A pathophysiological study of the hippocampus in a presenilin 1 M146V rat model of Alzheimer's disease

Ruth Pybus

Submitted for the degree of

Doctor of Philosophy

in the Faculty of Medicine, University of Edinburgh

August 2001

Declaration

I declare that this thesis was composed by myself. The contributions of others to this work are clearly indicated.

Ruth Pybus

Acknowledgements

I would like to thank Dr Nikki MacLeod and Dr John Curtis for their support, encouragement and advice throughout this project and for making my time spent working in their group such a productive and positive part of my life.

I am grateful for the technical help I have received from Dr Peter Estibeiro, Dr Eleanor Barnard, Dr Emma Wood and Professor Ironside and co-workers, who have generously given their time and resources to assist with experimental procedures out with the electrophysiological focus of our laboratory.

I have received excellent support from research support staff in the Medical Faculty, and would like to thank in particular Vivian Allison and Grace Grant in the histology service laboratory, the staff in the animal facility, and the staff in the workshop. Their dedication and knowledge has been invaluable to the progress of this research.

I am grateful for the financial backing I have received from the BBSRC and my parents, without which this project would not have been possible.

Contents

Abstract

Alzheimer's disease (AD) is the most prevalent cause of senile dementia in industrialized nations. The financial and organizational challenges it presents will increase with the projected rise in the proportion of older people in the population. Elucidation of the causes and progression of AD and development of effective treatments has been hampered by the lack of an animal model suitable for laboratory research. The discovery of rare heritable AD cases coupled with the development of transgenic technology has provided the possibility of generating powerful research tools. Resulting transgenic animal models have already aided understanding of the disease progression and suggested possible treatments. This thesis investigates the hippocampal electrophysiology and pathology of a rat model of the presenilin 1 gene M146V mutation, and is the first rat model of presenilin 1 AD. This mutation causes dominant inheritance of AD in a Finnish family. Since affected subjects show early disease onset and rapid deterioration, it was hoped that the $PS1_{M146V}$ transgene would promote generation of a phenotype within the life-span of the rat. In this study, extracellular field potential recordings of medial perforant pathway/dentate gyrus and CA3/CA1 synaptic properties and plasticity have been made in the $PS1_{M146V}$ transgenic rats and their non-transgenic littermates at 6 and 18 months old. No changes were observed in the half-maximal EPSP amplitude. At 6 months, no changes were seen in the expression of long-term potentiation, post-tetanic potentiation or paired pulse plasticity in either pathway. Synaptic plasticity recorded in the dentate gyrus in 18 month animals was also unchanged. However, long-term potentiation was significantly increased in the CA3/CA1 pathway in 18 month old transgenic animals, which showed a striking difference in its pattern of development. Paired pulse facilitation and post-tetanic potentiation were unchanged. This age-dependent and pathway-specific change is consistent with the progression of AD in human subjects, and results published on presenilin 1 mouse models. Intracellular sharp electrode recordings were made from CA1 pyramidal neurones from the 18 month old animals to investigate the source of the changes in long-term potentiation. No changes were observed in the passive membrane properties, action potential properties, the duration or amplitude of slow, medium and fast afterhyperpolarization and action potential

adaptation. However, the half width of the EPSP was significantly increased, which may be attributable to slower membrane repolarization. A similar lengthening of EPSP decay time has been reported for the conditioned response during paired pulse facilitation, and this has been attributed to autoinhibition of GABAergic interneurones via $GABA_B$ receptors. Further studies are required to establish whether GABAergic mechanisms are responsible for the observation in the $PS1_{M146V}$ rat. A preliminary histological investigation using congo red failed to reveal amyloid deposition or neurofibrillary tangles in the $PS1_{M146V}$ rat and this has since been supported by another laboratory using more rigorous immunohistological techniques. This observation is consistent with the findings reported in a presenilin 1 mouse model. These results support the success of the $PS1_{M146V}$ transgene in creating a phenotype with possible use in AD research. Its future contribution would probably be in generating a double transgenic model by cross breeding with a mutated amyloid precursor protein line, which has proved to be a successful approach for generating more robust and rapid development of AD-like phenotype in mouse models.

Chapter 1

Alzheimer's Disease

Alzheimer's disease (AD) is a fatal neurodegenerative disorder usually associated with the elderly. It is characterized by insidious deterioration of cognitive functions, which leaves the sufferer increasingly dependent on carers. The disease is prolonged, often lasting 8 to 12 years following diagnosis, severely impairing quality of life for sufferers and generating a huge emotional burden on relatives. It also causes economic and organizational challenges for both carers and society. This burden will increase given the projected growth in the ageing population. Current treatments are limited, and at best give only temporary alleviation of symptoms, with eventual incapacitation and death being inevitable. These considerations make the search for the cause of AD and development of effective treatments of great importance.

1.1 Epidemiology and Diagnosis

AD is the most common form of dementia in industrialized nations. Estimated prevalence varies greatly, but is usually quoted between 5 to twenty per cent for the population over sixty-five years old and twenty to fifty per cent for those over eighty-five years old (Bachman et al 1992, Rosenberg 1997, Evans et al 1989, Skoog et al 1993). Despite the variation in figures, all studies show a trend of increased AD prevalence from around sixty to eighty-five years of age. In men there is an approximate doubling in incidence every decade from sixty years, reaching a plateau after eighty-five years (Skoog et al 1993). Such a plateau is not seen in women.

The variability in prevalence figures arises from diagnostic difficulties. These are due to the heterogenous nature of the disease and the overlap of symptoms with other illnesses, particularly vascular dementia and Creutzfeld Jacob disease. Mild AD is particularly hard to diagnose, and some epidemiological studies have chosen to quantify only moderate and severe cases, creating further discrepancy in prevalence figures.

In 1984, a task force consisting of the National Institute of Neurological and Cognitive Disorders (USA) and the Alzheimer's Disease and Related Disorders Association developed a set of criteria to improve diagnostic accuracy (Appendix I) (McKhann et al 1984). It was agreed that a definite diagnosis of AD is not possible using current clinical tests. Instead, the task force decided that diagnosis of 'probable AD' could be made upon demonstration of typical clinical symptoms according

to their criteria, and having eliminated other dementing illnesses as the cause. Even with these clinical criteria, the accuracy of pre-mortem diagnosis is variable, with the most experienced assessors correctly diagnosing about ninety per cent of cases (Galasko et al 1994), and accuracy identifying the disease in its early stages can be much lower. For this reason, the task force stated that a definite diagnosis can only be made when the clinical assessment is combined with positive autopsy results.

For effective treatments to be developed, early diagnosis of AD is especially important. Towards this goal, various approaches are being investigated. Computerized tomography scans and magnetic resonance imaging can be used to identify other conditions as the source of dementia by detecting abnormalities such as ischaemic lesions caused by stroke and tumours. These techniques also reveal cortical atrophy and dilation of ventricles typical of AD, however, the extent of atrophy overlaps extensively with that associated with normal ageing and is not diagnostic.

Magnetic resonance imaging is particularly sensitive and is helping to improve early diagnosis by detecting reduced hippocampal volume (Jack et al 1999). Hippocampal cell loss is correlated to the severity of dementia, making this test particularly relevant to the clinical condition. Increased resolution of magnetic resonance imaging is now allowing visualization of larger senile plaques in experimental conditions (Benveniste et al 1999), which in the future will hopefully allow definite antemortem diagnosis. More recently, plaque stains derived from congo red have been developed that are able to cross the blood brain barrier. It is intended that these will allow antemortem staining of neuritic plaques to improve visualization using techniques such as magnetic resonance imaging (Skovronsky et al 2000a).

Although there is no current antemortem test for AD, some factors strongly support a diagnosis. Amongst these are the presence of the ε4 allele at the apolipoprotein E (apoE) locus, which is a known genetic risk factor. Cerebrospinal fluid of AD subjects consistently shows significant elevation of tau and reduction in the $A\beta_{42}$ protein (Mehta et al 2000, Kanai et al 1998). Blood tests would be more acceptable since cerebrospinal fluid tests require lumbar puncture. Recent efforts are focussing on AD-specific changes in the forms of beta-amyloid precursor protein (AβPP) isolated from platelets, which are correlated with the clinical severity of AD and reflect AβPP composition in the cerebrospinal fluid (Sennvik et al 2000).

Although promising, most of these techniques are currently either still experimental, too expensive or too time-consuming for a large scale epidemiological studies or general use.

1.2 Clinical Symptoms

Alzheimer's disease was first described by Alois Alzheimer in 1907. He documented the case of a fifty-one year old woman who presented with extreme jealousy that was soon accompanied by memory impairment and paranoid behaviour. She displayed violent outbursts and suffered from auditory hallucinations, and was often too disturbed to be properly examined. During successful examinations she was confused, lacked concentration and failed to perform simple verbal and writing tasks. She showed no sign of significant motor impairment. Towards the end of her illness she was bedridden, incontinent and apathetic. The patient declined steadily and died after 4 ½ years.

At autopsy the brain showed severe and widespread atrophy and arteriosclerosis. Histological examination revealed intracellular fibrillar bundles, which persisted in regions of cell loss. Throughout the cortex, extracellular deposits described as a 'peculiar substance' were observed (Alzheimer 1907).

At the time, dementia was considered a rare disease since cognitive decline in the elderly was seen as a normal consequence of ageing. It was only later that the symptoms and pathology observed in this middle-aged woman were linked to dementia in older subjects.

The typical early symptoms of AD are mild memory loss, particularly of anterograde declarative memory, and subtle behavioural changes. Memory impairment gradually extends to all forms of memory. Aphasia, manifest in difficulty naming objects and recognizing words, develops into mutism in the late stages. Agnosia confers impaired judgement and reasoning, resulting in difficulty planning and executing tasks. Subjects' ability to recognize objects and familiar faces deteriorates. Apraxias involve physical inability to perform daily tasks. Subjects tend to be unaware of their deficits (anosagnosia) and so are often reluctant to seek medical help. Sensory-motor function tends to be spared although limb rigidity, coupled with extreme confusion and apathy leads to subjects frequently becoming bedridden in the late disease stages.

Sufferers may also display a wide range of behavioural disturbances, which are often more distressing for carers than the cognitive problems. These include verbal and physical aggression,

paranoid delusions, hallucinations, sleep disturbances, depression, apathy, social withdrawal, wandering and pacing, repetitive actions, incontinence and inappropriate social behaviour.

1.3 Neuropathology

Three forms of pathology are recognised as diagnostic abnormalities in AD:

- Amyloid plaques
- Neurofibrillary deposition
- Specific nerve cell loss

The brain areas most severly affected are the association areas of the neocortex, the hippocampus, the amygdala and cholinergic neurones of the basal forebrain. This pattern of pathology accords with the typical AD deficits in memory, analytical thought, perception, and motivation.

1.31 Amyloid Plaques

These are extracellular lesions of which there are three forms; diffuse, neuritic and dense-core. All contain deposits of beta-amyloid (Aβ; a globular protein cleaved from AβPP). In healthy tissue, the major cleavage product is 40 amino acids long ($A\beta_{40}$), but some longer $A\beta_{42/43}$ is also produced. $A\beta_{42/43}$ seems to be the important isoform in plaque formation, since it is less soluble due to its additional N-terminal β-pleated sheet structure which increases its tendancy for fibril formation and aggregation (Xia et al 1997). Plaques form when $A\beta_{42}$ levels increase in conjunction with a high $A\beta_{42}/A\beta_{40}$ ratio, and *in vitro* studies have suggested that $A\beta_{40}$ hinders $A\beta_{42}$ deposition (Snyder 1994).

Neuritic plaques comprise a distinct Aβ core surrounded by dystrophic neurites and reactive astrocytes. Fibrillar $A\beta_{42/43}$ is the initial species to be deposited in neuritic plaques (Iwatsubo et al 1995), which is believed to seed the later deposition of $A\beta_{40}$ (Jarrett et al 1993). Other factors associated with plaques are microglia and proteins such as AβPP, α1-antichymotrypsin, apoE, apolipoprotein J, heparin-sulphate proteoglycan (HSPG), butyrylcholinesterase and non-amyloid

plaque component. Neuritic plaques are stained by congo red and show green bifringence when observed under polarized light.

Diffuse plaques also contain aggregated $A\beta_{42/43}$, but have far fewer fibrils and lack the distinct amyloid core. They are not associated with dystrophic neurites, are not stained by congo red and attract very few astrocytes or microglia. It has been proposed that diffuse plaques are precursors to neuritic plaques, possibly being converted by a butyrylcholinesterase-dependent mechanism, since butyrylcholinesterase is only associated with plaques with high levels of β-sheet amyloid (Guillozet et al 1997) and it induces Aβ aggregation *in vitro*. However, diffuse plaques are not restricted to areas of the brain that show degeneration in AD, for example, they are often found in the cerebellum. Also, they occur in the brains of aged, non-demented individuals, (although this may represent preclinical change). It has therefore been suggested that they are non-pathogenic and are either generated independently from neuritic plaques or are converted to neuritic plaque by factors that are restricted to limbic and association cortex areas. Alternatively, diffuse plaques are potentially pathogenic but not all brain areas are susceptible.

Dense-core or 'burnt-out' plaques are the final stage of plaque development. Associated neurites are degenerated and they no longer attract astrocytes. At this stage they are probably most effectively degraded by microglia.

There are also Aβ deposits in the cerebral vasculature, especially in vessels associated with the cerebral cortex. Vascular amyloid comprises mainly of $A\beta_{40}$, suggesting that the vasculature is not the source of amyloid deposited in the brain. The amount of vascular deposition is not correlated with the degree of dementia, and so it is unlikely that it contributes to AD-related deficits.

1.32 Neurofibrillary Deposition

Neurofibrillary deposits are intracellular and mainly comprise the tandem repeat region of tau. This microtubule binding protein undergoes various post-translational modifications, including phosphorylation, glycosylation and glycation, which have been implicated in AD pathology.

The affinity of tau for microtubules is regulated by its level of phosphorylation. In AD, tau is hyperphosphorylated (tau-p), which reduces its binding capacity and causes destabilization of microtubules. This may compromise neurone viability by impairing intracellular trafficking. Tau-p

forms non-soluble paired-helical filaments, that aggregate into neurofibrillary tangles (NFT). These build up in the cytoplasm, dislocating the nucleus and spreading into apical dendrites (but not axons) of pyramidal cells. They are associated with vimentin, actin, ubiquitin, tau, Aβ and neurofilament proteins, which form a fuzzy coat around the tau-p paired-helical filament core.

Glycation of tau is observed in AD brain but not in age-matched non-demented controls (Ko et al 1999b). Tau becomes an advanced glycation end-product (AGE); a protein heavily glycated by non-enzymatic formation of covalent bonds between the amino-groups of proteins and sugars. The bonds may be important for paired-helical filament formation; glycation can alter protein structure making proteins inactive and increasing their stability, which may explain the persistence of tangles. In addition, AGEs encourage formation of reactive oxygen species, which at low levels stimulate neuroprotective NFκB activity and cytokines (Yan et al 1995) and at higher levels can cause oxidative cell damage.

Tangles persist even when the cell is destroyed, leaving ghosts tangles that are eventually degraded by astrocytes. Ghost tangles are prevalent in the nucleus basalis of Meynert and hippocampus but are rare in the neocortex, even in the presence of intracellular NFTs. This suggests that they may only invade the neocortex in the later stages of the disease and are not the main cause of cell loss, or that they are more effectively cleared from the neocortex. Their distribution is specific to areas that show degeneration, such as the entorhinal cortex (LII and LIV), the subiculum, CA1, and prosubiculum. Other areas less affected include the accessory basal nucleus of the amygdala, the nucleus basalis of Meynert and the association neocortex, where they are mostly in LIII and LV.

Tangles are associated with other diseases such as Pick's, Down's syndrome (DS) and progressive supranuclear palsy, however they receive special interest in AD since they have a predictable distribution through various stages of the disease and their numbers correlate well with levels of dementia. This pattern was recognised by Braak & Braak (1991) who used it to categorise AD pathology into stages;

Transentorhinal Stages : Mild to severe deposition in the entorhinal cortex, targeting large stellate neurones of the pre-α layer.

Limbic Stages :	Pre-α strongly affected in the transentorhinal cortex. Some weak deposition in the CA1 and subiculum.
Isocortical Stages :	Ghost tangles in the transentorhinal and entorhinal cortices. Severe pathology in all isocortical association and limbic areas. Primary motor and sensory areas are spared.

Clinical changes relating to transentorhinal and limbic stages seem to be very subtle with obvious decline observable only once tau pathology extends beyond the limbic areas in the isocortical stage.

1.33 Specific Cell Loss

This predominantly affects large neurones in the association neocortex and limbic structures (Bundgaard et al 2001). Cell loss is co-localized with areas affected by tangles and to a large extent, neuritic plaques, with the level of cell loss correlating well with the severity of dementia (Gomez-Isla et al 1997).

There is increasing evidence for apoptotic mechanisms in AD neurodegeneration. DNA fragmentations has been identified by TUNEL labelling (Overmyer et al 2000) and brains of Alzheimer's disease subjects show upregulation of factors linked to apoptosis such as caspase 3 (Stadelmann et al 1999) Bcl-2 interacting mediator of cell death, Bcl-2 related ovarian death gene and p21 (Engidawork et al 2001). However, there is still controversy over whether necrotic cell death is also involved. Evidence of necrosis and lack of apoptosis reported in some studies may be artefactual since experimental conditions are manipulated to accelerate potential toxic effects and whilst a cytotoxic insult may cause apoptosis when delivered chronically at a low level, the same insult often results in necrosis when presented acutely and at a higher dose (Bonfoco et al 1995). This suggests that apoptotic mechanisms may be more relevant to the gradual, insidious nature of AD progression.

The following cell types are targeted in AD:

- Pyramidal neurones in the CA1 (forty per cent cell loss) and subiculum degenerate. CA3 neurones are largely spared.
- Large stellate neurones in the entorhinal cortex. This results in almost total destruction of LII and reduced cell density in LIII. These neurones give rise to the perforant pathway, which is the major source of cortical input into the hippocampus.
- Large multipolar neurones in LIV of the entorhinal cortex. These are the sole cortical output targets of the hippocampal formation. Surviving cells have a high tangle load, which suggests impaired function.
- Accessory basal nucleus cells in the amygdala, which project to the hippocampus.
- Large pyramidal cells of the neocortex association areas, especially the upper laminae.
- Cholinergic neurones of the nucleus basalis of Meynert (forty to seventy per cent cell loss) as well as the medial septum and vertical limb of the diagonal band of Broca. These form the main cholinergic projections to the neocortex and hippocampus and seem to be important for cognitive function. Their loss is demonstrated by the lack of cholinergic markers in the cortex and hippocampus.

The gross effects of cell loss are functional isolation of the hippocampus from the neocortex and other limbic areas and impaired cholinergic modulation of limbic and associational isocortex activity, disrupting pathways that are important for normal cognitive function.

1.34 Other Pathological Changes

AD subjects are affected by other non-specific pathologies. Some AD subjects have Lewy bodies without Parkinsonism, for which Lewy bodies are a typical pathological feature. These are found in smaller pyramidal neurones in the deep cortical layers (Wakabayashi et al 1995). There seems to be a correlation between Lewy body pathology and the incidence of hallucinations in AD subjects, especially in conjunction with poor eyesight (McShane et al 1995). However cases of Lewy body-variant AD are often considered to be a distinct form of dementia since the clinical traits are specific

enough to allow Lewy body involvement to be predicted antemortem (Liberini et al 1995). Also, there is evidence that the neurodegenerative process is different, for example inflammatory processes do not seem to feature in Lewy body variants of AD, which show much lower immunoreactivity for microglia than brains from non-Lewy body AD subjects (Rozemuller et al 2000). Lewy body subjects also lack tau immunoreactivity (Shepherd et al 2000).

In normal ageing, the apical dendrites of dentate gyrus granule cells and LII pyramidal cells of the parahippocampal gyrus are extended, presumably to compensate for mild cell loss, allowing maintenance of synaptic density. In AD subjects, this compensatory dendrite lengthening does not occur (Callahan et al 1998).

Hirano bodies, which are restricted to the CA1 and subiculum, are eosinophillic rods or spindle shaped bodies that contain actin and actin-associated proteins. Their function is unknown. Granulovascular change is seen in hippocampal pyramidal cells coincident with tangles (Ball 1978). They are clear, membrane-bound inclusions with a black granular core, which can distort neurone shape and displace the nucleus. They are immunoreactive for tau and tubulin filaments (Price et al 1986, Dickson et al 1993). These lesions are considered to be secondary AD pathology since they are found in many types of neurodegeneration, have a restricted distribution and in the case of hirano bodies may be evident in subjects as young as twenty years old.

1.4 Genetic basis

AD has been commonly understood to be a sporadic disease occurring in the elderly. This was termed senile dementia of the Alzheimer's type, to distinguish it from other forms of senile dementia such as Parkinson's disease or vascular dementia. However, it was recognized that some cases of AD occur at a much earlier age. Thus, cases in subjects under sixty years of age came to be termed pre-senile dementia of the Alzheimer's type, with evidence that it was distinct from that observed in elderly subjects (Pro et al 1980). It was also noted that some presenile cases are not sporadic, but are inherited in a fully penetrant, autosomal dominant manner. This familial Alzheimer's disease (FAD) tends to be

more aggressive than late-onset AD with subjects showing rapid cognitive decline and a shorter survival time (Swearer et al 1996).

To date, mutations on 3 genes have been connected with FAD. These code for the AβPP, presenilin 1 (PS1) and presenilin 2 (PS2). Mutations to PS1 are most common and may account for about fifty per cent of all FAD (Campion et al 1999) (although estimates are as low as 18% (Cruts et al 1998)). Late-onset FAD pedigrees exist but these are more difficult to identify. They are often masked by family members dying from other causes before AD is evident, and so a genetic susceptibility is not suspected. This may be especially relevant to PS2 mutations, which are not fully penetrant and seem to cause a pattern of clinical development more typical of sporadic Alzheimer's disease (SAD), being longer in duration and later in onset (Bird et al 1996). Conversely, it is possible that some cases appear to be familial but are actually due to a common environmental factor, or that since age is a risk factor for AD, familial longevity may increase the chances of SAD occuring in multiple family members and being mistaken for FAD.

Although FAD is only thought to account for about 0.5 to 1 per cent of AD cases (Rosenberg 1997), it is hoped that studying the effects of these mutations will aid understanding of the processes involved in the more prevalent sporadic forms. A major problem in the study of AD has been trying to establish cause and effect. The predictable nature of FAD transmission has allowed monitoring of preclinical family members known to carry the pathogenic mutation. This has led to identification of preclinical abnormalities in cerebrospinal fluid, blood composition and brain volume, which help to determine the order in which features of AD contribute to the disease and suggest possible treatments and diagnostic tools. For example magnetic resonance imaging can detect decreased hippocampal volume in FAD subjects up to 10 years before clinical symptoms develop.

SAD cases also seem to be influenced by genes. Although not sufficient or necessary for causing AD, these genes may predispose individuals to the disease, making its onset more likely in conjunction with other genetic or environmental risk factors. That genes are involved in AD concurs with the observation that about 10 per cent of AD subjects have at least one relative who has had the disease (Rosenberg 1997). The best understood risk factor associated with SAD is the ε4 allele of apoE. Mutations and dimorphisms in other genes have been suggested but these seem to have weaker effects and are less well studied.

1.41 The nature and roles of proteins involved in AD genetics

β-Amyloid precursor protein and β-amyloid

AβPP is an ubiquitously expressed glycosylated transmembrane protein that is especially prevalent in the brain (Kang et al 1987, Selkoe et al 1988, Shimokawa et al 1993). The full-length protein ($AβPP_{fl}$) is seven-hundred and seventy amino acids long ($AβPP_{770}$) with other isoforms arising from alternative mRNA splice variants. The most common isoform in the brain is $AβPP_{695}$, which is mainly generated in neurones (Tanaka et al 1988).

AβPP is processed by either α-secretase (Maruyama et al 1991), which is the main route in healthy cells, or β-secretase (figure 1.1). α-Secretase is located at the cell membrane, where it cleaves AβPP within the Aβ domain to release a secreted N-terminal fragment, sAβPPα and a C-terminal stub. The C-terminal stub is further cleaved by γ-secretase to release p3 (Haass et al 1993) and a rapidly degraded C-terminal fragment. Since α-secretase cleaves AβPP within the Aβ domain, this pathway is non-amyloidogenic (Golde et al 1992).

The β-secretase amyloidogenic pathway is also active in healthy cells (Shoji et al 1992). β-secretase is located in the endoplasmic reticulum and trans-golgi (Haass et al 1993). It cleaves AβPP at the N-terminal of the Aβ domain to release the secreted sAβPPβ fragment. The remaining C-100 stub is cleaved by γ-secretase to release Aβ (Golde et al 1992).

The identities of the secretases are as yet undetermined although there is growing evidence that PS1 may have γ-secretase activity (Li et al 2000a) and β-secretase may be the beta-amyloid converting enzyme (Cai et al 2001).

Different lengths of Aβ, varying from thirty-nine to forty-three amino acids, are produced depending on the exact cleavage site of γ-secretase. The more common forty amino acid variant is formed in the late golgi, whilst the longer $Aβ_{42/43}$ variants, ($Aβ_{42}$ being more prevalent,) are formed in the endoplasmic reticulum, suggesting that there are two types of γ-secretase with different subcellular localizations and AβPP cleavage sites (Citron et al 1996). These γ-secretases compete for the common substrate, C-100, such that if $Aβ_{40}$ secretion is inhibited, the levels of intracellular $Aβ_{42/43}$ increase (Skovronsky et al 2000b).

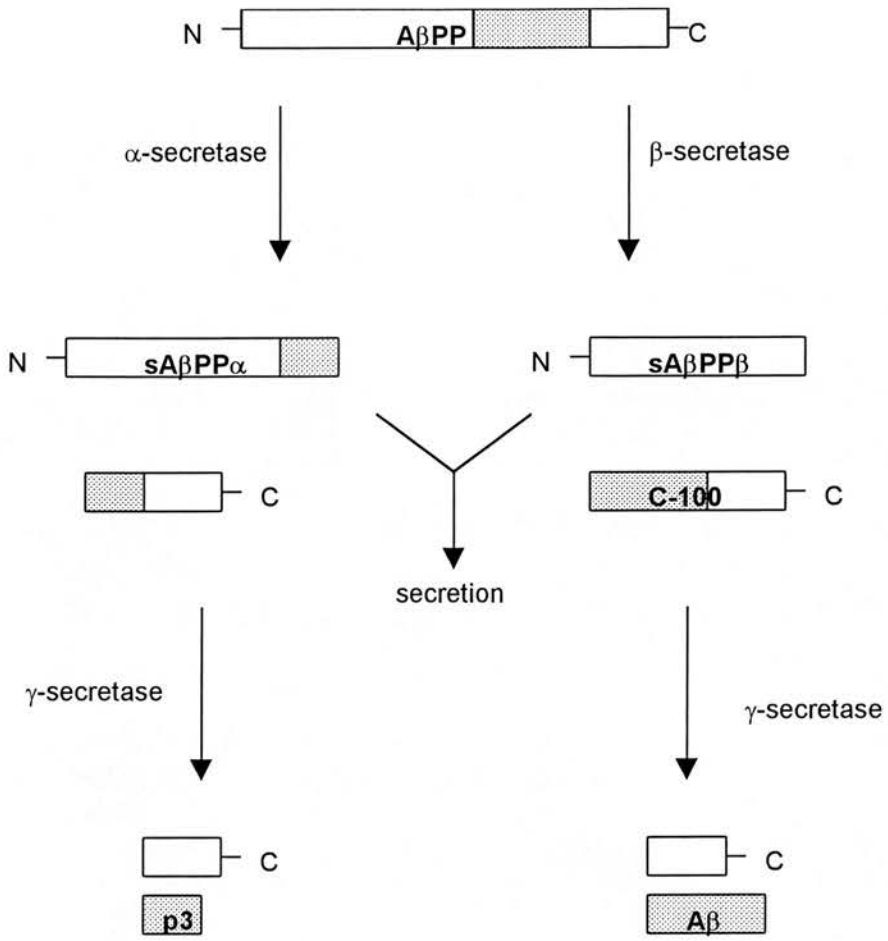

Figure 1.1 AβPP α-secretase and β-secretase processing pathways

The Aβ domain is highlighted.

AβPP is a *house-keeping* gene; an ubiquitously expressed gene that is important for non-specialized cellular processes. As such, it is highly conserved and abundant, comprising about 0.2 per cent of neuronal mRNA. Full length AβPP ($AβPP_{fl}$) and sAβPPα have recognized physiological roles in neurite outgrowth, synaptic plasticity and neuroprotection.

sAβPPα appears to protect neurones against excitotoxic insults and oxidative stress. Its expression is increased following neurone injury and cells pretreated with physiological concentrations of sAβPPα show reduced excitotoxicity in response to glutamate or Aβ. It reduces neurone excitability by activating the high conductance charybdoxin-sensitive Ca^{2+}-dependent K^+ channel, which carries a hyperpolarizating K^+ current. This may decrease the activity of voltage-gated

Ca^{2+} channels and NMDA receptor channels and so lower both basal and glutamate-induced increases in intracellular Ca^{2+} concentration. sAβPPα also decreases NMDA receptor activity by altering its phosphorylation state via a cGMP/PKG dependent pathway (Furukawa et al 1998). This does not affect kainate or AMPA receptor activity. sAβPPα release is stimulated by nerve growth factor, suggesting it has a role in neurotrophic activities.

sAβPPα levels are increased in the cerebrospinal fluid following *in vivo* induction of the putative physiological correlate of memory; long-term potentiation, and when infused into adult rat brains sAβPPα improves performance in learning and memory tasks. Rats reared in a stimulus enriched environment have more AβPP immunoreactive synapses and perform better in shock avoidance and water maze behavioural tests than rats from impoverished environments (Huber et al 1997). AβPP overexpressing mice show upregulation of growth associated protein 43 (GAP-43) and increased synapse density in the frontal cortex when examined using *in situ* immunohistochemistry (Mucke et al 1994). GAP-43 is important for neurite outgrowth in synaptic remodelling, and in healthy adult brain is expressed specifically in areas associated with AD; the association neocortex and hippocampus. However, its levels are reduced in the hippocampus and frontal cortex in AD brain which may contribute to cognitive impairment (Bogdanovic et al 2000, de la Monte et al 1995).

Membrane bound $AβPP_{fl}$ promotes neurite outgrowth and may contribute to synaptic plasticity. It binds proteoglycans (Buee et al 1993), which mediate cell-cell and cell-matrix adhesion and neurite extension and so may be involved in morphological changes and target finding during expression of synaptic plasticity.

The roles of β-secretase products; Aβ, sAβPPβ and C100, at normal physiologically levels of 10pM to 1nM are less well understood, however, micromolar doses of fibrillar Aβ trigger apoptosis-like cell death in neurone cultures (Loo et al 1993), and more recently, soluble oligomers and protofibrils of Aβ have shown neurotoxicity in culture (Lambert et al 1998, Hartley et al 1999). C100 is also neurotoxic (Yankner et al 1989). sAβPPβ activates cultured microglia to release potentially cytotoxic products such as reactive oxygen species and inflammatory cytokines. Although sAβPPα has similar activity, the detrimental effects seem to be compensated by its neurotrophic properties (Barger & Harmon 1997).

Presenilin 1 and 2

PS1 and 2 are ubiquitously expressed in the CNS but are especially prevalent in areas most susceptible to AD. Their distribution is similar to that of Aβ and is unchanged in AD. They are found exclusively in neurones (Kovacs et al 1996), specifically in the cell soma, with PS1 also spreading into some neurites. They are restricted to the early compartments of the protein secretory pathway, including the endoplasmic reticulum, intermediate compartment and the early cis-golgi compartment (Annaert & De Strooper 1999) although it has recently been suggested that small amounts may be found in the cell membrane (Takashima et al 1996). Their homology lies mostly within the 8 transmembrane domains and the large cytoplasmic loop, suggesting that these regions are particularly important for protein function.

The level of PS is strictly regulated, possibly by calsenilin (Buxbaum et al 1998), as demonstrated in TG mice designed to overexpress human PS1 (Thinakaran et al 1996, Thinakaran et al 1997). In these animals, although human PS1 is expressed, the level of total PS1 is little changed. PS is processed in the ER where the full length protein is rapidly cleaved within the cytoplasmic loop. The resulting C-terminal and N-terminal fragments remain closely associated to form a heterodimer.

PS has aspartate protease activity and can cleave proteins within transmembrane domains. It is involved in development, protein processing and apoptosis. Whilst the heterodimer is usually considered to be the active form, the full length protein must also be functional since it can reverse deficits in Caenorhabditis elegans caused by mutations in its PS homologue Sel-12.

The PS1 heterodimer is necessary for normal γ-secretase processing of AβPP (Xia et al 1998) and it is possible that PS1 is γ-secretase since it has the necessary property of being an aspartate protease with access to cleavage sites within the membrane (Wolfe et al 1999) and it is bound by γ-secretase inhibitors (Li et al 2000a). Neurones in PS1 null animals have reduced γ-secretase activity as indicated by the accumulation of P3- and Aβ-containing C-terminal stubs (De Strooper et al 1998). However, presenilin1 lacks sequence homology with know protease domains (Sherrington et al 1995) and there is residual amyloid secretion in PS1 null animals (De Strooper et al 1998). Also, there is increasing evidence for the existance of distinct γ-secretases that result in the different lengths of Aβ. However, PS1 mutations inhibited the production of both cleavage products to an equal extent (Murphey et al 2000). This would suggest that to be γ-secretase, then it must perform both Aβ42 and

Ab42 cleavage and have two distinct active sites for these roles. Given the lack of sequence homology with known proteases for even one domain, this is unlikely. However, it is clear that PS1 is important in promoting and regulating γ-secretase cleavage by an as yet unresolved mechanism. FAD mutations to PS1 result in elevated $A\beta_{42/43}$ production, which is a possible source of AD development in affected families.

A pro-apoptotic role is suggested for PS2. Cultured PC12 cells overexpressing human PS2 show increased vulnerability to apoptosis in response to Aβ exposure and withdrawl of neurotrophins. A similar response is seen in cells carrying normal levels of PS2 with an FAD-causing mutation (Deng et al 1996, Janicki et al 1997). In COS-7 cells overexpressing PS2, AβPP is abnormally processed by mechanisms suggesting apopotic, caspase-like activity and this response is heightened in cells expressing PS2 with FAD mutations (Weidermann et al 1999). Conversely, downregulation of PS2 is neuroprotective.

The interaction of PS1 with apoptotic pathways seems to be more complex. Upregulation of PS1 may cause either facilitation of (Czech et al 1998) or protection against (Bursztajn et al 1998) apoptosis whilst downregulation of PS1 has been shown to increase cell vulnerability (Roperch et al 1998).

PS1 may exert neuroprotection by interacting with the anti-apoptosis protein, β-catenin, in the endoplasmic reticulum. Free β-catenin is phosphorylated by glycogen synthase kinase-3β and tagged by ubiquitin for degredation. PS1 stabilizes β-catenin preventing its clearance and presumably promotes its anti-apoptotic activity. Cells expressing FAD PS1 are more sensitive to Aβ-induced apoptosis (Tanii et al 1999, Mattson et al 2000, Guo et al 1997). This may be explained by the failure of mutated PS1 to bind β-catenin, which is then depleted in association with an increased risk of apoptosis (Zhang et al 1998). However, another report in which PS1 was overexpressed in COS-7 cells suggests that PS1 binding inhibits β-catenin activity (Murayama et al 1998), although it did not show the effect of this binding on cell viability.

Where PS1 has been seen to facilitate apoptosis, identified mechanisms have included increased Ca^{2+} release from the endoplasmic reticulum (Guo et al 1997), free radical production (Guo et al 1999b), mitochondrial dysfunction (Guo et al 1998) and caspase activation (Kovacs et al 1999).

A role for PS1 in development was suggested by its homology with the Caenorhabditis elegans Notch signalling peptide, Sel-12. PS1 null animals have severe developmental defects, similar to those observed in Sel-12 null nematodes, which prevent offspring from surviving beyond a few days. However, this role does not seem to be disrupted in AD, since FAD mutations to PS in mice do not cause loss of function during development, and indeed mutated PS can rescue PS null animals as effectively as normal PS (Davis et al 1998).

Apolipoprotein E

ApoE is involved in plasma cholesterol and lipid homeostasis. In the cerebrospinal fluid, apoE is invariably associated with liposomes as a lipoprotein complex, which binds cell surface receptors such as the low density lipoprotein receptor, very low density lipoprotein receptor and the low density lipoprotein receptor-like receptor. Binding leads to internalization of the lipoprotein complex and its degradation by the lysosomal. Elevated apoE is associated with reduced plasma cholesterol (for review see Nimpf & Schneider 2000).

In the CNS, apoE is mainly produced by astrocytes (Boyles et al 1985) but it is also expressed at a lower level by selective neurones. In particular, apoE immunoreactive neurones are found in the frontal lobe of the cerebral cortex, CA1-4 hippocampal pyramidal cell populations and the granule cells of the dentate gyrus. ApoE is not produced in cerebellar neurones (Xu et al 1999). This pattern of neuronal apoE production mimics the distribution of AD pathology, suggesting that it may have a role in AD pathogenesis and confer regional specificity.

Additional roles for apoE relating to AD include modulation of AβPP processing and clearance (Vincent et al 2001), promotion of tau stability and microtubule formation (Benzing et al 1995, Wang et al 1998, Scott et al 1998) and synaptic remodelling (Arendt et al 1997).

1.42 AD-related gene mutations and allelic variants

β-Amyloid precursor protein

The first FAD mutation to be identified was on the AβPP gene. AβPP had been mapped to chromosome twenty-one in 1987 (Goldgaber et al 1987, Tanzi et al 1987, St George-Hyslop et al 1987). Meanwhile, it had been recognised that DS subjects invariably develop pathology indistinguishable from AD by thirty-five years (Jervis & Thiells 1948) and about seventy-five per cent

are diagnosed with AD by sixty years (Wisniewski et al 1985, Olson & Shaw 1969). Since DS is caused by trisomy of chromosome twenty-one it was possible that overexpression of a gene found on this chromosome could cause AD. The association of Aβ with amyloid plaques made AβPP a prime potential locus for FAD-inducing mutations.

In 1991, a missense mutation was identified at codon 717 of AβPP, replacing valine with isoleucine (V717I) (Goate et al 1991). This resulted in increased $A\beta_{42/43}$ levels in the CNS and onset of AD at about fifty years. Eight other unrelated families have subsequently been found to carry the same mutation. Ten other AβPP missense mutations have been found (Appendix II). They are all located at or near the Aβ domain and cause an increase in the level of $A\beta_{42/43}$. They all cause presenile onset at of Alzheimer's disease and an aggressive disease progression.

The most extensively studied AβPP mutation is the K670M/N671L Swedish double mutation on exon 16, close to the β-secretase site. Age of onset is between forty-four and sixty-one years (Axelman et al 1994). At autopsy, subjects show cortical atrophy, especially of the hippocampus, and dilated ventricles. There are high concentrations of NFTs and amyloid plaques mainly comprising $A\beta_{42/43}$ (Lannfelt et al 1994, Kalaria et al 1996).

Aβ levels in skin fibroblasts from living subjects are trebled (Ingelson et al 1996), suggesting that this tissue might replicate some of the pathogenic cellular processes of affected neurones making it a useful experimental tool. Human kidney 293 and neuroblastoma cells carrying the Swedish mutation produce 6 to 8 times more Aβ than those expressing wildtype AβPP (Citron et al 1992, Cai et al 1993) supporting amyloid upregulation as the source of AD changes.

Presenilin 1

It is often cited that about forty per cent of early-onset FAD cases are linked to PS1 mutations (Tanzi et al 1996) although some estimates are as low as 18 per cent (Cruts et al 1998). The involvement of chromosome 14 in FAD was recognised in 1992 (Schellenberg 1992) and the PS1 gene was identified in 1995 (Sherrington et al 1995) since when over seventy FAD-causing PS1 mutations have been described (Appendix III).

Mutations are found at many sites throughout the primary protein structure of PS1, but are particularly focused on the highly conserved transmembrane regions with a significant cluster along one face of an α-helix. These areas are all thought to be important for the function of the protein.

Although PS1 mutations are many and widespread, the resulting phenotypes are very similar. They lead to especially virulent AD with a mean age of onset of forty-five years and a rapid disease progression. In all cases, $A\beta_{42/43}$ is elevated without any change in $A\beta_{40}$, AβPPs or $A\beta PP_{fl}$ levels (Citron et al 1997). This implies that the α- and β-secretase pathways can be independently regulated. These observations have been made in both blood plasma and cultured skin fibroblasts from affected individuals. More importantly, $A\beta_{42/43}$ is elevated in cultured cells from healthy tissue when transfected with mutated PS1 and in transgenic mice carrying the mutated human gene (Citron 1997), showing that altered AβPP processing in the AD subjects can be attributed exclusively to the PS1 mutation.

PS1 mutations (M146V, L286V) predispose cells to apoptosis, including that induced by Aβ toxicity. Cell viability is restored by overexpression of the Ca^{2+} binding protein calbindin (Guo et al 1998), suggesting that impaired Ca^{2+} homeostasis is involved. Cells carrying the mutations A246E, ΔE10 and L286V express activated caspase 3 which is part of the classic apoptotic pathway (Kovacs et al 1999).

The mutation that will be studied in this thesis is the methionine to valine substitution at codon 146 (M146V). This mutation was linked to chromosome 14 in 1994 (Hardy 1994) and subsequently identified in 3 unrelated families (Clark et al 1995). Inheritance is autosomal dominant and the age of onset is especially low, commonly being between thirty-six and forty years and the mean disease duration is 6 years.

A typical case study describes a thirty-nine year old woman who presented with mild memory deficit. Medical examination revealed moderate deficits in other cognitive functions; spatial orientation, visual agnosia, constructional apraxias and agraphia in conjunction with cortical atrophy and ventricular dilation. The patient also had mild myoclonic jerking, which seems to be particular to M146V FAD. Her cognitive and physical problems worsened rapidly and she died 4 years after diagnosis in a bedridden state. Autopsy showed the expected pattern of amyloid plaques, NFTs and cell loss. Unusually, there was also mild vacuolar change, which suggested a form of prion disease but

this was discounted by the presence of AD pathology and a lack of altered prion protein (Hardy et al 1994).

Plasma and fibroblasts from M146V subjects showed a specific increase in $A\beta_{42/43}$ (Scheuner et al 1996). HK293 cells and transgenic mice expressing human $PS1_{M146V}$ both showed elevated levels of $A\beta_{42/43}$ when compared to controls carrying the wildtype human gene (Ancolio et al 1997, Duff et al 1996), and transfected cells also show increased sensitivity to $A\beta_{42/43}$ toxicity.

Presenilin 2

Six FAD-causing mutations have been described in the PS2 gene on chromosome 1 (Appendix IV). The time course of the disease resembles SAD, showing a later age of onset and longer disease duration than FAD attributed to PS1 and AβPP. The timing is also less predictable suggesting that environmental factors are significant modifiers of disease expression (Sherrington et al 1996).

One pedigree is the Volga-German line N141I found in 8 families with a common ancestor. The mean age of onset is fifty-five years and the duration is eleven years (Iwatsubo et al, 1998). A second mutation, in an Italian family (M239V) has a mean onset of over sixty years and lasts up to twenty years although commonly the duration is much shorter. $A\beta_{42/43}$ levels are elevated but as in SAD the total Aβ level is unchanged. Cells transfected with N141I produce 5 times more $A\beta_{42/43}$ (Citron et al 1997) and show increased susceptibility to apoptosis (Janicki & Monteiro 1997).

Apolipoprotein E

Apoε was identified as the SAD-linked chromosome 19 gene in 1993 (Strittmatter et al 1993), which marked a significant discovery towards understanding the nature of the most prevalent cases of AD. The three allelic variants of apoε differ at two loci (table 1.1).

Table 1.1 Allelic variants of apoE

Allele	Locus 112	Locus 158
ε2	cys	cys
ε3	cys	arg
ε4	arg	arg

Amongst AD cases, the ε4 allele occurs at a higher than expected frequency. The risk conferred by ε4 is dose dependent with homozygotes being the most likely to develop AD. ε4 promotes early disease onset, rapidly deteriorating neurone function and Aβ over-production. It also seems to increase the chance of developing AD in conjunction with other risk factors, for example, Aβ deposition in response to traumatic head injury is more severe in ε4 carriers (Nicholl et al 1995). Conversely, AD subjects carrying the ε2 allele occur at a frequency lower than would be expected suggesting that this allele is protective.

The apoε genotype also interacts with FAD mutations in AβPP. In the AβPP V717F and K670M/N671L pedigrees, apoε4 carriers have a significantly earlier age of AD onset (Noguchi et al 1993). It does not seem to interact with PS mutations (Houlden et al 1998). A polymorphism in the apoε promoter also affects AD susceptibility. There is a higher prevalence of alanine homozygotes at the -491 A/T locus in AD cases regardless of the apoε genotype (Wang et al 2000).

The apoE protein may influence AβPP processing, clearance of extracellular AβPP and Aβ and plaque formation. Carriers of the ε4 allele have lower apoE levels, which leads to impaired lipid and cholesterol catabolism and elevated levels of total cholesterol and triglycerides (Tiret et al 1994, Luc et al 1994). This may explain the perceived link between AD and cardiovascular disease. Inhibiting cholesterol production in cultured cells by seventy per cent impairs Aβ production without affecting the level of AβPP (Simons et al 1998). Therefore, elevated cholesterol levels in ε4 subjects may increase Aβ production.

ApoE binds AβPP, which allows it to be internalized for degradation by the low density lipoprotein receptor-like receptor. However, in AD, apoE associated with senile plaques may impair Aβ clearance and contribute to plaque development (Namba et al 1991). ApoE4 binds Aβ with higher affinity than E3 or E2 and promotes Aβ aggregation and fibrillogenesis (Wisniewski et al 1994). One study reported that apoE4 reduces Aβ polymerization and toxicity in culture (Evans et al 1995), however they used free apoE, which may act differently to apoE in its usual lipoprotein complex.

Aβ (and especially $A\beta_{42/43}$,) promotes apoE binding to hippocampal neurones in culture, which leads to internalization of the Aβ/apoE complex. This suggests a putative pathway for plaque formation whereby $A\beta_{42/43}$ is preferentially internalized by neurones, generating intracellular concentrations that promote aggregation. This Aβ aggregate is released when the neurone dies and seeds plaque formation. This process would be accelerated in apoε4 carriers since apoE4 is much more readily bound and internalized by neurones in response to Aβ.

ApoE binds tau to promote microtubule formation and stability. The E2 and E3 isoforms have the highest affinity for tau, suggesting that microtubule stabilization may be impaired in ε4 carriers. *In vitro*, apoE prevents tau hyperphosphorylation and tangle formation (Flaherty et al 1999) and ε4 carriers exhibit elevated cerebrospinal fluid tau levels (Kanai et al 1999), which in AD cases correlate with disease duration and level of cognitive deficit.

ApoE4 may potentiate pro-inflammatory mechanisms in AD, since cultured microglia are activated by sera from apoε4 AD subjects, but not by sera from other AD patients or healthy apoε4 subjects (Lombardi et al 1998). Also, apoE3 hinders microglial activation by sAβPP, whilst apoE4 is far less effective (Barger & Harmon 1997).

ApoE is expressed in response to injury (Snipes et al 1986) may have a role in synaptic plasticity (Krugers et al 1997, Arendt et al 1997). ApoE3 enhances neurite outgrowth in cultured dorsal root ganglion neurones, whilst apoE4 reduces outgrowth (Nathan et al 1994) which may indicate impaired reinnervation and formation of new synaptic connections following cell loss *in vivo*. This could explain the early age of AD-onset in ε4 carriers who could have impaired compensatory mechanisms for preclinical cell loss, and may also explain the lack of age-associated neurite extention in AD neurones (Callahan et al 1998).

Central Student Micro Lab

Login Name :	PS_Class_3M.MS.MED.ED
Full Name :	Class3M
Document :	Microsoft Word - Chapter 1 Alzheimer's diseas
	Phys Class.MS.MED.ED
Account Balance :	
Date and Time :	2002-02-12 14:54:08

Remainder of incomplete job follows this page

Alzheimer's disease (AD) is a fatal neurodegenerative disorder usually associated with the elderly. It is characterized by insidious deterioration of cognitive functions, which leaves the sufferer increasingly dependent on carers. The disease is prolonged, often lasting 8 to 12 years following diagnosis, severely impairing quality of life for sufferers and generating a huge emotional burden on relatives. It also causes economic and organizational challenges for both carers and society. This burden will increase given the projected growth in the ageing population. Current treatments are limited, and at best give only temporary alleviation of symptoms, with eventual incapacitation and death being inevitable. These considerations make the search for the cause of AD and development of effective treatments of great importance.

1.1 Epidemiology and Diagnosis

AD is the most common form of dementia in industrialized nations. Estimated prevalence varies greatly, but is usually quoted between 5 to twenty per cent for the population over sixty-five years old and twenty to fifty per cent for those over eighty-five years old (Bachman et al 1992, Rosenberg 1997, Evans et al 1989, Skoog et al 1993). Despite the variation in figures, all studies show a trend of increased AD prevalence from around sixty to eighty-five years of age. In men there is an approximate doubling in incidence every decade from sixty years, reaching a plateau after eighty-five years (Skoog et al 1993). Such a plateau is not seen in women.

The variability in prevalence figures arises from diagnostic difficulties. These are due to the heterogenous nature of the disease and the overlap of symptoms with other illnesses, particularly vascular dementia and Creutzfeld Jacob disease. Mild AD is particularly hard to diagnose, and some epidemiological studies have chosen to quantify only moderate and severe cases, creating further discrepancy in prevalence figures.

In 1984, a task force consisting of the National Institute of Neurological and Cognitive Disorders (USA) and the Alzheimer's Disease and Related Disorders Association developed a set of criteria to improve diagnostic accuracy (Appendix I) (McKhann et al 1984). It was agreed that a definite diagnosis of AD is not possible using current clinical tests. Instead, the task force decided that diagnosis of 'probable AD' could be made upon demonstration of typical clinical symptoms according

to their criteria, and having eliminated other dementing illnesses as the cause. Even with these clinical criteria, the accuracy of pre-mortem diagnosis is variable, with the most experienced assessors correctly diagnosing about ninety per cent of cases (Galasko et al 1994), and accuracy identifying the disease in its early stages can be much lower. For this reason, the task force stated that a definite diagnosis can only be made when the clinical assessment is combined with positive autopsy results.

For effective treatments to be developed, early diagnosis of AD is especially important. Towards this goal, various approaches are being investigated. Computerized tomography scans and magnetic resonance imaging can be used to identify other conditions as the source of dementia by detecting abnormalities such as ischaemic lesions caused by stroke and tumours. These techniques also reveal cortical atrophy and dilation of ventricles typical of AD, however, the extent of atrophy overlaps extensively with that associated with normal ageing and is not diagnostic.

Magnetic resonance imaging is particularly sensitive and is helping to improve early diagnosis by detecting reduced hippocampal volume (Jack et al 1999). Hippocampal cell loss is correlated to the severity of dementia, making this test particularly relevant to the clinical condition. Increased resolution of magnetic resonance imaging is now allowing visualization of larger senile plaques in experimental conditions (Benveniste et al 1999), which in the future will hopefully allow definite antemortem diagnosis. More recently, plaque stains derived from congo red have been developed that are able to cross the blood brain barrier. It is intended that these will allow antemortem staining of neuritic plaques to improve visualization using techniques such as magnetic resonance imaging (Skovronsky et al 2000a).

Although there is no current antemortem test for AD, some factors strongly support a diagnosis. Amongst these are the presence of the ε4 allele at the apolipoprotein E (apoE) locus, which is a known genetic risk factor. Cerebrospinal fluid of AD subjects consistently shows significant elevation of tau and reduction in the $A\beta_{42}$ protein (Mehta et al 2000, Kanai et al 1998). Blood tests would be more acceptable since cerebrospinal fluid tests require lumbar puncture. Recent efforts are focussing on AD-specific changes in the forms of beta-amyloid precursor protein (AβPP) isolated from platelets, which are correlated with the clinical severity of AD and reflect AβPP composition in the cerebrospinal fluid (Sennvik et al 2000).

Although promising, most of these techniques are currently either still experimental, too expensive or too time-consuming for a large scale epidemiological studies or general use.

1.2 Clinical Symptoms

Alzheimer's disease was first described by Alois Alzheimer in 1907. He documented the case of a fifty-one year old woman who presented with extreme jealousy that was soon accompanied by memory impairment and paranoid behaviour. She displayed violent outbursts and suffered from auditory hallucinations, and was often too disturbed to be properly examined. During successful examinations she was confused, lacked concentration and failed to perform simple verbal and writing tasks. She showed no sign of significant motor impairment. Towards the end of her illness she was bedridden, incontinent and apathetic. The patient declined steadily and died after 4 ½ years.

At autopsy the brain showed severe and widespread atrophy and arteriosclerosis. Histological examination revealed intracellular fibrillar bundles, which persisted in regions of cell loss. Throughout the cortex, extracellular deposits described as a 'peculiar substance' were observed (Alzheimer 1907).

At the time, dementia was considered a rare disease since cognitive decline in the elderly was seen as a normal consequence of ageing. It was only later that the symptoms and pathology observed in this middle-aged woman were linked to dementia in older subjects.

The typical early symptoms of AD are mild memory loss, particularly of anterograde declarative memory, and subtle behavioural changes. Memory impairment gradually extends to all forms of memory. Aphasia, manifest in difficulty naming objects and recognizing words, develops into mutism in the late stages. Agnosia confers impaired judgement and reasoning, resulting in difficulty planning and executing tasks. Subjects' ability to recognize objects and familiar faces deteriorates. Apraxias involve physical inability to perform daily tasks. Subjects tend to be unaware of their deficits (anosagnosia) and so are often reluctant to seek medical help. Sensory-motor function tends to be spared although limb rigidity, coupled with extreme confusion and apathy leads to subjects frequently becoming bedridden in the late disease stages.

Sufferers may also display a wide range of behavioural disturbances, which are often more distressing for carers than the cognitive problems. These include verbal and physical aggression,

paranoid delusions, hallucinations, sleep disturbances, depression, apathy, social withdrawal, wandering and pacing, repetitive actions, incontinence and inappropriate social behaviour.

1.3 Neuropathology

Three forms of pathology are recognised as diagnostic abnormalities in AD:

- Amyloid plaques
- Neurofibrillary deposition
- Specific nerve cell loss

The brain areas most severly affected are the association areas of the neocortex, the hippocampus, the amygdala and cholinergic neurones of the basal forebrain. This pattern of pathology accords with the typical AD deficits in memory, analytical thought, perception, and motivation.

1.31 Amyloid Plaques

These are extracellular lesions of which there are three forms; diffuse, neuritic and dense-core. All contain deposits of beta-amyloid (Aβ; a globular protein cleaved from AβPP). In healthy tissue, the major cleavage product is 40 amino acids long ($A\beta_{40}$), but some longer $A\beta_{42/43}$ is also produced. $A\beta_{42/43}$ seems to be the important isoform in plaque formation, since it is less soluble due to its additional N-terminal β-pleated sheet structure which increases its tendancy for fibril formation and aggregation (Xia et al 1997). Plaques form when $A\beta_{42}$ levels increase in conjunction with a high $A\beta_{42}/A\beta_{40}$ ratio, and *in vitro* studies have suggested that $A\beta_{40}$ hinders $A\beta_{42}$ deposition (Snyder 1994).

Neuritic plaques comprise a distinct Aβ core surrounded by dystrophic neurites and reactive astrocytes. Fibrillar $A\beta_{42/43}$ is the initial species to be deposited in neuritic plaques (Iwatsubo et al 1995), which is believed to seed the later deposition of $A\beta_{40}$ (Jarrett et al 1993). Other factors associated with plaques are microglia and proteins such as AβPP, α1-antichymotrypsin, apoE, apolipoprotein J, heparin-sulphate proteoglycan (HSPG), butyrylcholinesterase and non-amyloid

plaque component. Neuritic plaques are stained by congo red and show green bifringence when observed under polarized light.

Diffuse plaques also contain aggregated $A\beta_{42/43}$, but have far fewer fibrils and lack the distinct amyloid core. They are not associated with dystrophic neurites, are not stained by congo red and attract very few astrocytes or microglia. It has been proposed that diffuse plaques are precursors to neuritic plaques, possibly being converted by a butyrylcholinesterase-dependent mechanism, since butyrylcholinesterase is only associated with plaques with high levels of β-sheet amyloid (Guillozet et al 1997) and it induces Aβ aggregation *in vitro*. However, diffuse plaques are not restricted to areas of the brain that show degeneration in AD, for example, they are often found in the cerebellum. Also, they occur in the brains of aged, non-demented individuals, (although this may represent preclinical change). It has therefore been suggested that they are non-pathogenic and are either generated independently from neuritic plaques or are converted to neuritic plaque by factors that are restricted to limbic and association cortex areas. Alternatively, diffuse plaques are potentially pathogenic but not all brain areas are susceptible.

Dense-core or 'burnt-out' plaques are the final stage of plaque development. Associated neurites are degenerated and they no longer attract astrocytes. At this stage they are probably most effectively degraded by microglia.

There are also Aβ deposits in the cerebral vasculature, especially in vessels associated with the cerebral cortex. Vascular amyloid comprises mainly of $A\beta_{40}$, suggesting that the vasculature is not the source of amyloid deposited in the brain. The amount of vascular deposition is not correlated with the degree of dementia, and so it is unlikely that it contributes to AD-related deficits.

1.32 Neurofibrillary Deposition

Neurofibrillary deposits are intracellular and mainly comprise the tandem repeat region of tau. This microtubule binding protein undergoes various post-translational modifications, including phosphorylation, glycosylation and glycation, which have been implicated in AD pathology.

The affinity of tau for microtubules is regulated by its level of phosphorylation. In AD, tau is hyperphosphorylated (tau-p), which reduces its binding capacity and causes destabilization of microtubules. This may compromise neurone viability by impairing intracellular trafficking. Tau-p

forms non-soluble paired-helical filaments, that aggregate into neurofibrillary tangles (NFT). These build up in the cytoplasm, dislocating the nucleus and spreading into apical dendrites (but not axons) of pyramidal cells. They are associated with vimentin, actin, ubiquitin, tau, Aβ and neurofilament proteins, which form a fuzzy coat around the tau-p paired-helical filament core.

Glycation of tau is observed in AD brain but not in age-matched non-demented controls (Ko et al 1999b). Tau becomes an advanced glycation end-product (AGE); a protein heavily glycated by non-enzymatic formation of covalent bonds between the amino-groups of proteins and sugars. The bonds may be important for paired-helical filament formation; glycation can alter protein structure making proteins inactive and increasing their stability, which may explain the persistence of tangles. In addition, AGEs encourage formation of reactive oxygen species, which at low levels stimulate neuroprotective NFκB activity and cytokines (Yan et al 1995) and at higher levels can cause oxidative cell damage.

Tangles persist even when the cell is destroyed, leaving ghosts tangles that are eventually degraded by astrocytes. Ghost tangles are prevalent in the nucleus basalis of Meynert and hippocampus but are rare in the neocortex, even in the presence of intracellular NFTs. This suggests that they may only invade the neocortex in the later stages of the disease and are not the main cause of cell loss, or that they are more effectively cleared from the neocortex. Their distribution is specific to areas that show degeneration, such as the entorhinal cortex (LII and LIV), the subiculum, CA1, and prosubiculum. Other areas less affected include the accessory basal nucleus of the amygdala, the nucleus basalis of Meynert and the association neocortex, where they are mostly in LIII and LV.

Tangles are associated with other diseases such as Pick's, Down's syndrome (DS) and progressive supranuclear palsy, however they receive special interest in AD since they have a predictable distribution through various stages of the disease and their numbers correlate well with levels of dementia. This pattern was recognised by Braak & Braak (1991) who used it to categorise AD pathology into stages;

Transentorhinal Stages : Mild to severe deposition in the entorhinal cortex, targeting large stellate neurones of the pre-α layer.

Limbic Stages :	Pre-α strongly affected in the transentorhinal cortex. Some weak deposition in the CA1 and subiculum.
Isocortical Stages :	Ghost tangles in the transentorhinal and entorhinal cortices. Severe pathology in all isocortical association and limbic areas. Primary motor and sensory areas are spared.

Clinical changes relating to transentorhinal and limbic stages seem to be very subtle with obvious decline observable only once tau pathology extends beyond the limbic areas in the isocortical stage.

1.33 Specific Cell Loss

This predominantly affects large neurones in the association neocortex and limbic structures (Bundgaard et al 2001). Cell loss is co-localized with areas affected by tangles and to a large extent, neuritic plaques, with the level of cell loss correlating well with the severity of dementia (Gomez-Isla et al 1997).

There is increasing evidence for apoptotic mechanisms in AD neurodegeneration. DNA fragmentations has been identified by TUNEL labelling (Overmyer et al 2000) and brains of Alzheimer's disease subjects show upregulation of factors linked to apoptosis such as caspase 3 (Stadelmann et al 1999) Bcl-2 interacting mediator of cell death, Bcl-2 related ovarian death gene and p21 (Engidawork et al 2001). However, there is still controversy over whether necrotic cell death is also involved. Evidence of necrosis and lack of apoptosis reported in some studies may be artefactual since experimental conditions are manipulated to accelerate potential toxic effects and whilst a cytotoxic insult may cause apoptosis when delivered chronically at a low level, the same insult often results in necrosis when presented acutely and at a higher dose (Bonfoco et al 1995). This suggests that apoptotic mechanisms may be more relevant to the gradual, insidious nature of AD progression.

The following cell types are targeted in AD:

- Pyramidal neurones in the CA1 (forty per cent cell loss) and subiculum degenerate. CA3 neurones are largely spared.
- Large stellate neurones in the entorhinal cortex. This results in almost total destruction of LII and reduced cell density in LIII. These neurones give rise to the perforant pathway, which is the major source of cortical input into the hippocampus.
- Large multipolar neurones in LIV of the entorhinal cortex. These are the sole cortical output targets of the hippocampal formation. Surviving cells have a high tangle load, which suggests impaired function.
- Accessory basal nucleus cells in the amygdala, which project to the hippocampus.
- Large pyramidal cells of the neocortex association areas, especially the upper laminae.
- Cholinergic neurones of the nucleus basalis of Meynert (forty to seventy per cent cell loss) as well as the medial septum and vertical limb of the diagonal band of Broca. These form the main cholinergic projections to the neocortex and hippocampus and seem to be important for cognitive function. Their loss is demonstrated by the lack of cholinergic markers in the cortex and hippocampus.

The gross effects of cell loss are functional isolation of the hippocampus from the neocortex and other limbic areas and impaired cholinergic modulation of limbic and associational isocortex activity, disrupting pathways that are important for normal cognitive function.

1.34 Other Pathological Changes

AD subjects are affected by other non-specific pathologies. Some AD subjects have Lewy bodies without Parkinsonism, for which Lewy bodies are a typical pathological feature. These are found in smaller pyramidal neurones in the deep cortical layers (Wakabayashi et al 1995). There seems to be a correlation between Lewy body pathology and the incidence of hallucinations in AD subjects, especially in conjunction with poor eyesight (McShane et al 1995). However cases of Lewy body-variant AD are often considered to be a distinct form of dementia since the clinical traits are specific

enough to allow Lewy body involvement to be predicted antemortem (Liberini et al 1995). Also, there is evidence that the neurodegenerative process is different, for example inflammatory processes do not seem to feature in Lewy body variants of AD, which show much lower immunoreactivity for microglia than brains from non-Lewy body AD subjects (Rozemuller et al 2000). Lewy body subjects also lack tau immunoreactivity (Shepherd et al 2000).

In normal ageing, the apical dendrites of dentate gyrus granule cells and LII pyramidal cells of the parahippocampal gyrus are extended, presumably to compensate for mild cell loss, allowing maintenance of synaptic density. In AD subjects, this compensatory dendrite lengthening does not occur (Callahan et al 1998).

Hirano bodies, which are restricted to the CA1 and subiculum, are eosinophillic rods or spindle shaped bodies that contain actin and actin-associated proteins. Their function is unknown. Granulovascular change is seen in hippocampal pyramidal cells coincident with tangles (Ball 1978). They are clear, membrane-bound inclusions with a black granular core, which can distort neurone shape and displace the nucleus. They are immunoreactive for tau and tubulin filaments (Price et al 1986, Dickson et al 1993). These lesions are considered to be secondary AD pathology since they are found in many types of neurodegeneration, have a restricted distribution and in the case of hirano bodies may be evident in subjects as young as twenty years old.

1.4 Genetic basis

AD has been commonly understood to be a sporadic disease occurring in the elderly. This was termed senile dementia of the Alzheimer's type, to distinguish it from other forms of senile dementia such as Parkinson's disease or vascular dementia. However, it was recognized that some cases of AD occur at a much earlier age. Thus, cases in subjects under sixty years of age came to be termed pre-senile dementia of the Alzheimer's type, with evidence that it was distinct from that observed in elderly subjects (Pro et al 1980). It was also noted that some presenile cases are not sporadic, but are inherited in a fully penetrant, autosomal dominant manner. This familial Alzheimer's disease (FAD) tends to be

more aggressive than late-onset AD with subjects showing rapid cognitive decline and a shorter survival time (Swearer et al 1996).

To date, mutations on 3 genes have been connected with FAD. These code for the AβPP, presenilin 1 (PS1) and presenilin 2 (PS2). Mutations to PS1 are most common and may account for about fifty per cent of all FAD (Campion et al 1999) (although estimates are as low as 18% (Cruts et al 1998)). Late-onset FAD pedigrees exist but these are more difficult to identify. They are often masked by family members dying from other causes before AD is evident, and so a genetic susceptibility is not suspected. This may be especially relevant to PS2 mutations, which are not fully penetrant and seem to cause a pattern of clinical development more typical of sporadic Alzheimer's disease (SAD), being longer in duration and later in onset (Bird et al 1996). Conversely, it is possible that some cases appear to be familial but are actually due to a common environmental factor, or that since age is a risk factor for AD, familial longevity may increase the chances of SAD occuring in multiple family members and being mistaken for FAD.

Although FAD is only thought to account for about 0.5 to 1 per cent of AD cases (Rosenberg 1997), it is hoped that studying the effects of these mutations will aid understanding of the processes involved in the more prevalent sporadic forms. A major problem in the study of AD has been trying to establish cause and effect. The predictable nature of FAD transmission has allowed monitoring of preclinical family members known to carry the pathogenic mutation. This has led to identification of preclinical abnormalities in cerebrospinal fluid, blood composition and brain volume, which help to determine the order in which features of AD contribute to the disease and suggest possible treatments and diagnostic tools. For example magnetic resonance imaging can detect decreased hippocampal volume in FAD subjects up to 10 years before clinical symptoms develop.

SAD cases also seem to be influenced by genes. Although not sufficient or necessary for causing AD, these genes may predispose individuals to the disease, making its onset more likely in conjunction with other genetic or environmental risk factors. That genes are involved in AD concurs with the observation that about 10 per cent of AD subjects have at least one relative who has had the disease (Rosenberg 1997). The best understood risk factor associated with SAD is the ε4 allele of apoE. Mutations and dimorphisms in other genes have been suggested but these seem to have weaker effects and are less well studied.

1.41 The nature and roles of proteins involved in AD genetics

β-Amyloid precursor protein and β-amyloid

AβPP is an ubiquitously expressed glycosylated transmembrane protein that is especially prevalent in the brain (Kang et al 1987, Selkoe et al 1988, Shimokawa et al 1993). The full-length protein ($AβPP_{fl}$) is seven-hundred and seventy amino acids long ($AβPP_{770}$) with other isoforms arising from alternative mRNA splice variants. The most common isoform in the brain is $AβPP_{695}$, which is mainly generated in neurones (Tanaka et al 1988).

AβPP is processed by either α-secretase (Maruyama et al 1991), which is the main route in healthy cells, or β-secretase (figure 1.1). α-Secretase is located at the cell membrane, where it cleaves AβPP within the Aβ domain to release a secreted N-terminal fragment, sAβPPα and a C-terminal stub. The C-terminal stub is further cleaved by γ-secretase to release p3 (Haass et al 1993) and a rapidly degraded C-terminal fragment. Since α-secretase cleaves AβPP within the Aβ domain, this pathway is non-amyloidogenic (Golde et al 1992).

The β-secretase amyloidogenic pathway is also active in healthy cells (Shoji et al 1992). β-secretase is located in the endoplasmic reticulum and trans-golgi (Haass et al 1993). It cleaves AβPP at the N-terminal of the Aβ domain to release the secreted sAβPPβ fragment. The remaining C-100 stub is cleaved by γ-secretase to release Aβ (Golde et al 1992).

The identities of the secretases are as yet undetermined although there is growing evidence that PS1 may have γ-secretase activity (Li et al 2000a) and β-secretase may be the beta-amyloid converting enzyme (Cai et al 2001).

Different lengths of Aβ, varying from thirty-nine to forty-three amino acids, are produced depending on the exact cleavage site of γ-secretase. The more common forty amino acid variant is formed in the late golgi, whilst the longer $Aβ_{42/43}$ variants, ($Aβ_{42}$ being more prevalent,) are formed in the endoplasmic reticulum, suggesting that there are two types of γ-secretase with different subcellular localizations and AβPP cleavage sites (Citron et al 1996). These γ-secretases compete for the common substrate, C-100, such that if $Aβ_{40}$ secretion is inhibited, the levels of intracellular $Aβ_{42/43}$ increase (Skovronsky et al 2000b).

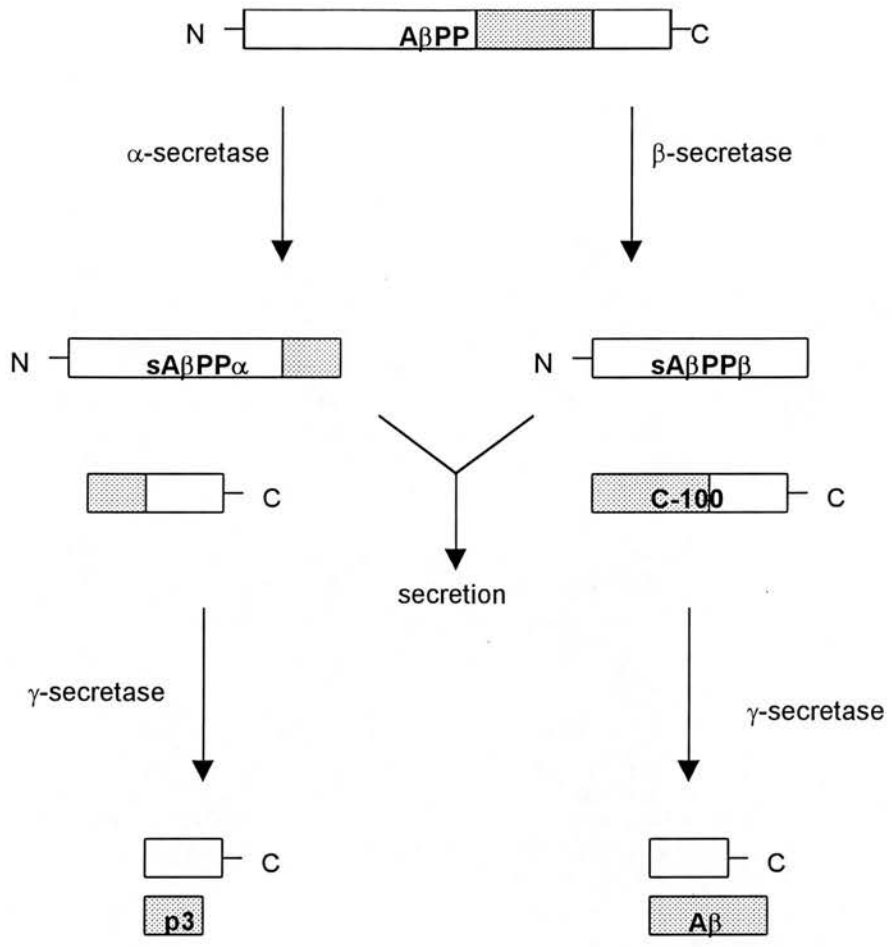

Figure 1.1 AβPP α-secretase and β-secretase processing pathways

The Aβ domain is highlighted.

AβPP is a *house-keeping* gene; an ubiquitously expressed gene that is important for non-specialized cellular processes. As such, it is highly conserved and abundant, comprising about 0.2 per cent of neuronal mRNA. Full length AβPP ($AβPP_{fl}$) and sAβPPα have recognized physiological roles in neurite outgrowth, synaptic plasticity and neuroprotection.

sAβPPα appears to protect neurones against excitotoxic insults and oxidative stress. Its expression is increased following neurone injury and cells pretreated with physiological concentrations of sAβPPα show reduced excitotoxicity in response to glutamate or Aβ. It reduces neurone excitability by activating the high conductance charybdoxin-sensitive Ca^{2+}-dependent K^+ channel, which carries a hyperpolarizating K^+ current. This may decrease the activity of voltage-gated

Ca^{2+} channels and NMDA receptor channels and so lower both basal and glutamate-induced increases in intracellular Ca^{2+} concentration. sAβPPα also decreases NMDA receptor activity by altering its phosphorylation state via a cGMP/PKG dependent pathway (Furukawa et al 1998). This does not affect kainate or AMPA receptor activity. sAβPPα release is stimulated by nerve growth factor, suggesting it has a role in neurotrophic activities.

sAβPPα levels are increased in the cerebrospinal fluid following *in vivo* induction of the putative physiological correlate of memory; long-term potentiation, and when infused into adult rat brains sAβPPα improves performance in learning and memory tasks. Rats reared in a stimulus enriched environment have more AβPP immunoreactive synapses and perform better in shock avoidance and water maze behavioural tests than rats from impoverished environments (Huber et al 1997). AβPP overexpressing mice show upregulation of growth associated protein 43 (GAP-43) and increased synapse density in the frontal cortex when examined using *in situ* immunohistochemistry (Mucke et al 1994). GAP-43 is important for neurite outgrowth in synaptic remodelling, and in healthy adult brain is expressed specifically in areas associated with AD; the association neocortex and hippocampus. However, its levels are reduced in the hippocampus and frontal cortex in AD brain which may contribute to cognitive impairment (Bogdanovic et al 2000, de la Monte et al 1995).

Membrane bound $AβPP_{fl}$ promotes neurite outgrowth and may contribute to synaptic plasticity. It binds proteoglycans (Buee et al 1993), which mediate cell-cell and cell-matrix adhesion and neurite extension and so may be involved in morphological changes and target finding during expression of synaptic plasticity.

The roles of β-secretase products; Aβ, sAβPPβ and C100, at normal physiologically levels of 10pM to 1nM are less well understood, however, micromolar doses of fibrillar Aβ trigger apoptosis-like cell death in neurone cultures (Loo et al 1993), and more recently, soluble oligomers and protofibrils of Aβ have shown neurotoxicity in culture (Lambert et al 1998, Hartley et al 1999). C100 is also neurotoxic (Yankner et al 1989). sAβPPβ activates cultured microglia to release potentially cytotoxic products such as reactive oxygen species and inflammatory cytokines. Although sAβPPα has similar activity, the detrimental effects seem to be compensated by its neurotrophic properties (Barger & Harmon 1997).

Presenilin 1 and 2

PS1 and 2 are ubiquitously expressed in the CNS but are especially prevalent in areas most susceptible to AD. Their distribution is similar to that of Aβ and is unchanged in AD. They are found exclusively in neurones (Kovacs et al 1996), specifically in the cell soma, with PS1 also spreading into some neurites. They are restricted to the early compartments of the protein secretory pathway, including the endoplasmic reticulum, intermediate compartment and the early cis-golgi compartment (Annaert & De Strooper 1999) although it has recently been suggested that small amounts may be found in the cell membrane (Takashima et al 1996). Their homology lies mostly within the 8 transmembrane domains and the large cytoplasmic loop, suggesting that these regions are particularly important for protein function.

The level of PS is strictly regulated, possibly by calsenilin (Buxbaum et al 1998), as demonstrated in TG mice designed to overexpress human PS1 (Thinakaran et al 1996, Thinakaran et al 1997). In these animals, although human PS1 is expressed, the level of total PS1 is little changed. PS is processed in the ER where the full length protein is rapidly cleaved within the cytoplasmic loop. The resulting C-terminal and N-terminal fragments remain closely associated to form a heterodimer.

PS has aspartate protease activity and can cleave proteins within transmembrane domains. It is involved in development, protein processing and apoptosis. Whilst the heterodimer is usually considered to be the active form, the full length protein must also be functional since it can reverse deficits in Caenorhabditis elegans caused by mutations in its PS homologue Sel-12.

The PS1 heterodimer is necessary for normal γ-secretase processing of AβPP (Xia et al 1998) and it is possible that PS1 is γ-secretase since it has the necessary property of being an aspartate protease with access to cleavage sites within the membrane (Wolfe et al 1999) and it is bound by γ-secretase inhibitors (Li et al 2000a). Neurones in PS1 null animals have reduced γ-secretase activity as indicated by the accumulation of P3- and Aβ-containing C-terminal stubs (De Strooper et al 1998). However, presenilin1 lacks sequence homology with know protease domains (Sherrington et al 1995) and there is residual amyloid secretion in PS1 null animals (De Strooper et al 1998). Also, there is increasing evidence for the existance of distinct γ-secretases that result in the different lengths of Aβ. However, PS1 mutations inhibited the production of both cleavage products to an equal extent (Murphey et al 2000). This would suggest that to be γ-secretase, then it must perform both Aβ42 and

Ab42 cleavage and have two distinct active sites for these roles. Given the lack of sequence homology with known proteases for even one domain, this is unlikely. However, it is clear that PS1 is important in promoting and regulating γ-secretase cleavage by an as yet unresolved mechanism. FAD mutations to PS1 result in elevated $A\beta_{42/43}$ production, which is a possible source of AD development in affected families.

A pro-apoptotic role is suggested for PS2. Cultured PC12 cells overexpressing human PS2 show increased vulnerability to apoptosis in response to Aβ exposure and withdrawl of neurotrophins. A similar response is seen in cells carrying normal levels of PS2 with an FAD-causing mutation (Deng et al 1996, Janicki et al 1997). In COS-7 cells overexpressing PS2, AβPP is abnormally processed by mechanisms suggesting apopotic, caspase-like activity and this response is heightened in cells expressing PS2 with FAD mutations (Weidermann et al 1999). Conversely, downregulation of PS2 is neuroprotective.

The interaction of PS1 with apoptotic pathways seems to be more complex. Upregulation of PS1 may cause either facilitation of (Czech et al 1998) or protection against (Bursztajn et al 1998) apoptosis whilst downregulation of PS1 has been shown to increase cell vulnerability (Roperch et al 1998).

PS1 may exert neuroprotection by interacting with the anti-apoptosis protein, β-catenin, in the endoplasmic reticulum. Free β-catenin is phosphorylated by glycogen synthase kinase-3β and tagged by ubiquitin for degredation. PS1 stabilizes β-catenin preventing its clearance and presumably promotes its anti-apoptotic activity. Cells expressing FAD PS1 are more sensitive to Aβ-induced apoptosis (Tanii et al 1999, Mattson et al 2000, Guo et al 1997). This may be explained by the failure of mutated PS1 to bind β-catenin, which is then depleted in association with an increased risk of apoptosis (Zhang et al 1998). However, another report in which PS1 was overexpressed in COS-7 cells suggests that PS1 binding inhibits β-catenin activity (Murayama et al 1998), although it did not show the effect of this binding on cell viability.

Where PS1 has been seen to facilitate apoptosis, identified mechanisms have included increased Ca^{2+} release from the endoplasmic reticulum (Guo et al 1997), free radical production (Guo et al 1999b), mitochondrial dysfunction (Guo et al 1998) and caspase activation (Kovacs et al 1999).

A role for PS1 in development was suggested by its homology with the Caenorhabditis elegans Notch signalling peptide, Sel-12. PS1 null animals have severe developmental defects, similar to those observed in Sel-12 null nematodes, which prevent offspring from surviving beyond a few days. However, this role does not seem to be disrupted in AD, since FAD mutations to PS in mice do not cause loss of function during development, and indeed mutated PS can rescue PS null animals as effectively as normal PS (Davis et al 1998).

Apolipoprotein E

ApoE is involved in plasma cholesterol and lipid homeostasis. In the cerebrospinal fluid, apoE is invariably associated with liposomes as a lipoprotein complex, which binds cell surface receptors such as the low density lipoprotein receptor, very low density lipoprotein receptor and the low density lipoprotein receptor-like receptor. Binding leads to internalization of the lipoprotein complex and its degradation by the lysosomal. Elevated apoE is associated with reduced plasma cholesterol (for review see Nimpf & Schneider 2000).

In the CNS, apoE is mainly produced by astrocytes (Boyles et al 1985) but it is also expressed at a lower level by selective neurones. In particular, apoE immunoreactive neurones are found in the frontal lobe of the cerebral cortex, CA1-4 hippocampal pyramidal cell populations and the granule cells of the dentate gyrus. ApoE is not produced in cerebellar neurones (Xu et al 1999). This pattern of neuronal apoE production mimics the distribution of AD pathology, suggesting that it may have a role in AD pathogenesis and confer regional specificity.

Additional roles for apoE relating to AD include modulation of AβPP processing and clearance (Vincent et al 2001), promotion of tau stability and microtubule formation (Benzing et al 1995, Wang et al 1998, Scott et al 1998) and synaptic remodelling (Arendt et al 1997).

1.42 AD-related gene mutations and allelic variants

β-Amyloid precursor protein

The first FAD mutation to be identified was on the AβPP gene. AβPP had been mapped to chromosome twenty-one in 1987 (Goldgaber et al 1987, Tanzi et al 1987, St George-Hyslop et al 1987). Meanwhile, it had been recognised that DS subjects invariably develop pathology indistinguishable from AD by thirty-five years (Jervis & Thiells 1948) and about seventy-five per cent

are diagnosed with AD by sixty years (Wisniewski et al 1985, Olson & Shaw 1969). Since DS is caused by trisomy of chromosome twenty-one it was possible that overexpression of a gene found on this chromosome could cause AD. The association of Aβ with amyloid plaques made AβPP a prime potential locus for FAD-inducing mutations.

In 1991, a missense mutation was identified at codon 717 of AβPP, replacing valine with isoleucine (V717I) (Goate et al 1991). This resulted in increased $A\beta_{42/43}$ levels in the CNS and onset of AD at about fifty years. Eight other unrelated families have subsequently been found to carry the same mutation. Ten other AβPP missense mutations have been found (Appendix II). They are all located at or near the Aβ domain and cause an increase in the level of $A\beta_{42/43}$. They all cause presenile onset at of Alzheimer's disease and an aggressive disease progression.

The most extensively studied AβPP mutation is the K670M/N671L Swedish double mutation on exon 16, close to the β-secretase site. Age of onset is between forty-four and sixty-one years (Axelman et al 1994). At autopsy, subjects show cortical atrophy, especially of the hippocampus, and dilated ventricles. There are high concentrations of NFTs and amyloid plaques mainly comprising $A\beta_{42/43}$ (Lannfelt et al 1994, Kalaria et al 1996).

Aβ levels in skin fibroblasts from living subjects are trebled (Ingelson et al 1996), suggesting that this tissue might replicate some of the pathogenic cellular processes of affected neurones making it a useful experimental tool. Human kidney 293 and neuroblastoma cells carrying the Swedish mutation produce 6 to 8 times more Aβ than those expressing wildtype AβPP (Citron et al 1992, Cai et al 1993) supporting amyloid upregulation as the source of AD changes.

Presenilin 1

It is often cited that about forty per cent of early-onset FAD cases are linked to PS1 mutations (Tanzi et al 1996) although some estimates are as low as 18 per cent (Cruts et al 1998). The involvement of chromosome 14 in FAD was recognised in 1992 (Schellenberg 1992) and the PS1 gene was identified in 1995 (Sherrington et al 1995) since when over seventy FAD-causing PS1 mutations have been described (Appendix III).

Mutations are found at many sites throughout the primary protein structure of PS1, but are particularly focused on the highly conserved transmembrane regions with a significant cluster along one face of an α-helix. These areas are all thought to be important for the function of the protein.

Although PS1 mutations are many and widespread, the resulting phenotypes are very similar. They lead to especially virulent AD with a mean age of onset of forty-five years and a rapid disease progression. In all cases, $A\beta_{42/43}$ is elevated without any change in $A\beta_{40}$, AβPPs or $A\beta PP_{fl}$ levels (Citron et al 1997). This implies that the α- and β-secretase pathways can be independently regulated. These observations have been made in both blood plasma and cultured skin fibroblasts from affected individuals. More importantly, $A\beta_{42/43}$ is elevated in cultured cells from healthy tissue when transfected with mutated PS1 and in transgenic mice carrying the mutated human gene (Citron 1997), showing that altered AβPP processing in the AD subjects can be attributed exclusively to the PS1 mutation.

PS1 mutations (M146V, L286V) predispose cells to apoptosis, including that induced by Aβ toxicity. Cell viability is restored by overexpression of the Ca^{2+} binding protein calbindin (Guo et al 1998), suggesting that impaired Ca^{2+} homeostasis is involved. Cells carrying the mutations A246E, ΔE10 and L286V express activated caspase 3 which is part of the classic apoptotic pathway (Kovacs et al 1999).

The mutation that will be studied in this thesis is the methionine to valine substitution at codon 146 (M146V). This mutation was linked to chromosome 14 in 1994 (Hardy 1994) and subsequently identified in 3 unrelated families (Clark et al 1995). Inheritance is autosomal dominant and the age of onset is especially low, commonly being between thirty-six and forty years and the mean disease duration is 6 years.

A typical case study describes a thirty-nine year old woman who presented with mild memory deficit. Medical examination revealed moderate deficits in other cognitive functions; spatial orientation, visual agnosia, constructional apraxias and agraphia in conjunction with cortical atrophy and ventricular dilation. The patient also had mild myoclonic jerking, which seems to be particular to M146V FAD. Her cognitive and physical problems worsened rapidly and she died 4 years after diagnosis in a bedridden state. Autopsy showed the expected pattern of amyloid plaques, NFTs and cell loss. Unusually, there was also mild vacuolar change, which suggested a form of prion disease but

this was discounted by the presence of AD pathology and a lack of altered prion protein (Hardy et al 1994).

Plasma and fibroblasts from M146V subjects showed a specific increase in $A\beta_{42/43}$ (Scheuner et al 1996). HK293 cells and transgenic mice expressing human $PS1_{M146V}$ both showed elevated levels of $A\beta_{42/43}$ when compared to controls carrying the wildtype human gene (Ancolio et al 1997, Duff et al 1996), and transfected cells also show increased sensitivity to $A\beta_{42/43}$ toxicity.

Presenilin 2

Six FAD-causing mutations have been described in the PS2 gene on chromosome 1 (Appendix IV). The time course of the disease resembles SAD, showing a later age of onset and longer disease duration than FAD attributed to PS1 and AβPP. The timing is also less predictable suggesting that environmental factors are significant modifiers of disease expression (Sherrington et al 1996).

One pedigree is the Volga-German line N141I found in 8 families with a common ancestor. The mean age of onset is fifty-five years and the duration is eleven years (Iwatsubo et al, 1998). A second mutation, in an Italian family (M239V) has a mean onset of over sixty years and lasts up to twenty years although commonly the duration is much shorter. $A\beta_{42/43}$ levels are elevated but as in SAD the total Aβ level is unchanged. Cells transfected with N141I produce 5 times more $A\beta_{42/43}$ (Citron et al 1997) and show increased susceptibility to apoptosis (Janicki & Monteiro 1997).

Apolipoprotein E

Apoε was identified as the SAD-linked chromosome 19 gene in 1993 (Strittmatter et al 1993), which marked a significant discovery towards understanding the nature of the most prevalent cases of AD. The three allelic variants of apoε differ at two loci (table 1.1).

Table 1.1 Allelic variants of apoE

Allele	Locus 112	Locus 158
ε2	cys	cys
ε3	cys	arg
ε4	arg	arg

Amongst AD cases, the ε4 allele occurs at a higher than expected frequency. The risk conferred by ε4 is dose dependent with homozygotes being the most likely to develop AD. ε4 promotes early disease onset, rapidly deteriorating neurone function and Aβ over-production. It also seems to increase the chance of developing AD in conjunction with other risk factors, for example, Aβ deposition in response to traumatic head injury is more severe in ε4 carriers (Nicholl et al 1995). Conversely, AD subjects carrying the ε2 allele occur at a frequency lower than would be expected suggesting that this allele is protective.

The apoε genotype also interacts with FAD mutations in AβPP. In the AβPP V717F and K670M/N671L pedigrees, apoε4 carriers have a significantly earlier age of AD onset (Noguchi et al 1993). It does not seem to interact with PS mutations (Houlden et al 1998). A polymorphism in the apoε promoter also affects AD susceptibility. There is a higher prevalence of alanine homozygotes at the -491 A/T locus in AD cases regardless of the apoε genotype (Wang et al 2000).

The apoE protein may influence AβPP processing, clearance of extracellular AβPP and Aβ and plaque formation. Carriers of the ε4 allele have lower apoE levels, which leads to impaired lipid and cholesterol catabolism and elevated levels of total cholesterol and triglycerides (Tiret et al 1994, Luc et al 1994). This may explain the perceived link between AD and cardiovascular disease. Inhibiting cholesterol production in cultured cells by seventy per cent impairs Aβ production without affecting the level of AβPP (Simons et al 1998). Therefore, elevated cholesterol levels in ε4 subjects may increase Aβ production.

ApoE binds AβPP, which allows it to be internalized for degradation by the low density lipoprotein receptor-like receptor. However, in AD, apoE associated with senile plaques may impair Aβ clearance and contribute to plaque development (Namba et al 1991). ApoE4 binds Aβ with higher affinity than E3 or E2 and promotes Aβ aggregation and fibrillogenesis (Wisniewski et al 1994). One study reported that apoE4 reduces Aβ polymerization and toxicity in culture (Evans et al 1995), however they used free apoE, which may act differently to apoE in its usual lipoprotein complex.

Aβ (and especially $A\beta_{42/43,}$) promotes apoE binding to hippocampal neurones in culture, which leads to internalization of the Aβ/apoE complex. This suggests a putative pathway for plaque formation whereby $A\beta_{42/43}$ is preferentially internalized by neurones, generating intracellular concentrations that promote aggregation. This Aβ aggregate is released when the neurone dies and seeds plaque formation. This process would be accelerated in apoε4 carriers since apoE4 is much more readily bound and internalized by neurones in response to Aβ.

ApoE binds tau to promote microtubule formation and stability. The E2 and E3 isoforms have the highest affinity for tau, suggesting that microtubule stabilization may be impaired in ε4 carriers. *In vitro*, apoE prevents tau hyperphosphorylation and tangle formation (Flaherty et al 1999) and ε4 carriers exhibit elevated cerebrospinal fluid tau levels (Kanai et al 1999), which in AD cases correlate with disease duration and level of cognitive deficit.

ApoE4 may potentiate pro-inflammatory mechanisms in AD, since cultured microglia are activated by sera from apoε4 AD subjects, but not by sera from other AD patients or healthy apoε4 subjects (Lombardi et al 1998). Also, apoE3 hinders microglial activation by sAβPP, whilst apoE4 is far less effective (Barger & Harmon 1997).

ApoE is expressed in response to injury (Snipes et al 1986) may have a role in synaptic plasticity (Krugers et al 1997, Arendt et al 1997). ApoE3 enhances neurite outgrowth in cultured dorsal root ganglion neurones, whilst apoE4 reduces outgrowth (Nathan et al 1994) which may indicate impaired reinnervation and formation of new synaptic connections following cell loss *in vivo*. This could explain the early age of AD-onset in ε4 carriers who could have impaired compensatory mechanisms for preclinical cell loss, and may also explain the lack of age-associated neurite extention in AD neurones (Callahan et al 1998).

1.5 Predisposition and protection for Alzheimer's disease

1.51 Risk Factors

The commonly accepted risk factors for AD are old age and family history. Many other risk factors have been proposed but most are poorly substantiated, or have been refuted by subsequent studies. In 1991, the importance of some major potential risk factors was reassessed by collating data from numerous studies, on the premise that the subject groups in many individual studies were too small to give the statistical power required to provide conclusive results (Graves et al 1991). Large subject groups are especially important in these studies since individual cases will only be associated with a subset of the proposed risk factors.

Age is the most obvious risk. AD is rare in subjects below sixty-five years old, but prevalence increases over the following decades reaching upto fifty per cent in the over eighty-five age group. Maternal age also seems to be important since a dispropotionate number of AD subjects are born to mothers over forty years old (Rocca et al 1991) although another study failed to find a significant correlation (Dewey et al 1988).

Genetic predisposition for AD is suggested by the high frequency of dementing illness (including Parkinson's disease) in first degree relatives of SAD subjects (van Duijn et al 1991). AD also seems to be preferentially transmitted down the maternal line, which suggests genetic susceptibility factors on the X-chromosome or in mitochondrial DNA. In the rare FAD cases, mutations cause autosomal dominant transmission of AD with close to full penetrance.

DS and diabetes are also linked with AD. DS subjects commonly develop pathology indistinguishable from AD by around thirty years of age and show clinical signs of AD by about forty years (Jervis & Thiells 1948, Wisniewski et al 1985). A weaker link is made with adult-onset diabetes on the basis of traits shared with AD such as amyloid deposition, impaired glucose metabolism, AGE formation, energy depletion and oxidative stress (Ott et al 1996, Leibson et al 1997). Amyloid deposits in diabetes are formed from amylin, which has little sequence homology with Aβ but does form β-enriched fibrils. Amylin activates microglia with interleukin-β and tumour necrosis factor α release kinetics identical to fibrillar Aβ. (Yates et al 2000). Presumably, deficits in diabetes are potentially capable of activating AD-causing pathways.

Between 1.5 and 3 times more women have AD as men, and this cannot be explained by the higher life-expectancy of women. This gender bias may be related to reduced oestrogen levels in post-menopausal women (Fratiglioni et al 1997).

However, studies of monozygotic twins with discordant incidence of AD or varied age of onset demonstrate the importance of environmental influences in SAD. This is supported by a study of communities of African origin in the USA, who had a higher incidence of AD than people living in Africa (Hendrie et al 1995). Also, there is a higher incidence of AD in urban compared to rural populations (Prince et al 1994).

Clinical depression has been sited as a cause, especially in cases where it occurs more than 10 years before diagnosis of AD and so is not merely an early symptom of dementia (Jorm et al 1991).

Traumatic head injury, defined as an incident causing loss of consciousness, induces elevation of the plaque-associated $A\beta_{42/43}$ in the cerebrospinal fluid within a week of the impact. Boxers often develop dementia pugilistica, which although distinct from AD, does involve NFT formation, Aβ deposition and loss of cholinergic function. That traumatic head injury does not consistently lead to AD in later life may be due to variability in the site of Aβ deposition depending on the site of impact and the observation that Aβ deposition following head injury is usually reversed (Mortimer et al 1991, Raby et al 1998)

Exposure to aluminium as a cause for AD became a popular theory when tangles were observed in the brains of animals that had received aluminium injections. However, these tangles were later found to comprise normal, and not hyperphosphorylated tau and much of the supporting research has since been discredited. AD subjects do not have elevated plasma aluminium and high exposure to the metal either through working environment or frequent use of antacids is not a risk factor (Munoz 1998). Other metals such as copper, zinc and iron may have a role in AD, but it has been recognised that endogenous levels of metal ions are high enough to be neurotoxic and possible pathogenic roles are likely to involve impaired regulation of metal ion storage and transport rather than exposure to exogenous sources.

Physical underactivity is particularly connected to early onset AD and this may link with hypothyroidism being a risk factor (Breteler et al 1991).

1.52 Protective Factors

There has been an equal interest in identifying environmental factors that might protect against AD. It was noticed that the incidence of AD is lower amongst arthritis sufferers (McGeer et al 1996). Anti-inflammatories used to treat arthritis have been cited as the probable reason for this and several antiinflammatory drugs are currently being trialled as treatments for AD.

Low oestrogen levels following the female menopause are a risk factor and AD prevalence is reduced in post-menopausal women on hormone replacement therapy (Kawas et al 1998). Oestrogen has many potentially neuroprotective activities such as increasing cerebral blood flow, augmenting glucose use, promoting neurite outgrowth and synapse formation and as an antioxidant. Oestrogen replacement improves cognitive performance in healthy post-menopausal women (Henderson 1997) and some female AD subjects.

Use of the antioxidants, vitamins E and C, to treat AD subjects reflects the importance of oxidative processes in the disease (Morris et al 1998). Vitamin E seems to have some efficacy, particularly in alleviating behavioural symptoms.

The protective effects of smoking in AD are controversial. Whilst demonstrated in some studies (Graves et al 1991), and supported by improved cognitive performance in demented subjects treated with nicotine patches, many studies have found smoking to either have no influence or to potentiate the risk for AD (Launer et al 1999, Merchant 1999).

Folic acid is depressed in the plasma of AD subjects (Clarke et al 1998), and folic acid deficits are linked to impaired performance on cognitive tests (Riggs et al 1996), suggesting a potential line of investigation.

Higher levels of education have been proposed as a protective factor. The observed link between AD and education may be due to increased synapse density or elevated expression of neuroprotective factors; however, this is speculative. Suggestions that the correlation may be due to subjects with poorer education coming from a lower social strata are refuted by a study of an Italian population with low education but good socio-economic status. They confirmed a link between AD and lack of education, regardless of social status, particularly amongst subjects in their sixties (De Ronchi et al 1998).

There is a low incidence of severe headaches and migraines in AD subjects (Dewey et al 1988, Heyman et al 1984). During a phase of severe headaches, cerebral blood flow is increased suggesting a possible protective mechanism.

1.6 Alzheimer's disease pathogenesis

Elucidating the mechanisms of AD pathogenesis is complicated by the heterogeneity of the possible causative and risk factors and the diversity of clinical symptoms. The variety of characteristic abnormalities in AD brain have inspired different theories of disease progression, emphasizing in turn the potential roles of abnormal proteins, genetic mutations and polymorphisms, inflammatory processes, oxidising agents, metal ions, neurotransmitter deficits and metabolic defects, all of which are likely to contribute to some extent.

A full theory of AD should explain how the different risk factors feed into a common pathway resulting in the observed complement of pathologies and clinical symptoms. It must also explain why only certain brain areas are targeted to generate the specific cognitive deficits characteristic of this disease, and why it is predominantly a disease of ageing.

The current prevailing theory of AD pathogenesis is the amyloid cascade hypothesis. According to this view, pathogenic changes in the processing and accumulation of Aβ comprise the common pathway into which risk and causative factors feed and from which the full range of pathology develops. In particular, the non-soluble, fibrillar form of Aβ associated with plaques is seen as the primary pathogenic species.

There is strong evidence that Aβ plays a central role in disease progression. This was initially suggested by the invariable appearance of fibrillar Aβ in AD brains, forming amyloid plaques and vascular deposits. The occurance of AD in DS subjects supports a role for Aβ since this condition leads to AβPP over-production. FAD mutations on the AβPP and PS genes all cause an increase in either total Aβ or the $A\beta_{42/43}/A\beta_{40}$ ratio. Fibrillar Aβ can induce neurotoxicity *in vitro* (Yankner et al 1989, Pike et al 1993) and this has been attributed to its additional β-sheet structure, the significance of which is consolidated by the link between other β-sheet enriched proteins and neurodegenerative diseases such as prion protein in transmissible spongiform encephalopathies, huntingtin protein in

Huntington's disease and α-synuclein in Parkinson's disease.

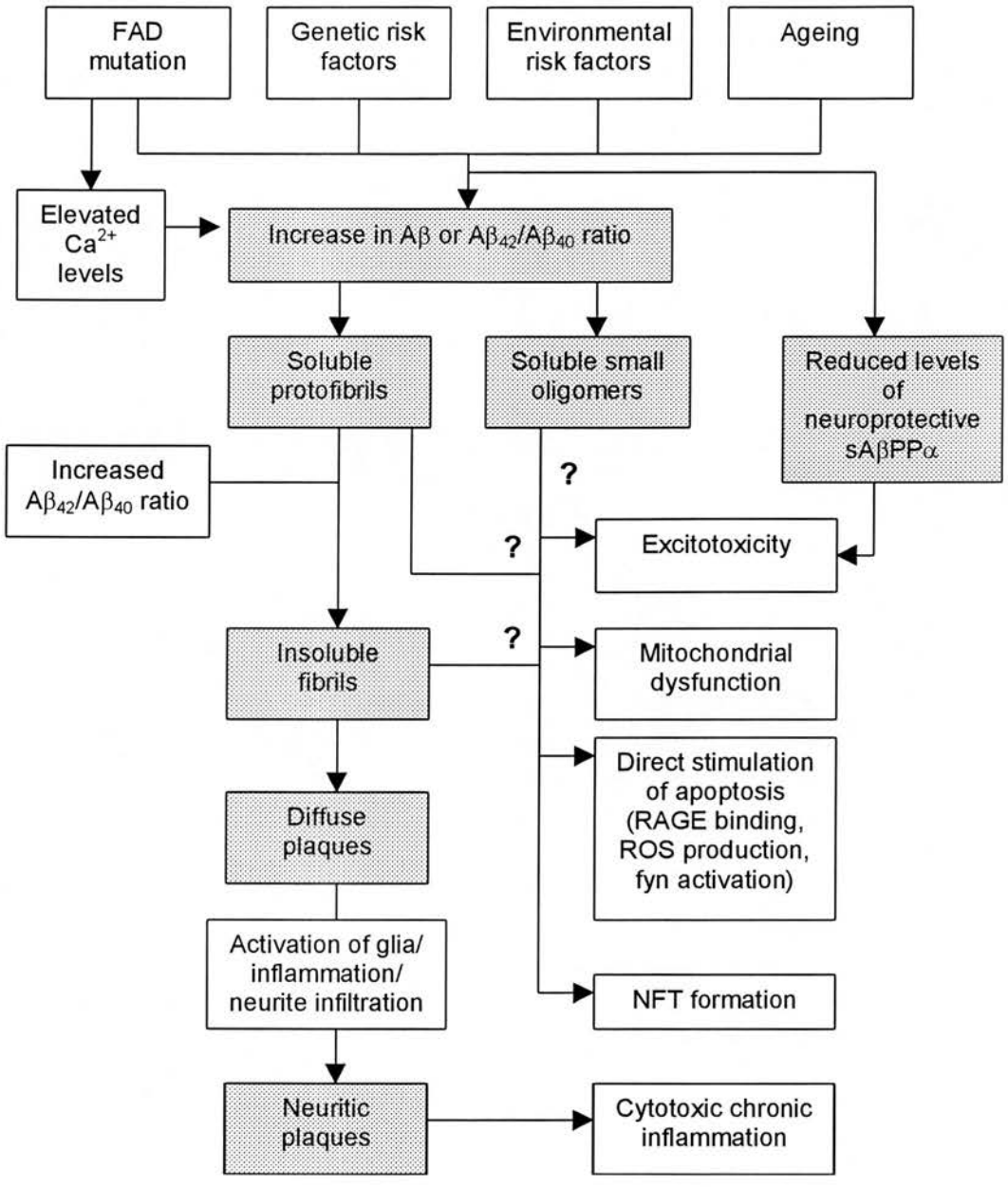

Figure 1.61 Amyloid toxicity in Alzheimer's disease

The pathways showing development of Aβ toxic species and plaques are highlighted. ? indicates insufficient evidence to attribute various types of pathology with specific states of Aβ aggregation.

PS mutations cause disruption of Ca^{2+} homeostasis. Cultured cells expressing mutated PS1 have an elevated Ca^{2+} response to depolarization and the source of this Ca^{2+} is the endoplasmic reticulum (Guo et al 1997), where PS1 is localized. Altered Ca^{2+} regulation in the ER could disrupt normal gene expression and protein processing and elevated Ca^{2+} promotes Aβ production (Querforth & Selkoe 1994).The major arguments against a central role for fibrillar Aβ are the poor correlation between neuritic plaque density and the severity of dementia cited by many studies (Gomez-Isla et al 1997, Bierer et al 1995), which has been explained by microglial clearance of plaques; and the transgenic mouse models of FAD that show amyloid deposition in the absence of neurodegeneration. This has been explained by species differences in sensitivity to human Aβ fibrils, which induce neurodegeneration, microglial activation and tau phosphorylation when injected into aged primates but do not generate pathology in rats when injected in plaque-equivalent doses (Geula et al 1998b). A further suggestion is that the transgenic animals were not allowed to age sufficiently since Aβ is toxic when injected into the brain of aged but not young adult primates (Geula et al 1998b). These explanations have however not yet satisfied critics of the amyloid hypothesis.

Recently, a more convincing explanation of these discrepancies has emerged that continues to support Aβ toxicity but questions the amyloid hypothesis assumption that it is only highly aggregated fibrils of Aβ that are toxic (figure 1.61). Whilst soluble Aβ monomers are benign, small oligomers (usually comprising 3-6 Aβ units) and protofibrils (precursors to fibrils) are toxic (Lambert et al 1998, Hartley et al 1999). Both are more readily formed by the β-sheet enriched $Aβ_{42/43}$, but whilst protofibrils tend to evolve into fibrillar deposits, the small oligomers are quite stable.

Levels of soluble Aβ are elevated in AD (McLean et al 1999) and correlate well with synapse loss (Lue et al 1999). This implies a correlation with dementia levels, which are linked to the degree of cell loss. Similar observations have been made in transgenic mouse FAD models (Mucke et al 2000). Soluble Aβ toxicity may also explain cell loss in the absence of plaque formation reported in some FAD mouse models (Chui et al 1999, Mucke et al 2000). Elevated levels of soluble Aβ are not seen in brain from non-demented subjects with AD-equivalent plaque density, suggesting that plaque Aβ is less pathogenic. Deposited amyloid in the form of diffuse plaques may even be neuroprotective by depleting reservoirs of soluble Aβ. This is not to ignore a possible pathogenic role for plaque-

associated fibrillar Aβ but suggests that it may be unavailable to damage neurones directly.

A second distinguishing feature of non-demented subjects with high levels of AD-like pathology is the lack of inflammatory markers, which are a significant feature of AD brain. The AD brain may provide conditions that allow fibrillar Aβ to exert indirect toxicity by activating microglia and astrocytes, leading to neuritic plaque formation and chronic, cytotoxic inflammation.

Since many papers do not indicate the state of Aβ used in toxicity studies, or use 'aged' fibrillar Aβ without ruling out the possible presence of protofibrils and oligomers, it is not possible to predict which forms contribute to the various modes of toxicity, although the evidence cited above does suggest that soluble Aβ aggregates may be the predominant species, especially regarding direct toxicity. These ambiguities should be considered in the following sections where results are often cited as being specific to fibrillar Aβ, which in fact may not be the case.

Aβ can exert direct toxicity by activating *fyn* tyrosine kinase (Lambert et al 1998), which induces apoptosis by increasing the rectifying potassium channel current I_k (Yu et al 1998) (although excitotoxicity has also been recorded due to Aβ-induced inactivation of I_k (Good et al 1996)), free-radical generation, calcium influx via L-type voltage sensitive channels, and PKA-mediated impairment of mitochondrial activity (Ueda et al 1994). Aβ facilitates glutamate excitotoxicity (Koh et al 1990) by impairing glutamate uptake by astrocytes both directly and by reducing glucose uptake, which creates a deficit of ATP and so impairs glutamate sequestration (Parpura-Gill et al 1997).

As well as increasing levels of toxic Aβ, altered AβPP processing in AD decreases levels of the neuroprotective sAβPPα (Sennvik et al 2000). sAβPPα is upregulated in healthy neurones in response to metabotropic glutamate receptor activation (Stephenson & Clemens 1998) and confers protection against excitotoxicity. It acts through the membrane-associated cGMP to dephosphorylate charybdotoxin-sensitive K^+ channels and NMDA receptor channels. This selectively suppresses NMDA currents, attenuating Ca^{2+} influx in response to high levels of presynaptic activity, and activating charybdotoxin-sensitive K^+ channels in a Ca^{2+}-independent manner (Furukawa et al 1996, Barger et al 1995), which carry a hyperpolarizing current, reducing neurone excitability.

1.61 Neurofibrillary tangles

The potential for NFTs to play a pathogenic role in AD was largely overlooked as the amyloid hypothesis gained increasing support and abnormal amyloid protein became the focus of research. NFTs were seen as a largely irrelevant by-product of the disease process. Interest in NFTs was rekindled by the discovery of tau gene mutations that are responsible for the heritable fronto-temporal dementias with parkinsonism (FTDP-17). Patients with FTDP-17 show similar clinical presentation to AD, although behavioural deficits are more prevalent. Brains from FTDP-17 subjects contain hyperphosphorylated tau which either forms paired helical filaments as in AD or ribbons depending on the mutation. These cases demonstrate that tau dysfunction can cause neurodegeneration and dementia in the absense of aberrant Aβ.

Fibrillar Aβcan induce hyperphosphorylation of tau *in vitro*, in the absence of amyloid deposition (Busciglio et al 1995). This may explain how Aβ can induce NFT formation before plaques develop. Aβ causes tau hyperphosphorylation by activating tau protein kinase I (TPKI). TPKI is upregulated in AD brain and in hippocampal cells incubated with Aβ, and blockers of TPKI reduce Aβ toxicity (Takashima et al 1993). Tau-p has reduced capacity for binding microtubules, which leads to microtubule destabilization. This impairs intracellular trafficking and maintenance of neuronal polarity. Dephosphorylation of tau restores microtubule binding function (Busciglio et al 1995). Tau is usually localized in distal axons, but fibrillar Aβ treatment results in tau-p accumulation in the somatodendritic compartment, possibly due to impaired axonal transport (Busciglio et al 1995).

Tau is not the only microtubule associated protein in cells and it has been questioned why others fail to compensate for the loss of tau function. The primary candidates for assuming the role of tau are MAP-1 and MAP-2. MAP-2 has a tandem repeat sequence similar to tau that could possibly also be hyperphosphorylated, reducing its binding efficiency (Zhang et al 1996). Also, tau-p directly prevents MAP-1 and MAP-2 from compensating for loss of tau function by binding to them in competition with microtubules (Alonso et al 1997). MAP-2 is phosphorylated by a nitric oxide synthase-dependent pathway in response to NMDA receptor activity (Llansola et al 2001) and so may contribute to synaptic plasticity by inducing microtubule destabilisation to allow remodelling of the synapse. Loss of MAP activity would therefore be expected to destabilise existing synapses and prevent the establishment of new synaptices in response to induction stimuli for synaptic plasticity.

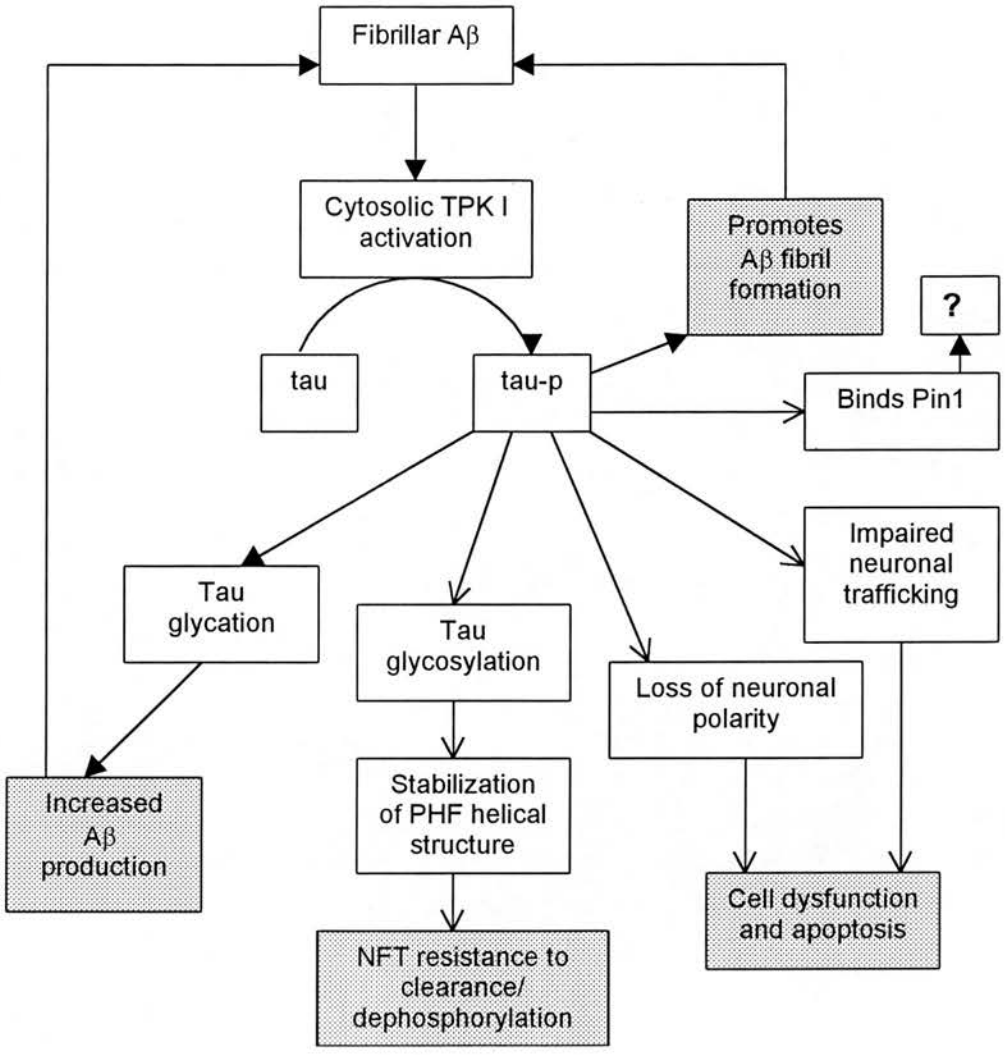

Figure 1.62 Pathogenic actions of hyperphosphorylated tau.

⟶ *indicate possible positive feedback into the pathogenic Aβ pathway. Major consequences of tau hyperphosphorylation are highlighted.*

Tau-p is both glycated and glycosylated. Glycated tau is capable of causing oxidative stress which results in cytokine activation and Aβ release (Takashima et al 1993, Yan et al 1995). Glycosylation of tau-p seems to stabilize the helical structure of paired helical filaments (Wang et al 1996a) and promote hyperphosphorylation. Deglycosylation leads to the formation of tau ribbons as

seen in FTDP-17 brain, and facilitates release of normal tau upon treatment with phosphatases (Wang et al 1996a).

Tau is also involved in the cell cycle. It binds the mitosis regulating protein prolyl isomerase (Pin1) (Lu et al 1999a), and is upregulated during mitosis in neuronal cultures (Nelson et al 1996). Although most neurones are post-mitotic, other cell cycle proteins are detected in AD, the purpose or consequences of which are unclear. Pin1 restores the microtubule binding activity of tau-p. It has been suggested that high levels of tau-p in AD brain may sequester Pin1 depleting soluble reserves and that this might have adverse consequences for cell viability (Lu et al 1999a).

Tau-p may promote fibril formation since paired helical filaments extracted from human AD subjects causes Aβ deposition when injected into the cerebral cortex and hippocampus of rats (Shin et al 1993). Injection of the phosphatase inhibitor, okadaic acid, into rat brain causes tau phosphorylation, amyloid plaque formation and memory impairment (Arendt et al 1995).

1.62 Inflammation

Interest in a possible role for inflammatory mechanisms in AD, long neglected due to the view that the brain holds an immuno-privileged status, came with the recognition that long-term users of anti-inflammatory drugs have a lower risk of developing AD (McGeer et al 1996). Inflammation is confined to areas affected by AD and is localized around plaques and NFTs (Oka et al 1998). Aβ is capable of triggering inflammatory responses (Bournemann et al 2001). Also, several polymorphisms are now being identified in genes for proteins involved in inflammation that co-segregate with cases of late-onset AD (Collins et al 2000).

Inflammation in the CNS is mediated by microglia and astrocytes that are attracted to sites of tissue damage or foreign material where they act to both remove abnormal material and protect healthy tissue. Activated glia become phagocytic and release inflammatory proteins, including cytokines, chemokines, complement and acute phase proteins, that interact in complex cascades. In normal circumstances, the upregulation of inflammatory proteins is transient and beneficial (for reviews see Eddelston and Mucke 1993, Zielasek & Hartung 1996). In AD these pathways become chronically activated so may become neurotoxic (Marty et al 1991). The inflammatory mechanisms in the CNS are poorly understood and the protective and pathological actions of individual inflammatory

proteins in AD remain ambiguous. However, this section will highlight some of the mechanisms that possibly contribute to AD pathology (figure 1.63).

Glia and plaque development

Inflammation occurs early in the disease process and may be important for transforming diffuse Aβ deposits into neuritic plaques. Inflammation could be crucial for initiating neurotoxicity, since brains from non-demented subjects with AD-like levels of diffuse plaques and NFTs have far fewer inflammatory markers than AD brains and have no neuritic plaques or cell loss (Lue et al 1996).

Aβ acts as a chemotactic signal, triggering the initial migration of microglia and astrocytes to sites of Aβ aggregation. Microglia phagocytose plaques and generate proteolytic enzymes to degrade Aβ fibrils, however, microglia may be disabled by plaque toxins (Korotzer et al 1993). Astrocytes gather around the periphery of plaques and shield surrounding tissue from plaque-associated toxins. However, they also impede clearance of amyloid by microglia, which allows plaques to persist and induce chronic inflammation (DeWitt et al 1998).

Aβ activates microglia, possibly by binding the receptor for advanced glycation end-products (RAGE) or scavenger receptors, both of which are upregulated in microglia from AD brain, and this is enhanced by numerous cytokines (Meda et al 1995). sAβPPβ also induces microglia activation and cytotoxicity in culture, which can be blocked by pre-incubating microglia with apoE3. ApoE4 is ineffective (Barger & Harmon 1997). Microglia are fully activated in AD, showing MHCII immunoreactivity. Astrocytes are reactive rather than fully activated, showing elevated GFAP but no MHCII expression. They are stimulated by cytokines released from activated microglia (Akama & van Eldic 2000).

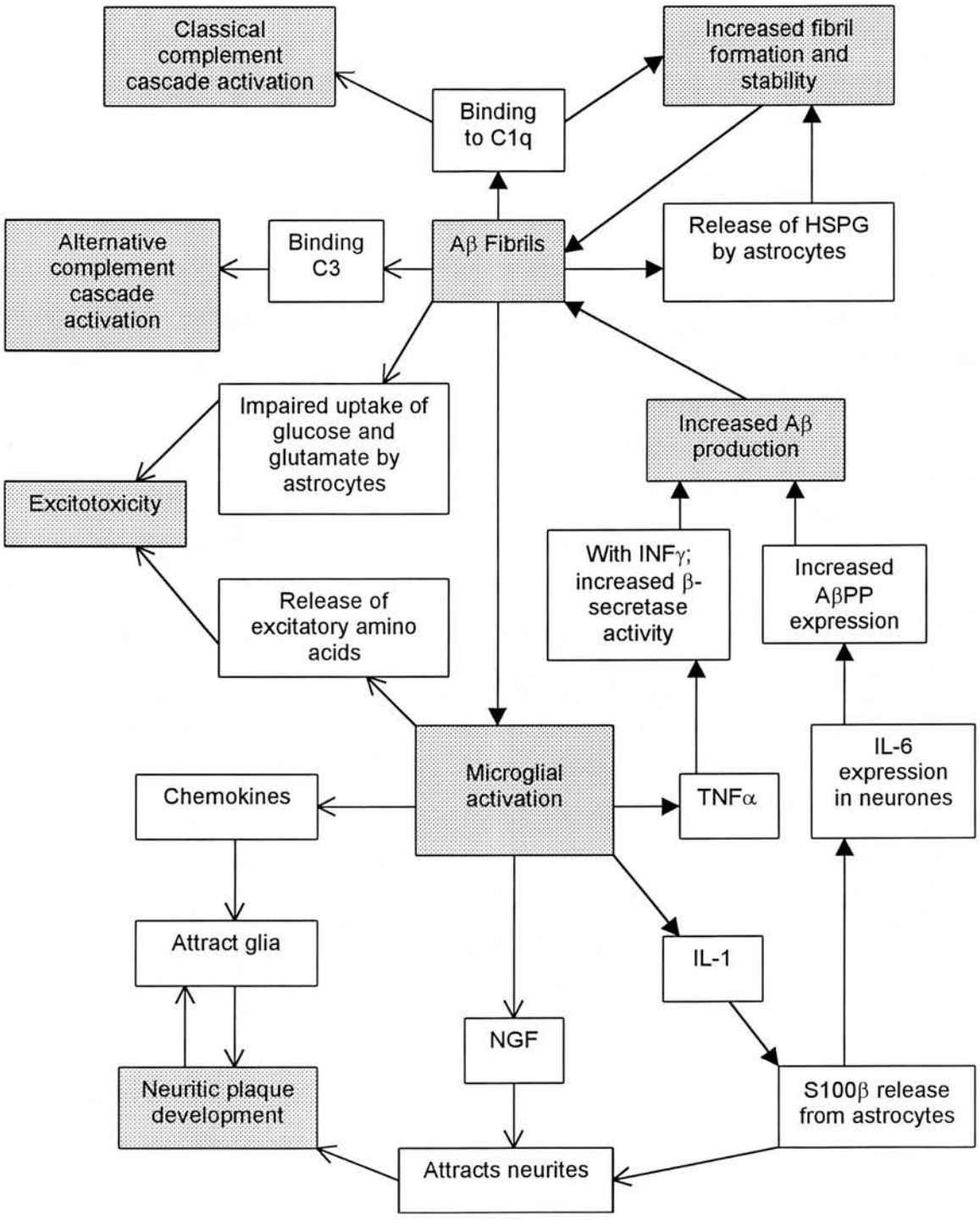

Figure 1.63 Immune responses to Aβ fibrils

→ *Indicate possible positive feedback into the pathogenic Aβ pathway. Major consequences of inflammation are highlighted.*

Glia contribute to plaque development by producing AβPP, promoting Aβ fibrillogenesis, attracting neurites and improving plaque stability. Although neurones are the major source of Aβ, elevated levels of the cytokine TGF-β in AD (Gray & Patel 1993) may promote astrocyte expression of AβPP. Astrocytes release HSPGs, which promote β-secretase processing of AβPP (Leveugle et al 1997) and formation of Aβ fibrils (McLaurin et al 1999) as well as protecting Aβ aggregates from degradation (Verbeek et al 1999). Microglia release nerve growth factor in response to $A\beta_{25-35}$, the complement protein C3a and the synergistic actions of cytokines IL-1β and TNFα (Heese et al 1988), which could attract neurites to areas of Aβ accumulation where they are exposed to neurotoxins.

Cytokines and Chemokines

All cytokines and chemokines so far investigated are centrally generated (Licastro et al 2000) and are elevated in brain areas showing AD pathology (Luterman et al 2000). A variety of cytokines and chemokines are released from cultured microglia in response to Aβ, including MCP-1 and TNFα, IL-6, IL-1α and IL-1β (Szczepanik et al 2001).

In the periphery, chemokines provide chemotactic signals for leucocytes, and in the CNS of AD subjects they may promote migration of microglia and astrocytes towards plaques, degenerating neurones and NFTs. The chemokine MCP1 induces peripheral monocyte migration across the blood-brain barrier and can also stimulate cytokine activity and superoxide radical formation.

The inflammatory cytokines best studied in AD are IL-1, IL-6, TGFβ, TNFα and S100β. IL1 immunoreactive microglia are present during the early stages of plaque formation and IL-1 levels increase as dystrophic neurites become associated with the plaque. IL-1 triggers S100β release from astrocytes.

S100β promotes dendritic outgrowth and may attract neurites to the site of Aβ accumulation, leading to the formation of neuritic plaques. Indeed there is a strong correlation between S100β levels and the number of plaque-associated dystrophic neurites. An early role for S100β in plaque development is supported by the $A\beta PP_{V717F}$ mouse model of AD (Sheng et al, 2000). In this model, activation of cytokine S100β preceded Aβ deposition. This suggests that accumulation of soluble Aβ oligomers in the early (pre-clinical) stages of AD could attract microglia and activate expression of

IL-1. S100β release from astrocytes would attract neurites to form neuritic plaques, which degenerate in the absence of neuronal targets and presence of inflammatory cytotoxins.

S100β upregulates neuronal expression of IL-6 (Li et al 2000b). Elevated IL-6 levels may promote cognitive impairment since chronic expression in mice interferes with avoidance learning (Heyser et al 1997) and human individuals expressing the C allele of the IL-6 gene show decreased IL-6 activity and delayed AD development (Papassotiropoulos et al 1999).

Cytokines also affect Aβ production. Although TGFβ can protect against ischaemia and excitotoxicity and has been shown to facilitate plaque clearance by microglia in transgenic mice (Wyss-Coray et al 2001), it can also induce increased AβPP release from astrocytes (Gray & Patel 1993). TNFα and INFγ act synergistically on neurones to increase Aβ and decrease sAβPPα production (Blasko et al 1999). The factors that determine the role TGFβ plays in AD have not been determined.

Complement

The classical complement pathway is an amplifying cascade mainly comprising serine proteases. The pathway starts with activation of C1q and terminates with the formation of the membrane attack complex (figure 1.64). An alternative pathway of complement activation requires covalent bonding of a stimulating molecule to C3. Membrane attack complex units combine to form transmembrane channels capable of conducting ions and disrupting cellular homeostasis. Intermediate complement components trigger the release of cytokines from microglia, tag material for phagocytosis and act as glia chemoattractants.

Non-demented elderly subjects show little CNS complement activity but in AD brain full complement activation is seen in areas affected by pathology (Yasojima et al 1999). In the hippocampus and temporal cotex, neurones are the main source of complement (Yasojima et al 1999) and plaque-associated dystrophic neurites express membrane attack complex.

Aβ stimulates the classical complement pathway by binding to C1q, which has 6 homologous subunits each with a binding site for Aβ. $A\beta_{42}$ binds more effectively than $A\beta_{40}$ and fibrillar Aβ is more effective at activating the complement cascade (Webster et al 1997). C1q protects bound Aβ from phagocytosis by microglia (Webster et al 2000) and promotes fibrillogenesis (Webster & Rogers

1996). It is possible that difficulty generating plaques in rodent models of AD overexpressing muAβPP or huPS1 carrying FAD mutations is due to the lower affinity of rodent Aβ for C1q (Webster et al 1999). C1q can also be activated by DNA released from damaged neurones, which binds the same domain as Aβ (Jiang et al 1992). This could amplify complement activation as neurones degenerate and accelerate cognitive decline. $A\beta_{42}$ also forms covalent bonds with C3 and so is capable of activating the alternative complement pathway (Bradt et al, 1998).

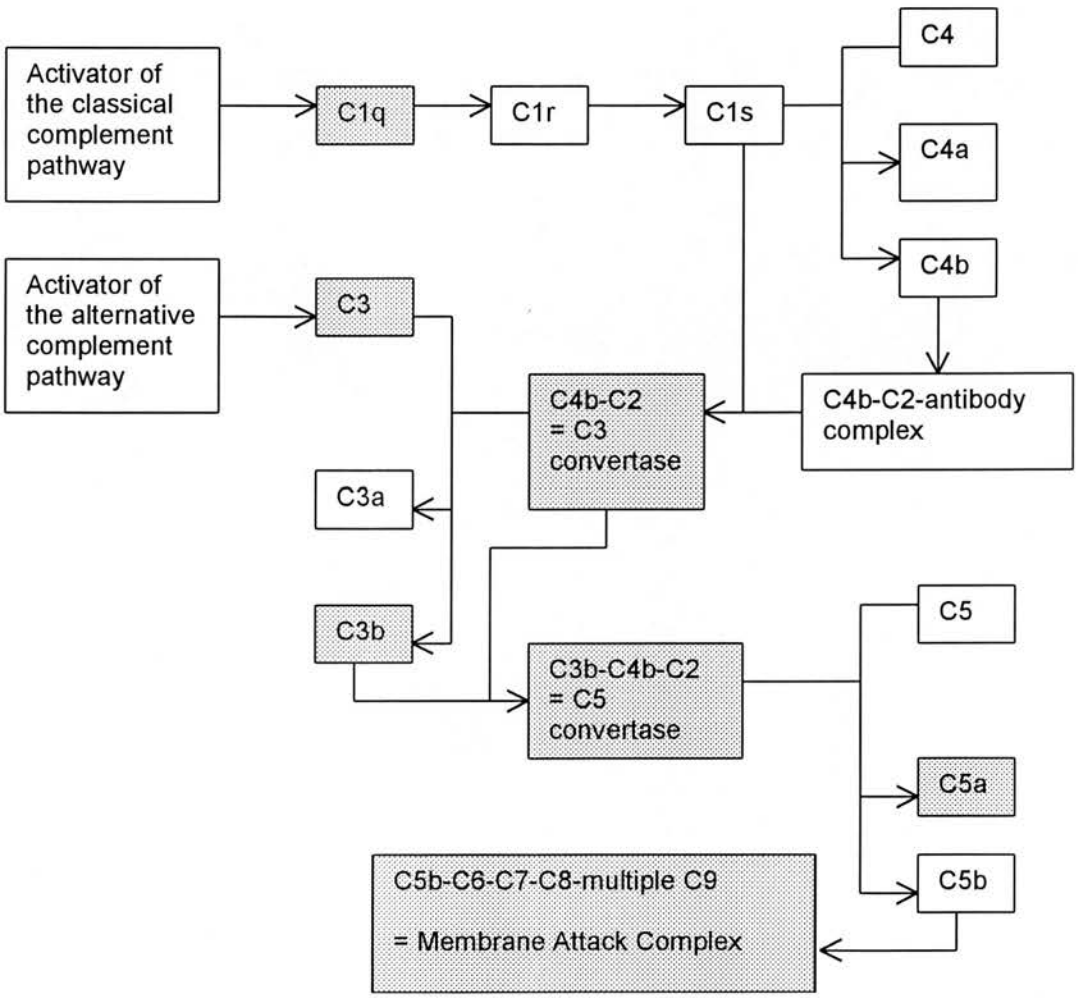

Figure 1.64 The classical complement pathway

Factors referred to in the text are highlighted.

Complement is active early in the development of AD. In a study using Down's syndrome brains as a temporal model of AD, diffuse plaques and $A\beta_{42}$ immunoreactivity were observed in a 12 year old in the absense of complement activity or AD pathology. In a 15 year old, $A\beta_{42}$ was colocalized with C1q, C3 and apoJ in neuritic plaques in addition to reactive astrocytes and activated microglia leading to full AD patholgy and complement immunoreactivity by the late 20s. Brains from thirty to forty year old subjects showed C1q and C3 mostly in neuritic plaques with C5b-9 also associated with dystrophic neurites, some neurones and NFTs. Therefore, complement becomes activated in conjunction with neuritic plaque formation, which leads to MAC formation and neurodegeneration. (Stoltzner et al 2000).

Fibrillar Aβ is opsonized by C3b which attracts microglia and stimulates the production C5a. C5a potentiates Aβ-induced release of cytokines IL-6 and IL-1β from cultured microglia (O'Barr & Cooper 2000).

To avoid inappropriate opsonization by complement, healthy endogenous cells have membrane-bound complement regulators that block the complement cascade either at the C3/C5 convertase level (membrane cofactor protein, decay accelerating factor and complement receptor 1) or at the level of MAC formation (CD59). These regulators are highly expressed in peripheral tissue. In the brain, cultured astrocytes express CD59, membrane cofactor protein and at a lower level, decay accelerating factor. Neurones have low levels of CD59 and membrane cofactor protein and lack decay accelerating factor and complement receptor 1 therefore may be more susceptibly to damage by complement, which could explain the neuritic damage in the vicinity of AD plaques (Singhrao et al 1999).

Acute phase protein

Plaques are associated with Aβ–binding acute phase proteins such as α2-macroglobulin and α1-antichymotrypsin. α2-macroglobin can have either neuroprotective of neurotoxic actions. It binds and inactivates neuroprotective NGFβ, which can lead to cell death (Fabrizi et al, 1999). However, it also contributes to Aβ clearance (Qui et al 1996). Both of these acute phase proteins reduced neurone loss under the same culture conditions, but whilst α2-macroglobin prevented fibril formation, this was

promoted by α1-antichymotrypsin (Du et al 1988) The authors suggest that α1-antichymotrypsin obscures the Aβ active site to prevent toxicity (Du et al 1988). However, it may be that both α1-antichymotrypsin and α2-macroglobin prevented Aβ toxicity by interferring with the toxic actions of soluble Aβ and the presence or absence of fibrils was largely irrelevant to neurone viability.

1.63 Mitochondrial dysfunction

The main role of mitochondria is energy production. Neurones have an exceptionally high energy demand making it particularly vulnerable to ATP deficiency. This is reflected in the large number of neurological disorders amongst diseases caused by mitochondrial dysfunction (Schoffner & Wallace, 1994).

Mitochondria metabolise pyruvate, the end-product of glycolysis, in the Krebs cycle and electron transport chain. The electron transport chain is especially important since it releases the majority of the ATP produced by aerobic respiration by the process of oxidative phosphorylation (for review see Sherratt 1991). The electron transport chain substrates are NADH and $FADH_2$, which are formed during glycolysis and the Krebs cycle. In the electron transport chain the pair of high energy electrons carried by NADH or $FADH_2$ are passed through a series of protein complexes (I to IV) of decreasing energy levels, to drive the movement of protons across the inner mitochondrial membrane from the matrix into the intermembrane space. The inner membrane is highly impermeable and so holds protons against their electrochemical gradient, generating a proton-motive force, which drives the release of ATP.

As well as producing energy, mitochondria buffer cytosolic Ca^{2+} and so are important for maintaining Ca^{2+} homeostasis (Budd & Nicholls 1996). However, extreme or prolonged increases in cytosolic Ca^{2+} can saturate mitochondrial buffering capacity. These conditions cause the opening of mitochondrial permeability transition pores that span both inner and outer membranes (Dubinsky and Levi 1998). In their partially open state, these non-specific channels allow release of Ca^{2+} and exchange of other small molecules. More seriously, when fully open, they cause mitochondrial swelling (Puka-Sundvall et al 2000) and may also allow release of NADH, $FADH_2$ and GSH, depleting substrate availability for the electron transport chain.

Free radicals are formed during oxidative phosphorylation. Electrons escape the electron transport chain, and react with molecular oxygen to form the superoxide radical. This is converted into oxygen and hydrogen peroxide by superoxide dismutase. Hydrogen peroxide can be converted by catalase into water and oxygen or by glutathione peroxidase into water (reviewed in Boveris & Cadenas 1982). Deficits in this antioxidant system or increases in the production of reactive oxygen species in a dysfunctional electron transport chain lead to oxidative stress, which damages proteins, lipids and DNA.

Oxidative stress leads to the opening of mitochondrial transition pores and disrupts the electron transport chain, creating a cellular energy deficit and promoting further production of reactive oxygen species. Oxidants stimulate mitochondrial permeability transition pores to open either directly or by activating phospholipase A to produce free fatty acids (Wieckowski et al 2000).

Mitochondria carry their own DNA that codes for some components of the electron transport chain complexes. Damage to mitochondrial DNA or disfunction in the transcription pathways reduces the efficiency of oxidative phosphorylation and ATP production and increases the release of reactive oxygen species. Since these are produced in the mitochondria, this organelle is a prime target for oxidative damage. Mitochondrial DNA is especially fragile since it lacks histones and has less efficient DNA repair enzymes than nuclear DNA. Impaired mitochondrial function encourages further reactive oxygen species production, generating a positive feedback loop of escalating damage. Resulting energy deficits disrupt ion homeostasis and membrane potential, cell excitability and increase the availability of free metal ions.

Mitochondria from AD subjects show impaired activity in the electron transport chain complexes I (NADH dehydrogenase) and IV (cytochrome oxidase) (Aksenov et al 1999) and in pyruvate dehydrogenase (Gibson et al 1998). One of the complex I subunits, normally coded by mitochondrial DNA, appears to be missing in AD. Complex I dysfunction is also seen in Parkinson's disease and Huntington's disease.

Complex IV function is decreased by about fifty per cent in AD. This is not observed in healthy aged subjects or in subjects with other neurodegenerative diseases such as Parkinson's disease. The loss of function is observed in AD-affected brain areas but not in the cerebellum (Aksenov et al 1999).

Pyruvate dehydrogenase is deactivated by TPKI. Mitochondria have their own form of TPKI which is more sensitive to activation by Aβ than cytosolic TPKI (Imahori et al 1998). In mitochondria, pyruvate dehydrogenase converts pyruvate, the product of glycolysis, into acetyl CoA. In AD, its activity is depleted, leading to reduced glucose metabolism and increased lactate production. This causes acetyl CoA depletion and consequent decrease in ATP production. Acetyl CoA depletion may also be a source of the cholinergic deficit typical of AD.

Some cases of SAD are linked to mutations in mitochondrial DNA coding subunits CO1 and CO2 of cytochrome oxidase (complex IV). SAD cases show preferential transmission down the maternal line, which may be explained by AD susceptibility genes in the maternally transmitted mitochondrial DNA.

1.64 Metal Ions

Metal ions are abundant in healthy brain, where they bind metalloproteins to facilitate enzyme function. Free metal ions are highly toxic; iron, copper, zinc and manganese all have redox activity and can cause oxidative damage. Therefore, free metal ion concentrations are strictly controlled by ATPase pumps and high capacity storage proteins.

Many studies have measured levels of metal ions in healthy and AD brain with poor replicability. An early report measured increased zinc and iron and decreased copper levels in the hippocampus and amygdala but no change in the cerebellum of AD brain (Deibel et al 1996). A further study confirmed the increase of zinc and iron (Cornett et al 1998). Others have failed to measure changes in cerebrospinal fluid levels of iron or zinc or have measured a decrease in zinc (Molina et al 1998, Rulon et al 2000). Serum levels of metal ions are affected by apoE genotype. Carriers of the SAD-linked apoε4 allele have elevated levels of serum copper and zinc (Gonzalez et al 1999). However, these studies have measured total metal levels rather than levels of the potentially toxic free metal ions. Increased amounts of the iron storage protein, ferritin, have also been recorded (Kuiper et al 1994), suggesting that any increase in iron in the AD brain can be accommodated safely. More convincing evidence for the involvelment of metal ions in AD is their association with pathological markers. Zinc is strongly associated with amyloid plaques, NFT-bearing neurones and

vascular amyloid (Suh et al 2000). Iron and copper are also associated with plaques (Lovell et al 1998).

Conditions in the AD brain could promote metal ion availability. The AD brain shows cerebral acidosis (Yates et al 1990). This could be caused by lactate generation in response to energy deficit and by chronic inflammation. Mild acidosis causes release of metal ions from metalloproteases and so could free a variety of enzyme associated metal ions. Energy depletion could impair control of metal ion compartmentalisation by inactivating ATPase ion pumps. Zinc is released in neurotransmitter vesicles from some glutamatergic synaptic terminals. Excitotoxicity, associated with AD, could cause excessive release of zinc, elevating it to toxic levels. Elevated zinc levels may suppress synaptic plasticity. Zinc can modulate the kinetics of $GABA_A$ (Smart 1992), NMDA and non-NMDA glutamate receptors (Xie et al 1993), and blocks LTP in both mossy fibre/CA3 and Schaffer collateral/CA1 hippocampal pathways (Xie & Smart 1994). Therefore, elevated zinc concentration in the hippocampus could contribute to impaired cognitive function in AD prior to severe levels of cell loss.

These metals may actually contribute to the formation of plaques and tangles. Aβ has binding sites for copper (Atwood et al 2000) and zinc (Yang et al 2000a). Copper II binds Aβ and induces aggregation, especially of $A\beta_{42}$ (Atwood et al 2000) and this is enhanced under acidic conditions (Atwood et al 1998). It also binds AβPP, and is reduced to CuI with the release of free radicals (Multhaup et al 1996). Zinc causes Aβ aggregation but preferentially of α-helix conformation Aβ (Huang et al 2000). As well as promoting aggregation, copper and zinc also defibrillize established Aβ aggregates (Chauhan et al 1997) and so the interaction between Aβ and metal ions promotes the formation of non-fibrillar Aβ aggregates.

Metal ions can also cause aggregation of tau protein. Calcium and magnesium selectively aggregate tau-p whereas aluminium and iron both induce aggregation of tau and tau-p. Copper and zinc have no effect (Yang et al 1999a).

Binding of copper (and iron) to Aβ generates hydrogen peroxide (Huang et al 1999b) and peptide-bound redox metal ions (Huang et al 1999c, Sayre et al 2000) which can both cause oxidative damage. Bound metal ions can react with hydrogen peroxide to release the highly reactive hydroxyl ion, making metalloproteins particularly susceptible to oxidative damage. Zinc prevents the

production of hydrogen peroxide caused by the interaction of Aβ with iron and copper. Therefore, although zinc contributes to Aβ deposition, it may then act to resist plaque-associated production of reactive oxygen species (Huang et al 2000b).

The copper/iron binding protein and antioxidant, ceruloplasmin, is expressed in the neurones of healthy brain, but in AD it is preferentially upregulated in the neuropil (Loeffler et al 1996, Castellani et al 1999). It has been suggested that this reflects a lack of ability in neurones to upregulate ceruloplasmin in response to elevated metal ion levels in AD and this represents a deficit in AD antioxidative activity that contributes to oxidative stress (Castellani et al 1999). This suggestion is supported by observations of low ceruloplasmin, as well as superoxide dismutase, activity in the plasma of AD subjects (Snaedal et al 1998).

1.65 Oxidative Stress

The previous sections have shown the possible mechanisms by which changes in a single protein, Aβ, could generate the wealth of pathological features recorded in cases of AD. The culmination of these changes must ultimately be cell death, and evidence is growing that the primary mechanism of neurotoxicity is oxidative stress. This is caused by an imbalance between the production of harmful reactive oxygen species, such as the hydroxyl radical, the superoxide radical, hydrogen peroxide and peroxynitrate and the availability of protective antioxidants. Aβ aggregates, NFTs, inflammation, dysfunctional mitochondria and free metal ions all have the capacity to generate reactive oxygen species. Antioxidant activity decreases with age and neurones are especially susceptible to oxidative damage having relatively poor antioxidant activity and in general being post-mitotic. The AD brain shows typical signs of oxidative damage; oxidation of proteins and release of carbonyl peptides, peroxidation of lipids, production of 4-hydroxynonenal and acrolein and oxidative damage causing fragmentation of DNA, especially in mitochondria. This section will summarize the sources of reactive oxygen species in AD pathology and suggest some mechanisms by which these can cause neurodegeneration.

Aβ can be directly neurotoxic by binding metal ions to produce hydrogen peroxide and peptide-bound redox metal ions. Aβ targets the cell membrane, where it damages the Na^+/K^+/ATPase leading to ion imbalance (Mark et al 1997). It oxidises the astrocyte glutamate transporter, impairing

glutamate clearance from the synaptic cleft (Keller et al 1997). It also inactivates glutamine synthase that converts glutamate into glutamine (Pike et al 1997). These actions all contribute to excitotoxicity. Aβ oxidises lipids forming lipid free radicals and the by-products of lipid peroxidation, HNE and acrolein (Mark et al 1997, Keller et al 1997). Although these are less toxic than Aβ, they have a longer half-life and so can act at greater distances from the initial site of free radical formation. Aβ reacts non-enzymatically with carbohydrates by the Maillard reaction to release free radicals and form advanced glycation end-products. Glycated Aβ can bind RAGE, a receptor that mediates cellular oxidative stress in glia, endothelial cells and neurones (Yan et al 1996) and can stimulate apoptosis.

Aβ can indirectly induce iNOS from astrocytes by stimulating IL1β release from microglia. IL-1β binds astrocyte interleukin receptors to activate the TNFa receptor associated factor 6, which stimulates iNOS expression and NO release (Akama & van Eldic, 2000). NO has potentially neurotoxic and neuroprotective roles in AD. It can exert toxicity indirectly by reacting with superoxide radicals to form peroxynitrate. However, its direct roles seem to be protective. It has a putative neurotransmitter/retrograde messenger role in synaptic plasticity, promotes vasodilation and may protect against excitotoxicity. In AD brain, the level of cerebrospinal fluid NO is inversely correlated to the level of dementia and glutamate toxicity is attenuated in cerebellar granule cells which produce iNOS and are spared in AD (Tarkowski et al, 2000) supporting a predominantly protective role.

The mitochondrial electron transport chain releases superoxide radicals. Mitochondria are especially prone to oxidative damage due to their proximity to this significant source of free radical production and the vulnerability of their DNA, and such damage potentiates further superoxide radical formation making mitochondria a site of potential amplification of oxidative stress. Cells exposed to $A\beta_{42/43}$ produce increased levels of reactive oxygen species, have impaired mitochondrial function and eventually become apoptotic. This is prevented by the Ca^{2+} binding agent, calbindin, suggesting that Ca^{2+} influx is an early event in the pathway (Guo et al 1998).

Oxidative stress activates a PKC-dependent increase in Aβ production (Paolo et al 2000). This specifically increases the intracellular Aβ pool and may be an important positive feedback loop in AD, contributing to the formation of toxic $A\beta_{42/43}$ aggregates.

Whether neurodegeneration in AD is primarily a necrotic or apoptotic event, or is subserved by some distinct mechanism, is still a matter for debate. In experimental conditions, chronic, low level toxic insults are more likely to induce apoptosis, whilst the same insult applied acutely may induce necrosis. This possibly explains reports of both necrosis (Sutton et al 1997, Suzuki 1997) and apoptosis (Ohyagi et al 2000, Li et al 1996) in different studies on Aβ toxicity in cell cultures. Since AD is a chronic illness, apoptosis may be the more likely mechanism but identifying apoptotic cells in AD tissue is difficult since only a very small proportion of cells will be undergoing apoptosis at any time. Oxidative stress has been cited as a likely cause of neurodegeneration in AD, and this is commonly linked to apoptosis.

1.66 Age-dependence

The brain becomes increasingly vulnerable to Aβ-mediated toxicity with age as shown by Aβ injections into primate brain that causes neurodegeneration in aged but not young animals (Geula et al 1998b). The ageing brain has impaired defences against excitotoxicity and oxidative stress (Clementi et al 1996) and so may accumulate toxins that make it more susceptible to disease. In women, risk of AD with age is increased at the menopause with the associated decrease in oestrogen levels (Fratiglioni et al 1997).

The age-dependence of AD could be caused by accumulation of mutations in mitochondrial DNA. Mitochondria divide independently of cell mitosis. Mutations to mtDNA occur more frequently than in nuclear DNA (Richter et al 1988). This is exacerbated in AD brain in which the rate of mitochondrial DNA mutation is 15 times greater than in healthy age-matched controls (Corral-Debrinski et al 1994). Cells develop a heteroplasmic population of mitochondria (ie having mitochondria with differences in their complement of mutations) and those carrying mutations proliferate either by increased division or persistence (de Grey 1997). In post-mitotic cells, such as neurones, this unfortunately encourages proliferation of dysfunctional mitochondria tending towards homoplasmy for deliterious mutations, and this gradual build-up of impaired mitochondria contributes to the observed decrease in ETC efficiency and increase in reactive oxygen species production with age. This would make the aged brain more susceptible to illnesses such as AD that are linked to energy deprivation and oxidative stress.

Polyunsaturated fats are more prone to oxidative damage than other membrane bound lipids (Laganiere & Yu 1993). Mitochondrial and neuronal membranes become more vulnerable to Aβ toxicity with ageing as the levels of polyunsaturated fats (already relatively high in these membranes) increases (Huber et al 1991).

Chronic inflammation has a major role in AD. Basal and stimulus-induced levels of inflammatory cytokines are increased in the ageing brain (Ershler 1993, Saurwein-Teissl 2000) facilitating the excessive immune response to amyloid deposition that leads to the sustained and toxic activity of inflammatory proteins.

1.67 Site specificity

AD pathology is focussed on the hippocampus and association cortices. There is also significant neurodegeneration of cholinergic pathways from the basal forebrain nuclei to the hippocampus and neocortex.

The importance of inflammation in AD partly explains the site-specificity of neurone loss since the hippocampus and the entorhinal cortex are especially sensitive to inflammatory cytotoxins. Chronic low-dose infusion of the inflammogen, bacterial lipopolysaccharide, into the ventricles of experimental animals result in increased AβPP and cytokine (IL1β and TNFα) expression and atrophy limited to the hippocampus and entorhinal cortex, and the animals show memory impairment (Hauss-Wegrzyniak et al 1998).

Soluble Aβ oligomers are selectively toxic to neurones in the hippocampus CA1, dentate gyrus, and entorhinal cortex and spare cerebellar neurones and some CA3 neurones. ApoE is more strongly expressed in brain areas that are sensitive to damage in AD (Xu et al 1999).

Cytokine activation often involves nuclear factor-κB (NFκB) -dependent transcription. In most cells, NFκB exists in an inactivated form in the cytoplasm. However, in some cortical and hippocampal cells it is constitutively active (Kaltschmidt 1994), which may explain why these areas suffer high levels of pathology and cell loss in AD. NFκB mediates both neuroprotective and cytotoxic pathways, and is central to apoptosis, and so may act as a discriminator of incoming signals to decide cell fate.

The influence of apoE in AD may confer site specificity since this protein is expressed in the

cerebral cortex and hippocampus, but not in the cerebellum (Xu et al 1999).

There are two possible explanations for specific loss of cholinergic projections from the basal forebrain nuclei to the hippocampus and cerebral cortex. First, Aβ-induced oxidative stress disrupts G-protein signalling of muscarinic receptors. Second, Aβ activates tau protein kinase, which impairs pyruvate dehydrogenase function. This depletes levels of acetyl CoA, required to produce acetylcholine. Disruption of cholinergic transmission in the hippocampus and neocortex may then cause retrograde degeneration of neurones in the medial septum and nucleus basalis of Meynert. The loss of cholinergic fibres correlates with density of NFTs suggesting a link between the two pathologies (Geula et al 1998a).

Chapter 2

Transgenic Animal Models

The study of AD is hampered by the lack of a naturally occurring animal model. Post-mortem examination of AD brain allows the affected areas to be identified and patterns of pathological markers to be described, but disease progression cannot be studied and components of the pathological markers do not reliably indicate factors that are of primary importance in pathogenesis. An animal model would allow the progression of changes in the AD brain to be plotted from the earliest stages and provide a tool for testing new treatments. In recent years, transgenic technology, coupled with the discovery of genetic mutations that cause FAD, has provided a possible means of generating animals that express AD.

Transgenic technology involves the introduction of foreign genetic material into an animal's genome and the subsequent transmission of this mutation in a stable manner to offspring, creating a sustainable pedigree of animals carrying the donated DNA in all their cells. Transgenic technology has the benefit of allowing human genes to be expressed in laboratory animals, so overcoming some of the species-difference problems faced when studying human conditions in animals. Transgenic animals can be used to examine gene control sequences and their activity in disease development. The function of proteins can be studied by inference of the effects of overexpressing or inhibiting the expression of the gene. The consequences of disease-causing mutations can be studied by inserting human genes carrying a known disease-related mutation into laboratory animals.

2.1 Historical overview

The first step in the development of transgenic technology was to show that foreign cells could be incorporated into the tissues of a host. Rather than producing a transgenic animal; one which carries a copy of donor DNA in every cell, this generated chimaeric animals, in which some tissues contained cells of both host and donor origin. Two 8-cell stage embryos were cultured together until they formed a single blastocyst, which was then implanted into pseudopregnant mice to develop to term (Tarkowski 1961). Successful contribution of both cell lines to the offspring was demonstrated by sex-chimaerism, in about half of the offspring. Production of chimaeric mice was developed by Gardner, (1968) who used a blastocyst as the host into which foreign cells from the inner mass of a blastocyst of the same age were injected. Brinster (1974) used teratocarcinoma cells as the donor material to

confirm that cells from different developmental stages could participate in embryonic development. The advantage of using teratocarcinoma cells was that they could be maintained in culture making them available for genetic manipulation prior to insertion. However, the use of teratocarcinoma cells precluded the production of sustainable lines of genetically altered animals since the offspring often developed fatal tumours which prevented them from reaching adulthood and progeny of chimaeric mice seldom carried the donor cells, suggesting that teratocarcinoma cells rarely contribute to the germline (Papaioannou et al 1975). Evans and Kaufman (1981), succeeded in finding suitable culture conditions for maintaining embryonic stem cell lines. Using embryonic stem cells instead of teratocarcinoma cells gave higher rates of success in generating chimaeras, and these mice successfully transmitted the donor cells to their offspring, giving the first evidence that lines of animals carrying foreign genetic material could be reliably sustained (Bradley et al 1984). Transgenic lines were generated from the first generation progeny of the chimeric animals, by selecting those offspring derived from gametes containing the donor DNA.

Transgenic animals can also be generated directly by injection of donor DNA into the fertilized egg at the 1-cell (pronuclear) stage, as was first shown by Gordon et al (1980). This is the method of choice for production of transgenic rats since culture conditions for maintaining rat embryonic stem cells have still not been devised. At the pronuclear stage, within a few hours of fertilization, the male and female nuclei have not yet fused. The DNA of the transgene is injected into the male nucleus of the fertilized egg (figure 2.1). The male nucleus is larger than the female nucleus and is usually closer to the surface of the oocyte (Rülicke & Hübscher 2000). It is incorporated into the nucleus of the zygote as the male and female nuclei fuse and so will be present in all the cells of the offspring. The manipulated zygote is then inserted into a pseudopregnant female to develop to term.

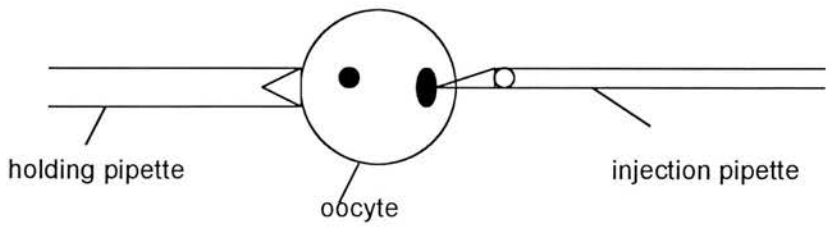

Figure 2.1 Pronuclear injection

2.2 Limitations of transgenic technology

Although transgenic animals have already been very useful in scientific research and their contribution continues to expand, the technology has pitfalls that can affect the reliability of protein expression and activity.

2.21 Genetic background

Transgenes are usually expressed in inbred strains of laboratory animal. These are lines of animals which are homozygous at every gene locus as a result of consecutive brother/sister matings over more than twenty generations. This provides a background free of genetic variability suitable for assessing the specific effects of the transgene.

Some inbred lines show abnormalities due to homozygosity of deleterious mutations and these may affect assessment of the effects of the transgene. The ola129 mouse strain shows particularly severe abnormalities such as deficits in behavioural tests and in the development of the corpus collosum, which make it a poor choice for studying the effects of a transgene on development or on learning and memory.

The same transgene can show qualitative or quantitative differences in phenotype depending on the background upon which it is expressed and so it is often worth examing a transgene in more than 1 strain.

2.22 Co-segregation

Unfortunately, ola129 is often the strain of choice for generating a transgenic line since embryonic stem cells from these animals are cultured with the greatest success. The resulting transgenic animals are often backcrossed onto another strain such as C57B, which confers a more normal physiological background and more robust breeding. With each generation of back-crossing, the transgenic offspring lose more of the ola genome. However, even after many generations, the transgene will continue to be associated with neighbouring ola129 genes. It is possible that any differences seen in the transgenic group are due to the co-segregating ola129 genes and not the transgene, generating false-positive results.

2.23 Limits to insert size

Bacterial plasmid DNA is the usual vectors for cloning a transgene. However, they can only handle gene fragments of about one hundred kilobase pairs; much smaller than most of the genes being studied. Also, longer DNA fragments are more prone to damage from the shearing forces exerted during purification and pronuclear injection. As a result, the non-coding introns are omitted from the transgene. This allows cloning of sufficient DNA for successful expression of the full protein. However, the introns can be important for efficient gene transcription, which may explain the difficulties often experienced in generating high levels of protein expression (Brinster et al 1988). Introns control splicing of mRNA into gene product variants and so functionally important isoforms may not be produced. Introns can also signal transport of mRNA to the cytoplasm, therefore their omission may result in abnormal intracellular distribution of the protein.

The introduction of larger DNA fragments has been made possible by the use of yeast artificial chromosomes, which have the potential to carry up to 2 megabase-pairs of genetic material. Also, endogenous mechanisms for gene rearrangement in yeast can be exploited to introduce mutations of the transgene before cloning. Lamb et al (1993) used yeast artificial chromosomes to transfer an entire human gene, AβPP (about four hundred kilobase pairs), to mice, this being the first example of yeast artificial chromosomes being used to transfer considerably longer DNA fragments.

2.24 Variable insertion site

Although a transgene usually only has one insertion site in the host genome, its position is unpredictable. Therefore, two transgenic lines may carry the same transgene but in different parts of the genome. Neighbouring genes can affect the expression of the transgene and so the two lines may exhibit different phenotypes. These positional effects are often only quantitative, so a number of lines are generated and the one with the strongest protein expression or most robust phenotype is chosen for maintaining a permanent line. Creating multiple lines allows false positives, caused by unusual interactions between the transgene and the host DNA or by rare cases of the transgene disrupting an endogenous gene, to be identified.

Positional effects are overcome by directing the transgene to a specific part of the chromosome. This is known as homologous recombination and involves the transgene recognizing its

analogous sequence in the host DNA and inserting at that locus, simultaneously removing or disrupting the endogenous gene. This technique has also allowed the production of gene knockout animals.

2.25 Redundancy

Many genes, especially those fundamental for cell function, have homologues with similar capabilities. The effect of knockout or loss of function mutations can be masked by the recruitment of homologues to restore function and leads to false-negative results.

2.26 Problems with homozygous mutations

Knockout of or loss of function mutations to a gene that is important for development is usually developmentally lethal. Therefore, heterozygote animals are often used as the experimental group, and so some normal gene function remains, possibly masking the phenotype of the transgene.

More recent developments are allowing increasing control over the tissues in which or at what developmental stage a mutation is effected. This conditional mutagenesis commonly uses an intrinsic plasmid gene rearrangement mechanism using two 34-base pair lox-p sequences to mark the target gene and the 'causes recombination' CRE effector, which recognises lox-p and makes either a reversal or removal of the target gene, depending on the orientation of the lox-p markers. A line of animals can be generated that carry lox-p marking the gene of interest. A second line of animals carries the CRE gene with a promotor which confers upon it site or time specific expression. When the two lines are crossed, offspring will express the mutation in the tissues or at the developmental stage as determined by the CRE promotor. Other similar genes capable of performing these alterations have been subsequently identified.

2.27 Variable copy number

Although there is usually only one transgene insertion site, this may carry multiple copies of the transgene in a head-to-tail array. Not all copies are necessarily complete, therefore, although a higher copy number gives a greater chance of transcribing the full length transgene, the expression levels of the gene does not necessarily reflect the copy number. If each copy has its own direct control region

then they each appear to be independently regulated and copy number is reflected by expression level (Stief et al 1989).

2.28 Changes in expression of other genes

Transgenic animals can show altered expression of proteins other than those targeted by transgenesis. This may be due to the transgene directly interfering with transcription of endogenous genes or indirectly by the transgene product (or lack of a protein in the case of knockout transgenic animals) leading to modified expression of other genes.

2.3 Animal models of Alzheimer's disease

Transgenic approaches have been a focus of recent AD research. Some AD-like pathology has been reported in apes and dogs, but these animals are not suitable for extensive scientific studies due to ethical, financial and time constraints. Ideally, an AD model would be a traditional laboratory animal, however, aged rodents do not naturally show any AD-type of illness.

Rodents transgenic for human genes carrying FAD-causing mutations have been produced in an attempt to provide an AD model. A perfect animal model would show all aspects of the human condition. In AD this is perhaps unlikely due to the cognitive focus of the disease. It affects mostly phylogenetically recent brain areas, which underlie cognition and are particularly well developed in the human brain. Since rodents do not posses such sophisticated cognitive traits, it is likely that some of the systems affected by AD are not developed in rodent brain. However, it is possible that many of the traits of AD can be recreated, and that cognitive dysfunction can be studied in relation to normal rodent behaviour.

Potential AD models are typically studied for signs of pathology and alterations in their behaviour, levels of neurochemicals, electrophysiology and biochemistry. A perfect model should show amyloid plaques, neurofibrillary tangles and specific nerve loss. This should be focussed in the neocortex, hippocampus, amygdala and basal forebrain nuclei.

Since AD pathology is especially concentrated in the hippocampus of AD subjects, animal models should show deficits in forms of memory subserved by the hippocampus. In rodents, the hippocampus subserves spatial memory, and so impaired performance in maze tests is expected.

AD brain shows particularly severe loss of cholinergic innervation to the hippocampus and neocortex from the cholinergic forebrain nuclei. An AD model would be expected to show a reduction in cholinergic markers in these brain areas, reflecting synapse loss and degeneration of cells in the forebrain nuclei.

Electrophysiological studies can detect changes in the activity of neurones and in the properties of pathways, such as expression of synaptic plasticity in the hippocampus and neocortex. Altered expression of synaptic plasticity would be particularly interesting in an AD model, since these mechanisms are believed to underly memory storage and retrieval.

A major effect of FAD mutations in human subjects is increased Aβ production. AβPP mutations cause an increase in total Aβ whilst presenilin FAD mutations cause a selective increase in $A\beta_{42/43}$, therefore, any FAD model of AD should show the appropriate change in Aβ levels. Transitional metals such as iron and copper should be colocalized with plaques and tangles and the activity of protein kinases and phosphatases could be altered. Markers of apoptosis should be upregulated, along with signs of oxidative damage such as lipid peroxidation, protein oxidation and DNA fragmentation.

2.31 Transgenic rodent models of AβPP familial Alzheimer's disease

The AβPP mutations used most to generate transgenic models of FAD are Indiana V717F and Swedish K670N/M671L, both of which have successfully recapitulated some important features of human AD.

A popular model for studying the Indiana mutation is the PDAPP mouse, which shows dramatic upregulation of Aβ, and in particular $A\beta_{42}$ in the hippocampus and cerebral cortex but not in the cerebellum (Games et al 1995, Johnson-Wood et al 1997). This leads to Aβ deposition and plaque formation in the neocortex and hippocampus from about 6 months onwards. The density of plaques increases with age and they become associated with dystrophic neurites (Games et al 1995, Johnson-Wood 1997). Dentate gyrus synaptic and dendritic density are lower in the transgenic mice (Games et

al 1995), however, this does not correlate with amyloid load and in fact high Aβ levels can accompany decreased synaptic density in the absence of Aβ deposition (Mucke et al 2000). This is supported by another PDAPP study that revealed deficits in synaptic transmission and reduced synaptic density in the absence of plaques (Hsia et al 1999). NFTs have not been observed in this model (Games et al 1995).

The amyloid plaques of PDAPP mice are surrounded by microglia and astrocytes (Games et al 1995). Microglia are strongly activated and have increased expression of macrophage colony-stimulating factor receptors, that can modulated interactions between Aβ and glia (Murphy et al 2000).

Impaired cognition increases with age and plaque load as shown using the water maze (Chen et al 2000). This is accompanied by altered neurone excitability and synaptic plasticity. The maximum EPSP amplitude of hippocampal pyramidal neurones from PDAPP mice is decreased. Young (4 to 5 month old) mice show increased paired pulse facilitation and decreased long-term potentiation whilst aged (twenty-seven to twenty-nine month old) mice show decreased paired pulse facilitation and increased long-term potentiation suggesting that synaptic transmission can be compromised prior to amyloid deposition, and that the mechanisms of cognitive impairment differ in young and aged animals (Larson et al 1999).

Indiana mutation mice show age-dependent deficiencies in glucose metabolism, that concurs with the energy deficit observed in human AD brain (Dodart et al 1999).

The main Swedish mutation models are TG2576 and APP23. Swedish mutation mice show increased β-cleavage of AβPP that results in Aβ elevation and sAβPPα depletion (Moechars et al 1999). The level of $A\beta_{42}$ is the most strongly enhanced (Hsiao et al 1996). As Aβ accumulation progresses, the proportion of insoluble Aβ increases and CSF and plasma Aβ levels drop (Kawarabayashi et al 2001). Mice show age-dependent amyloid deposition and plaque formation in the neocortex and limbic areas (Hsiao et al 1996, Chapman et al 1999, Phinney et al 1999). Plaques develop more rapidly in female mice (Sturchler-Pierrat & Staufenbiel 2000) and so this model may be useful for studying the reasons for increased AD susceptibility in women.

APP23 mice at 14 to 18 months show selective cell loss in brain areas affected by congophillic plaques, which are localized in the neocortex and hippocampus (Sturchler-Pierrat et al 1997, Calhoun

et al 1998), although a study of a different line; TG2576 mice failed to show significant cell loss (Yang et al 2000b). That plaques can induce neurodegeneration is supported by the positive correlation between loss of CA1 pyramidal neurones and plaque load and the signs of degeneration seen in some neurons that are near to plaques. There was qualitative evidence for cell loss in the neocortex although no significant global cell loss was measured (Calhoun et al 1998). These findings concur with studies of human AD brain. Some plaque-associated neurites were positive for α-synuclein (Yang et al 2000b), as is observed in human AD brain. Aβ deposits of APP23 mice were associated with neurites that show ectopic projections and swollen axons resembling dystrophic neurites of AD (Sturchler-Pierrat et al 1997, Phinney et al 1999). Aged APP23 mice show dystrophy of cholinergic fibres (Sturchler-Pierrat & Staufenbiel 2000).

Paired helical filaments of tau have not been observed (Yang et al 2000b) although tau-p was detected in the APP23 line (Sturchler-Pierrat et al 1997, Sturchler-Pierrat & Staufenbiel 2000).

Congophyllic (but not diffuse) plaques from APP23 mice are associated with activated microglia and reactive astrocytes (Sturchler-Pierrat et al 1997). The microglia are found on the plaque periphery and are associated with amyloid fibrils and dystrophic neurites. Microglia exhibit signs of phagocytic activity when associated with neurites but not amyloid fibrils suggesting that Aβ fails to stimulate microglia to phagocytose amyloid deposits (Stalder et al 1999). Aβ probably activates microglia via scavenger receptor A, which was upregulated in these mice, rather than by RAGE, which was absent from the majority of plaques. The activated microglia express major histocompatibility complex II but fail to activate B and T lymphocytes (Bornemann et al 2001), which do not seem to be involved in the immune response in human AD. Rather, Swedish mutation mice do have microglia that are positive for the cytokines IL-1β and TNFα and astrocytes that are positive for IL-6, and it is such inflammatory factors that appear to be activated in human AD brain (Benzing et al 1999) (although a further study only managed to detect IL-1β activity (Mehlhorn et al 2000)).

An age-dependent deficit in long-term potentiation was recorded both at the Schaffer collateral/CA1 and perforant pathway/DG synapses. Paired pulse facilitation and post-tetanic potentiation were unchanged (Moechars et al 1999, Chapman et al 1999). There was no change in the amplitude of the EPSP and no reduction in synaptophysin labelling suggesting that the decrease in long-term potentiation was not due to altered synaptic transmission (Chapman et al 1999).

Swedish mutation mice show altered behaviour in the home cage; alternate aggression, anxiety and hyperactivity behaviour emerges in mice from about 8 weeks old. They have impaired performance in the water maze (Hsiao etal 1996), and in the T-maze when aged sufficiently to show impaired long-term potentiation expression (in the absense of cell loss) (Chapman et al 1999). The performance level in the maze correlates well with the size of the long-term potentiation response. Therefore, cognitive impairment can occur before cell loss, due to dysfunction of neuronal activity. Some tests reveal cognitive impairment in transgenic mice even prior to amyloid deposition (King et al 1999), suggesting that soluble Aβ rather than amyloid fibrils could alter neuronal activity. Gender differences in cognitive impairment have also been recorded, with females being more susceptible, which may be relevant to the gender bias in human AD (King et al 1999).

Models of other AβPP mutations have confirmed observations of elevated Aβ42 and sAβPPβ, abnormal homecage behaviour, impaired glucose metabolism and impaired perfomance in behavioural tests (Moechars et al 1999, Pedersen et al 1999). Transgenic mouse brain has also shown signs of apoptotic cell death in the absense of plaque formation (Kumar-Singh et al 2000) supporting a toxic role for soluble Aβ and apoptosis as the mechanism for cell death in AD. Amyloid deposition has been observed in the cerebral vasculature (Van Dorpe et al 2000).

2.32 Transgenic rodent models of presenilin familial Alzheimer's disease

Levels of presenilin are very tightly regulated and so it has not been possible to generate PS transgenic animals with the high levels of mutated protein expression achieved in AβPP transgenic models. However, lines of mutated presenilin mice have still successfully expressed some AD-like pathology.

Mice expressing human PS1 carrying a variety of FAD-causing mutations show a selective increase in $A\beta_{42}$ production (Duff et al 1996, Citron et al 1997) confirming that PS1 influences AβPP processing and substantiating the theory that all FAD mutations discovered so far probably cause AD by interfering with Aβ expression. Although no amyloid plaques develop in these mice, neurones show increased intracellular Aβ load and cell loss in the hippocampus, neocortex and cerebellum (Chui et al 1999), supporting a role for soluble Aβ aggregates in neurotoxicity. PS1 mutations caused impaired Ca^{2+} homeostasis and mitochondrial function in synaptosomes from transgenic mice (Begley et al 1999), which could be responsible for the observed hypersensitivity to excitotoxins shown by

neurones from these mice (Guo et al 1999a). Cell death was prevented by treatment with antioxidants that prevent Ca^{2+} influx (Guo et al 1999b) supporting a role for Ca^{2+} in PS1-mediated neurotoxicity.

Altered Ca^{2+} regulation has been recorded in electrophysiological studies that observed enlarged medium and late afterhyperpolarising potentials, increased Ca^{2+} influx in response to cell depolarisation and elevated long-term potentiation in neurones from mice expressing PS1 mutations (Barrow et al 2000).

FAD mutations to PS1 do not impair its developmental role. This is confirmed by the ability of mutated PS1 to prevent the developmental defects usually observed in PS1 null animals with almost equal efficacy to wildtype PS1 (Qian et al 1998, Davis et al 1998). This supports the view that PS1 mutations initiate AD via altered AβPP processing and impairment of Ca^{2+} homeostasis rather than by influencing development.

2.33 Double mutation transgenic rodent models Alzheimer's disease

The most robust rodent models of AD have been produced by cross-breeding existing single transgenic lines to generate double transgenic lines, co-expressing the AβPP Swedish mutation and a PS1 mutation. Borchelt et al (1996) combined the AβPPswe model, with high over-production of Aβ with a $PS1_{A246E}$ model that showed an increased proportion of the putatively more pathogenic $A\beta_{42}$, to generate a mouse that at 2 to 3 months old already expressed a much higher level of $A\beta_{42}$ than either of the single transgenic lines. By 12 months old, the brains of double transgenic mice were positive for amyloid deposits, gliosis and neuritic dystrophy mainly in the hippocampus and neocortex (Borchelt et al 1997). Similar substantial elevation of $A\beta_{42}$ levels and speed of amyloid deposition have been reported by studies using other PS1mutations (Holcomb et al 1998, Lamb et al 1999, McGowan et al 1999, Wengenack et al 2000). Expression of the double mutations did not significantly increase the level of neurone loss (Takeuchi et al 2000) but did result in the basal forebrain cholinergic nuclei forming smaller and less dense synapses in the cortex and hippocampus (Wong et al 1999). The double mutation mice also replicated deficits in the Y-maze seen in PS1 but not $A\beta PP_{swedish}$ transgenic lines (Holcomb et al 1998).

The novel approach of immunizing double-transgenic mice with $A\beta_{42/43}$ shows that even these imperfect models are providing valuable insights into possible treatments for AD. Immunization prior

to development of pathology prevented development of plaques. Animals immunized once Aβ deposition was apparent retarded the development of further pathology (Schenk et al 1999). Behavioural tests have further shown the vaccine to alleviate cognitive deficits (Janus et al 2000a, Morgan et al 2000).

Chapter 3

Synaptic Plasticity in the Hippocampus

The regular cytoarchitecture of the hippocampus has made it popular for extracellular studies of synaptic function and in particular synaptic plasticity. The basic tri-synaptic circuit of the hippocampus is preserved in transverse sections (figure 3.1) and the clearly defined cell body layers allow reliable electrode placement. The line of $PS1_{M146V}$ rats described in this thesis have been tested for altered expression of synaptic plasticity, focussing on paired-pulse facilitation (PPF), paired-pulse depression (PPD), post-tetanic potentiation (PTP) and long-term potentiation (LTP).

In addition, short-term potentiation, long-term depression and short-term depression can all be generated in the hippocampus.

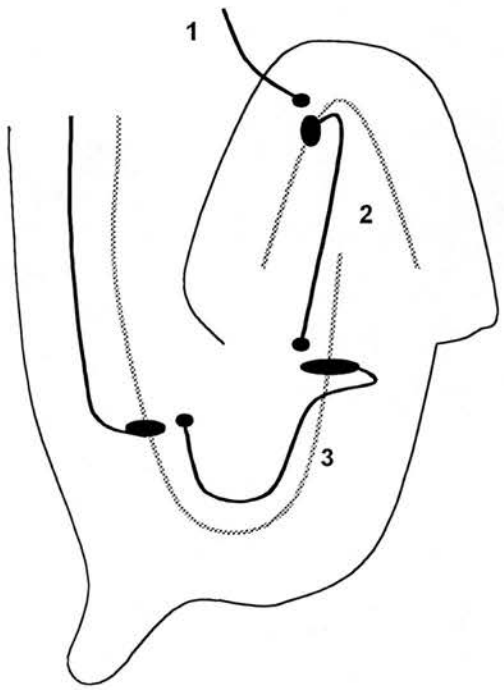

Figure 3.1 The Hippocampal Trisynaptic Pathway

This diagram shows the trisynaptic pathway in a transverse section of the hippocampus. The perforant pathway ***(1)*** *projects from the entorhinal cortex to the dentate gyrus granule cells. Axons from the granule cells form the mossy fibres* ***(2)****, which synapse onto CA3 pyramidal neurones. Axons from CA3 pyramidal neurones form the Schaffer collaterals* ***(3)****, which synapse onto CA1 pyramidal neurones.*

3.1 Paired pulse plasticity

When two stimuli are given to presynaptic neurones with a short interpulse interval (<2 seconds), the postsynaptic response to the second stimulus may be either depressed (PPD) or facilitated (PPF) with respect to the response to the first stimulus. When studied using field potential recordings, a specific synaptic connection tends to reliably show plasticity in one direction. For example, PPF is commonly observed in CA1 pyramidal neurones in response to Schaffer collateral stimulation and in dentate gyrus granule cells in response to lateral perforant pathway stimulation, whereas stimulating the medial perforant pathway generates PPD in dentate gyrus cells. When recorded intracellularly both PPF and PPD can be generated by the same cell. If the response to the first pulse is large then the then the response to the second pulse is depressed (PPD). Conversely, if the first response is small, the second response is facilitated (PPF) (Debanne et al 1996).

3.11 Paired pulse facilitation

Paired pulse facilitation is believed to be presynaptically generated by mechanisms that control the level of neurotransmitter release. Katz and Miledi described the *Residual Calcium Hypothesis of PPF* in 1968, which states that the influx of Ca^{2+} into the presynaptic bouton in response to the second stimulus is supplemented by calcium remaining in the bouton from the first stimulus. This elevated concentration of Ca^{2+} increases the release probability of available neurotransmitter vesicles (Katz & Miledi 1968). CA3/CA1 glutamatergic synapses have an average of 5 vesicles ready for release (Dobrunz & Stevens 1997) but only one active zone (Sorra & Harris 1993) and so they release either 1 or no vesicles in response to an action potential. If the probability of release is low then many synapses will fail to release neurotransmitter in response to the first stimulus, generating a small EPSP. However, the probability of release in response to the second stimulus is greater due to the elevated Ca^{2+} concentration so more synapses release neurotransmitter and the second response is larger. The low probability of neurotransmitter release in response to the first stimulus may be due to the lower density of neurotransmitter vesicles observed in synapses that express PPF (Bower and Haberly 1986).

It takes less than 1 second for the concentration of cytosolic Ca^{2+} in the presynaptic terminal to return to normal following a single action potential (Regehr et al 1994). That PPF can outlast the elevation of Ca^{2+} suggests additional mechanisms are involved, and these may not necessarily be presynaptic. Postsynaptic calcium-calmodulin kinase IIα (CaMKIIα) may contribute, since mice lacking this protein show weaker PPF (Silva et al 1992).

3.12 Paired pulse depression

The mechanisms of PPD in dentate granule cells are not well understood due to the paucity of intracellular studies on these relatively small neurones, however, the tri-phasic change in PPD magnitude with changing interpulse interval (figure 3.2) suggests that the situation is more complex than for PPF and that it is not merely due to neurotransmitter depletion.

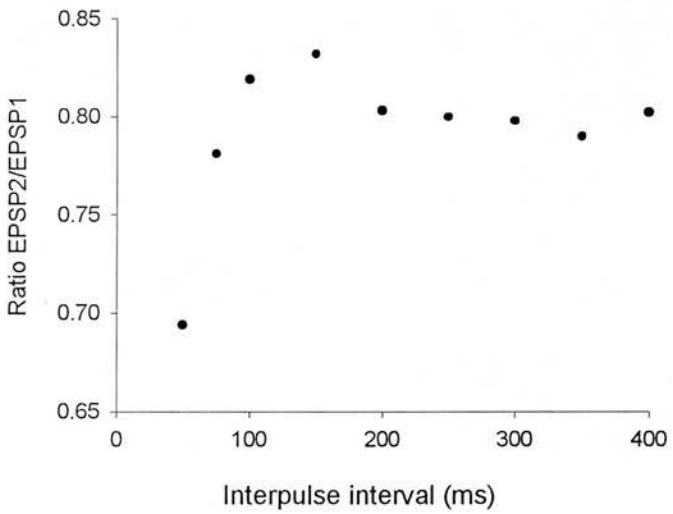

Figure 3.2 Dentate Gyrus Granule Cell Paired Pulse Depression

The level of depression decreases dramatically between interpulse intervals of about 50-100ms after which it increases gradually until a plateau of depression is achieved from intervals of about 200ms.

Depression at short interpulse intervals (up to about one-hundred milliseconds) has been attributed to GABAergic feed-forward inhibition (Burdette & Gilbert 1995). It appears that only $GABA_A$ receptors are active on dentate gyrus granule cells, generating IPSPs that peak at about forty milliseconds and last for about two-hundred milliseconds in single cell recordings (Steffensen & Henriksen 1991). This could account for the inhibition at short interpulse intervals, perhaps slightly longer than two-hundred milliseconds when imperfect synchronicity of neuronal firing in field studies is considered.

However, other mechanisms are needed to explain the persistance of PPD well beyond the time scale of a $GABA_A$ IPSP. It is possible that PPD is also mediated by the slow potassium-dependent afterhyperpolarization that has been observed following perforant pathway stimulation (Rausche et al 1989). This lasts for over a second and so might become the dominant influence of PPD at longer interpulse intervals. The mechanisms that generate PPD must exert strong inhibition to override the events that lead to PPF generation.

3.2 Post-tetanic potentiation

Following a transient, high intensity burst of stimuli (or tetanus) the postsynaptic response increases rapidly, often to 2 or 3 times the resting level. This potentiation reaches its peak typically within 2 minutes and lasts for less than 10 minutes. Like paired pulse facilitation, it is generated by elevated Ca^{2+} concentrations in the presynaptic bouton. Mitochondria allow potentiation to persist by sequestering Ca^{2+} during the tetanus. This is gradually released back into the cytosol, retarding the rate of Ca^{2+} buffering (Tang & Zucker 1997).

3.3 Long-term changes in synaptic strength

Paired-pulse plasticity and post-tetanic potentiation only account for changes in synaptic strength that last for seconds or minutes. More persistent synaptic modifications, LTP and LTD, last for at least an hour and can persist for several days *in vivo* (Bliss & Lomo 1973) and involve far more complex mechanisms involving both presynaptic and postsynaptic sites, which are as yet only partially

understood. Potentiation that obviously outlasts PTP but decays before 1 hour is termed short-term potentiation (STP) and is normally evoked by smaller conditioning trains of stimuli than those that induce LTP, which has a higher threshold for induction, and may involve different expression mechanisms (Schultz & Fitzgibbons 1997b).

LTP in the dentate gyrus was the first long-lasting form of synaptic plasticity to be described (Bliss & Lomo 1973), since when similar modifications have been observed in many excitatory and inhibitory synapses throughout the brain. LTP is generated experimentally by a high frequency burst of stimuli (HFS), usually comprising a one-hundred Hertz burst lasting for 1 second or multiple bursts (for example, 10 bursts of 4 pulses at 100 Hertz every two-hundred milliseconds) termed theta burst stimulation (TBS), argued to mimic more physiological patterns of hippocampal activity. Long-term depression (LTD) in the hippocampus is best induced by low frequency stimulation (LFS) of around 1 Hertz for 10 to 15 minutes.

Various types of LTP and LTD have been described as it has become apparent that there are pathway- and stimulation protocol-specific differences in the mechanisms of induction and expression. Long-term synaptic plasticity in the perforant pathway/dentate gyrus and CA3/CA1 pathways are commonly described as NMDA-dependent (although non-NMDA components have been isolated) whilst mossy fibre/CA3 LTP is NMDA-independent. The following discussion relates to NMDA-dependent long-term synaptic plasticity recorded in the dentate gyrus and CA1. NMDA-independent LTP mechanisms are described at the end of the chapter.

3.31 Properties of long-term plasticity

LTP exhibits the properties of cooperativity, persistence, associativity, input specificity and metaplasticity. LTP is induced when excitation of a postsynaptic cell reaches a physiologically determined threshold. This requires multiple inputs to be active together and/or to fire with a certain pattern (McNaughton et al 1978). In experimental conditions, the stimulus used to induce LTP is often as little as 1 second long, but potentiation can persist for hours. LTP can be induced in synapses receiving a sub-threshold input when an LTP-inducing stimulus is given simultaneously onto the same neurone (Levy & Steward 1979). Such a mechanism may underly associational learning during classical conditioning. Formally, it was believed that only synapses that are active during induction

are able to express LTP (Andersen et al 1977, Lynch et al 1977). This allows much greater capacity for storing memories since plasticity occurs at the level of the synapse rather than at the level of the neurone. However, more recently it has been found that specificity may not be absolute. Superperfusion techniques developed by Engerg and Bonhoeffer allow activation of synapses to be restricted to within approximately thirty micrometres from the electrode. However, synapses within seventy micrometres were potentiated by tetanic stimulation in the CA1 (Engert and Bonhoeffer 1997). This suggests that localized groups of synapses rather than individual synapses may be the unit of memory formation. The threshold for inducing LTP is not fixed, but can change in response to the history of synaptic activity. As a pathway becomes more potentiated, its threshold increases whereas a relatively quiet pathway has a lower threshold (Ngezahayo et al 2000). This *metaplasticity* could function to preserve responsiveness in quiet pathways and prevent saturation and seizure activity in more active pathways. LTD in the adult hippocampus has also been shown to exhibit cooperativity, persistence, associativity, input specificity and metaplasticity (Ngezahayo et al 2000).

3.32 Induction of NMDA-dependent plasticity

LTP induction in the CA1/CA3 pathway is dependent on Ca^{2+} influx through NMDA receptor-linked ion channels (Collingridge et al 1983). During low level synaptic activity, the NMDA receptor contributes little to the EPSP. Its ion channel is blocked by a magnesium ion that is only removed once the postsynaptic membrane is depolarized. Therefore, the NMDA receptor acts as a detector of coincident presynaptic and postsynaptic activity. Due to the channel's slow activation kinetics, any contribution made by NMDA receptor-mediated currents are swamped by feedforward and feedback GABAergic inhibition.

During and after an LTP-inducing tetanus, NMDA receptor activity makes a greater contribution to postsynaptic depolarization. EPSP summation during the tetanus prolongs postsynaptic membrane depolarization, which removes the magnesium block. Also, $GABA_B$ autoreceptors inhibit GABAergic interneurone activity by approximately 10 milliseconds into the tetanus (Davies et al 1991). Indeed, activation of presynaptic $GABA_B$ receptors is necessary for LTP (Davies et al 1991). Slow NMDA receptor inactivation allows efficient EPSP summation during the tetanus, which facilitates the build-up of Ca^{2+} in dendritic spines. There is evidence that this is supplemented by Ca^{2+}

released from intracellular stores, stimulated by metabotropic glutamate receptor activation and also by Ca^{2+} itself.

The potential for LTP to subserve memory was realized early on with the recognition of similarities between LTP properties and the theoretical mechanism of memory formation devised by the psychologist Donald Hebb (Hebb 1949). The rule for Hebbian learning states that;

'When an axon of cell A ... excite(s) cell B and repeatedly or persistently takes part in firing it, some growth process or metabolic change takes place in one or both cells so that A's efficiency as one of the cells firing B is increased.'

Ca^{2+} is thought to induce LTP by binding calmodulin, creating a complex capable of activating kinases such as CaMKIIα, PKC and tyrosine kinases. CaMKIIα is essential for both induction of LTP (Liu et al 1999) and spatial learning as demonstrated by deficits in CaMKIIα null mice (Silva et al 1992). During LTP induction, the increase in postsynaptic Ca^{2+} concentration stimulates CaMKIIα autophosphorylation within 15 minutes of the LTP-inducing stimulus (Barria et al 1997). Its activity is prolonged for over an hour (Fukunaga et al 1993) and so it may serve as a memory of the transient increase in Ca^{2+} concentration. It is possible that CaMKIIα levels in active dendritic spines are increased by protein synthesis in the dendrites since CaMKIIα levels increase within 5 minutes of an induction stimulus, which precludes transport of new protein from the soma, and CaMKIIα mRNA is abundant in forebrain neurone dendrites (Ouyang et al 1999).

Activated CaMKIIα is translocated to the postsynaptic density where it forms a complex with the NMDA NR2B subunit (Strack & Colbran 1998). The formation of this complex may allow CaMKIIα to remain active when Ca^{2+} levels have returned to normal by holding it near a site of Ca^{2+} influx. Persistent phosphorylation of CaMKIIα may also be facilitated by suppression of protein phosphatases. A stimulus that is subthreshold for LTP generation coupled with phosphatase inhibitors or adenylate cyclase activators leads to CaMKIIα autophosphorylation and induction of LTP (Makhinson et al 1999).

LTD induction is also dependent on Ca^{2+} influx through NMDA receptor-linked ion channels (Dudek & Bear 1992) but this leads to enhanced phosphatase rather than kinase activity (Mulkey et al 1993). The calcium calmodulin complex is formed as in LTP, but to generate LTD it activates the

phosphatase calcineurin. This can release protein phosphatase 1 from inhibition by suppressing inhibitor-1 activity (Mulkey et al 1994).

STP is NMDA-dependent and probably represents early plastic changes that are necessary but not always sufficient for initiating further mechanisms responsible for more sustained potentiation.

3.33 Bidirectional synaptic modification

Synaptic potentiation is not a permanent state. Both LTP and LTD can be induced in the same population of synapses and are mutually reversing. The first experimental evidence for bidirectional synaptic modification was described in dentate gyrus granule cells. HFS induction of LTP could be reversed by LFS induction of LTD (Xie et al 1992). Both LTP and LTD were NMDA receptor-dependent and were impaired by chelating intracellular Ca^{2+} with BAPTA, showing that they required postsynaptic Ca^{2+} influx (Xie et al 1992).

Applying stimuli of different frequencies to a modifiable pathway exposes the bidirectional nature of synaptic plasticity. *In vitro*, six-hundred pulse stimulation of the Schaffer collaterals at <5Hz generated LTD at CA1 pyramidal cell synapses whilst stimulation at >15Hz generated LTP. Stimulation at around 10Hz failed to generate lasting synaptic plasticity (Steel and Mauk 1999).

The nature of plasticity generated by a stimulus depends on the level of postsynaptic depolarization and the resulting increase in Ca^{2+} concentration. It is differences in these parameters that allows either LTP or LTD to be generated using different frequencies or strengths of stimulation. Postsynaptic depolarization and Ca^{2+} concentration increase must be strong to induce LTP and milder to induce LTD and manipulating these variables allows different responses to be generated by the same stimulus. In the CA1, LTD can be induced by HFS that usually generates LTP if it is paired with partial block of NMDA receptors (Cummings et al 1996), partial buffering of intracellular Ca^{2+} (Brocher et al 1992) or by perfusing tissue with low Ca^{2+} aCSF (Mulkey & Malenka 1992). Stimulation of around 10Hz, which usually fails to induce lasting synaptic plasticity, induces LTD when coupled with postsynaptic hyperpolarization (Xie et al 1992) or in tissue perfused with low Ca^{2+} buffer and LTP in tissue perfused with high Ca^{2+} buffer (Coussens & Teyler 1996).

The nature of synaptic plasticity may be influenced by the pattern as well as the magnitude of Ca^{2+} elevation. Under stimulus conditions that generate LTP and LTD with near-equal probability,

simultaneous release of caged Ca^{2+} to increasing the magnitude of Ca^{2+} concentration elevation generates LTP, whilst increasing the duration of Ca^{2+} elevation generates LTD (Yang et al 1999b). These observations are described by the Bienenstock, Cooper & Munro model (reviewed in Bear 1996) where the transition between LTD and LTP inducing levels of postsynaptic depolarization/Ca^{2+} accumulation occurs at the modification threshold Θ_m (Figure 3.3).

The NMDA receptor was a possible candidate for gating Ca^{2+} influx and so determining the value of Θ_m. LTD would be induced by stimuli that were too weak to activate NMDA receptors whilst strong stimuli would activate NMDA receptor-mediated Ca^{2+} influx and induce LTP. However, it was found that LTD is NMDA receptor-dependent (Dudek & Bear 1992). Also, stimulation of CA1 pyramidal neurones can cause NMDA receptor activation and NMDA-induced release of Ca^{2+} from intracellular stores without inducing synaptic plasticity (Emptage et al 1999).

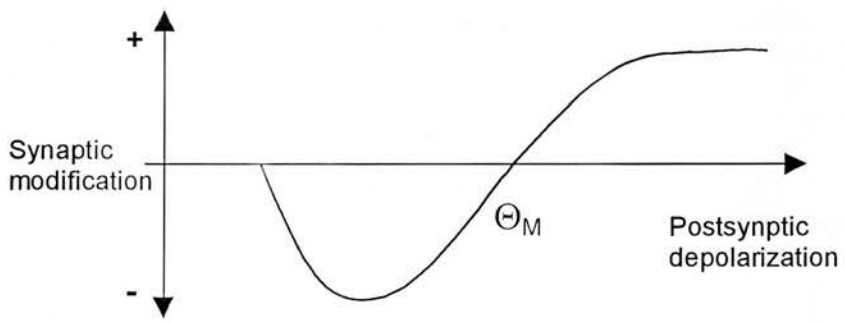

Figure 3.3** The Bienenstock, Cooper & Munro **Model of Bidirectional Synaptic Modification

Postsynaptic depolarization below Θ_m generates LTD and above Θ_m generates LTP. The value of Θ_m can change depending on the history of synaptic activity.

Induction of LTP leads to protein kinase activity (Huang & Hsin 1999a) whilst LTD involves phosphatase activity (Mulkey et al 1993). It was proposed that failure of 10Hz stimulation to induce synaptic plasticity was due to a balance between the induction of kinase and phosphatase activity. 10Hz stimulation of CA3/CA1 synapses treated with the protein kinase inhibitor, H-7 expressed LTD whilst those treated with the phosphatase inhibitor, tautomycin expressed LTP (Coussens & Tyler 1996) suggesting that the gating mechanisms for bidirectional synaptic modification regulate the relative activities of kinases and phosphatases in response to Ca^{2+} influx.

3.34 The modifiable threshold

The value of Θ_m is sensitive to the history of synaptic activity and so subserves metaplasticity. This is important since a static Θ_m would lead to persistent potentiation in some synapses and depression in others. A modifiable Θ_m allows for bidirectional synaptic modification and maintenance of synaptic sensitivity.

Modification of Θ_m can be generated by stimuli even if they fail to induce synaptic plasticity. The CA1 response to HFS varies following priming stimuli of six-hundred conditioning pulses at either 3, 10 or 30Hz. HFS generated no potentiation after 3Hz priming, weak transient potentiation following 10Hz priming and gradually developing, stable potentiation following 30Hz (Wang & Wagner 1999b).

LTP induction is enhanced by mGluR activation (Raymond et al 2000) and impaired by weak NMDA receptor activation. mGluR priming establishes a lasting threshold for LTP induction by a PKC-dependent mechanism (Bortolotto & Collingridge 2000) that results in local protein synthesis (Raymond et al 2000). PKC may act through the mitogen activated protein kinase p42 MAPK (Sweatt 2001) to increase local protein synthesis. A possible target would be CaMKIIα mRNA which is abundant in dendrites and CaMKIIα is upregulated and activated during LTP.

$GABA_A$ activity may modify Θ_m. $GABA_A$ agonists facilitate LTD induction by shifting the threshold to a more depolarized membrane potential whilst $GABA_A$ antagonists facilitate LTP by shifting the threshold to a more polarized postsynaptic membrane potential (Steel & Mauk 1999). Transgenic mice that express constitutively active *fyn* tyrosine kinase have depressed GABA activity. LTP can be generated in hippocampal slices from these mice using stimuli that fail to induce synaptic

modification in wild-type mice (Lu et al 1999b). In the CA1, pyramidal neurone activity is suppressed by recurrent GABAergic inhibition. The strength of the inhibition is proportional to the activity in pyramidal neurones and so may provide a mechanism of keeping the pathway within a functional range of activity (Steel & Mauk 1999).

3.35 Site of expression of long-lasting plasticity

The expression mechanisms of synaptic modification are still poorly understood. Elucidating these mechanisms has involved extensive research over nearly thirty years aimed at identifying the site of expression, whether presynaptic or postsynaptic. The methods most commonly employed are investigation of the interaction between long-term plasticity and PPF and quantal analysis.

PPF analysis of site of expression

PPF is believed to be presynaptically generated, and is weakened by manipulations that increase the probability of neurotransmitter release (for example, increased extracellular Ca^{2+} concentration (Creager et al 1980)). It is therefore suggested that putative presynaptic LTP expression would involve an increase in the probability of neurotransmitter release and so result in PPF depression whilst PPD would involve a decrease in neurotransmitter release and so result in PPD. McNaughton first studied LTP-linked changes in PPF at the lateral perforant pathway/dentate gyrus synapse (McNaughton 1982). He found that whilst PPF was initially depressed, it recovered to baseline levels by the end of the PTP phase. Similar results were recorded in the CA1 (for example Manabe et al 1993). However, more persistent depression of PPF during strong LTP expression has been observed in both pathways (for example in the CA1, Kuhnt & Voronin 1994 and in the DG, Christie & Abraham 1994). Kleschevnikov and collegues recognised that PPF depression is not observed during weak LTP expression, and in some cases PPF actually strengthened slightly, which may explain the negative results reported in the earlier papers (Kleschevnikov et al 1997).

Strong pre-tetanic PPF predicts strong LTP and a greater and more persistent decrease in PPF magnitude following LTP-inducing stimulation (Kleschevnikov et al 1997). During the first thirty minutes following a high frequency tetanus, the magnitude of LTP is most strongly correlated with the decrease in PPF strength, indicating a strong role for presynaptic mechanisms. By sixty minutes post-

tetanus, the magnitude of LTP correlates only weakly with the change in PPF strength, suggesting that postsynaptic mechanisms are more prominent. However, the magnitude of LTP correlates strongly with the strength of pre-tetanic PPF (Kleschevnikov et al 1997). Large PPF may reflect a greater capacity for plastic change in a pathway. This accords with the BCM model of synaptic modification since large PPF would reflect low probability of transmitter release associated with depressed synapses, in which Q_m would be shifted to a more hyperpolarized level, facilitating LTP.

Therefore, results from PPF studies suggest that presynaptic mechanisms may be important for the first thirty minutes of LTP with postsynaptic or intermediate changes becoming more influential as stable LTP becomes established.

Quantal analysis of site of expression

Quantal analysis is based on the theory that neurotransmitter is released in discrete units of uniform quantity, termed quanta. Spontaneous miniture postsynaptic potentials are assumed to represent single synaptic events and are equivalent in amplitude to quantal size. Quantal size is determined by the amount of transmitter per quanta (which is often assumed to be constant), the proportion of transmitter that reaches postsynaptic receptors and the sensitivity of those receptors, and can therefore be influenced by postsynaptic and intermediate changes in synaptic transmission. The number of neurotransmitter vesicles released in response to a stimulus is termed quantal content, which is determined by the number of vesicle release sites and the average release probability. Therefore, changes in quantal content are usually assumed to reflect presynaptic alterations.

The parameters often measured during quantal anaylsis of LTP are transmission failure rate, which is measured directly as the proportion of stimuli that do not generate a postsynaptic response; quantal size, which is equivalent to the miniture excitatory postsynaptic potential (mEPSP) or current (mEPSC) amplitude and quantal content that can be calculated as the evoked EPSP amplitude divided by the mEPSP amplitude.

mEPSC amplitude has been observed to increase during LTP without a change in frequency (Cormier & Kelly 1996), which suggests a postsynaptic increase in receptor sensitivity or an increase in the number of functional receptors. However, in another study the frequency of mEPSCs increased without a change in amplitude (Sastry and Bhagavatula, 1996) when LTP was induced using a

different method, suggesting increased presynaptic probability of transmitter release or up-regulation of functional release sites, although it might also reflect postsynaptic activation of receptors where transmission failure was due to lack of receptors rather than failure of transmitter release.

LTP induction leads to a decrease in the transmission failure rate (Stricker et al 1996, Sastry & Bhagavatula 1996, Kuhnt & Voronin 1994). This may reflect an increased probability of transmitter release. There is evidence that in the hippocampus, a single quantum of glutamate saturates the available postsynaptic receptors. However, the average probability of transmitter release is thought to be low (Hessler et al 1993), which suggests that a decrease in the transmission failure rate involves activation of transmitter release from previously inactive syanpses or activation of postsynaptic receptors that were previously either absent or not functional.

Both quantal content and quantal size increased in response to LTP inducing stimuli in one study (Stricker et al 1996), which failed to determine whether presynaptic or postsynaptic mechanisms had been recruited, whilst another study showed a significant change in quantal content with quantal size increase making only a small contribution to LTP (Voronin et al 1992), suggesting a presynaptic locus. Many studies have concluded that both presynaptic and postsynaptic mechanisms are responsible for LTP expression.

Kullmann et al (1992) concluded that various mechanisms could contribute to LTP expression, since they were able to generate LTP that increased either quantal content, quantal size or both parameters. Involvement of both presynaptic and postsynaptic mechanisms was also suggested by Larkman and collegues (Larkman et al 1992).

A more sophisticated study measured the changes in PPF quantal parameters before and after an LTP-inducing tetanus (Khunt & Voronin, 1994). Before the tetanus, the second stimulus for PPF had a larger quantal content value only, supporting a presynaptic locus for PPF. For twenty minutes following the tetanus, PPF was reduced and both quantal size and content increased in proportions that suggested both pre and postsyanptic changes were active. Synaptic transmission during LTP has been studied between individual pairs of CA3 and CA1 neurones, showing a post-tetanic decrease in failure of transmission and increase in quantal size (Malinow 1991). Therefore, as in the PPF studies, quantal analysis supports involvement of both presynaptic and postsynaptic mechanisms in LTP expression.

It is becoming clear that complex time-dependent synaptic alterations accompany the development of LTP expression. Early LTP expression (1 to 2 hours following induction) involves protein kinase activity and protein synthesis from existing mRNA, and is now distinguished from late LTP expression (over 10 hours) that requires gene expression. The complex development of these expression mechanisms may make the results of PPF and quantal analysis studies highly dependent on the time following the tetanus during which they are recorded.

3.36 Possible mechanisms of long-term synaptic modification

Possible mechanisms for LTP and LTD include mobilization of AMPA receptors to and from the postsynaptic density, morphological changes, receptor phosphorylation or dephosphorylation, altered glutamate release and retrograde messengers.

AMPA receptors and the silent synapse hypothesis

It has been assumed that both AMPA and NMDA receptors are present at all glutamatergic synapses. In fact, some hippocampal synapses fail to express AMPA mediated currents (Gomperts et al 1998) and following LTP induction the number of such so-called silent synapses decreases. This suggests that expression of LTP is dependent on an increase in AMPA mediated currents, either by activation of receptors that were previously present but not functional or by insertion of new receptors into the postsynaptic density. The conversion of silent synapses to active synapses is a postsynaptic event, but in quantal analysis would be detected as an increase in the frequency of mEPSCs, which would be interpreted as presynaptic. This highlights how the assumptions upon which quantal analysis is based can generate misleading conclusions.

The AMPA receptor, and the form containing the GluR1 subunit in particular, is required for LTP expression. Receptors consisting of GluR1/GluR2 heteromers are concentrated in the hippocampus. Mice lacking the GluR1 receptor develop normally, as other subunit types combine with GluR2 to maintain normal synaptic transmission, but these animals fail to express LTP in the CA1 and have impaired DG LTP (Zamanillo et al 1999).

The migration of new receptors into the postsynaptic density as a mechanism for LTP expression was hypothesized by Xie et al (1997b) to explain the differential contribution of NMDA

receptor- and AMPA receptor-mediated currents to LTP in dentate gyrus granule cells. Computer modelling showed that whilst changes in NMDA receptor conductance may be explained by increased receptor sensitivity, changes in AMPA receptor conductance were best explained by migration of receptors closer to the site of presynaptic transmitter release. Recent evidence has supported the importance of new AMPA receptors. NMDA-dependent LTP resulted in upregulation of AMPA receptors as was shown by ELISA to detect AMPA receptor proteins in the membrane fraction (Lu et al 2001). Immunostaining showed AMPA receptors to have clustered at the postsynaptic density (Lu et al 2001). AMPA insertion was blocked by tetanus toxin suggesting SNARE-dependent exocytosis (Lu et al 2001). GluR1 tagged with green fluorescent protein was shown to be concentrated in dendrites near the base of spines and to migrate into the spines following LTP induction (Shi et al 1999). AMPA receptor insertion explains the increase in quantal size measured at tetanized synapses, and concurs with the idea that neurotransmitter availability is not a limiting factor in the size of the postsynaptic response. The migration of GluR1 in response to a tetanus was dependent on NMDA receptor activation, further supporting the link between NMDA receptor activity and LTP. GluR1 was inserted into both silent and AMPA receptor-containing synapses and some of the new receptors were detected at the cell surface suggesting that they were available to participate in neurotransmission. Therefore phosphorylation of GluR1 possibly mediates AMPA receptor migration to the postsynaptic density to allow LTP expression.

Brefeldin, an inhibitor of protein trafficking, impaired NMDA-dependent LTP and western analysis of the membrane fraction showed it to have prevented an LTP-associated increase in membrane bound-GluR1 (Broutman and Baudry 2001).

This receptor migration occurred within about 15 minutes of the tetanus (Shi et al 1999), concurring with the observation that potentiation is stabilized within an hour of LTP induction. An increase in AMPA receptor sensitivity has been measured starting a few minutes after the tetanus but taking about an hour to reach a plateau, which may reflect the gradual addition and activation of new receptors at the postsynaptic density. Early increases in AMPA receptor sensitivity may be attributed to phosphorylation and increased conductance of active AMPA receptors, whilst increases after 15 minutes and more could involve the insertion of new receptors into silent synapses.

AMPA receptor insertion and removal from the postsynaptic density may be mediated by the interaction between GluR2 and the membrane fusion protein N-ethyl-maleimide-sensitive fusion protein (NSF). AMPA receptors are stabilized at the cell membrane by association of the GluR2 subunit with NSF. Impeding GluR2 association with NSF with pep2m leads to a decrease in the intracellular pyramidal CA1 response to locally applied AMPA and a decrease in cell surface GluR2 immunoreactivity. Neurones treated with pep2m showed no reduction in the level of dendritic GluR2, but less of the protein was located in the cell membrane suggesting that AMPA receptors can be removed from the postsynaptic density and held in a dendritic pool (Noel et al 1999).

LTD may be mediated by removal of AMPA receptors from the postsynaptic density. CA1 pyramidal neurones perfused intracellularly with pep2m failed to express LTD, whilst synapses that were expressing strong LTD following low frequency stimulation of the Schaffer collaterals failed to be further depressed by pep2m. That these two methods of synaptic depression are mutually occluding suggests that they use a common mechanism. No change in the kinetics of AMPA receptors was observed, suggesting that LTD and pep2m depress the AMPA response by reducing the number of functional receptors (Luthi et al 1999).

It has been suggested that LTP is generated at individual synapses in an all-or-none manner (Petersen et al 1998). Minimal stimulation intended to activate single synapses was paired with postsynaptic depolarization to induce LTP. The majority of synapses showed one of three responses when tested with a short pairing sequence followed by a long pairing sequence; potentiation in response to the short sequence only, potentiation in response to the long sequence only or no potentiation. Only one cell showed potentiation in response to both sequences. The short and long sequences generated potentiation of similar magnitude indicating all-or-none LTP generation. That some synapses required a longer pairing sequence indicates that they have different thresholds for LTP induction.

This data can be interpreted in the light of the silent-synapse hypothesis. If indeed Petersen et al were recruiting and potentiating single synapses then these already had functional AMPA receptors. Indeed, additional AMPA receptors have been observed to migrate into active synapses following LTP induction. This suggests that although the level of LTP generated in response to an induction event may be all-or-none, such step-wise increases in potentiation may be repeated. The second

pairing sequence in the Petersen experiment was given within only a few minutes of the first, during which time LTP expression would not have been established. If importation of AMPA receptors is the key event in stabilizing LTP then giving a second pairing sequence after an hour or more may allow further potentiation.

Potentiation at silent synapses necessitates activation of more than one synapse, since AMPA receptor activation at another site is needed to depolarize the postsynaptic cell and allow NMDA receptor activity. It is possible that individual synapses are only potentiated once, as implied by Petersen et al, but that the increase in response generated by their technique was due to recruitment of silent synapses. This would suggest that AMPA receptors migrating into active synapses do not become established in the postsynaptic membrane and do not contribute to LTP but that the all-or-none expression of LTP is due to the activation of an adjacent silent synapse.

Most studies have investigated silent synapses that lack functional postsynaptic AMPA receptors. However, silent synapses may have functional receptors but fail to release neurotransmitter. Late LTP is dependent on cAMP activity. LTP induced by cAMP leads to an increase in the level of active presynaptic terminals shown by fluorescent dye (Fm1-43), suggesting that late expression of LTP may involve facilitation of neurotransmitter release from previously inactive synapses (Ma et al 1999).

Morphological changes

Recent studies have shown that morphological changes can occur rapidly and may be important for LTP expression. Some active spines develop protrusions into the presynaptic bouton forming a spinule, which may develop to such an extent that independent active zones are formed within the same synapse, enhancing synaptic efficacy. These are known as perforated synapses. Electron microscopy analysis of synapses following LTP induction shows an increase in the proportion of perforated synapses by 5 minutes post-tetanus (Toni et al 1999).

The proportion of perforated synapses peaks by about thirty minutes and decays to baseline levels within an hour. This decline is concommitant with an increase in the proportion of boutons contacting multiple spines (Toni et al 1999). Three-dimensional reconstruction of neurones filled with the fluorescent dye calcein shows formation of new spines within forty minutes post-tetanus (Engert

and Boenhoeffer 1999). In untetanized sections the majority of multiple spine boutons are contacted by spines from different dendrites. In tetanized sections the number of multiple spine boutons increases and a greater proportion involve spines arising from the same dendrite. The new spines had a long neck, well developed postsynaptic density and were associated with vesicle-rich boutons suggesting that they could be fully functional (Toni et al 1999). However, Shi et al suggest that new AMPA receptors do not enter new spines (Shi et al 1999). Therefore, they may form silent synapses and be a means of preventing saturation of LTP at a neuronal level rather than contributing to potentiation resulting from the current induction events.

One electron microscopy study observed no significant change in synapse number or morphology following LTP induction, however, the authors acknowledged that their sample size was small, and so did not argue strongly against the possible contribution of morphological changes to LTP (Sorra & Harris 1998).

Guidance of morphological changes and stabilization of synapses may be regulated by the HSPG, N-syndecan. During LTP, N-syndecan forms a complex with *fyn* tyrosine kinase that accumulates in the cell membrane (Lauri et al 1999) where it would be available to mediate interactions between the neurone and the extracellular matrix.

Receptor phosphorylation

Src-family protein kinases can induce potentiation that occludes tetanic LTP induction (Huang & Hsin 1999a). The NMDA NR2B subunit is phosphorylated by the *src* tyrosine kinase during LTP, which increases the conductance of NMDA receptors (Huang et al 2001). This is mediated by cell adhesion kinase β/proline-rich tyrosine kinase 2 (CAKβ/Pyk2) which is activated by PKC following increases in intracellular Ca^{2+} concentration and binds *src* tyrosine kinase, releasing it from autoinhibition. This may facilitate Ca^{2+} influx during early LTP and promote Ca^{2+} dependent mechanisms of expression such as maintaining activity of CaMKIIα. Inhibition of CAKβ/Pyk2 blocks LTP induction whilst intracellular CAKβ/Pyk2 perfusion CA1 pyramidal neurones induces potentiation that occludes tetanic LTP induction (Huang et al 2001).

CaMKIIα can phosphorylate the AMPA receptor GluR1 subunit (Barria et al 1997), which increases the size of Na^+/K^+-mediated AMPA ESPCs. Other AMPAR subunits may also have

phosphorylation sites with similar functions. Stabilization of CaMKIIα at the postsynaptic density by binding the NMDA NR2B subunit may facilitate AMPA receptor phosphorylation (Leonard et al 1999).

PKA is activated 2 to 10 minutes following tetanization and may facilitate CaMKIIα activation by decreasing protein phosphatase activity and so promoting autophosphorylation. LTP induction in the dentate gyrus is also NMDA receptor dependent and probably involves autophosphorylation of CaMKIIα.

NMDA-dependent LTP expression involves activation of the mitogen activated protein kinase ERK (Kanterewicz 2000). ERK activation may have various roles including activation of gene expression, and so may be relevant to the transition from early to late LTP.

LTD involves increased phosphatase activity that could theoretically reverse LTP-induced receptor phosphorylation.

Glutamate release

Manabe and Nicoll argue that increased glutamate release is not a feature of CA1 LTP since the post-tetanic decline in currents through persistently open NMDA receptor-linked channels followed the same time course in tetanized and untetanized pathways (Manabe & Nicoll 1994). Whilst CA1 LTP expression appears to be increasingly postsynaptic with time, in the dentate gyrus, a persistent increase in glutamate release from the medial perforant pathway has been observed (Dolphin et al 1982, Bliss et al 1986, Errington et al 1987). Increase in glutamate release probability may result from the phosphorylation of synaptic proteins such as rabphilin-3A, which is phosphorylated by PKA and CaMKIIα (Fykse et al 1995).

Retrograde messengers

Experimental generation of associative LTP in the CA1 by linking a weak input with an LTP-inducing input, causes depression of PPF at synapses that receive only a weak input (Kleschevnikov et al 1997). This suggests that the probability of glutamate release is increased from these terminals even though they were not subject to the LTP-inducing stimulus. Therefore, it is suggested that induction events in dendritic spines lead to the release of a retrograde messenger that can modify the probability

neurotransmitter release from the presynaptic terminal. The identity of this putative retrograde messenger, required to coordinate presynaptic and postsynaptic changes, has not been resolved, although nitric oxide, carbon monoxide and arachadonic acid are all possible candidates. Of these, nitric oxide is a popular choice. Nitric oxide synthase can be activated by CaMKIIα. LTP is enhanced by nitric oxide donors (Malen & Chapman 1997) and impaired by nitric oxide synthase inhibitors (Haley et al 1992). LTP induced by postsynaptic injection of CaMKIIα is not sensistive to nitric oxide depletion (Ko & Kelly 1999a), which suggests that nitric oxide may maintain enhanced glutamate release to facilitate CaMKIIα autophosphorylation during LTP induction, which can then initiate postsynaptic changes.

3.37 NMDA-independent LTP

Mossy fibre/CA3 LTP

There is controversy over whether mossy fibre LTP induction is pre or postsynaptic. Kapur et al (1998) used two different stimuli and managed to isolate two forms of mossy fibre LTP. LTP induced by HFS comprising of few long bursts seemed not to involve postsynaptic NMDA or L-type channels. LTP induced by HFS comprising of many short bursts was also NMDA-independent but did require influx of Ca^{2+} through postsynaptic L-type voltage dependent Ca^{2+} channels and was blocked by nimodipine. Yeckel et al also tried to distinguish different mechanisms of LTP induction using different stimulation protocols but they observed an increase in postsynaptic Ca^{2+} concentration following brief HFS as well as following more prolonged stimulation. LTP induced by both protocols was blocked by intracellular Ca^{2+} buffer. They found that the rise in intracellular Ca^{2+} arose from intracellular stores and was dependent on mGluR activation (Yeckel et al 1999) This shows that this form of LTP at least does involve postsynaptic induction mechanisms, whilst it is possible that it is generated alongside LTP with different mechanisms that are not postsynaptically driven. Mossy fibre LTP does not involve activation of the mitogen-activated protein kinase ERK (Kanterewicz et al 2000). Lower frequency tetanization (25Hz) also induces mossy fibre LTP and this was not impeded by mGluR blockade or Ca^{2+} chelators (Mellor & Nicoll 2001).

CA1 NMDA-independent LTP

CA1 LTP is usually defined as being NMDA dependent. Whilst NMDA receptors are involved in CA1 LTP, NMDA antagonists have revealed an NMDA-independent component both *in vitro* (Grover & Teyler 1990, Stricker et al 1999) and *in vivo* (Morgan & Teyler 1999). NMDA antagonists reveal that about fifty per cent of the *in vivo* response is NMDA independent (Morgan and Teyler 1999). Instead it is induced by Ca^{2+} influx through L-type voltage dependent calcium channels. The cascades stimulated by these two forms of LTP are distinct. NMDA dependent LTP involves serine/threonine kinase activity and mGluR1 activity can modulate the LTP response. L-type voltage dependent calcium channels LTP involves tyrosine kinase activity. Gamma-protein activity and the group 1 mGluR1 and mGluR5 (that are abundant on CA1 pyramidal cells) do not contribute to NMDA-independent LTP induction however group 2 and group 3 mGluRs seem to be needed (Grover & Yan 1999).

Dentate gyrus NMDA-independent LTP

Dentate gyrus LTP can also be induced independently of NMDA receptor activation by either activating mGluR or stimulating Ca^{2+} influx through T-type voltage dependent calcium channels. All these forms of DG LTP are impaired by MAPK inhibitors (Coogan et al 1999).Medial perforant pathway-dentate gyrus synapses show NMDA-independent LTP and PPD. LTP induction by HFS was attenuated by high concentrations of MAPK inhibitors (Coogan et al 1999). The mitogen activated kinase p42 MAPK is involved in LTP expression. p38 MAPK, which can inhibit p42 MAPK activity, is active during NMDA-independent LTD expression (Bolshakov et al 2000). Therefore, whilst NMDA-dependent synaptic modification may be driven by relative activities of protein kinases and phosphatases, NMDA-independent synaptic modification may be driven by the opposing actions of p42 and p38 MAPK.

Chapter 4

Materials and Methods

4.1 Breeding programme

Fischer rats were genetically modified to carry the human PS1 gene with the Finnish M146V mutation (Estibeiro, Edinburgh University). In the affected human family, this mutation causes AD that has an especially early age of onset, which may facilitate the expression of AD-type abnormalities within the lifetime of a rat.

Mice have been the animal of choice in the majority of transgenic studies into AD. Although rats have a longer reproductive cycle, and so take longer to establish in transgenic lines, their neurophysiology is better understood since their larger size makes them preferable for intricate *in vivo* elecrophysiological studies.

In this transgenic line, the mutated human PS1 mRNA expression is 6 times greater than that of the endogenous rat PS1 mRNA. The mutated protein is expressed at a low, but detectable level. Mutated PS1 is thought to cause AD by increasing the level of $A\beta_{42/43}$ expression. Unfortunately, the $A\beta_{42/43}$ levels in these animals have not been quantified due to the lack of a commercially available ELISA kits for rat Aβ.

The rats were housed and bred in the Medical Faculty animal facility and monitored by trained staff. Rats from second litters were preferably chosen for breeding. Heterozygote rats were mated with wildtype partners to produce litters that gave approximately equal numbers of heterozygote and wildtype offspring. Ageing of Edinburgh rats beyond 18 months was prevented by illness, in particular the high incidence of tumours in rats approaching this age.

4.2 Genotyping offspring

4.21 Tagging and tail biopsy

Tail biopsies were taken from weaned offspring under general anaesthetic. Animals were anaesthetised by halothane inhalation in an anaesthetic chamber until the withdrawl reflex was absent in response to mild pinching of the hind paw. A tag was clipped to the ear of each animal bearing an identification number. Half a centimetre was taken from the end of the tail using a razor blade and placed in a microfuge tube labelled with the animal's tag number. The tail was pinched to minimize

bleeding while a drop of tail glue was applied to the cut end to induce blood coagulation and promote healing. The animal was then returned to their homecage where they recovered from the anaesthesia within a few minutes. Animals were observed until fully recovered.

4.22 DNA extraction

Microfuge tubes containing the tail biopsies were placed on ice and 500µl of PK digestion buffer was added to each. Samples were incubated at 55°C for about 36 hours after which they were spun for 10 minutes reducing any remaining solid material, which comprised mainly hair and bone, into a pellet. The supernatant was removed and treated with 500µls isopropanol. The tube was gently swirled to encourage the DNA to precipitate. The DNA was carefully picked out and the isopropanol drained off before being transferred into TE.1 pH7.5 (10mM pH7.5 tris, 0.1mM EDTA in sterile H_2O). This was heated for 15 minutes at 60°C. To fully resuspend the DNA, the microfuge tubes were periodically swirled. The samples were then stored at 4°C.

4.23 Southern blotting

Fifty microlitres of DNA solution was digested using 0.3µl EcoR1 in 40µl 10x H- (500mM NaCl, 100mM Tris 7.5, 100mM $MgCl_2$, 10mM DTT, 1mM spermidine and 1g BSA) and incubated in a water bath at 37°C overnight. The digests were heated to 67°C for 10 minutes after which $^1/_{10}$ volume NaAc and 2½ volume 100% EtOH was added. The digests were chilled at -20°C for 30 minutes to precipitate the DNA. They were centrifuged for 15 minutes to recover the DNA. Having removed the supernatant, the pellet was washed with 500µl 100% EtOH and centrifuged for a further 5 minutes. The EtOH was removed and the microfuge tubes left open on the bench to allow the pellet to dry. The DNA pellets were resuspended by heating in distilled water and Edye, which allowed the sample to be visualized on the gel.

Agarose gel was prepared in 1x TBE buffer with 5µls ethidium bromide, a DNA binder. The samples were loaded onto the gel and run at 150V for 1 to 2 hours. Once the marker had run about $^2/_3$ of the way down the gel, the gel was photographed under ultraviolet light to expose how far the samples had travelled, (poor sample mobility indicates incomplete DNA digestion by EcoR1). The gel was treated with 0.4M HCl for 15 minutes followed by 0.25M NaOH for 30 minutes. It was then

stacked overnight on top of a NaOH reservoir and against a sheet of positively charged nylon. The gel was exposed under ultraviolet light to ensure all of the DNA had transferred to the nylon sheet, which was rinsed in 4 x SCC and allowed to dry.

The probe for human PS1 was heated in a bath of boiling water for 10 minutes to denature the DNA into single strands. This was then cooled rapidly in an ice/water slurry to prevent reannealing of the DNA probe. To the probe was added nonaprimer mix, cATP, cGTP, cTTP, Kienow enzyme and the ^{32}PdCTP radioactive marker. This was heated at 35°C for 30 minutes. EDTA was added and the probe was heated again to 100°C for 10 minutes followed by rapid chilling in ice slurry. The nylon sheet was treated with prehybridisation solution in SSC to occupy vacant DNA binding sites. This was rotated slowly in a prehybridisation tube at 60°C for at least 15 minutes. The probe was added to the prehybridisation tube, which was returned to the rotisserie for a further 2 hours. The nylon sheet was then thoroughly washed at 65°C over an hour in gradually decreasing concentrations of SSC with 1% SDS following which, it was removed and washed at room temperature with 2 x SSC. A geiger counter was used throughout to be certain that all radioactive contamination was neutralized.

The nylon sheet, DNA side up, was placed in a photographic folder. In complete darkness, a piece of film was placed in the exposing folder on top of the nylon sheet. The folder was sealed and left at -70 °C for 20 to 24 hours to expose. The film was fully thawed and processed in an automatic film developer (Konica SRX-101A). Tracks that were marked indicated the transgenic animals. Figure 4.1 shows a typical southern blot result.

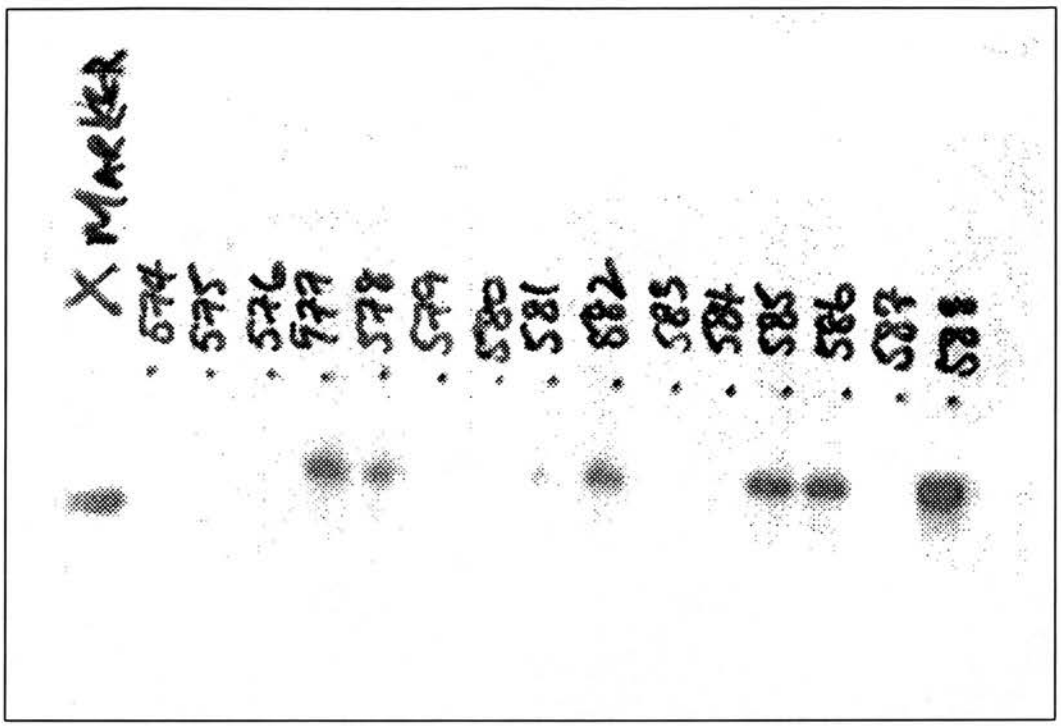

Figure 4.1 Southern blot impression for samples from 14 rats.

The marker serves as a positive control. The positive tracks indicate the transgenic offspring. The result for rat 581 was inconclusive and this sample was retested at a later date.

4.3 Recording chamber

An interface recording chamber as shown in figure 4.2 was used for all electrophysiological experiments. Heated, oxygenated aCSF passed through outlet (B) and flowed over the mesh-covered platform (E). The flow rate was high enough to allow a meniscus of aCSF to form around the slices (D). Water vapour from outlet (A) bubbled with oxygen (G) also helped keep the slices moist and oxygenated. aCSF was recycled to a heated, oxygenated reservoir (not shown). The temperature of aCSF was measured using a thermal probe (C) near the aCSF outlet and was regulated by the heating

element (H). The earth electrode (F) on the platform gave a reference point for measuring voltage changes at the recording electrode.

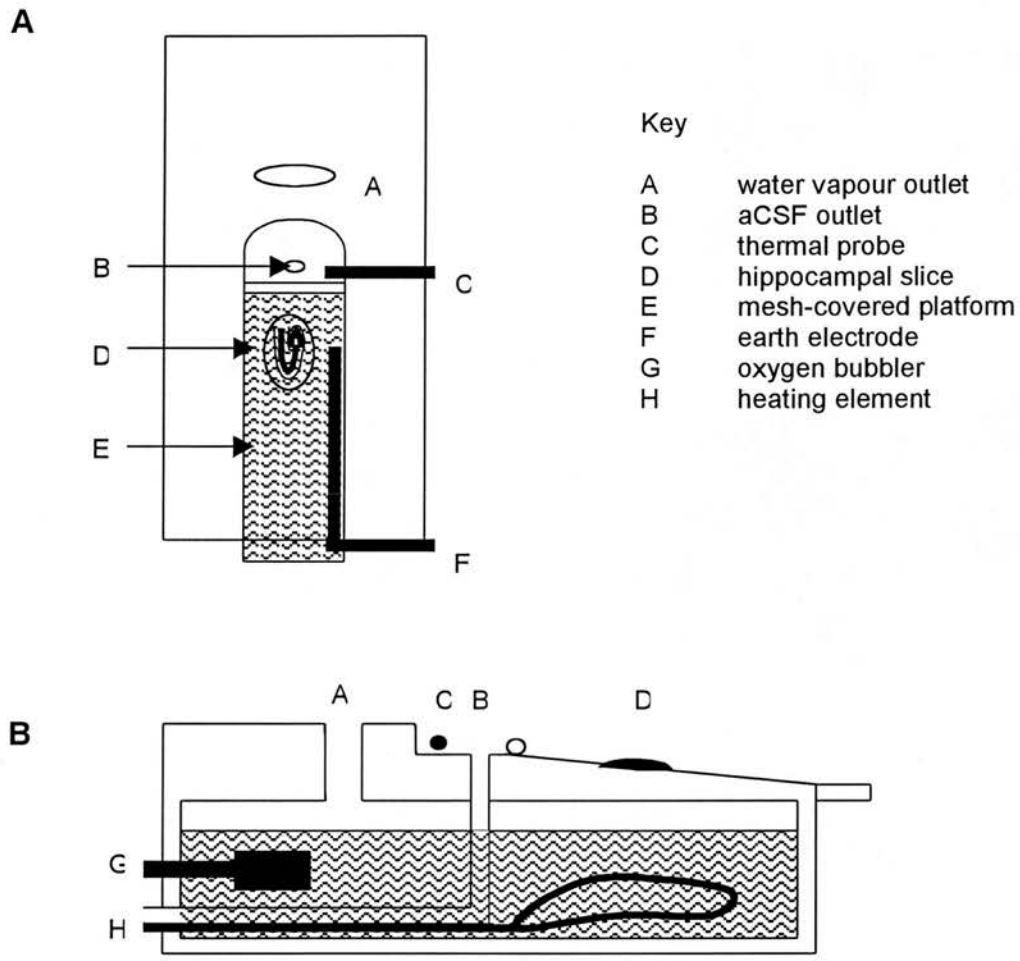

Figure 4.2 Schematic diagram of slice chamber.

(A) *Aerial view.* ***(B)*** *Side view in cross section.*

4.4 Preparation of hippocampal brain slices

Male Fischer rats were killed at 6 months or 18 months old by decapitation under halothane anaesthesia. The brain was quickly and carefully removed and cooled in aCSF of composition (mM); sucrose 252.0, KCl 2.5, NaH_2PO_4 1.2, $CaCl_2$ 2.4, $MgSO_4$ 10.0, $NaHCO_3$ 26, D-glucose 10, which was bubbled with 95% O_2/5% CO_2 and maintained at <4°C. The brain was trimmed and fixed to a cutting platform with cyanocryolite industrial superglue and supported against an agar block. Slices 400μm thick were cut using a vibrotome (Campden Instruments). The hippocampus was trimmed and 4 slices were transferred to the recording chamber where they were left to incubate for at least 1 hour at 30 to 31°C. To record from the CA1, the bath aCSF composition was (mM); NaCl 124.0, KCl 2.5, NaH_2PO_4 1.2, $CaCl_2$ 2.4, $MgSO_4$ 1.3, $NaHCO_3$ 26, D-glucose 10. To record from the dentate gyrus, the aCSF included 100μM picrotoxin to depress $GABA_A$ inhibition and was adjusted to 4.0mM $CaCl_2$ and 4.0mM $MgSO_4$ to prevent spontaneous synaptic activity. The flow rate was 1.5mls/minute.

At the end the pre-incubation period, slices were only used if the cell body layers were clearly visible and the slices were not sinking into the supporting mesh.

4.5 Extracellular field potential recordings

Electrode positions are shown in figure 4.3. Micropipettes were pulled using a Model P-87 Flaming Brown Micropipette puller (Sutter Instruments) using thin-walled (1.17mm inner diametre) filamented borosilicate glass (Clark Instruments). To record extracellular field potentials in the CA1, a glass recording electrode (5 to 10MΩ) was placed into the stratum radiatum of the CA1 and a concentric bipolar stimulating electrode was placed in the stratum lacunosum-moleculare of the CA3 to stimulate the Schaffer collaterals. To record field potentials from dentate gyrus granule cells, the stimulating electrode was placed on the perforant pathway at the apex of the granule cell body layer and the recording electrode was placed in molecular layer of the dentate gyrus.

The perforant pathway divides as it enters the dentate gyrus into medial and lateral pathways. All recordings were made in the medial pathway which can be identified by the expression of PPD rather than PPF. All extracellular protocols were run using an LTP Program written by W.W.

Anderson (University of Bristol, 1997). Data was collected and analysed online and offline using the same program.

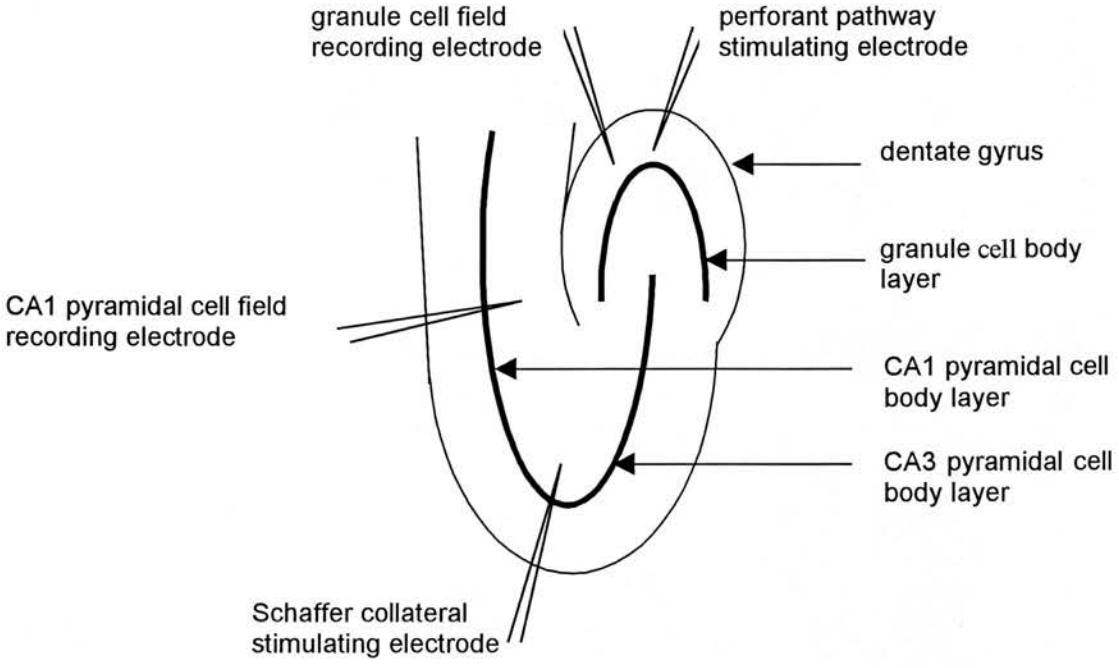

Figure 4.3 Electrode placement for extracellular field recording

Slices were deemed healthy if the fibre volley amplitude was less than 1/3 of the EPSP amplitude and stimulation of the slice did not elicit epileptiform activity. Stimulus intensity was increased until just subthreshold for generating a population spike. The rising slope of this maximal EPSP was measured and recorded (figure 4.4). The stimulus intensity was then reduced in order to generate a half-maximal EPSP as judged by slope magnitude.

The average amplitude, half width and rising slope of half-maximal field EPSPs were calculated. Maximal field EPSPs were generated by gradually increasing the stimulus intensity until evidence of a population spike was visible. Half-maximal field EPSPs were found by decreasing the stimulus intensity until the rising slope value was half that recorded in the maximal field EPSP.

Twenty consecutive field EPSPs were recorded from each slice. The field EPSP parameters measure in control and transgenic groups were averaged and analysed using a t-test. All statistics were performed using SigmaStat for Windows v2.03 (SPSS inc. 1997).

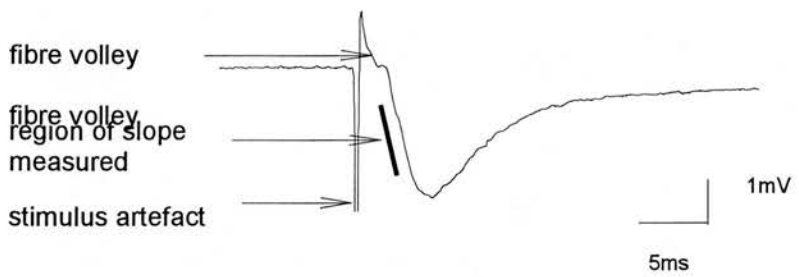

Figure 4.4 Example of a maximum EPSP

EPSP showing the measurement of the slope and the typical size of the fibre volley.

Paired pulse data were collected by giving pairs of stimuli at interpulse intervals of 400, 350, 300, 250, 200, 150, 100, 75 and 50ms. Paired stimulation was repeated every 15 seconds and 4 sweeps were averaged online at each interpulse interval. Paired pulse data were analysed using a repeat measure 2-way ANOVA.

To record LTP, first a stable baseline was recorded for at least 30 minutes with test stimuli given every 15 seconds. After 30 minutes of stable baseline had been recorded, a conditioning train consisting of 100 pulses at 100Hz was applied to the stimulating electrode. To generate dentate gyrus LTP, the stimulus intensity was doubled during the tetanus only. Test stimuli were given for an hour, followed by a second identical conditioning train and a further 30 minutes of test stimuli. This was repeated in 1 to 3 slices per day depending on the health of the slices. Reanalysis was performed if necessary using the LTP Program. To analyze post-tetanic potentiation, an unpaired t-test was performed on the values of the largest slope generated within 10 minutes of the conditioning train. LTP was analyzed over the last 10 minutes of expression recorded, using a nested ANOVA (SPSS);

LTP following the first conditioning train was analysed at the 80 to 89 minute interval and following the second tetanus was analysed over the 111 to 120 minute interval.

4.6 Intracellular sharp electrode recording

Intracellular recordings were made in CA1 pyramidal cells from 18 month old rats. Micropipettes were pulled from filamented borosilicate glass (30 to 70MΩ using thin wall glass or 80 to 150MΩ using thick wall glass). Electrodes were used if capable of passing more than 1nA of both positive and negative current. All data were collected using Clampex 8 and analysed offline using Clampfit (both, Axon Instruments Inc, 1999).

To make recordings, the tip of the electrode was place in the pyramidal cell body layer of the CA1, the offset adjusted to 0mV and the bridge current of the amplifier was balanced. The electrode was advanced in 1 to 3μm steps with a negative square current pulse being generated at 1Hz. As the electrode approached a cell, the increased resistance at the tip was observed as an unbalancing of the brigde. The *Buzz* feature of the amplifier was used to aid cell penetration. Negative holding current was applied to promote sealing of the cell membrane. Once the membrane potential was stable, the holding current was gradually removed and the offset value taken as the working membrane potential. If the cell showed spontaneous activity, negative holding current was briefly reapplied. Cells were only used if the resting membrane potential was stable at a minimum negative value of –60mV, the action potentials were at least 60mV in amplitude and the membrane resistance was at least 20MΩ. The offset was also noted when the electrode was withdrawn to allow the true resting membrane potential to be calculated. Data from cells where this showed the resting membrane potential to be more positive than -60mV were discarded. All intracellular data were analysed using an unpaired t-test or the Mann Whitney rank sum test if the data were not normally distributed.

4.61 Collection and analysis of data

Membrane resistance (R_n)

Square current pulses of 500ms duration were given via the recording electrode in 20pA steps from 35 to -205pA. This was repeated 13 times and the results were averaged. To calculate the membrane

resistance, the input current was plotted against the voltage of the response with the slope being the result. Cells with a membrane resistance lower than 20MΩ were rejected. The resistance was calculated using the initial voltage response to current injection, to minimize bias caused by rectifying currents (figure 4.5).

Adaptation of action potential firing frequency

Two second-long pulses of current, starting from 20pA and increasing in 40pA steps, were injected via the recording electrode to generate trains of action potentials. The current/frequency response were calculated for the interspike intervals for action potentials 1 to 2 (first interspike interval), action potentials 2 to 3 (second interspike interval) and by averaging the interspike intervals for the last 4 action potentials (steady state interval) (figure 4.6). Adaptation was analyzed by plotting the action potential number in a train generated by a 660pA current pulse against its firing frequency.

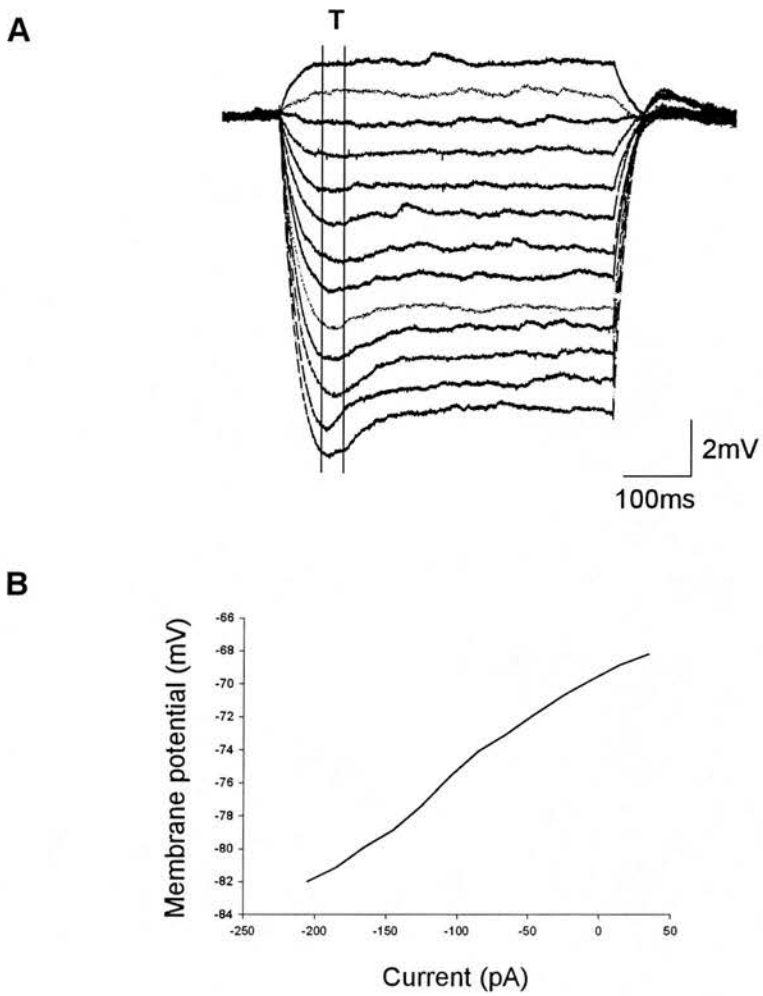

Figure 4.5 Neuronal resistance

(A) *The change in membrane resistance in response to current injection was measured during the trasient* ***(T)*** *phase.* ***(B)*** *The slope of the current/voltage plot gave the neuronal resistance.*

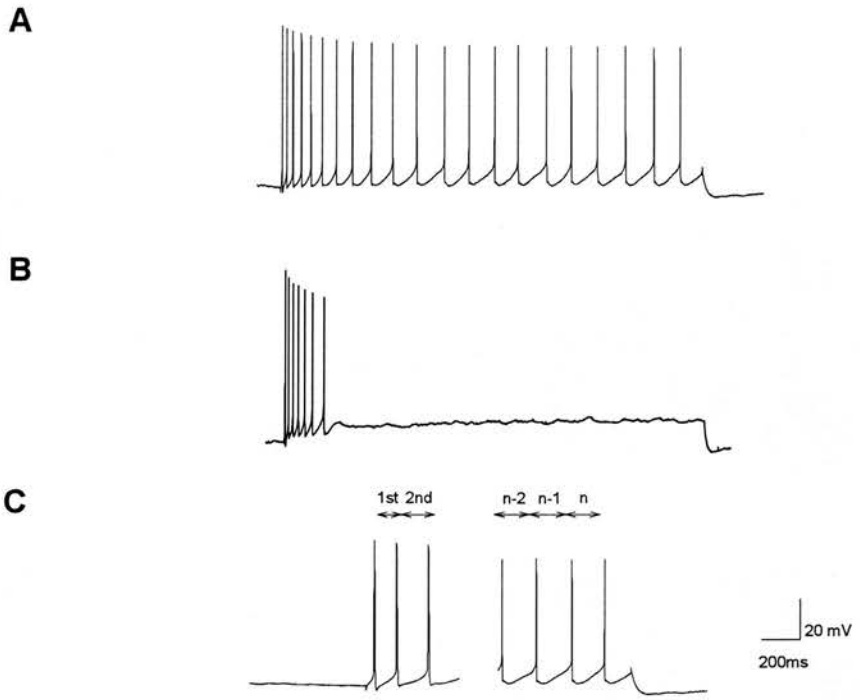

Figure 4.6 Action potential firing frequency adaptation

*Response to a 700pA current pulse of **(A)** a typical slow-adapting neurone and **(B)** a typical fast-adapting neurone. **(C)** Measurement of 1st, 2nd and steady-state firing frequencies (trace shows first three and last four action potentials from the response shown in **(A)**). The steady state firing frequency is calculated as the average interpulse interval of the last 4 action potentials (n, n-1,n-2).*

Action potential properties

One millisecond current pulses transmitted through the recording electrode were used to generate single action potentials, which were averaged over 30 sweeps. The parametres measured were spike amplitude, rise time, decay time, half width, and amplitudes of afterdepolarizing potentials or fast afterhyperpolarizing potentials if present (figure 4.7).

Medium and slow after-hyperpolarization

To measure the medium and slow AHPs, a 40Hz burst of current pulses transmitted through the recording electrode, each producing an action potential, was generated on a 4 second sweep. The burst generated 8, 12, 16 or 20 stimuli and the response was averaged over 30 sweeps. The medium AHP amplitude was taken as the maximum level of hyperpolarization. The maximum of the slow AHP was often obscured by the medium AHP and so the level of hyperpolarization 1 second after the end of the end of the action potential burst was taken as a representative measurement of the slow AHP amplitude (figure 4.8). By 1 second, the medium AHP no longer contributes to the hyperpolarization .

Synaptically evoked EPSP properties

A concentric bipolar stimulating electrode was placed in the stratum lacunosum-moleculare of the CA3 to stimulate the Schaffer collaterals. The stimulus intensity was increased until an action potential was generated with a 50% success rate. The amplitude of the maximum EPSP (recorded in the absence of an action potential) was measured and the stimulus intensity was reduced until an EPSP of half-maximal amplitude was generated. All subsequent procedures used this stimulus intensity. To characterize the EPSP, 50 sweeps each generating 1 EPSP were averaged. The amplitude, rise time, decay time and half width were recorded offline (figure 4.9).

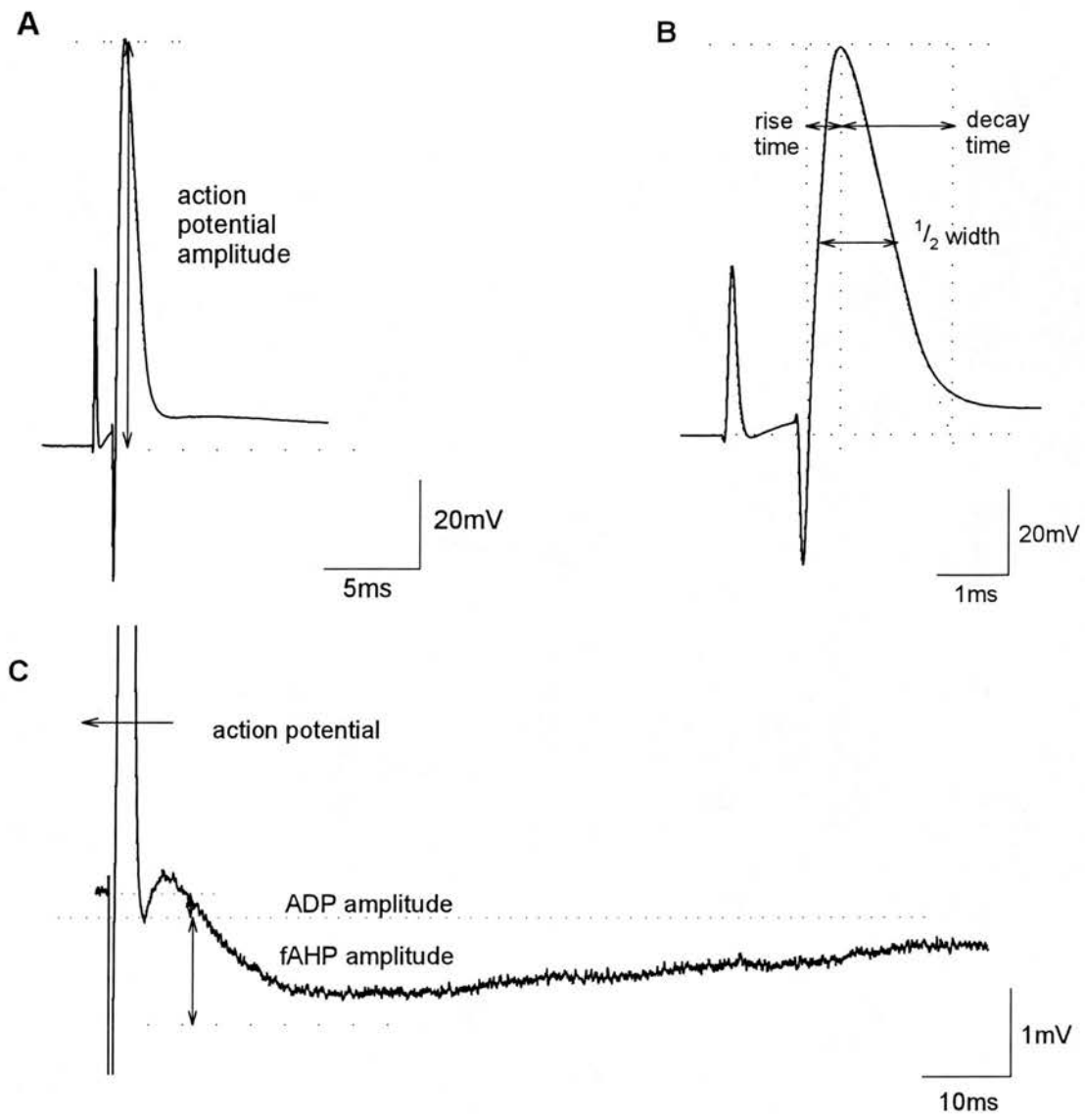

Figure 4.7 Action potential properties

(A) *The action potential amplitude was measured from the resting membrane potential.* ***(B)*** *The rise and decay times were measured from the peak of the action potential to the resting membrane potential (or projected if an ADP extended the decay phase). The half width was measured where the action potential had reached its half maximal amplitude.* ***(C)*** *ADP and AHP amplitudes were measured from the resting membrane potential.*

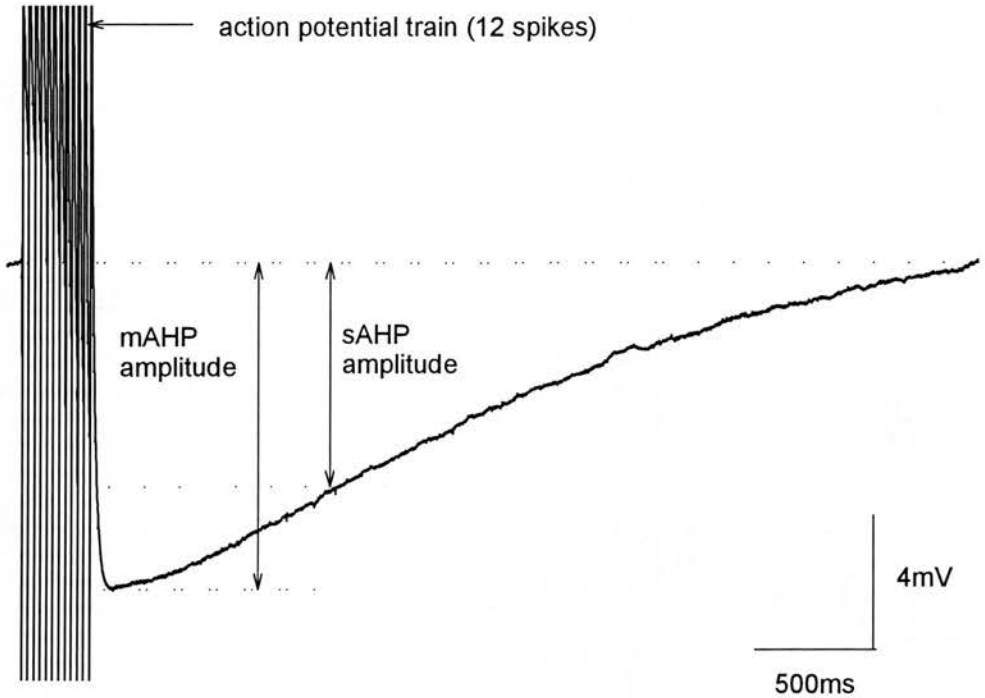

Figure 4.8 Medium and slow after-hyperpolarization

After-hyperpolarization amplitude was measured from the resting membrane potential. The mAHP maxima was the point of strongest hyperpolarization. The sAHP maxima was usually masked by the mAHP and so was taken as the amplitude of hyperpolarization 1 second after the end of the action potential train.

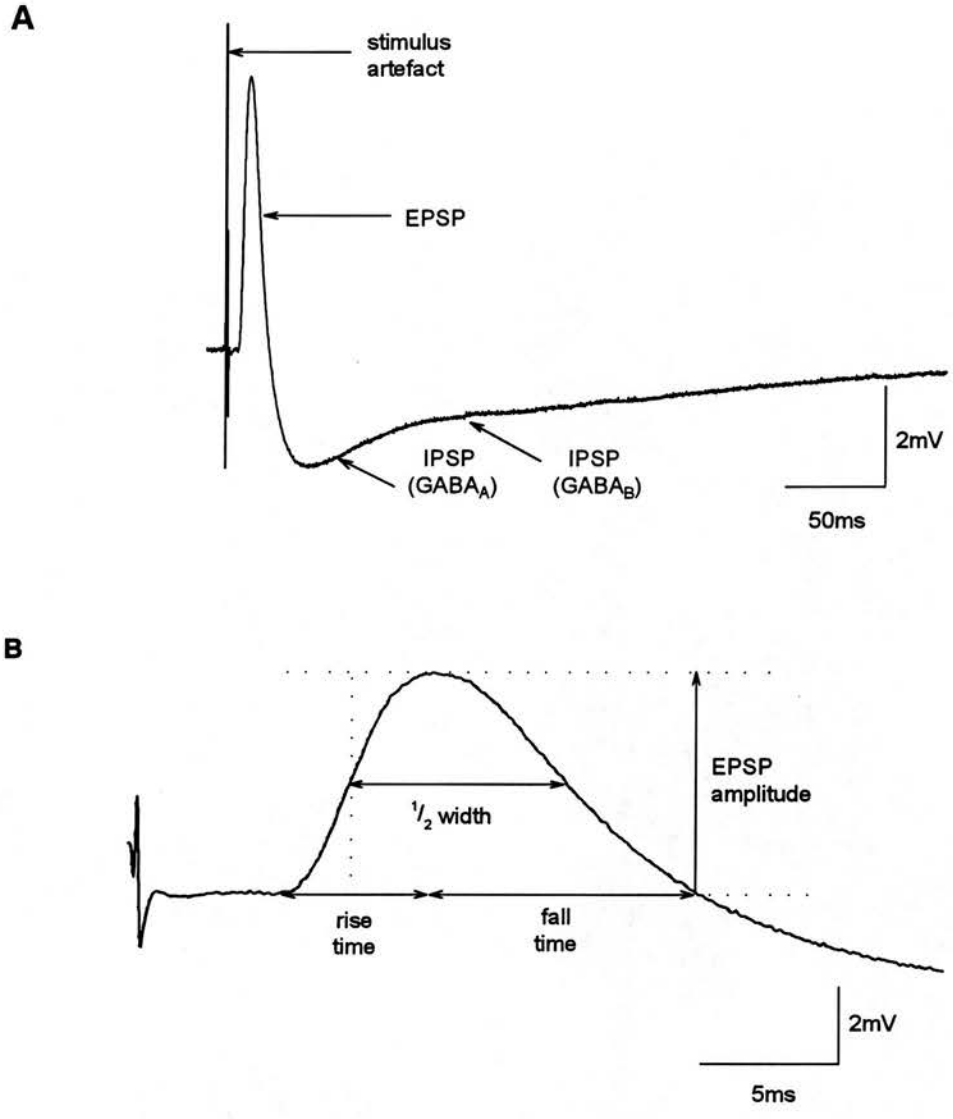

Figure 4.9 EPSP properties
(A) *Features of a typical mixed synaptic potential* ***(B)*** *Measurement of EPSP properties.*

Time constant (τ)

A 0.5ms depolarizing current pulse transmitted via the recording electrode was used to calculate the time constant. This pulse should be too small to activate voltage-dependent ion channels. About 300 sweeps were averaged for each cell. A curve with 2 exponentials consistently gave the best fit to the membrane response, giving values for the first time constant (τ_0) and an equalizing time constant (τ_1). If the potential of the entire neuronal membrane could be changed uniformally, then only 1 time constant would be observed, which would be an accurate measure of the membrane time constant (τ_m). However, current injection into the cell soma causes differential depolarization of the dendrites, which generate equalizing time constants. τ_0 was used to describe the cells in this study, which tends to be a slight overestimate of τm (Rall 1969) (figure 4.10).

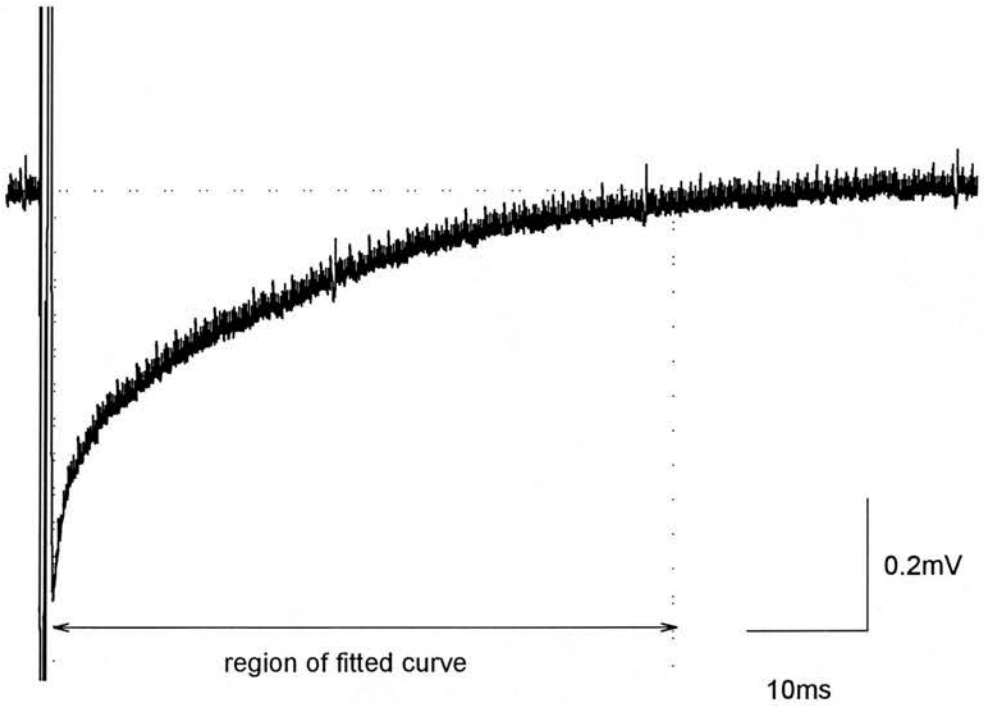

Figure 4.10 Time constant

A curve was fitted to the cell response from the peak of the response to the point where the membrane potential returned to baseline levels. Limits of the fitter region of the response are shown.

4.7 Histology

4.71 Transcardiac perfusion

The rats were deeply anaesthetised by intraperitoneal injection of 25% urethane (1.25g/kg body weight). Full anaesthesia was determined by lack of withdrawl reflex on applying a strong pinch to the hind paw.

The animal was pinned onto a polystyrene board, in a fume hood, ventral side uppermost with its forelimbs splayed to present the thorax for dissection. A button-hole incision was made with blunt scissors and the skin was cut to expose the thorax. The base of the sternum was held with forceps and the ribs cut through on either side of the sternum, which was pinned to the polystyrene board to reveal the thoracic cavity. The heart was held firmly but gently using toothed forceps and the apex of the left ventrical snipped. A catheter was carefully inserted into the aorta and taped to the animal's body to hold it in place. The right atrium was snipped to provide an outlet for perfusate. To flush blood from the brain, heparinized phosphate buffered saline was pumped into the aorta for about 10 minutes. Fixative (4% paraformaldehyde, 0.1% gluteraldehyde in 0.1M phosphate buffer, pH 7.4,) was then pumped into the aorta for about 30 minutes. Successful infusion of the brain was suggested by stiffening of the forelimbs and neck. The rat was decapitated and the brain removed and stored in fixative overnight. The brain was transferred to 70% EtOH for at least 24 hours before being automatically processed overnight and mounted in a wax block.

4.72 Slicing and preparing samples for water-based stain

The wax block was trimmed and mounted onto a chuck. Eight micrometre parasagital sections containing the dorsal hippocampus were cut on a microtome (Glen Creston, Stanmore). About 160 sections were cut from one hemisphere of each animal. These were floated in a water bath at 40°C until smooth and then floated onto microscope slides coated with gelatin with 4 sections per slide. These were dried overnight at 36°C.

The sections were dewaxed by immersion in xylene for 20 to 30 minutes, dehydrated by passage through EtOH (absolute, 90%, 70%) and washed in tap water. Every 5th slide was selected for

each type of basic stain used to allow a representative spread of the hippocampus to be examined with each of the staining regimens. About thirty sections from each animal were tested with each stain.

4.73 Histological staining

Haematoxylin and eosin

Heamatoxylin stains cell nuclei dark blue. Eosin stains cytoplasm pink. Combined haematoxylin and eosin staining can expose faint irregularities in the neuropil indicating amyloid plaques and evidence of NFTs through distorted, tadpole-shaped cell bodies.

Sections were immersed in filtered haematoxylin for 5 minutes and checked under a light microscope. If necessary, they were differentiated with acid alcohol before washing with Scott's tap water substitute for 3 minutes. The sections were washed for 3 minutes in tap water before immersion in filtered eosin for 2 minutes and potassium alum for 2 minutes. The sections were dehydrated through EtOH (70%, 90%, 95%, absolute) and cleared in xylene. DPX mountant was added drop-wise over the sections and a coverslip fixed carefully on top to avoid damage to sections or trapping air bubbles. The mountant hardened overnight.

Congo Red (Highman method)

Congo red stains amyloid plaques red, showing the dense amyloid core in mature plaques. The plaques have green bifringence under polarized light. This is a traditional stain for AD amyloid plaques that has now been supersceded by immunohistology and silver staining methods. It was used here to give an initial indication of the presence of pathology, that could later be corroborated by the use of more rigorous techniques.

Sections were immersed in a mordant of saturated picric acid for 15 minutes and washed well. They were then immersed in 0.5% congo red in 50% EtOH for 15 minutes or more and differentiated with 0.2% potassium hydroxide in 80% EtOH if necessary. The sections were then washed and the nuclei lightly counterstained in haematoxylin. They were then dehydrated and mounted as previously described.

Aims

The aim of this investigation was to characterize a new line of transgenic rats carrying the human PS1 gene with the AD-causing M146V mutation, with the intention of identifying abnormalities to support the use of these animals as a model of AD and to suggest mechanisms by which PS1 mutations may cause the deficits typical of AD. The study focussed on the hippocampus, which is a major target of AD pathology. Since the hippocampus subserves some forms of memory, deficits in the physiology of this structure could underlie some of the memory impairment indicative of AD. Synaptic plasticity was investigated as a measure of hippocampal function and intracellular recordings were made from CA1 pyramidal neurones as a means of elucidating the possible mechanisms of altered synaptic plasticity in the transgenic animals. Basic histological staining was used to expose any AD-type pathology particularly the presence of amyloid plaques and cell loss.

Chapter 5

Results

Part I

Extracellular recordings of field potentials and synaptic plasticity

5.1 Extracellular field potentials

Extracellular field potentials generated in the CA1 and the dentate gyrus were analyzed in 6 and 18 month old animals. All fields showed a rapid rising phase and a slightly slower decay phase. In some recordings, the fibre volley was evident (eg figure 5.1A control), although in many cases this was obscured by the rising phase of the EPSP.

From each slice, the amplitude, rising slope and half width of 20 field EPSPs were measured. The field EPSPs generated during the baseline of LTP experiments were used (see section 5.4). These were half maximal field EPSPs. Maximal EPSPs were found by increasing the stimulus intensity until a population spike was evident. The rising slope of the EPSP was measured and then the stimulus intensity was reduced to generate an EPSPs with half the maximum slope value. The results are summarized in table 5.1 at the end of this section.

5.11 Field EPSP parameters in the CA1

Typical CA1 field EPSPs recorded in control and transgenic animals at 6 and 18 months old are shown in figure 5.1A and B. Histograms comparing the mean amplitude, half width and slope in control and transgenic animals are shown for animals aged approximately 6 months (figure 5.1C) and 18 months (figure 5.1D). All analyses were performed using the student's t-test on data averaged for each animal.

There was no significant difference in the amplitude, half width or slope of field EPSPs recorded in control and transgenic groups of animals aged 6 months (amplitude P=0.915; half width P=0.344; slope P=0.961; control n=4 rats, transgenic n=3 rats). In 18 month old animals there was also no significant difference in the amplitude, half-width or slope of field EPSPs recorded in control and transgenic groups (amplitude P=0.632; half width P=0.489; slope P=0.658; control n=6 rats, transgenic n=6 rats).

The field EPSPs shown in figure 5.1A and B were chosen to represent as close as possible the mean amplitude and slope parameters of their group. The field EPSPs generated at 18 months were visibly larger in both the control and transgenic groups. Repeat measure analysis showed the amplitude and slope, but not the half width of the field EPSPs, to be highly significantly increased at 18 months in both control (amplitude $P \leq 0.010$ $F_{(1,228)}$=9.239; slope $P<0.01$ $F_{(1,228)}$=9.847; half width P=0.943 $F_{(1,228)}$=0.005) and transgenic (amplitude P=0.021 $F_{(1,228)}$=6.993; slope P=0.031 $F_{(1,228)}$=5.937; half width P=0.621 $F_{(1,228)}$=0.257) groups.

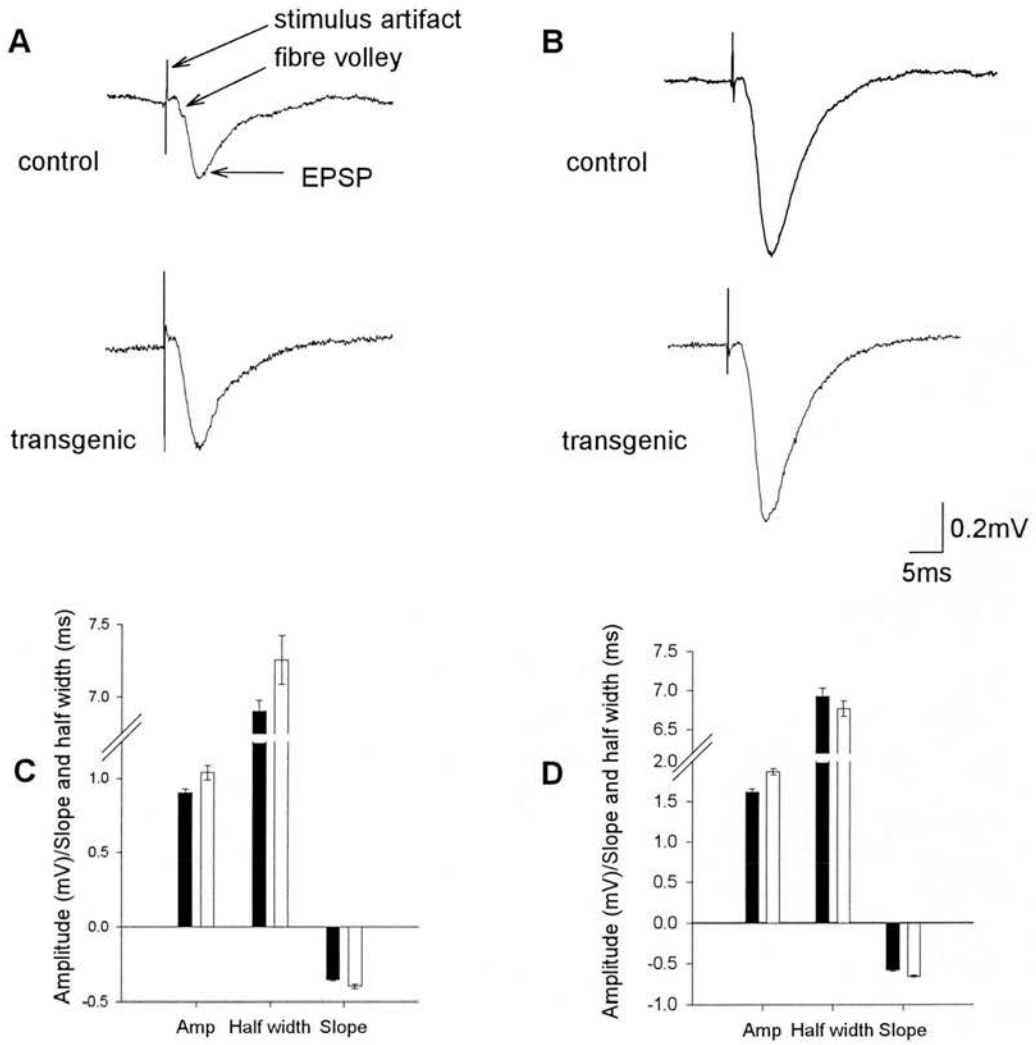

Figure 5.1 CA1 field EPSP properties

Examples of CA1 field EPSPs recorded from ***(A)*** *6 month and* ***(B)*** *18 month old animals. The upper traces were recorded from control animals and the lower traces were recorded from transgenic animals. Histograms show the mean amplitude, half width and slope values measured in* ***(C)*** *6 month and* ***(D)*** *18 month animals (control - black, transgenic - white). There was no significant difference between control and transgenic groups in the field EPSP amplitude, half width or slope values (t-test. 6 months; amplitude P=0.915 , half width P=0.344 , slope P=0.961; control n=4 rats, transgenic n=3 rats. 18 months; amplitude P=0.632, half width P=0.489, slope P=0.658; control n=6 rats, transgenic n=6 rats.)*

5.12 Field EPSP parameters in the dentate gyrus

Typical field EPSPs recorded in the dentate gyrus of control and transgenic animals at 6 and 18 months old are shown in figure 5.2A and B. Histograms comparing the amplitude, half width and slope mean in control and transgenic animals are shown at 6 months (figure 5.2C) and 18 months (figure 5.2D). All statistical analyses were performed using the student's t-test on the average EPSP values for each animal.

At 6 months, there was no significant difference in the amplitude, half width or slope of field EPSPs recorded in control and transgenic groups (amplitude P=0.252; half width P=0.730; slope P=0.741; control n=3 rats, transgenic n=4 rats). Unlike the CA1 field potentials, at 18 months there was a significant difference in the amplitude, and slope but not half width of field EPSPs recorded in control and transgenic groups in the dentate gyrus (amplitude P=0.048; slope P=0.030; half width P=0.690; control n=9 rats, transgenic n=4 rats).

The field EPSPs shown in figure 5.2A and B were again chosen to represent as close as possible the mean amplitude and slope parameters of their group. The field EPSPs generated in the transgenic group at 18 months were visibly larger than those generated at 6 months, but there was little apparent age-related change in field EPSP size in the control group. T-test analysis showed the amplitude and slope, but not the half width of the field EPSPs recorded in the transgenic group to be significantly increased at 18 months (amplitude $P<0.05$ $F_{(1,265)}=5.833$; slope $P<0.01$ $F_{(1,265)}=11.722$; half width $P=0.697$ $F_{(1,265)}=0.158$). There was no age-related change in any of the three parameters in the control group (amplitude $P=0.218$ $F_{(1,342)}=1.629$; slope $P=0.222$ $F_{(1,342)}=1.603$; half width $P=0.390$ $F_{(1,342)}=0.774$).

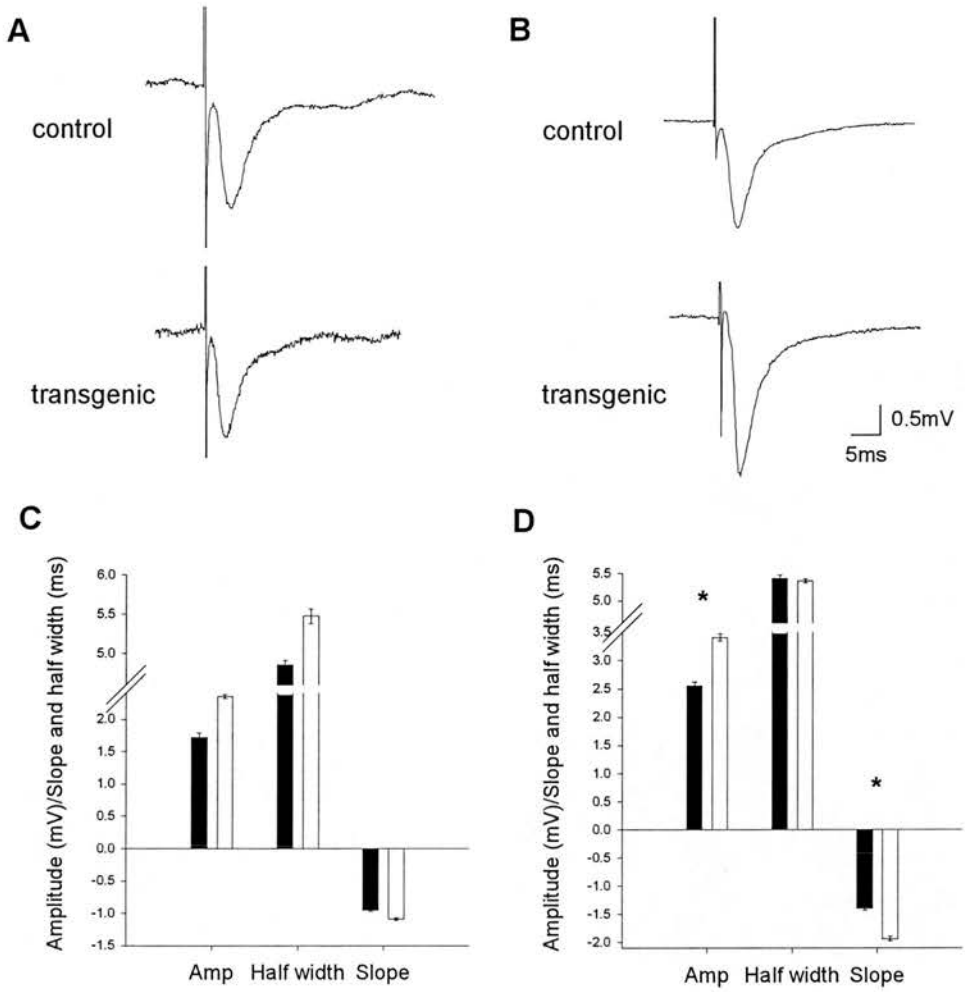

Figure 5.2 Dentate Gyrus field EPSP properties

Examples of DG field EPSPs recorded at ***(A)*** *6 months and* ***(B)*** *18 months. Histograms show the mean amplitude, half width and slope values ± SEM measured in* ***(C)*** *6 month and* ***(D)*** *18 month animals (black - control, white - transgenic). At 6 months, there was no significant difference in the field EPSP amplitude, half width or slope values measured in the control and transgenic groups (t-test. Amplitude P=0.252 half width P=0.730, slope P=0.741 ; control n=3 rats, transgenic n=4 rats). However, at 18 months, the transgenic groups generated field EPSPs with significantly greater amplitude and slope (but not half width) values (amplitude P=0.048; slope P=0.030; half width P=0.690; control n=9 rats, transgenic n=4 rats).*

Table 5.1 Properties of excitatory postsynaptic field potentials

	Control (mean ± SEM)	Transgenic (mean ± SEM)	P and F values
CA1 6 months			
Amplitude (mV)	0.905 ± 0.023 n=4	1.039 ± 0.051 n=3	P=0.915
Half width (ms)	6.903 ± 0.075 n=4	7.256 ± 0.167 n=3	P=0.344
Slope (mV/ms)	-0.354 ± 0.009 n=4	-0.398 ± 0.014 n=3	P=0.961
Dentate gyrus 6 months			
Amplitude (mV)	1.726 ± 0.061 n=3	2.355 ± 0.029 n=4	P=0.252
Half width (ms)	4.853 ± 0.055 n=3	5.474 ± 0.094 n=4	P=0.730
Slope (mV/ms)	-0.947 ± 0.027 n=3	-1.087 ± 0.190 n=4	P=0.741
CA1 18 months			
Amplitude (mV)	1.618 ± 0.036 n=6	1.872 ± 0.041 n=6	P=0.632
Half width (ms)	6.923 ± 0.104 n=6	6.770 ± 0.095 n=6	P=0.489
Slope (mV/ms)	-0.584 ± 0.010 n=6	-0.658 ± 0.015 n=6	P=0.658
Dentate gyrus 18 months			
Amplitude (mV)	2.557 ± 0.040 n=9	3.406 ± 0.065 n=4	P=0.048*
Half width (ms)	5.407 ± 0.062 n=9	5.362 ± 0.038 n=4	P=0.690
Slope (mV/ms)	-1.395 ± 0.033 n=9	-1.939 ± 0.040 n=4	P=0.030*

All statistics were performed using the t-test.
Sample sizes; n=number of animals.
* Statistically significant $P<0.05$.

5.2 Paired pulse plasticity

Paired pulse plasticity of the field EPSP was studied in the CA1 and dentate gyrus. Pairs of stimuli with interpulse intervals from 50 to 400ms were used to generate paired pulse facilitation (PPF) in Schaffer collateral/CA1 pyramidal cell synapses and paired pulse depression (PPD) in medial perforant pathway/dentate gyrus granule cell synapses. The level of facilitation or depression is given as a ratio, calculated by dividing the conditioned field EPSP slope by the conditioning field EPSP slope.

5.21 Paired pulse facilitation in the CA1

PPF in the CA1 was strongest in response to shorter interpulse intervals, and decreased in a non-linear manner as the interpulse interval was lengthened. PPF was expressed at all interpulse intervals tested. Representative examples of field EPSPs from control and transgenic groups demonstrating PPF in response to stimuli with a 50ms interpulse interval are shown at both 6 months (figure 5.3A and B) and 18 months (figure 5.4 A and B). The relationship between PPF and interpulse interval recorded at 6 months in slices from control and transgenic animals is shown in figure 5.3C. At 6 months, there was no significant difference in the strength of PPF recorded in control and transgenic groups (2-way repeat measure ANOVA. P=0.996 $F_{(1,128)}$=0.0000258; control n=9 slices from 4 animals, transgenic n=9 slices from 5 animals).

The change in PPF with interpulse interval recorded at 18 months in slices from control and transgenic animals is shown in Figure 5.4C. Typical PPF responses in control and transgenic groups are shown in figure 5.4A and B). At 18 months, there was also no significant difference in the strength of PPF recorded in control and transgenic groups (2-way repeat measure ANOVA. P=0.465 $F_{(1,144)}$=0.558; control n=10 slices from 5 animals, transgenic n=10 slices from 5 animals).

The strength of PPF was compared at 6 and 18 months within experimental groups (figure 5.5). This revealed an increase in the strength of PPF with age in both control (2-way repeat measure ANOVA. P<0.01 $F_{(1,136)}$=13.539; 6 months n=9 slices from 4 animals, 18 months n=10 slices from 5 animals) and transgenic groups (2-way repeat measure ANOVA. P<0.001 $F_{(1,136)}$=29.362; 6 months n=9 slices from 5 animals, 18 months n=10 slices from 5 animals).

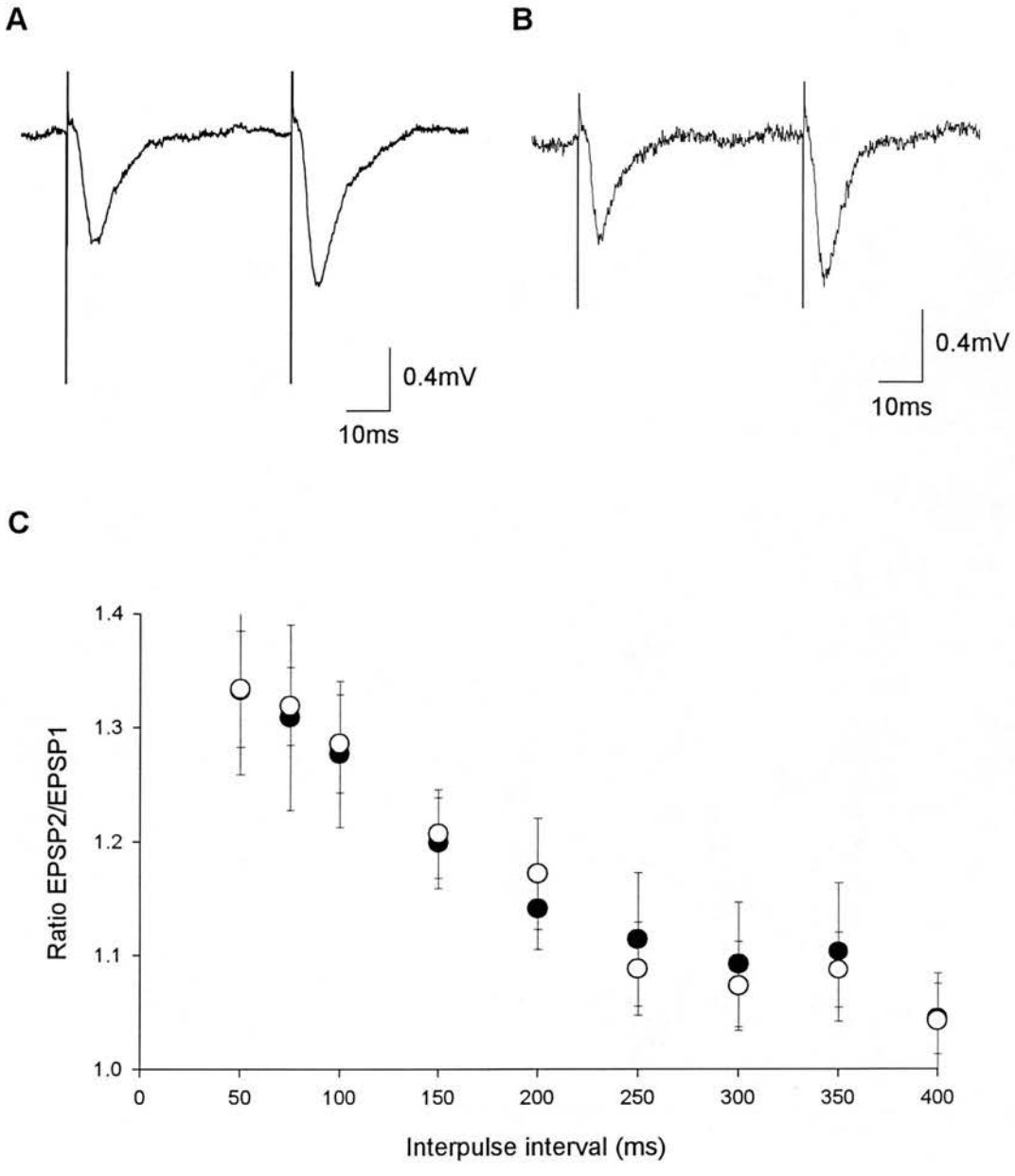

Figure 5.3 Paired pulse facilitation in the CA1 at 6 months

Examples of PPF in the CA1 of ***(A)*** *control and* ***(B)*** *transgenic animals at 6 months. Examples were chosen to show representative PPF strength.* ***(C)*** *shows the change in PPF magnitude with interpulse interval. (Black - control, white - transgenic). There was no significant difference in the strength of PPF generated by control and transgenic groups in the CA1 at 6 months (2-way repeat measure ANOVA. P=0.996* $F_{(1,128)}$*=0.0000258, control n=9 slices from 4 animals, transgenic n=9 slices from 5 animals).*

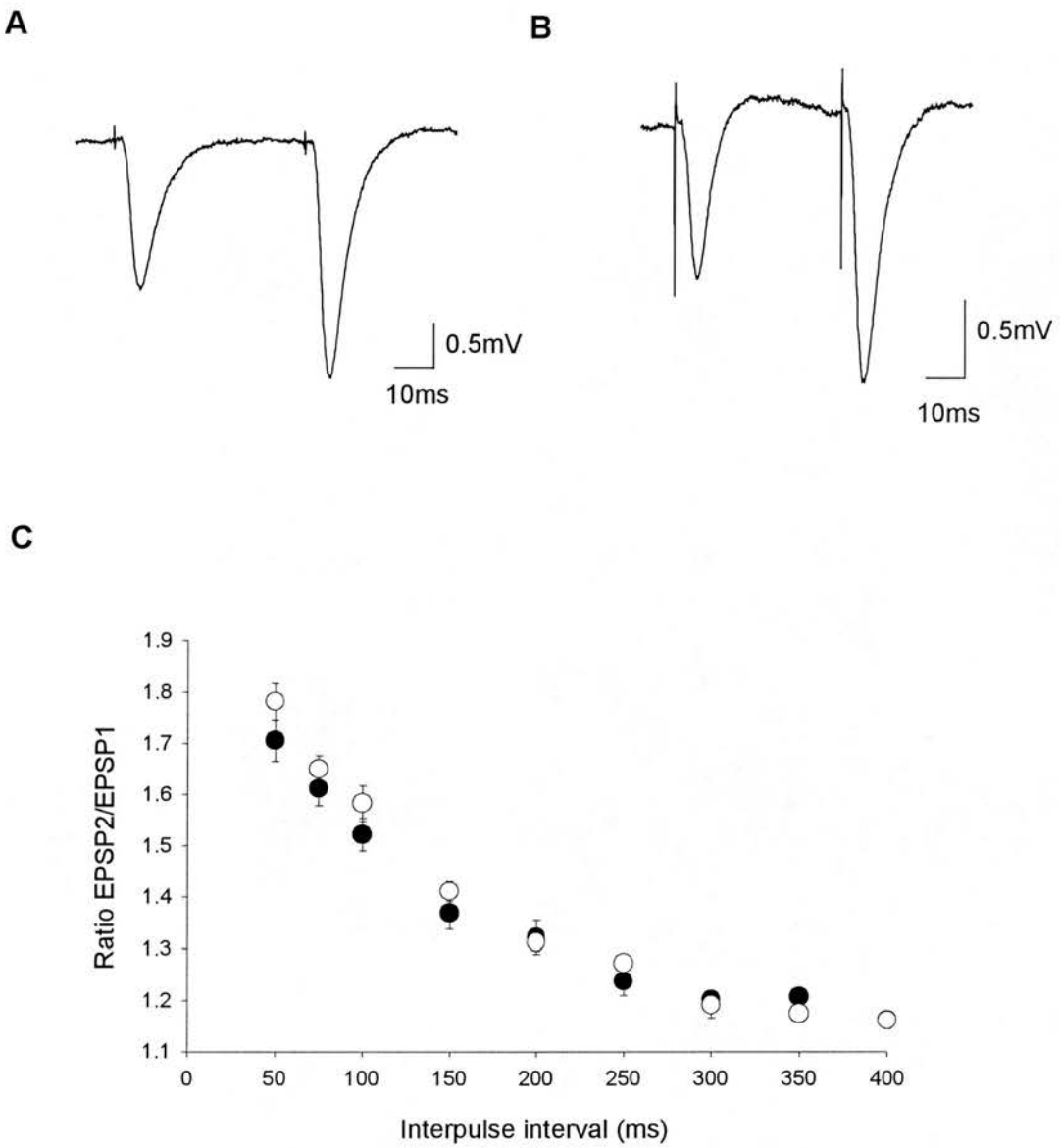

Figure 5.4 Paired pulse facilitation in the CA1 at 18 months

*Examples of PPF in the CA1 of **(A)** control and **(B)** transgenic animals at 18 months. Examples were chosen to show representative PPF strength. **(C)** shows the change in PPF magnitude with interpulse interval. (Black - control, white - transgenic).*

There was no significant difference in the strength of PPF generated by control and transgenic groups in the CA1 at 18 months (2-way repeat measure ANOVA. P=0.465 $F_{(1,144)}$=0.558, control n=10 slices from 5 animals, transgenic n=10 slices from 5 animals).

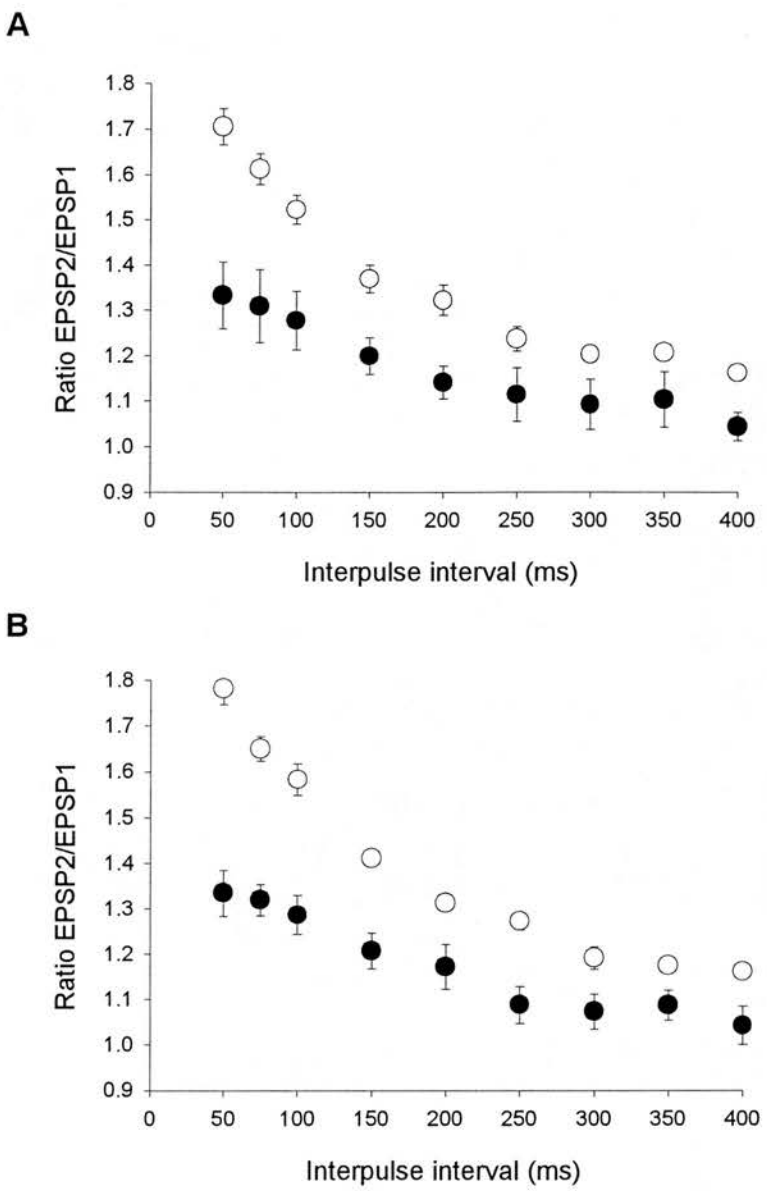

Figure 5.5 Age-dependent changes in CA1 PPF strength

The change in PPF magnitude with age is shown for ***(A)*** *control and* ***(B)*** *transgenic groups (6 months - black, 18 months - white). In both cases, there was a significant increase in the strength of PPF with age, which was especially prevalent at smaller interpulse intervals (2-way repeat measure ANOVA. Control P=0.002* $F_{(1,136)}$*=13.539, 6 months n=9 slices from 4 animals, 18 months n=10 slices from 5 animals). Transgenic (2-way repeat measure ANOVA. P<0.001* $F_{(1,136)}$*=29.362; 6 months n=9 slices from 5 animals, 18 months n=10 slices from 5 animals).*

5.22 Paired pulse depression in the dentate gyrus

The change in PPD with interpulse interval recorded in the dentate gyrus showed a triphasic response to the range of interpulse intervals used. PPD was strongest at 50ms, but fell rapidly as the interpulse interval increased to 150ms, where PPD was weakest. At the longer interpulse intervals (200-400ms) PPD strength was increased and established a plateau. PPD was expressed at all interpulse intervals tested. Representative examples of field EPSPs from control and transgenic groups demonstrating PPD in response to stimuli with a 50 ms interpulse interval are shown for both 6 months (figure 5.6A and B) and 18 months (figure 5.7 A and B). The triphasic pattern of PPD activity was observed at both 6 months (figure 5.6C) and 18 months (figure 5.7C).

At 6 months, there was no significant difference in the strength of PPD recorded in control and transgenic groups (2-way repeat measure ANOVA. P=0.144 $F_{(1,72)}$=2.566; control n=4 slices from 4 animals, transgenic n=7 slices from 4 animals). However, there was a consistent trend towards stronger PPD in the transgenic group at 6 months and the all-pairwise multiple comparison procedures (Tukey Test) showed a highly significant difference between control and transgenic groups at the 50ms interpulse interval only (50 ms $p<0.01$; 75ms p=0.067; 100ms p=0.084; 150ms p=0.214; 200ms p=0.364; 250ms p=0.471; 300ms p=0.411; 350ms p=0.506; 400ms p=0.559). At 18 months, there was also no significant difference in the strength of PPD recorded in control and transgenic animals (2-way repeat measure ANOVA. P=0.401 $F_{(1,272)}$=0.725; control n=24 slices from 10 animals, transgenic n=12 slices from 4 animals).

The strength of PPD was compared in 6 month and 18 month groups (figure 5.8). Unlike PPF, PPD showed no age-related change in strength in control and transgenic groups (2-way repeat measure ANOVA. Control; P=0.384 $F_{(1,208)}$=0.784; 6 months n=4 slices from 4 animals, 18 months n=24 slices from 10 animals. Transgenic; P=0.113 $F_{(1,136)}$=2.796; 6 months n=7 slices from 4 animals, 18 months n=12 slices from 4 animals).

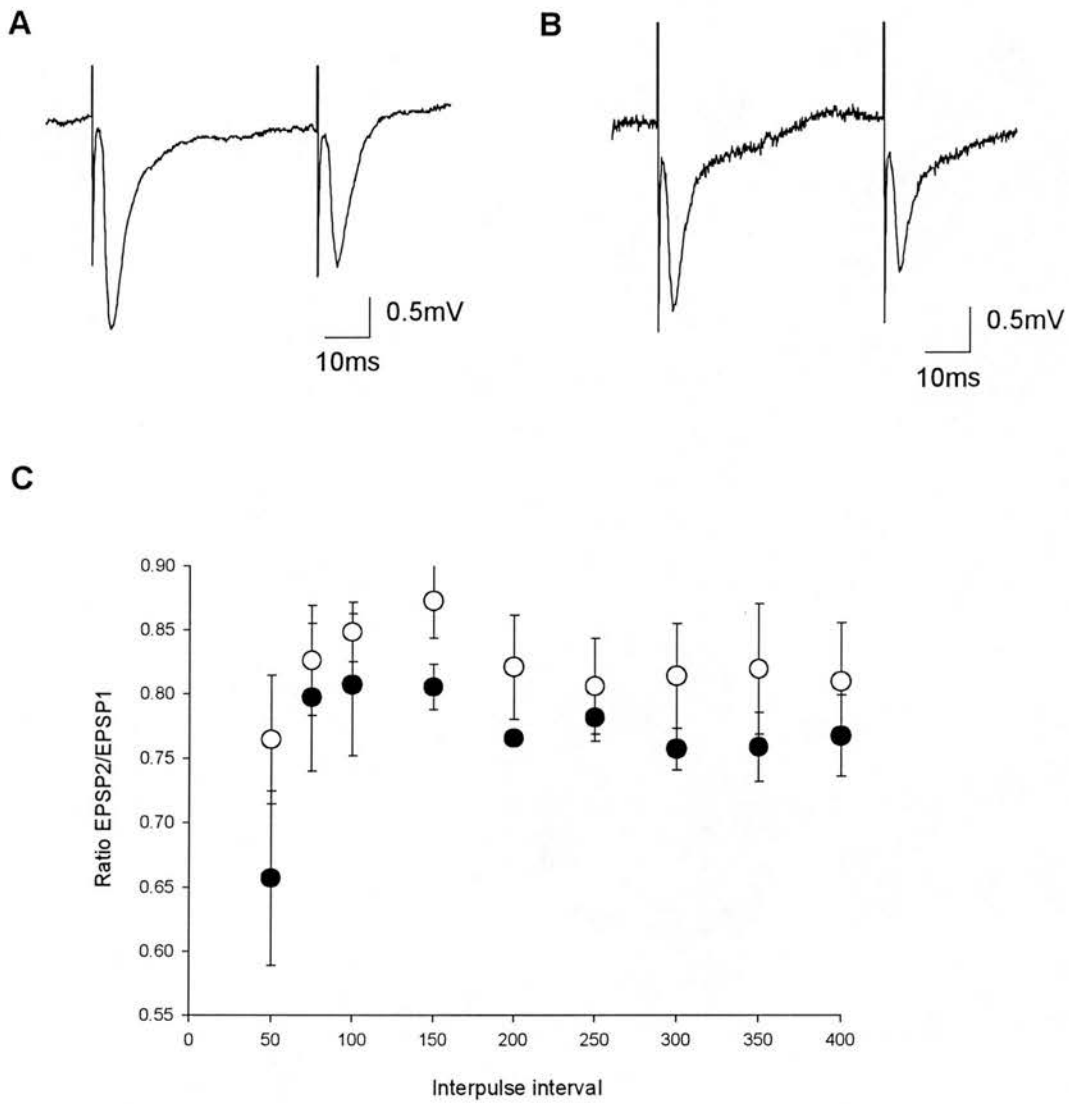

Figure 5.6 Paired pulse depression in the dentate gyrus at 6 months

*Examples of PPD in the dentate gyrus of **(A)** control and **(B)** transgenic animals at 6 months, generated with a 50ms interpulse interval. Examples were chosen to show representative PPD strength. **(C)** shows the change in PPD magnitude with interpulse interval (Black - control, white - transgenic).*

There was no significant difference in the strength of PPD generated in control and transgenic groups in the dentate gyrus at 6 months (2-way repeat measure ANOVA. $P=0.144$ $F_{(1,72)}=2.566$; control n=4 slices from 4 animals, transgenic n=7 slices from 4 animals) however, the all-pairwise multiple comparison procedure (Tukey test) showed that at 50ms, PPD in the transgenic group was significantly increased (P=0.006).

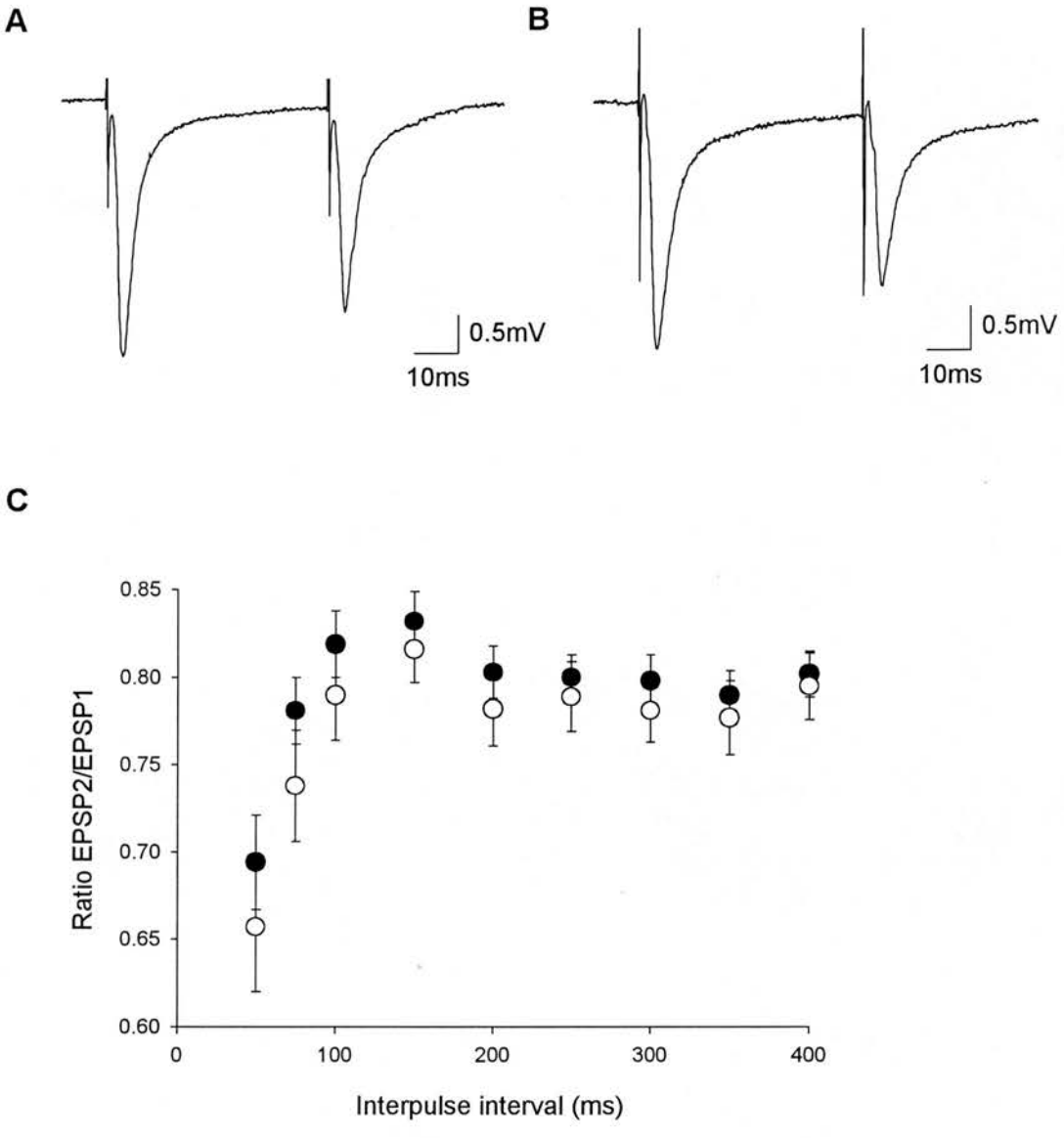

Figure 5.7 Paired pulse depression in the dentate gyrus at 18 months

*Examples of PPD in the dentate gyrus of **(A)** control and **(B)** transgenic animals at 18 months, generated with a 50ms interpulse interval. Examples were chosen to show representative PPD strength. **(C)** shows the change in PPD magnitude with interpulse interval (black - control, white - transgenic).*

There was no significant difference in the strength of PPD generated in control and transgenic groups in the dentate gyrus at 18 months (2-way repeat measure ANOVA. $P=0.401$ $F_{(1,272)}=0.725$; control n=24 slices from 10 animals, transgenic n=12 slices from 4 animals).

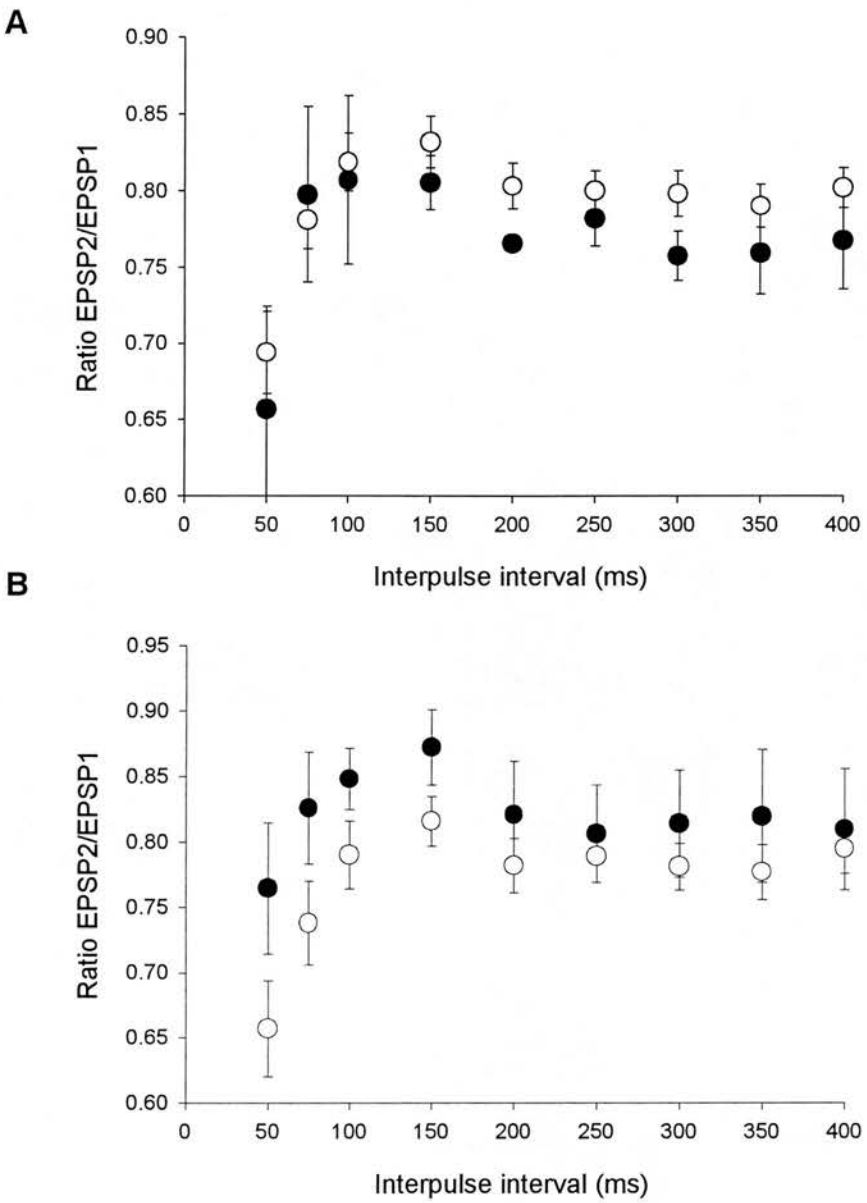

Figure 5.8 Age-dependent change in dentate gyrus PPD strength

The comparison of PPD magnitude generated at 6 months and 18 months is shown for ***(A)*** *control and* ***(B)*** *transgenic groups (black - 6 months, white - 18 months). There was no significant age-dependent change in PPD strength in either control or transgenic groups. (2-way repeat measure ANOVA. Control; P=0.384* $F_{(1,208)}$*=0.784; 6 months n=4 slices from 4 animals, 18 months n=24 slices from 10 animals. Transgenic; P=0.113* $F_{(1,136)}$*=2.796; 6 months n=7 slices from 4 animals, 18 months n=12 slices from 4 animals).*

5.3 Post-tetanic potentiation

Postetanic potentiation of the field EPSP was induced using a 1 second 100Hz high frequency stimulation train (HFS) and monitored by measuring the field EPSP slope in response to test stimuli given every 15 seconds. The field EPSP slope value increased rapidly in response to the HFS and was maximal within 5 minutes, before decaying more gradually into the STP/early LTP phase of potentiation.. The increase in EPSP slope was expressed as a percentage change from baseline (pre-HFS) values. The amplitude of PTP was taken as the largest increase in EPSP slope generated within 5 minutes of the HFS. The latency was the time (in seconds) from the end of the HFS to the maximal PTP response. PTP amplitude and latency values are summarized in Table 5.2 at the end of section 5.3.

5.31 Post-tetanic potentiation in the CA1

HFS consistently generated strong PTP in the CA1 in both control and transgenic groups at 6 and 18 months. Figure 5.9A shows the typical pattern of PTP development in the CA1 recorded from a 6 month old control animal. Histograms of the mean PTP peak amplitude and latency values are shown for control and transgenic groups at 6 months (figure 5.9B) and 18 months (figure 5.9C).

The mean (± SEM) PTP amplitude at 6 months was 160.531% ± 27.446 in the control group and 158.602% ± 16.853 in the transgenic group. The mean PTP amplitude at 18 months was 140.683% ± 17.366 in the control group and 128.519% ± 17.523 in the transgenic group. PTP amplitude varied greatly. At 6 months the range of amplitude values was 90.734 to 251.671% in the control group and 87.087 to 207.519% in the transgenic group. At 18 months the range of amplitude values was 64.547 to 206.044% in the control group and 64.941 to 212.864% in the transgenic group. There was no significant difference in the mean PTP amplitude generated in control and transgenic groups at either 6 months (t-test; P=0.951 control n=6 transgenic n=8) or 18 months (t-test; P=0.636 control n=7 transgenic n=9).

In the CA1, PTP reached maximum within 60s of the HFS in both control and transgenic groups (range; 6 months control 30-60s, transgenic 15-60s. 18 months control 15-60s, transgenic 15-45s). Since test stimuli were given every 15s the resolution of PTP latency was low. There was no significant difference in the PTP latencies recorded in control and transgenic groups at 6 months (t-test P=0.108 control n=6 transgenic n=8) or 18 months (t-test P=0.139 control n=7 transgenic n=9).

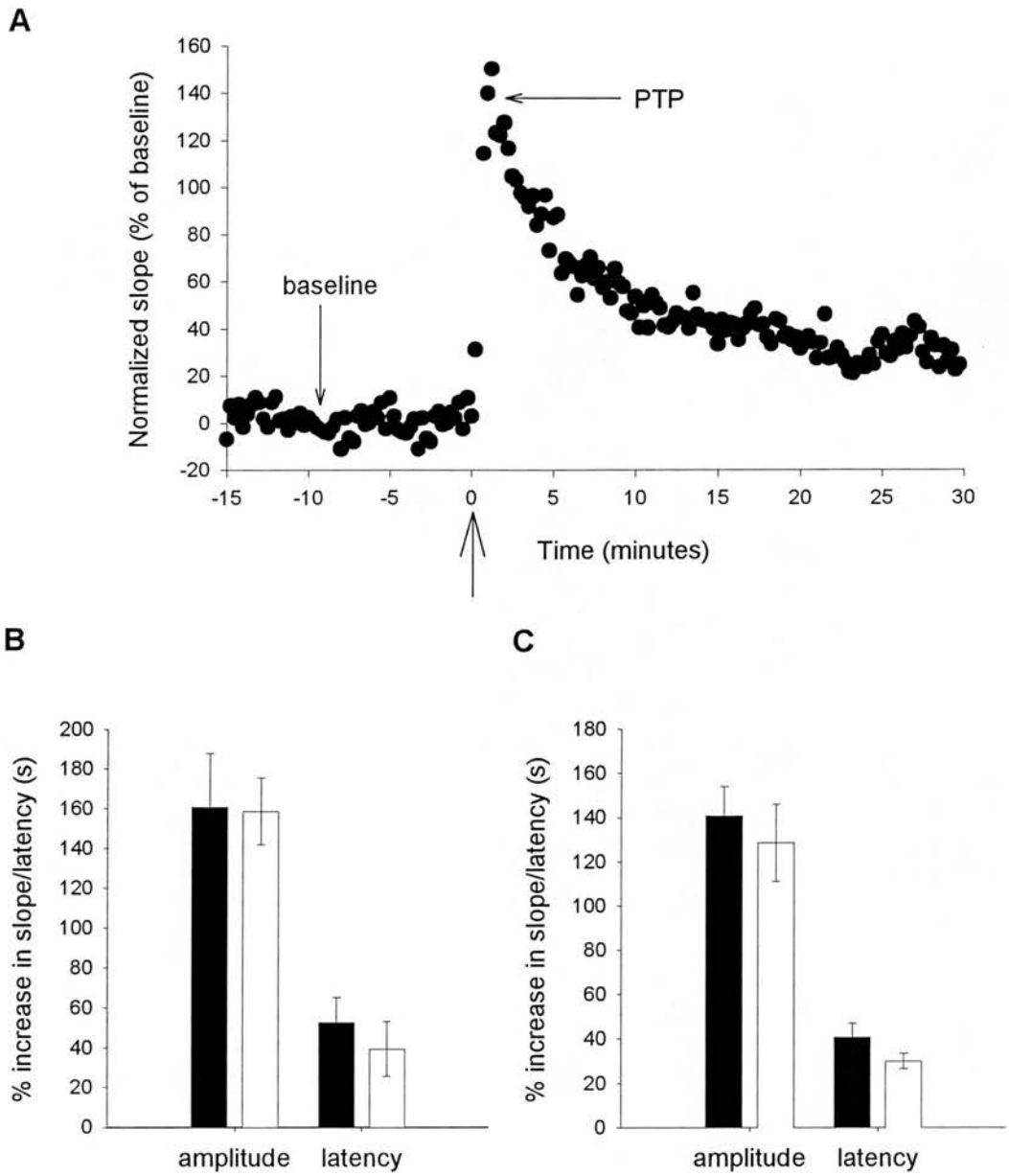

Figure 5.9 Post-tetanic potentiation in the CA1

(A) *shows a typical response to a tetanizing stimulus train (large arrow) recorded in a 6 month old control animal. PTP is demonstrated by the sharp peak following the tetanus. Histograms show the mean (± SEM) PTP amplitude and latency values at* ***(B)*** *6 months and* ***(C)*** *18 months (black - control, white - transgenic).*
There was no significant difference in the mean PTP amplitude or latency recorded in control and transgenic groups at 6 months (t-test: amplitude; P=0.951 control n=6 transgenic n=8. Latency; P=0.108 control n=6 transgenic n=8) or 18 months (t-test: amplitude; P=0.636 control n=7 transgenic n=9. Latency; P=0.139 control n=7 transgenic n=9).

5.31 Post-tetanic potentiation in the dentate gyrus

High frequency stimulation consistently generated PTP in the DG in both control and transgenic groups at 6 and 18 months. PTP generated in the dentate gyrus was weaker and took longer to reach peak levels than PTP generated in the CA1. An example of the pattern of PTP development in the dentate gyrus (recorded at 6 months from a control animal) is shown in figure 5.10A. Histograms of the mean PTP peak amplitude and latency values are shown for control and transgenic groups at 6 months (figure 5.10B) and 18 months (figure 5.10C).

The mean (± SEM) PTP amplitude at 6 months was 98.036% ± 12.345 in the control group and 104.868% ± 9.393 in the transgenic group. The mean PTP amplitude at 18 months was 102.173% ± 15.165 in the control group and 106.319% ± 15.247 in the transgenic group. As in the CA1, PTP amplitude varied greatly in the dentate gyrus. At 6 months the range of amplitude values was 65.354 to 136.892% in the control group and 79.925 to 144.574% in the transgenic group. At 18 months the range of amplitude values was 33.563 to 302.033% in the control group and 15.247 to 200.061% in the transgenic group. There was no significant difference in the mean PTP amplitude generated in control and transgenic groups at either 6 months (t-test; P=0.664 control n=5 transgenic n=6) or 18 months (t-test; P=0.859 control n=17 transgenic n=10).

In the DG, PTP was maximal within 3 minutes of the HFS in both control and transgenic groups (range: 6 months control. 30 to 165s, transgenic 30 to 135s; 18 months control 45 to 270s, transgenic 60 to 270s). There was no significant difference in the PTP latencies recorded in control and transgenic groups at 6 months (t-test P=0.477 control n=5 transgenic n=6) or 18 months (t-test P=0.303 control n=17 transgenic n=10).

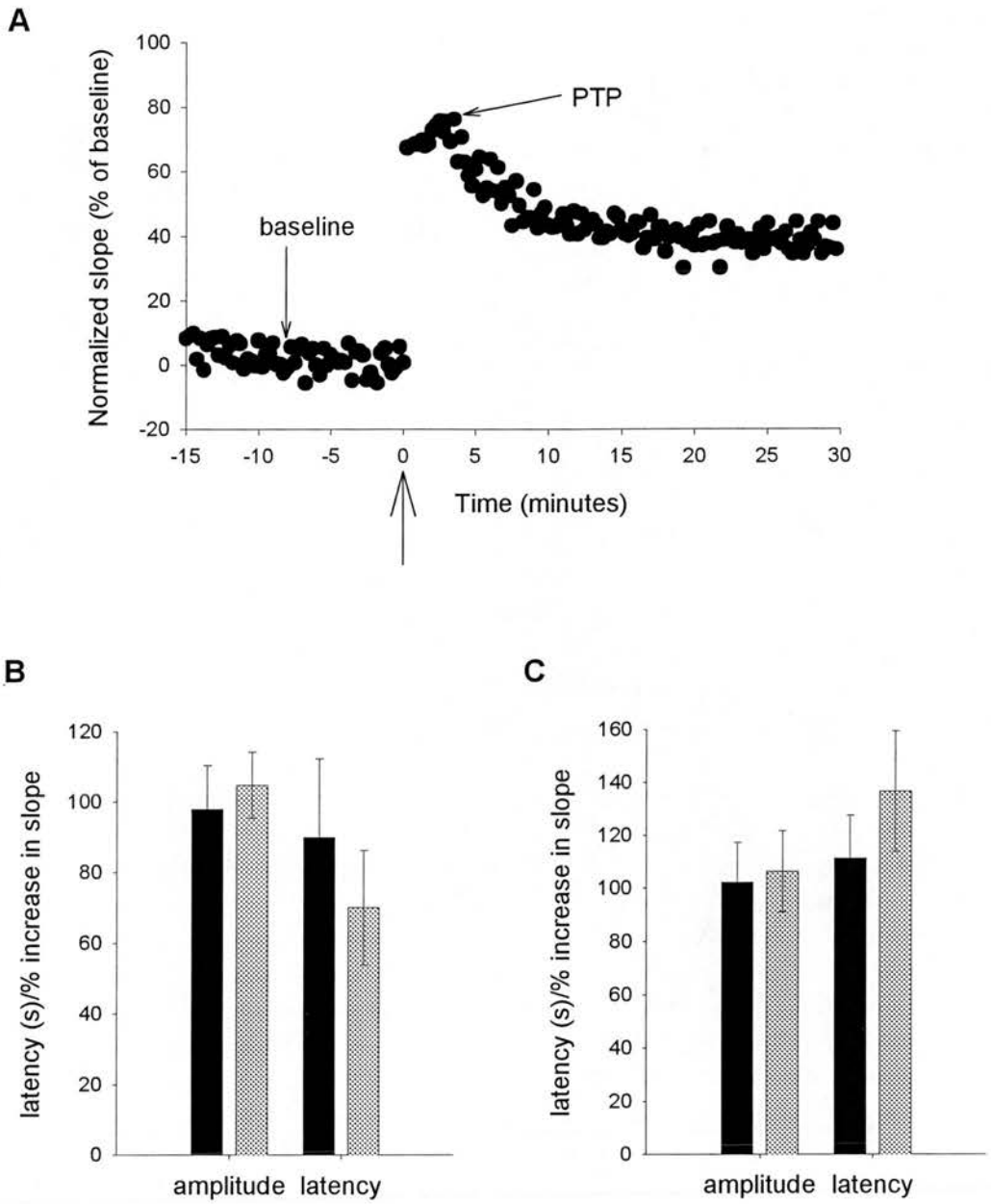

Figure 5.10 Post-tetanic potentiation in the dentate gyrus

(A) *shows a typical response to a tetanizing stimulus train (large arrow) recorded in the dentate gyrus ofa 6 month old control animal. PTP is demonstrated by the peak following the tetanus. Histograms show the mean (± SEM) PTP amplitude and latency values at* ***(B)*** *6 months and* ***(C)*** *18 months (black - control, white - transgenic).*

There was no significant difference in the mean PTP amplitude or latency recorded in control and transgenic groups at 6 months (t-test: amplitude; P=0.664 control n=5 transgenic n=6. Latency P=0.477 control n=5 transgenic n=6) or 18 months (t-test: amplitude; P=0.859 control n=17 transgenic n=10. Latency P=0.303 control n=17 transgenic n=10).

Table 5.2 Post-tetanic potentiation amplitude and time to peak latency

	Control (mean ± SEM)	Transgenic (mean ± SEM)	P values
CA1			
6 months			
PTP amplitude†	160.531 ± 27.446 n=6	158.602 ± 16.853 n=8	*P*=0.951
Latency (s)	52.5 ± 12.55 n=6	39.375 ± 13.742 n=8	*P*=0.108
18 months			
PTP amplitude†	140.683 ± 17.366 n=7	128.519 ± 17.523 n=9	*P*=0.636
Latency (s)	40.714 ± 6.308 n=7	30.00 ± 3.536 n=9	*P*=0.139
Dentate gyrus			
6 months			
PTP amplitude†	98.036 ± 12.345 n=5	104.869 ± 9.393 n=6	*P*=0.644
Latency (s)	90.00 ± 22.25 n=5	70.00 ± 16.28 n=6	*P*=0.477
18 months			
PTP amplitude†	102.173 ± 15.165 n=17	106.319 ± 15.247 n=10	*P*=0.859
Latency (s)	111.18 ± 16.273 n=17	136.50 ± 22.743 n=10	*P*=0.303

All statistics performed using the t-test.
†PTP amplitude is expressed as the per cent increase in field EPSP slope from pre-tetanized values.
There was no significant difference between control and transgenic groups in any of the values measured.

5.4 Long-term potentiation

Long-term potentiation (LTP) was generated in the Schaffer collateral/CA1 pathway and the medial perforant pathway/dentate gyrus pathway. A stable baseline was recorded for 30 minutes before using a 1 second, 100Hz high frequency tetanizing stimulus (HFS) to generate LTP. A second identical HFS was given an hour after the first. The field EPSP slope values measured during the baseline were averaged offline and all slope values were normalized as a percentage of the baseline slope value. Slope measurements made at 81 to 90 minutes were averaged to analyze the strength of LTP expression, and an increase of 10% or more above baseline values were accepted as LTP. To assess differences between groups, slope measurements made over the same 81-90 minute interval were analyzed by nested ANOVA. Further increase in synaptic strength following the second HFS was measured offline at 111-120 minutes.

5.41 Long-term potentiation in Schaffer-collateral/CA1 pathway

Figure 5.11 shows example of field EPSPs recorded in the CA1 of slices from 6 and 18 month old animals before and after HFS. Figures 5.12A and B show recordings from the CA1 for control and transgenic groups at 6 months and 18 months respectively. LTP was evoked by HFS at the time point indicated by the arrows. At 6 months, both control and transgenic groups showed the same qualitative response to the HFS; rapid PTP generation, which quickly decayed into the early-LTP phase, with stable LTP usually established within 1 hour. The strength of LTP expression varied greatly. At 6 months, the mean (± SEM) LTP expression level values were 22.64% ± 6.277 (control) and 18.029% ± 2.257 (transgenic) with ranges of 11.499 to 53.554% in the control group and 10.442 to 26.692% in the transgenic group. There was no significant difference in the strength of LTP expression recorded in control and transgenic groups at 6 months (nested ANOVA; P=0.519 F=0.444 control n=3, transgenic n=4). Figure 5.13 shows scatter plots of the relationship between the percentage of LTP and the baseline EPSP slope and stimulus intensity. No correlation was found to suggest that the increase in LTP recorded in the transgenic group was due to baseline effects (Pearson correlations; Control LTP and EPSP slope P=0.873, LTP and stimulus intensity P=0.139, transgenic LTP and EPSP slope P=0.131, LTP and stimulus intensity P=0.367).

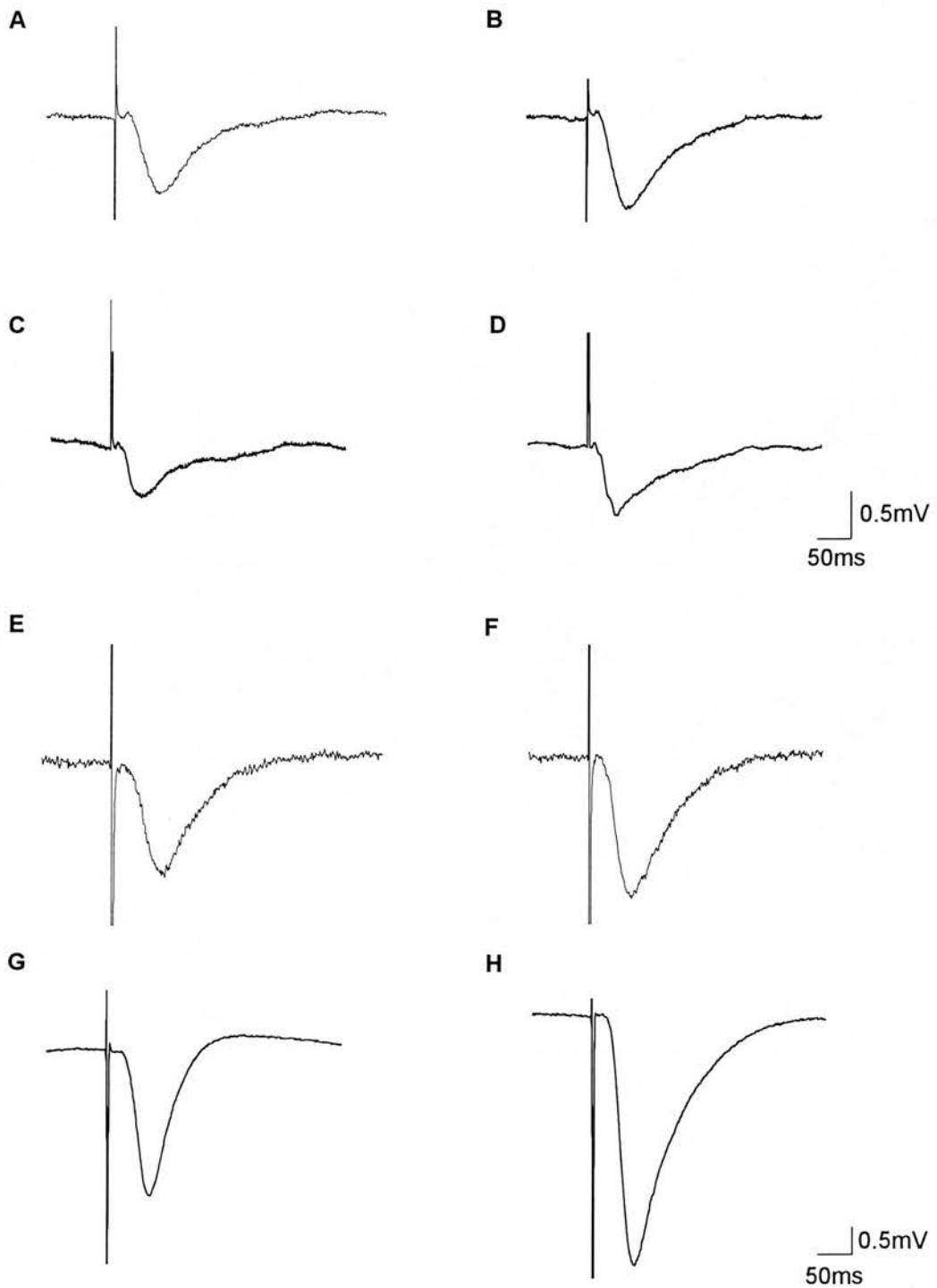

Figure 5.11 Field EPSPs in the CA1 before and after HFS
*Traces are shown of EPSPs recorded from slices of 6 month **(A-D)** and 18 month **(E-H)** old animals. **(A), (B), (E) & (F)** were recorded from control and **(C), (D), (G) & (H)** were recorded from transgenic animals. The traces on the left were recorded during the baseline. The traces on the right were recorded at 55 minutes following the HFS. The slope of fields recorded after the HFS were all potentiated.*
*Trace **(D)** shows evidence of a persisting population spike.*

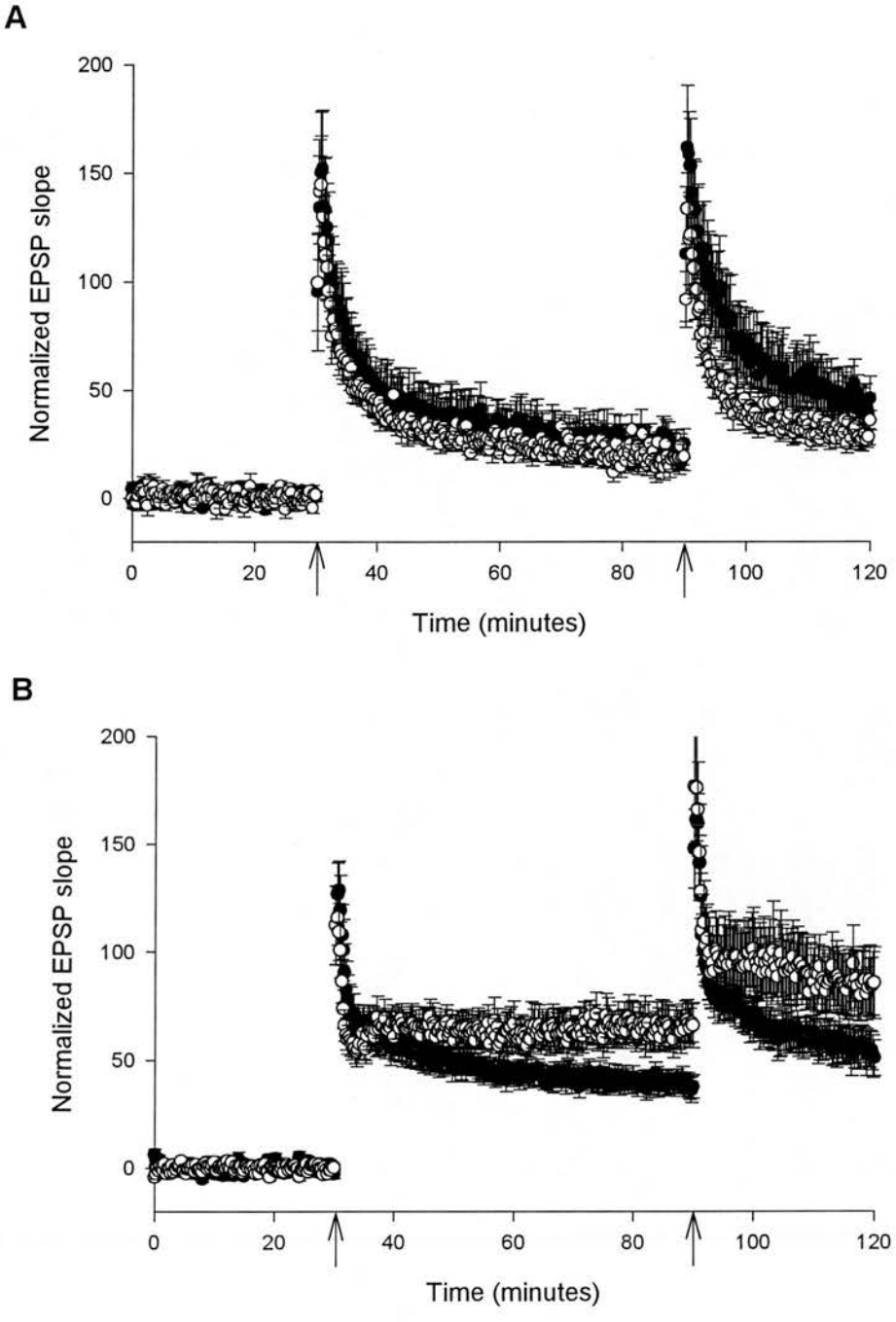

Figure 5.12 Long-term potentiation in the CA1

LTP recorded in the CA1 of control (black) and transgenic (white) animals at ***(A)*** *6 months and* ***(B)*** *18 months old. The Schaffer collaterals were tetanized at 30 and 90 minutes (arrows).* ***(A)*** *LTP recorded in slices from 6 month old transgenic rats was not significantly different from that recorded in slices from control rats (nested ANOVA; P=0.519* $F_{(1,99)}$*=0.444, control n=3 rats, transgenic n=4 rats.)*

(B) *LTP recorded in slices from 18 month old transgenic rats was significantly greater than that recorded in slices from control rats (nested ANOVA; P=0.011* $F_{(1,126)}$*=7.560 control n=6 rats, transgenic n=6 rats).*

The second HFS generated further potentiation of between 10.077 and 45.347% (x=24.687% ± 4.781) in the control group and between 16.014 and 37.018 (x=24.223% ± 2.861) in the transgenic group. Although the transgenic group still showed stronger LTP, there was no statistically significant difference in either the total level of LTP expression in the control and transgenic groups (nested ANOVA; P=0.227, $F_{(1,99)}$=1.635), or in the further increase in LTP expression measured in the two groups (t-test; P=0.938).

At 18 months, the control group showed the same qualitative response to the HFS as was described in the 6 month old animals. However, the LTP generated in the transgenic group showed a striking qualitative difference (figure 5.14B). Instead of showing the gradual decrease in potentiation following the end of the PTP phase, the level of potentiation in the transgenic group actually increased slightly. This increase rapidly stabilized into a robust plateau of LTP expression that was established within 10 minutes following the HFS. This was in stark contrast to the gradual decline of potentiation that was observed in the control group that takes usually 30 minutes to establish a stable level of LTP expression. There was a significant difference in the level of potentiation recorded for the first 20 minutes following HFS (2-way repeat measure ANOVA; P<0.001, F=22.117.). There was a statistically significant interaction between genotype and time (P<0.001, F=4.066). The strength of LTP expression varied from 23.484 to 53.912% in the control group (x=39.674% ± 4.448) and from 37.467 to 117.700% in the transgenic group (x=65.301% ± 8.413). The level of LTP expression 51-60 minutes following HFS was significantly greater in the transgenic group (nested ANOVA; P=0.011 $F_{(1,126)}$=7.560 control n=6 rats, transgenic n=6 rats).

The second HFS generated further potentiation of between 9.872 and 38.346% (x=17.229% ± 6.898) in the control group and between 0.354 and 72.397% (x=21.362% ± 7.191) in the transgenic group. In one control experiment, the second HFS caused an 18.44% depotentiation of LTP expression. There a statistically significant difference in the total level of LTP expression in control and transgenic groups following the second HFS (nested ANOVA; P=0.002 $F_{(1,126)}$=11.662), although there was no significance in the further increase in the level of LTP expression (t-test; P=0.691).

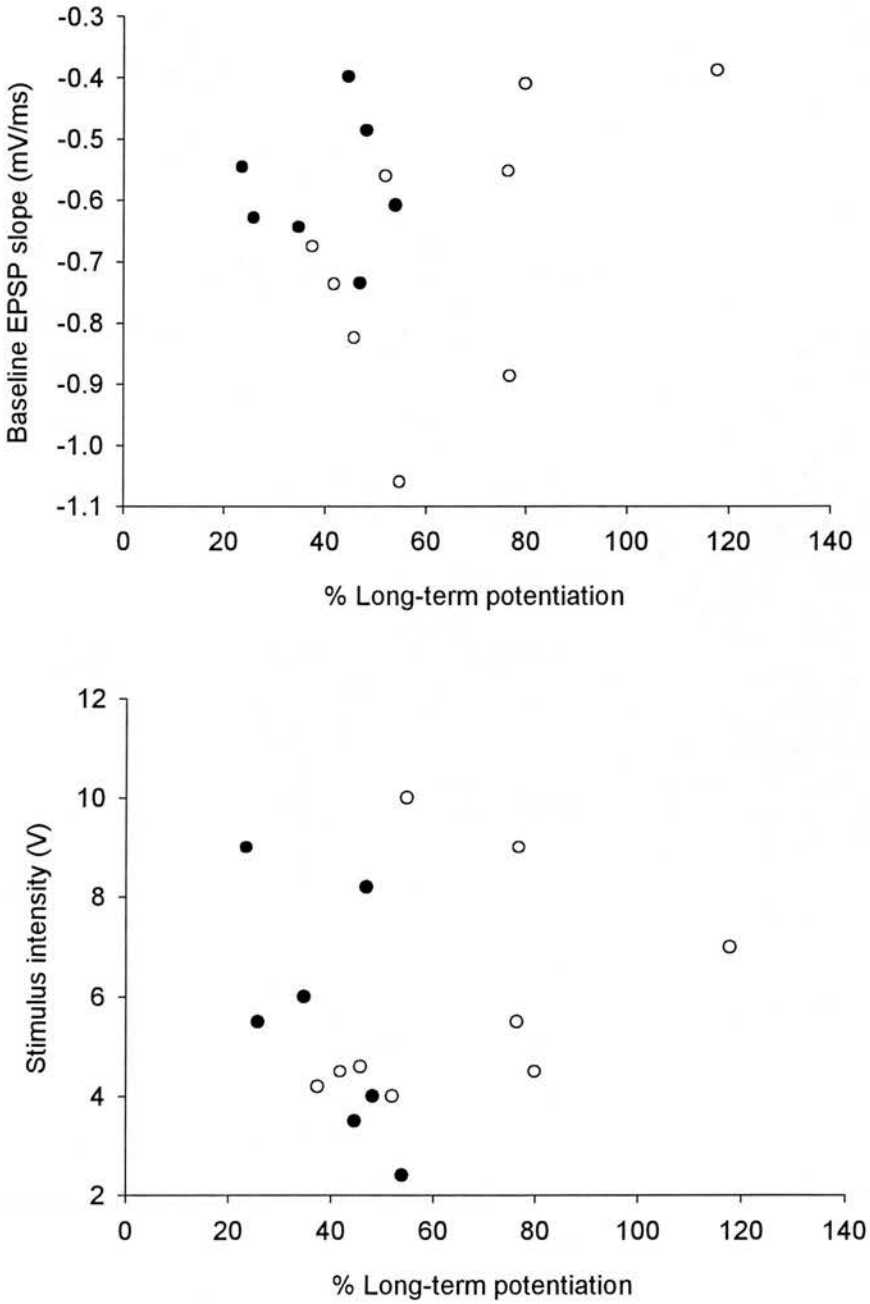

Figure 5.13 Correlations between percentage of CA1 LTP and baseline properties
Scatter plots show the relationship between percentage of LTP and average baseline EPSP slope (A) and stimulus intensity (B) in control (black circles) and transgenic (open circles) 18 month groups.
There was no significant correlation between the percentage of LTP and the baseline EPSP slope or stimulus intensity (Pearson correlations; Control LTP and EPSP slope P=0.873, LTP and stimulus intensity P=0.139, transgenic LTP and EPSP slope P=0.131, LTP and stimulus intensity P=0.367).

5.42 Long-term potentiation in medial perforant pathway/dentate gyrus pathway

Figure 5.14 shows example of field EPSPs recorded in the DG of slices from 6 and 18 month old animals before and after HFS. Figures 5.15A and B show LTP recorded in the CA1 for control and transgenic groups at 6 months and 18 months respectively. At 6 and 18 months, both control and transgenic groups showed the same qualitative response to the HFS; PTP decayed into the early-LTP phase, with stable LTP usually being established within 1 hour.

The strength of LTP expression varied greatly. At 6 months, the mean (± SEM) LTP expression level values were 40.323% ± 5.885 (control) and 40.666% ± 6.338 (transgenic) with ranges of 27.385 to 59.179% in the control group and 25.611 to 63.302% in the transgenic group. There was no significant difference in the strength of LTP expression recorded in control and transgenic groups at 6 months (nested ANOVA; P=0.7.21, $F_{(1,90)}$=0.136 control n=4 rats, transgenic n=4 rats). At 18 months, the mean (± SEM) LTP expression level values were 42.214 ± 5.585% (control) and 49.636 ± 10.122% (transgenic) with ranges of 14.813 to 96.864% in the control group and 21.706 to 122.448% in the transgenic group. There was no significant difference in the strength of LTP expression recorded in control and transgenic groups at 18 months (nested ANOVA; P=0.055, $F_{(1,126)}$=4.368 control n=9 rats, transgenic n=4 rats).

At 6 months, the second HFS generated further potentiation of between 0.53 and 41.25% (x=19.417% ± 8.559) in the control group and between 2.49 and 29.93% (x=20.699% ± 3.926) in the transgenic group. One slice in the control group showed 1.56% depotentiation. There was no statistically significant difference in the total level of LTP expression in control and transgenic groups following the second HFS (nested ANOVA; P=0.817 $F_{(1,90)}$=0.056), or in the level of further increase in LTP expression (t-test; P=0.888). At 18 months, the second HFS generated further potentiation of between 3.17 and 46.08% (x=14.499% ± 4.164) in the control group and between 0.300 and 57.700% (x=27.339% ± 4.876) in the transgenic group. Three slices in the control group showed 0.14, 1.41 and 19.97% depotentiation of LTP expression following the second HFS. There was no statistically significant difference in the total level of LTP expression in control and transgenic groups following the second HFS (nested ANOVA; P=0.061 $F_{(1,126)}$=4.149), or in the further increase in LTP expression (t-test; P=0.063) although this result was marginal and there was a trend towards stronger LTP expression in the transgenic group noticable after the second HFS.

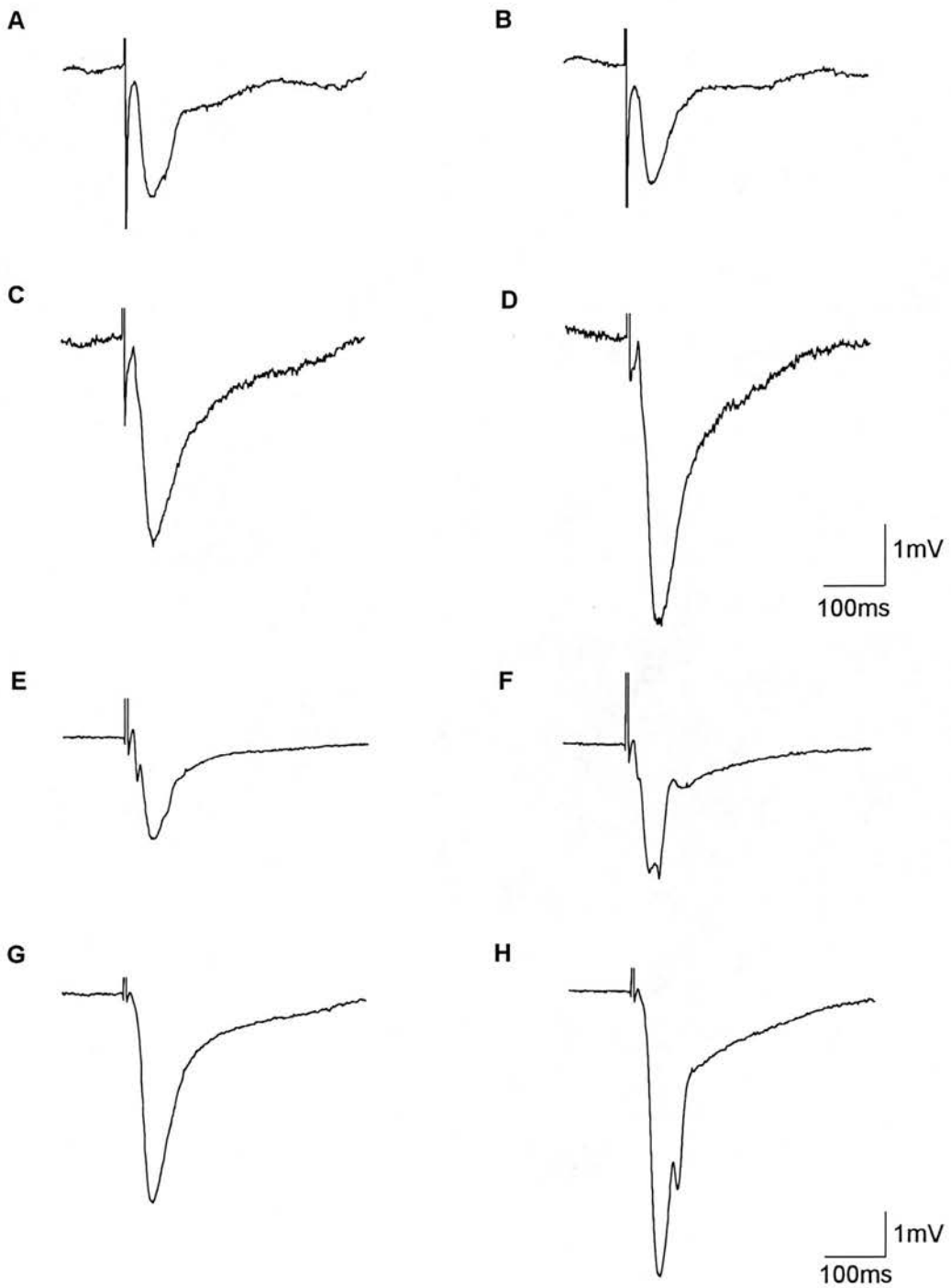

Figure 5.14 Field EPSPs in the DG before and after HFS
Traces are shown of EPSPs recorded from slices of 6 month ***(A-D)*** *and 18 month* ***(E-H)*** *old animals.* ***(A), (B), (E) & (F)*** *were recorded from control and* ***(C), (D), (G) & (H)*** *were recorded from transgenic animals. The traces on the left were recorded during the baseline. The traces on the right were recorded at 55 minutes following the HFS. The slope of fields recorded after the HFS were all potentiated.*
Traces ***(F) & (H)*** *shows evidence of a persisting population spike.*

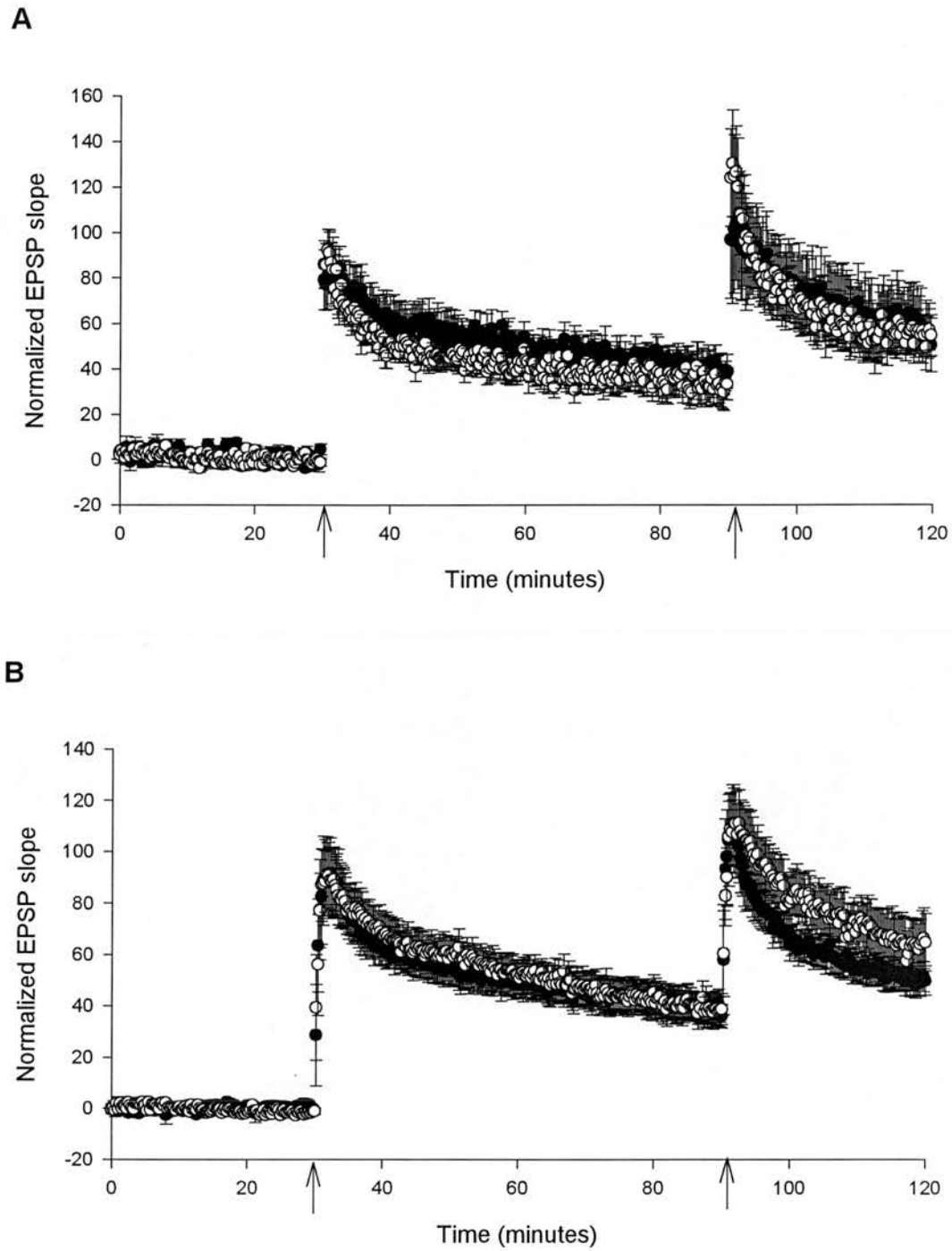

Figure 5.15 Long-term potentiation in the dentate gyrus

*LTP recorded in slices from control (black) and transgenic (white) animals at **(A)** 6 months and **(B)** 18 months. The perforant pathway was tetanized at 30 and 90 minutes (arrows). There was no significant difference in the level of LTP generated by slices from control and transgenic animals at either 6 or 18 months (nested ANOVA; 6 months: $P=0.721$ $F_{(1,90)}=0.136$. Control n=4 rats, transgenic n=4 rats.*

18 months: $P=0.055$ $F_{(1,216)}=4.368$. Control n=9 rats, transgenic n=4 rats).

Part II

Intracellular recordings from CA1 pyramidal neurones in 18 month old rats

Sharp electrode intracellular recordings were made from CA1 pyramidal neurones in 18 month old control and transgenic rats. The limited number of animals available prevented an intracellular investigation in 6 month old animals. Of the fifty-three animals available for intracellular study, 12 became ill and had to be killed without use (most commonly due to tumours) and twenty-two yielded slices that were not healthy enough to make successful intracellular recordings. This left nineteen animals that yielded healthy slices from which recordings were successfully made. Cells were accepted for analysis if the resting membrane potential had a negative value of at least -60mV, generated action potentials with amplitudes of at least 60mV and had a membrane resistance of more than 20MΩ. The findings of this study are summarized in table 5.3 at the end of part II.

5.5 Basic membrane properties of CA1 pyramidal neurones

5.51 Resting membrane potential

The provisional value for the resting membrane potential was recorded from impaled cells and adjusted if necessary if the voltage registered at the recording electrode when withdrawn from the neurone was not zero, to give the true resting membrane potential.

Figure 5.16 shows the frequency distribution of resting membrane potential values recorded in control and transgenic groups. The resting membrane potential values ranged from -60 to -87.5mV in the control group (x=-66.49mV ± 1.23) and -60 to -83.20mV in the transgenic groups (x=-63.39mV ± 0.61). The resting membrane potential values recorded in the control and transgenic groups was not significantly different (Mann-Whitney rank sum test; P=0.513 control n=36, transgenic n=54).

5.52 Membrane resistance

Hyperpolarizing and depolarizing current pulses were injected into neurones and the resulting change in membrane potential was recorded. Figure 5.17A shows the membrane responses to current injection. The membrane potential response was measured in the early part of the sweep to avoid bias of the result by rectifying voltage gated currents. Also to minimize bias caused by voltage activated currents, only responses to hyperpolarizing pulses of between -5 and -125pA were included in the analysis. The current voltage relationship was plotted as shown in figure 5.17B and the value of the slope is the membrane resistance.

Membrane resistance values ranged from 22.757 to 82.168MΩ in the control group (x=38.39MΩ ± 2.19) and 20.030 to 74.078MΩ in the transgenic group (x=40.18MΩ ± 1.94) (figure 5.17C). The mean (± SEM) membrane resistance values are shown in figure 5.17D. The difference in membrane resistance values recorded in neurones from control and transgenic groups was not statistically significant (t-test; P=0.549 control n=33, transgenic n=50).

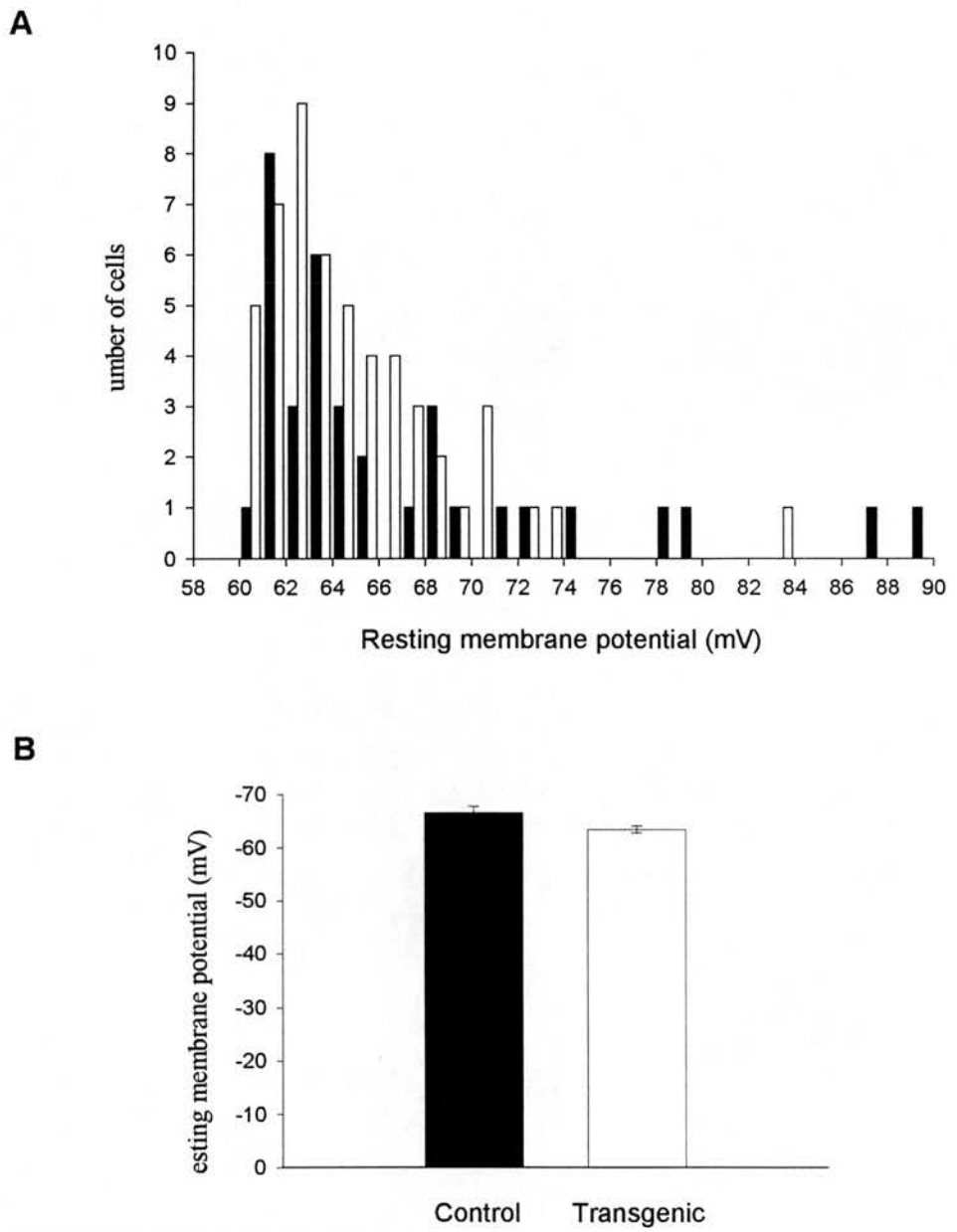

Figure 5.16 Resting membrane potential

(A) *Frequency distribution of resting membrane potential values in control and transgenic groups. Values are grouped into 1mV bins.* ***(B)*** *Mean resting membrane potential values (± SEM). The difference between values recorded in control and transgenic groups was not statistically significant (Mann-Whitney rank sum test P=0.513. Control; x = -66.46mV ± 1.23, n=36. Transgenic; x = -63.39mV ± 0.61 n=54).*

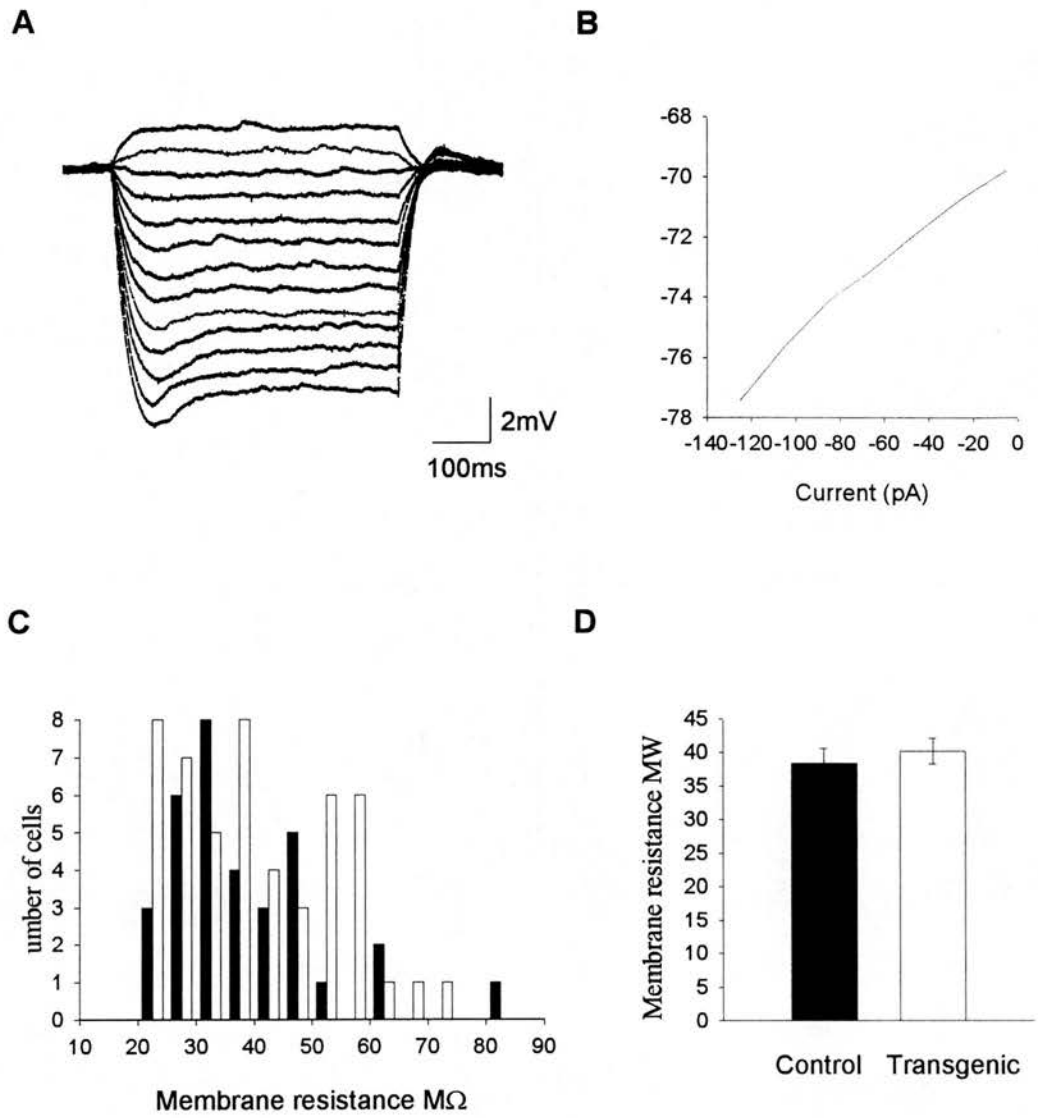

Figure 5.17 Membrane resistance

(A) *Membrane response to current pulses rangeing from -205 to 35pA.* ***(B)*** *The membrane responses to hyperpolarizing current pulses to -130pA were plotted to calculate the membrane resistance.* ***(C)*** *Frequency distribution of membrane resistance values in control and transgenic groups.* ***(D)*** *Comparing the mean membrane resistance values (± SEM). The difference in membrane resistance values in the control and transgenic groups was not statistically significant (t-test; P=0.549, control n=33, transgenic n=50).*

5.53 Time constant

A 0.5ms hyperpolarizing current pulse was used to generate a passive membrane response, to which a curve was fitted to calculate the neuronal time constant (figure 5.18A). Time constant values ranged from 7.427 to 59.824ms in the control group and from 11.229 to 67.177ms in the transgenic group. The frequency distributions are shown in figure 5.18B. Figure 5.18C shows the mean (±SEM) time constant values recorded in the control (x=30.62ms ± 2.41) and transgenic (x=27.81ms ± 1.79) groups. The difference in time constant values recorded in control and transgenic groups was not statistically significant (t-test; P=0.343 control n=28, transgenic n=41).

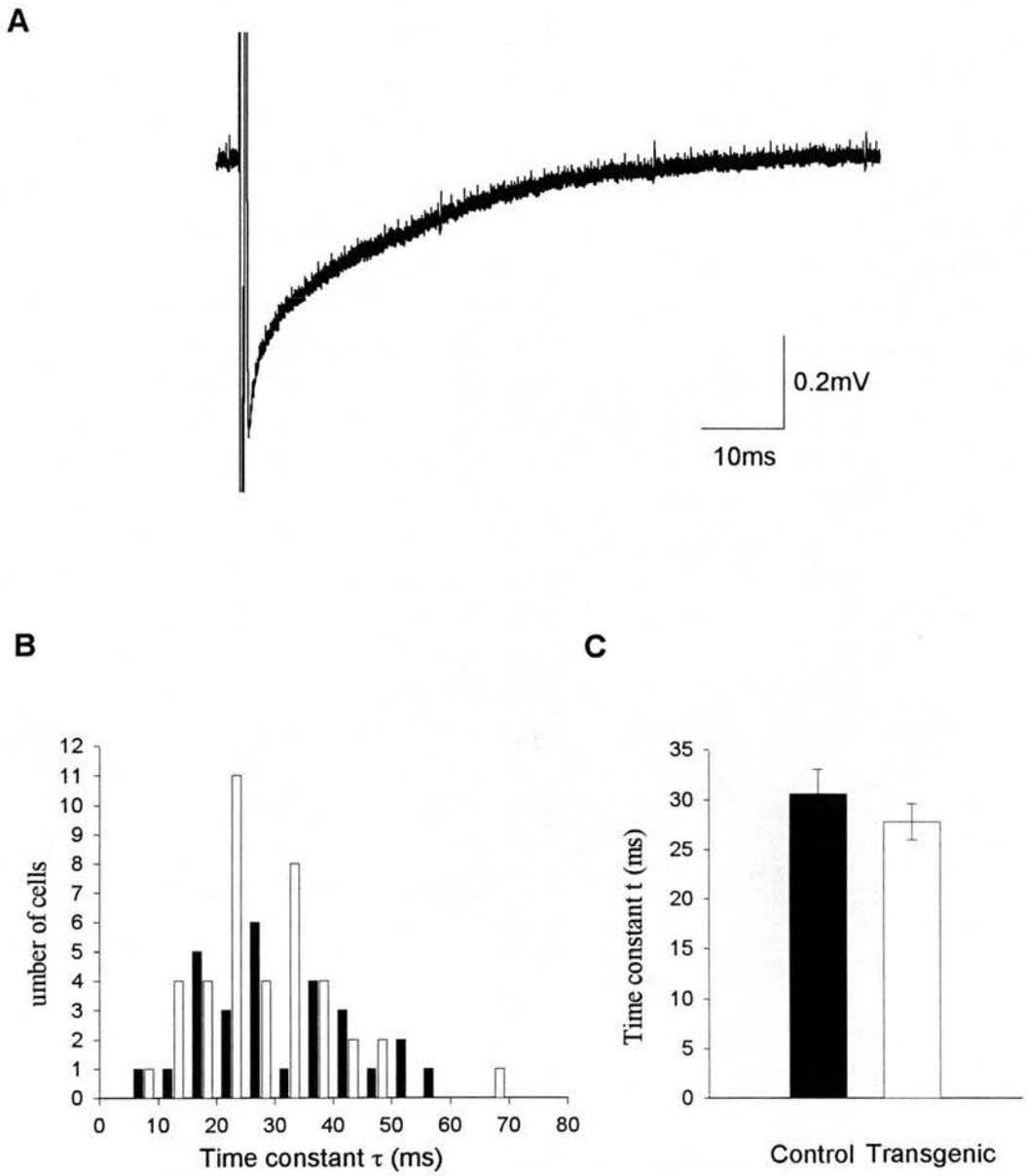

Figure 5.18 Time constant

(A) *Membrane response to a 0.5ms hyperpolarizing current pulse.* ***(B)*** *Frequency distribution of time constant values recorded in the control (black) and transgenic (white) groups. Time constant values are grouped into 5ms bins.* ***(C)*** *Comparing the mean (± SEM) of the time constant values. The difference in time constant values recorded in the control and transgenic groups was not statistically significant (t-test; P=0.343 control n=28, transgenic n=41).*

5.6 Action potential properties

Action potentials were generated by injecting depolarizing current into the neurone. The amplitude, rise time, decay time and half width of five action potentials were measured and the average gave representative values for each cell. An example of an action potential is shown in figure 5.19A.

Action potential amplitude values ranged from 64.46 to 79.80mV in the control group (x=72.867mV ± 0.686) and from 60.22 to 82.46mV in the transgenic group (x=71.703mV ± 0.772). The frequency distributions of amplitude values are shown in figure 5.19B and the mean values (± SEM) are shown in figure 5.19C. The difference in action potential amplitudes recorded in the control and transgenic groups was not statistically significant (Mann-Whitney rank sum test; P=0.465, control n=29 transgenic n=51).

Action potential rise time values ranged from 0.40 to 0.76ms in the control group (x=0.59ms ± 0.013) and from 0.44 to 0.76ms in the transgenic group (x=0.59ms ± 0.012). The frequency distributions are shown in figure 5.20A and the mean values (± SEM) are shown in figure 5.20B. The difference in action potential rise time recorded in the control and transgenic groups was not statistically significant (Mann-Whitney rank sum test; P=0.877, control n=29 transgenic n=51).

Action potential decay time values ranged from 0.84 to 1.46ms in the control group (x=1.078ms ± 0.023) and from 0.68 to 1.50ms in the transgenic group (x=1.068ms ± 0.024). The frequency distributions are shown in figure 5.20C and the mean values (± SEM) are shown in figure 5.20D. The difference in action potential decay time recorded in the control and transgenic groups was not statistically significant (t-test; P=0.778, control n=29 transgenic n=51).

Action potential half width values ranged from 0.76 to 0.98ms in the control group (x=0.851ms ± 0.010) and from 0.70 to 1.50ms in the transgenic group (x=0.869ms ± 0.011). The frequency distributions are shown in figure 5.20E and the mean values (± SEM) are shown in figure 5.20F. The difference in action potential half width recorded in the control and transgenic groups was not statistically significant (t-test; P=0.264, control n=29 transgenic n=51).

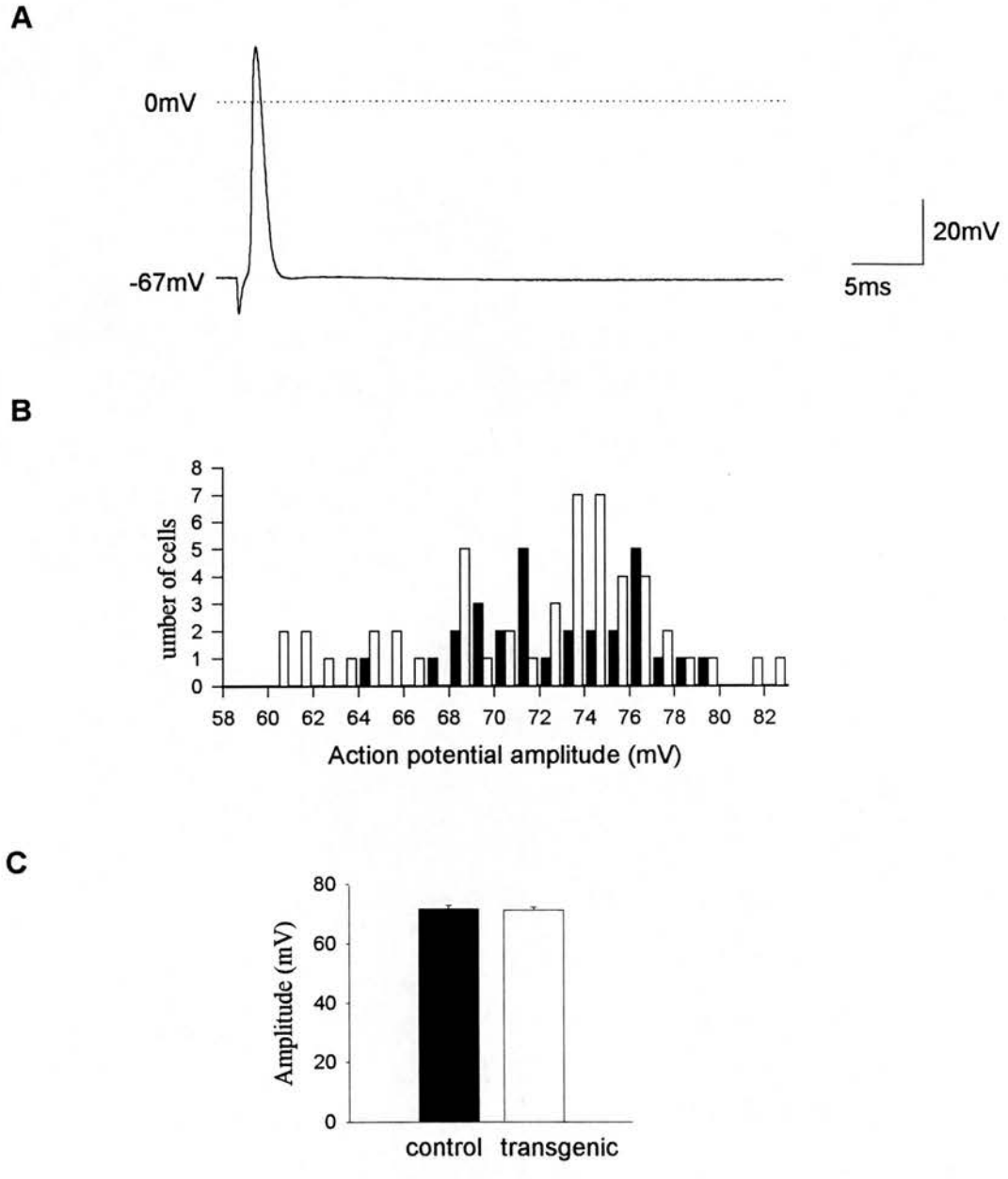

Figure 5.19 Action potential amplitude

(A) *Action potential induced by a single depolarizing current pulse.* ***(B)*** *Frequency distribution of action potential amplitude values in control (black) and transgenic (white) groups. Action potential amplitude values are grouped in 1mV bins.* ***(C)*** *Mean (± SEM) amplitude values.*

The difference in action potential amplitude values measured in control and transgenic groups was not statistically significant (Mann-Whitney rank sum test; P=0.465 control n=29 transgenic n=51).

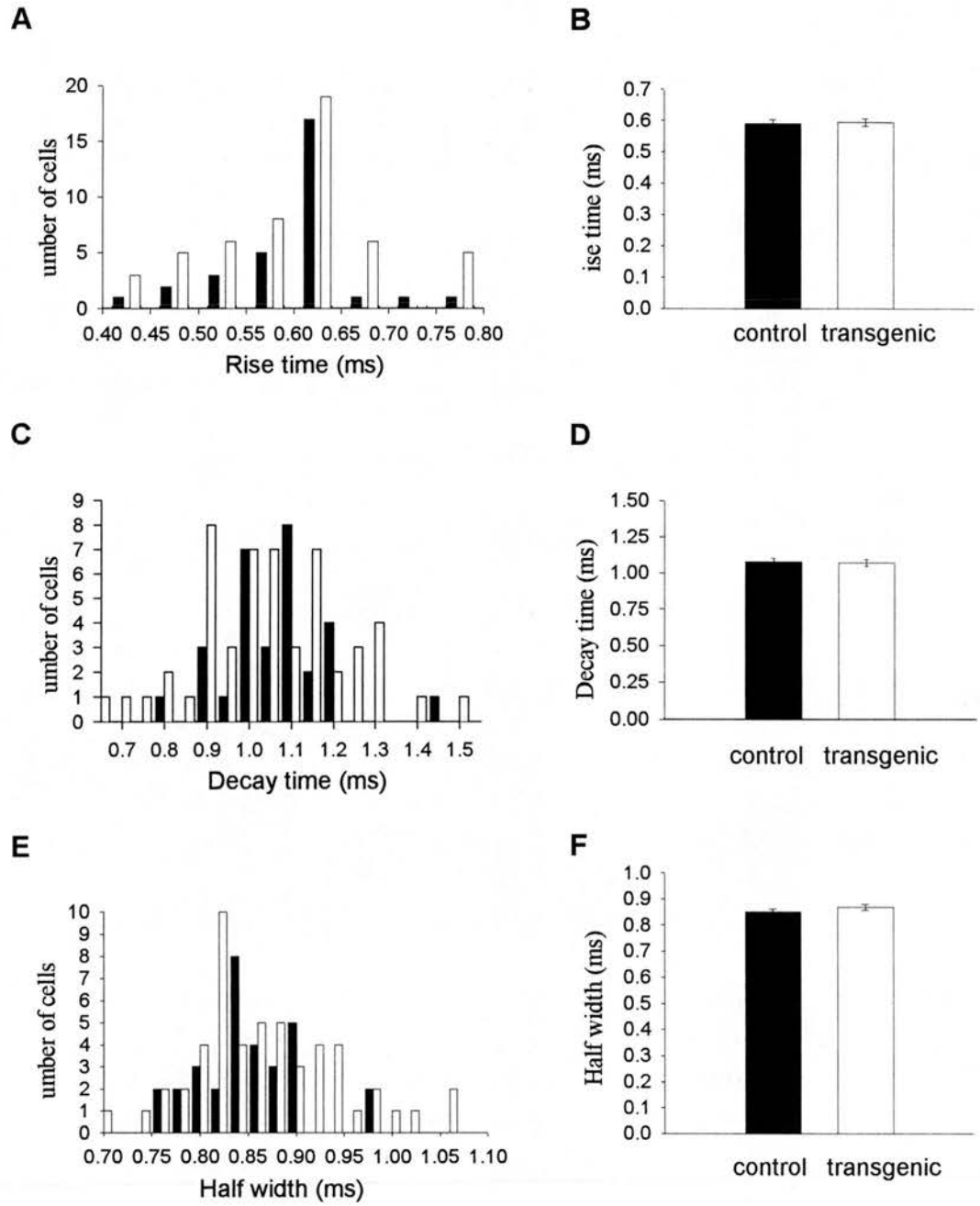

Figure 5.20 Action potential rise time, decay time and half width

*Frequency distribution graphs are shown for action potential **(A)** rise time, **(C)** decay time and **(E)** half width in control (black) and transgenic (white) groups. Action potential rise time and fall time values are grouped into 0.05ms bins and half width values are grouped into 0.02ms bins. Mean (± SEM) values are plotted for **(B)** rise time, **(D)** decay time and **(F)** half width.*

There was no significant difference in the action potential rise time (Mann-Whitney rank sum test P=0.877) decay time (t-test P=0.778) or half width (t-test P=0.264) measured in control and transgenic groups (control n=31, transgenic n=52).

An afterdepolarizing potential (ADP) followed single action potentials in 18 out of 31 (58%) control cells and 22 out of 52 (42%) transgenic cells. An example of both ADP and fAHP responses in a control cell is shown in figure 5.21A. Afterdepolarizing potential amplitudes ranged from 0.20 to 13.64mV (x=4.51mV ± 0.84) in the control group and from 0.11 to 11.06mV (x=4.058mV ± 0.612) in the transgenic group. Figure 5.21B shows frequency distributions of ADP amplitudes. The mean (±SEM) ADP amplitude values are shown in figure 5.21C. The difference in ADP amplitudes recorded in control and transgenic groups was not statistically significant (t-test; P=0.661 control n=18, transgenic n=22).

A fast afterhyperpolarizing potential (fAHP) followed the action potential in 21 out of 31 (67%) control cells and 34 out of 52 (65%) transgenic cells. Fast afterhyperpolarizing potential amplitudes ranged from 0.260 to 3.803mV (x=1.503mV ± 0.350) in the control group and from 0.140 to 8.480mV (x=1.271mV ± 0.267) in the transgenic group. Figure 5.21D shows frequency distributions of fAHP amplitudes. The mean (±SEM) fAHP amplitude values are shown in figure 5.22E. The difference in ADP amplitudes recorded in control and transgenic groups was not statistically significant (Mann-Whitney rank sum test; P=0.562 control n=21, transgenic n=34).

Single action potentials were followed by an fAHP and an ADP in 15 out of 31 (48%) control neurones and 22 out of 52 (42%) transgenic neurones (figure 5.21A). No afterpotential was observed following action potentials in 9 out of 31 (29%) control and 20 out of 52 (38%) transgenic neurones. There was no significant difference in the numbers of neurones showing an ADP, fAHP, both or none following the action potential in control and transgenic groups (Chi-squared test; P=0.213).

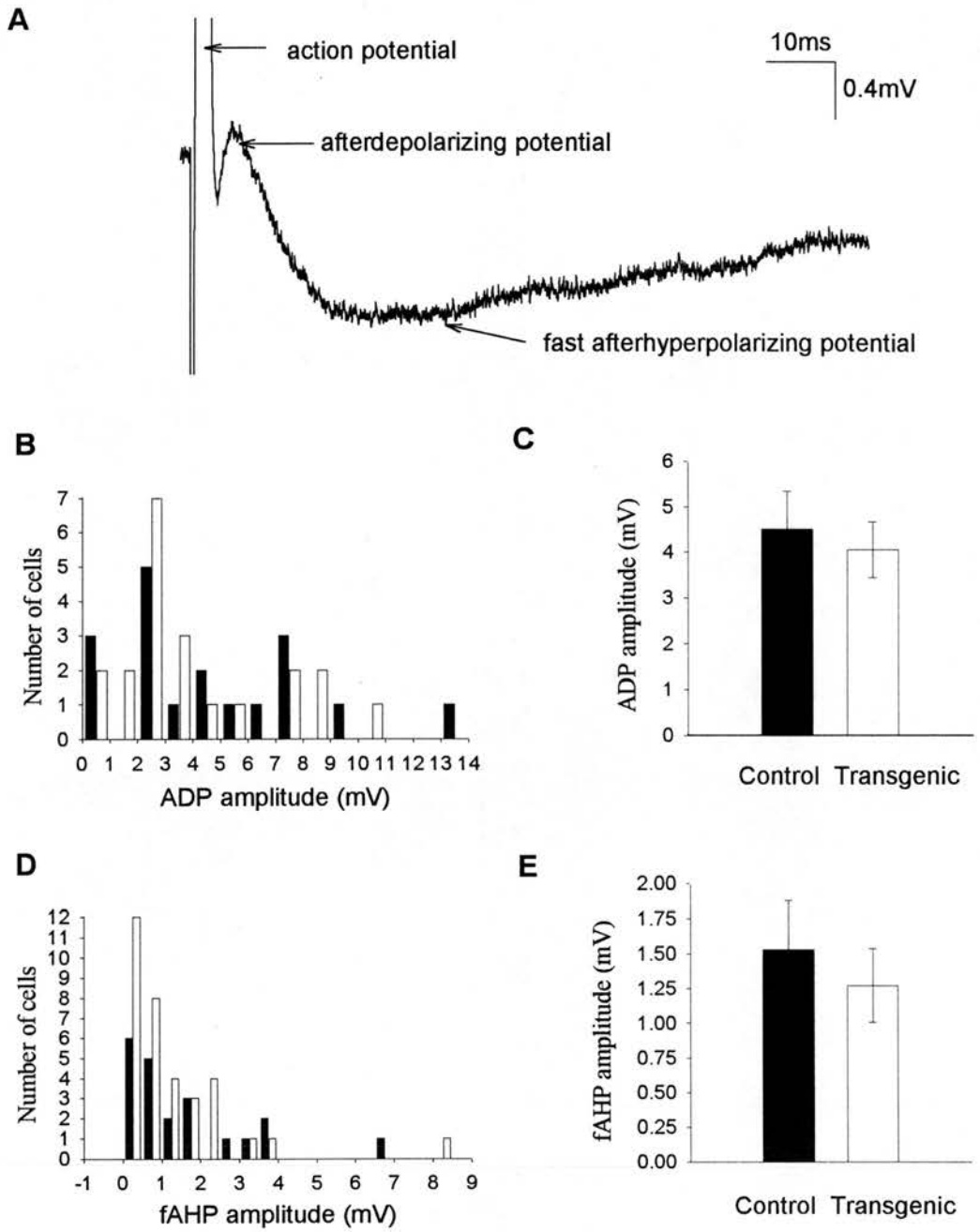

Figure 5.21 Action potential afterdepolarizing and fast hyperpolarizing potentials

(A) *Both a small ADP and a fAHP followed the action potential in this cell. Frequency distributions of ADPs* ***(B)*** *and fAHPs* ***(D)*** *in control (black) and transgenic (white) groups. Values were grouped into 1mV (ADP) and 0.5mV (fAHP) bins. The mean (± SEM) values are shown for the* ***(C)*** *ADP and* ***(E)*** *fAHP.*

The difference in ADP and fAHP values recorded in control and transgenic groups was not statistically significant (ADP: t-test; P=0.661, control n=18 transgenic n=22. fAHP: Mann-Whitney rank sum test; P=0.562. control n=21 transgenic n=34.)

5.7 EPSP properties

EPSPs in CA1 pyramidal neurones were generated by stimulation of the Schaffer collaterals in the stratum radiatum. For consistancy between cells and animals, measurements were made from half maximal EPSPs. To obtain synaptically generated half maximal EPSPs, the stimulus intensity was increased until an action potential was generated in response to 50% of stimuli. The amplitude was measured and the stimulus intensity decreased to obtain an EPSP with a half maximal amplitude value. Superimposed examples of EPSPs recorded in control and transgenic groups is shown in figure 5.22A.

EPSP amplitude values ranged from 2.181 to 11.369mV in the control group (x=5.704mV ± 0.512) and from 2.681 to 11.107mV in the transgenic group (x=5.995mV ± 0.369). The frequency distributions of amplitude values are shown in figure 5.22B and the mean values (± SEM) are shown in figure 5.22C. The difference in EPSP amplitudes recorded in the control and transgenic groups was not statistically significant (t-test; P=0.638, control n=22 transgenic n=30).

EPSP rise time values ranged from 3.5 to 13.2ms in the control group (x=5.65ms ± 0.49) and from 3.3 to 9.4ms in the transgenic group (x=6.03ms ± 0.34). The frequency distribution of rise time values is shown in figure 5.23A and the mean values (± SEM) are shown in figure 5.23B. The difference in EPSP rise time recorded in the control and transgenic groups was not statistically significant (Mann-Whitney rank sum test; P=0.251, control n=22 transgenic n=30).

EPSP decay time values ranged from 3.60 to 101.40ms in the control group (x=19.659ms ± 4.901) and from 3.0 to 84.1ms in the transgenic group (x=30.70ms ± 4.50). The frequency distributions of EPSP decay time values is shown in figure 5.23C and the mean values (± SEM) are shown in figure 5.23D. The difference in EPSP decay time recorded in the control and transgenic groups was not statistically significant (Mann-Whitney rank sum test; P=0.060, control n=22 transgenic n=30) although there was a trend towards a longer decay time in the transgenic group.

EPSP half width values ranged from 4.30 to 45.60ms in the control group (x=10.718ms ± 1.964) and from 4.10 to 37.49ms in the transgenic group (x=14.85ms ± 1.50). The frequency distribution of half width values is shown in figure 5.23E and the mean values (± SEM) are shown in figure 5.23F. The action potential half width recorded in the transgenic groups was significantly

longer than that recorded in the control group (Mann-Whitney rank sum test; P=0.016, control n=22 transgenic n=30).

Figure 5.24 shows scatter plots of EPSP properties against resting membrane potential. There was no significant correlation between resting membrane potentian and EPSP amplitude, rise time, decay time or half-width in either control or transgenic groups. (Pearson correlation. Control; resting membrane potential and EPSP amplitude P=0.699, EPSP rise time P=0.069, EPSP decay time P=0.198 and EPSP 1/2 width P=0.189. Transgenic; resting membrane potential and EPSP amplitude P=0.123, EPSP rise time P=0.175, EPSP decay time P=0.113 and EPSP 1/2 width P=0.232.)

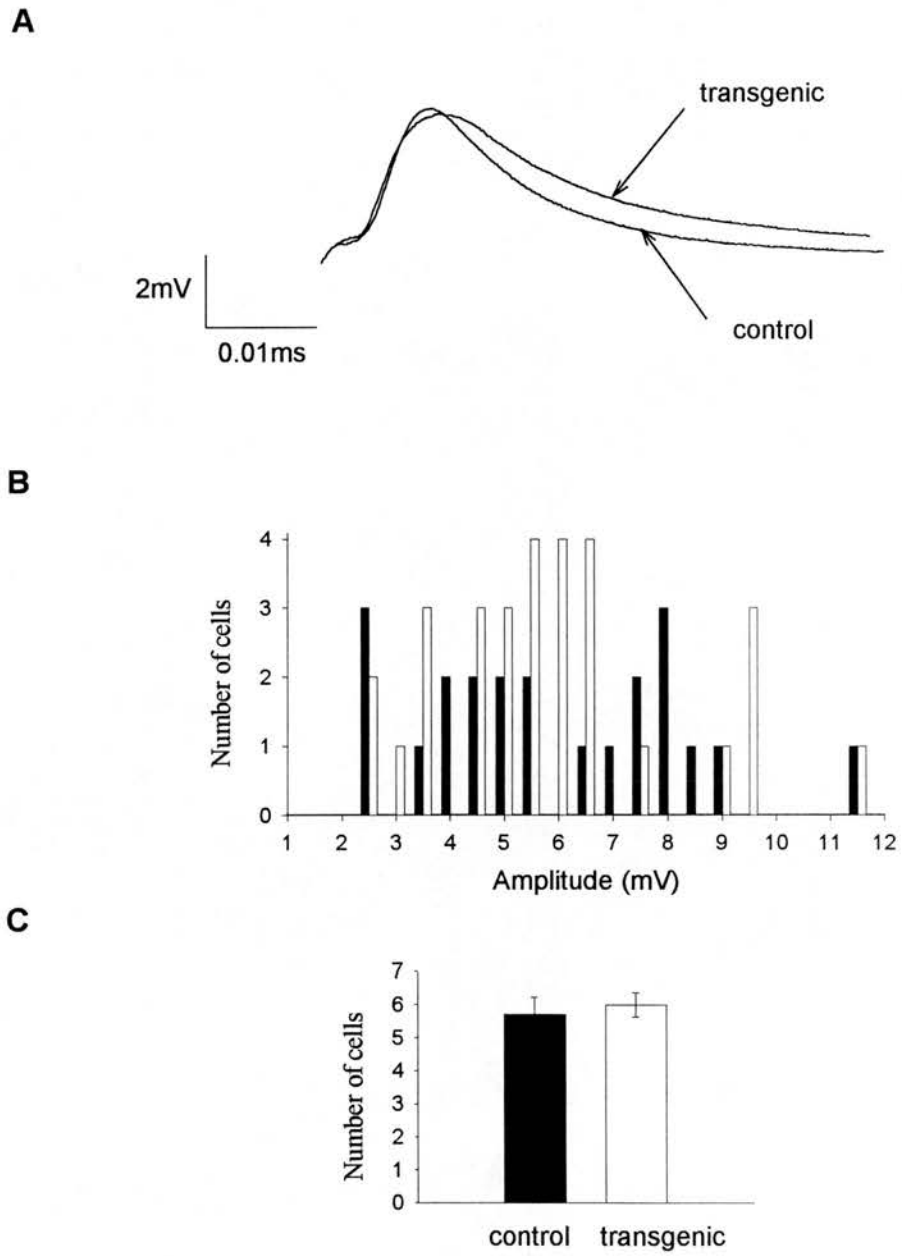

Figure 5.22 EPSP amplitude

(A) *Examples of synaptically generated EPSPs in control and transgenic groups, showing the increase half width in the transgenic group.* ***(B)*** *Frequency distribution of EPSP amplitudes in control (black) and transgenic (white) groups.* ***(C)*** *Mean (± SEM) amplitudes; there was no significant difference in the mean EPSP amplitudes recorded in control and transgenic groups (t-test; P=0.638, control n=22, transgenic n=30).*

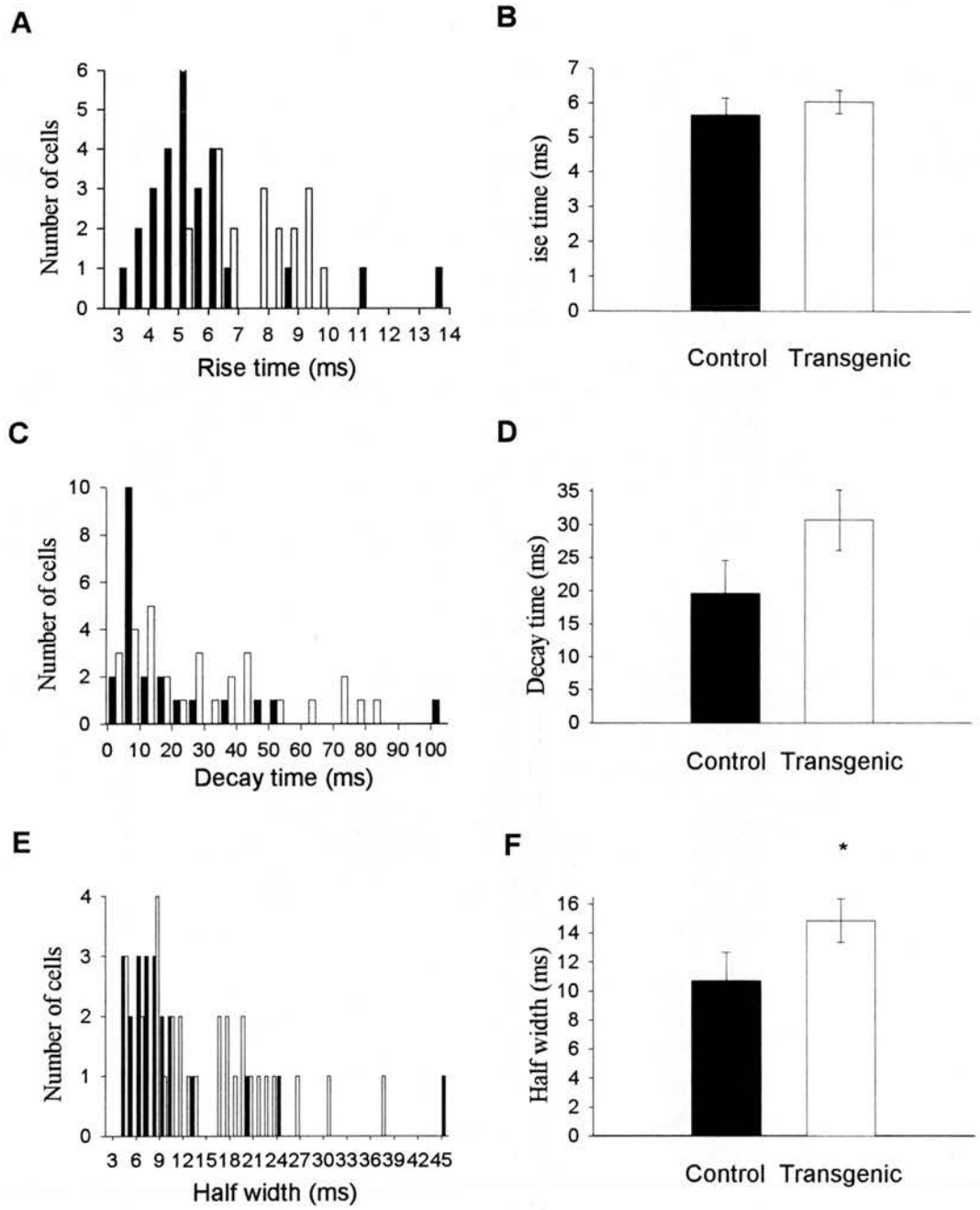

Figure 5.23 EPSP rise time, decay time and half width

*Distribution graphs are shown for EPSP **(A)** rise time, **(C)** decay time and **(E)** half width in control (black) and transgenic (white) groups. Values are grouped into (rise time) 0.5ms, (decay time) 5ms and (half width) 1ms bins. Mean (± SEM) values are plotted for **(B)** rise time, **(D)** decay time and **(F)** half width.*

There was no significant difference in the EPSP rise time (P=0.251) or fall time (P=0.060) values recorded in control and transgenic groups. The EPSP half width values recorded in the transgenic group were significantly longer (P=0.016). (All statistics using Mann-Whitney rank sum test, control n=22, transgenic n=30).

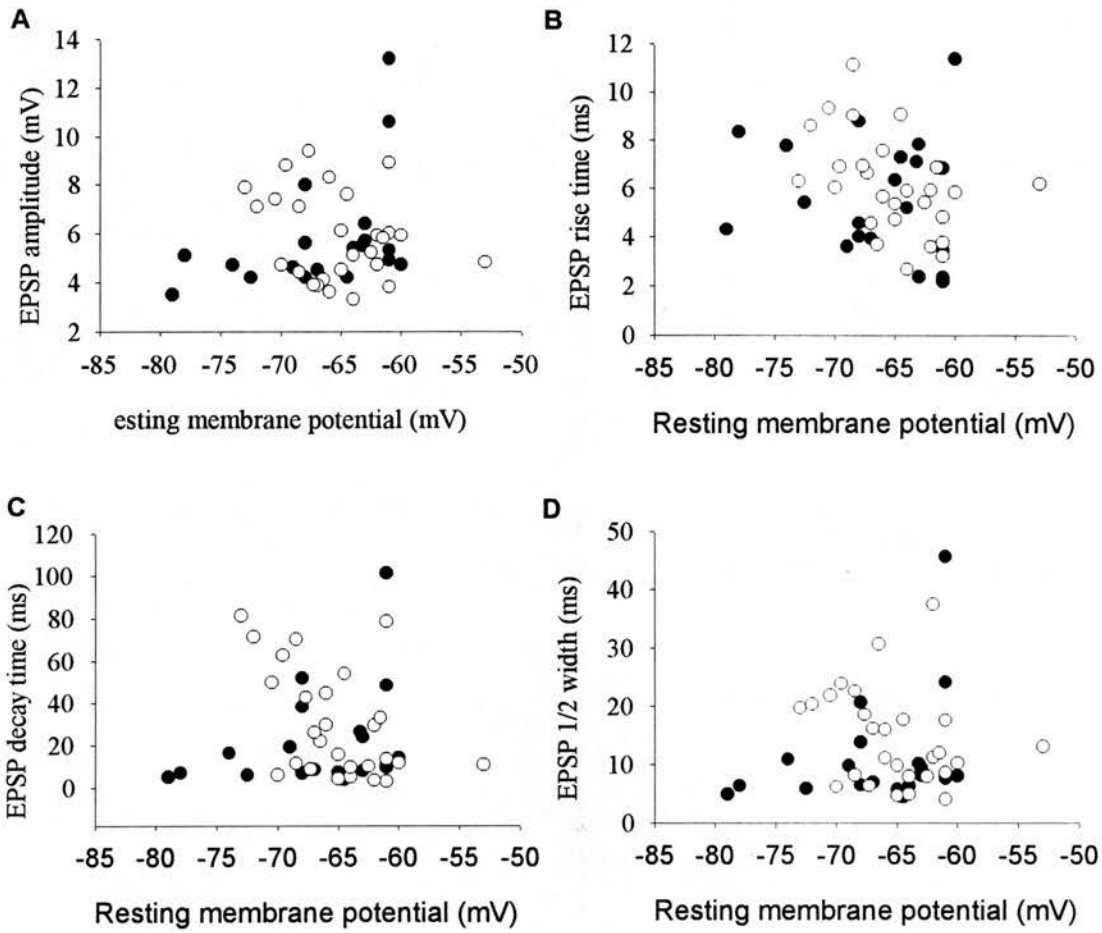

Figure 5.24 Resting membrane potential and EPSP properties
Scatter plots show the relationship between the resting membrane potential and (A) EPSP amplitude, (B) EPSP rise time, (C) EPSP decay time and (D) EPSP half width in control (black circles) and transgenic (open circles) groups. There was no significant correlation between resting membrane potential and EPSP properties in control or transgenic groups.

Control; resting membrane potential and ***(A)*** *EPSP amplitude P=0.699 ,* ***(B)*** *EPSP rise time P=0.069 ,* ***(C)*** *EPSP decay time P=0.198 and* ***(D)*** *EPSP 1/2 width P=0.189. Transgenic; resting membrane potential and* ***(A)*** *EPSP amplitude P=0.123,* ***(B)*** *EPSP rise time P=0.175 ,* ***(C)*** *EPSP decay time P=0.113 and* ***(D)*** *EPSP 1/2 width P=0.232 (Pearson correlation).*

5.8 Action potential firing frequency

Depolarizing current pulses of between 20 and 780pA were used to investigate the current/firing frequency relationship and firing frequency adaptation of action potentials. Neurones either showed rapid adaptation to silence or established a steady state of firing that persisted for the duration of the 2 second long current pulse. Neurones are referred to as rapidly or slowly adapting on the basis of these firing patterns. Examples of both types of response are shown in figure 5.25. Neurones showing persistent firing properties were used to investigate potential differences between the control and transgenic groups. Persistent firing was observed in 14 out of 29 (48.3%) control neurones and 31 out of 53 (58.5%) transgenic neurones.

Action potential frequencies were measured for spikes 1 and 2 (1st interspike interval), spikes 2 and 3 (2nd interspike interval) and averaged over the last 4 spike in the train (steady state). The relationship of these values with change in current strength is shown in figure 5.26. The action potential firing frequency over the 1st interpulse interval was not significantly different in control and transgenic groups (2-way repeat measure ANOVA; P=0.906 $F_{(1,607)}$=0.014. Control n=14, transgenic n=31). The maximum firing frequencies were 77.31Hz ± 4.36 (range 45.05 to 116.28Hz) in the control group and 70.05Hz ± 7.32 (range 25.00 to 138.89Hz) in the transgenic group. The action potential firing frequency over the 2nd interpulse interval was not significantly different in control and transgenic groups (2-way repeat measure ANOVA; P=0.730 $F_{(1,571)}$=0.120. Control n=14, transgenic n=30). The maximum firing frequencies were 62.36Hz ± 4.35 (range 28.57 to 81.97Hz) in the control group and 58.84Hz ± 5.91 (range 17.73 to 106.38Hz) in the transgenic group. The action potential firing frequency at steady state was not significantly different in control and transgenic groups (2-way repeat measure ANOVA; P=0.554 $F_{(1,437)}$=0.356. Control n=14, transgenic n=25). The maximum firing frequencies were 5.71Hz ± 0.97 (range 1.69 to 11.56Hz) in the control group and 7.72Hz ± 1.09 (range 1.66 to 15.40Hz) in the transgenic group.

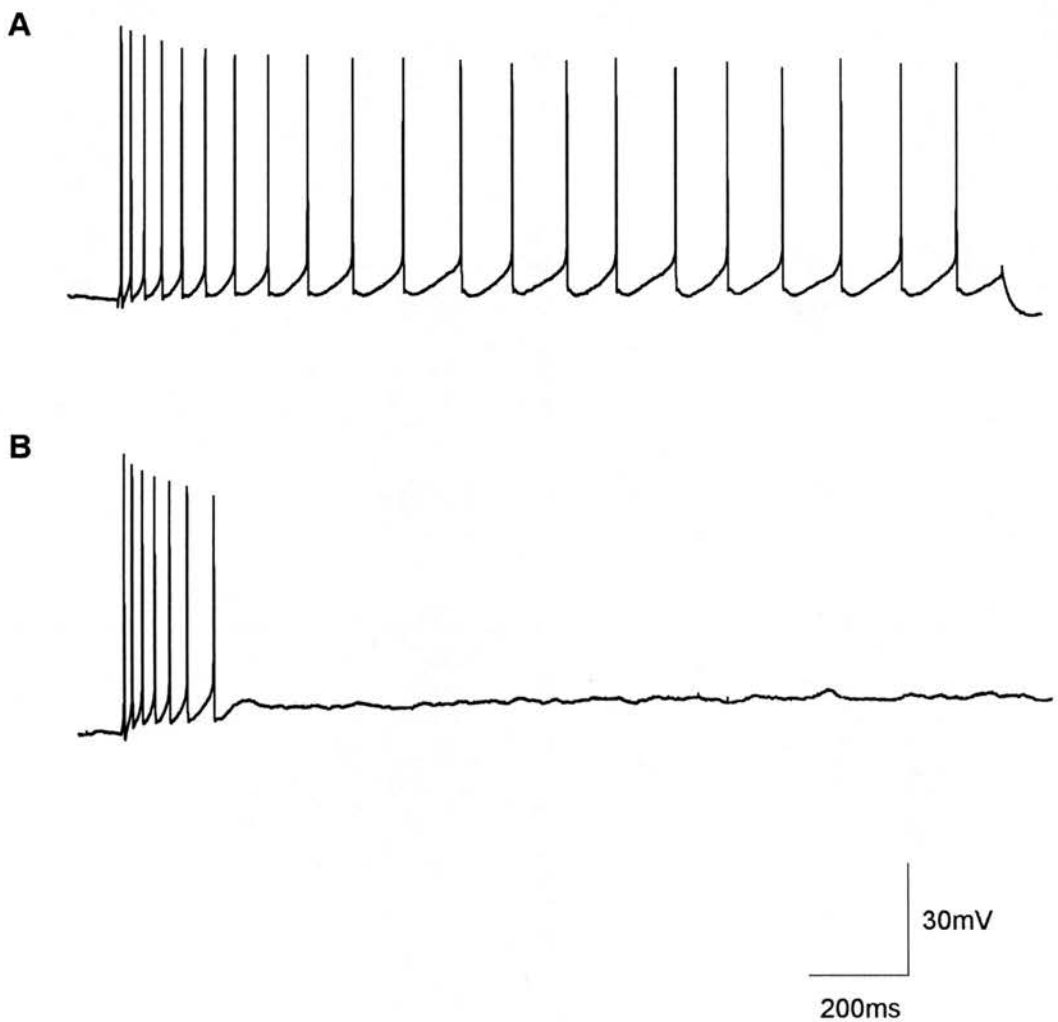

Figure 5.25 Action potential firing patterns

Responses to a 700pA depolarizing current pulse are shown for slowly and rapidly adapting neurones. ***(A)*** *shows action potential firing frequency adaptation to a steady state that persisted for the 2 second duration of the sweep.* ***(B)*** *shows rapid adaptation to silence. The two types of response were observed in neurones from both control and transgenic groups (control; adaptation to silence 15/29 neurones, persistent firing 14/29 neurones. Transgenic; adaptation to silence 22/53 neurones, persistent firing 31/53 neurones). There was no significant difference in the number of rapidly and slowly adapting neurones in the control and transgenic groups (Chi squared test with Yates correction P=0.511).*

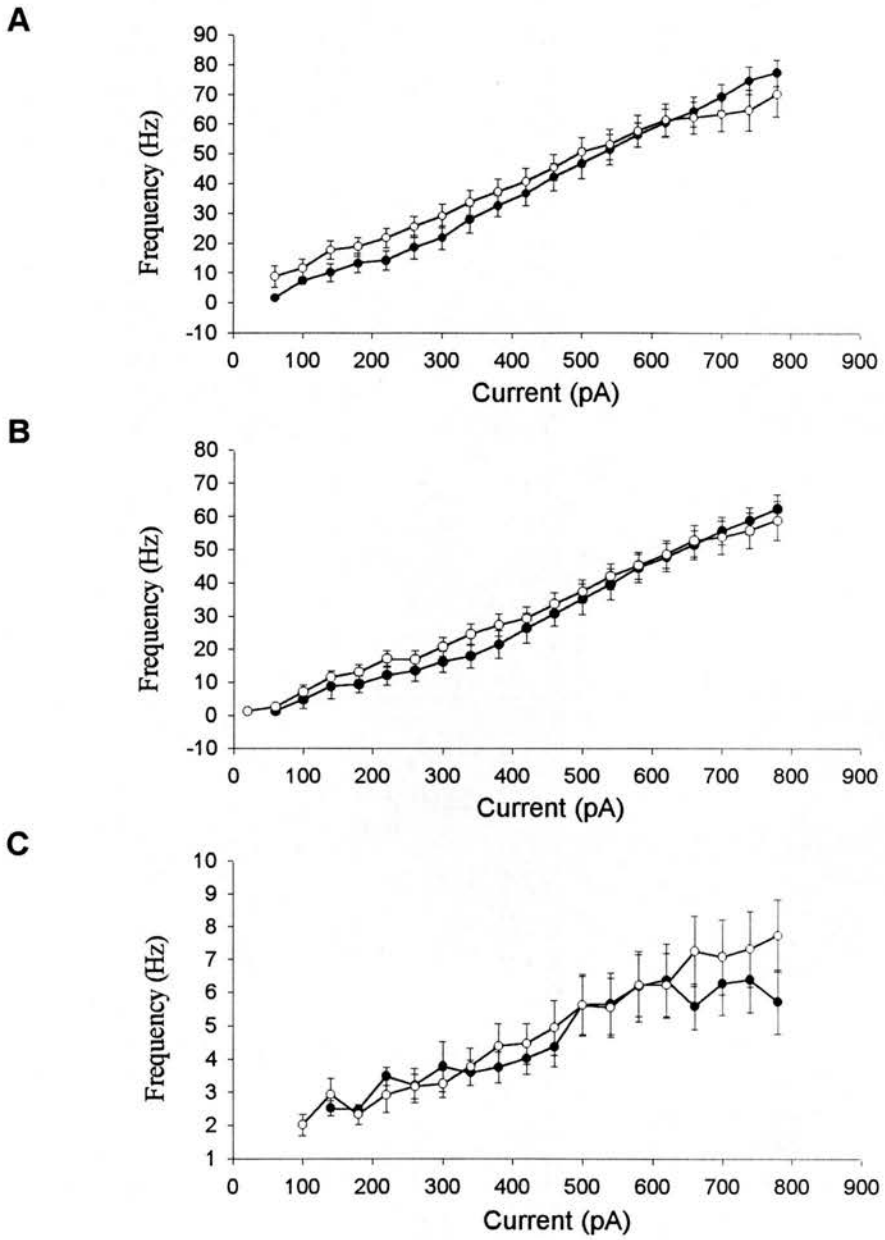

Figure 5.26 Current - action potential firing frequency relationship

*Current-frequency plots are shown for the **(A)** 1st, **(B)** 2nd and **(C)** steady state spike intervals. The difference in action potential firing frequency in control and transgenic groups was not significant at any of the intervals measured (2-way repeat measure ANOVA; 1st interspike interval P=0.906 $F_{(1,607)}$=0.014 control n=14 transgenic n=31. 2nd interspike interval P=0.730 $F_{(1,571)}$=0.120 control n=14 transgenic n=30. Steady state P=0.554 $F_{(1,437)}$=0.356 control n=14 transgenic n=25).*

A plot of action potential firing frequency adaptation in control and transgenic cells in response to a 660pA depolarizing current pulse is shown in figure 5.27. The first interval frequency values were 64.74Hz ± 5.16 in the control group (range 36.50 to 108.70Hz) and 64.49Hz ± 5.15 in the transgenic group (range 15.48 to 108.70Hz). The final interval frequency values were 13.73Hz ± 2.67 in the control group (range 2.67 to 16.39Hz) and 15.25Hz ± 1.96 in the transgenic group (range 1.95 to 19.16Hz). Neurones from both control and transgenic groups reached a plateau firing frequency by about the 8th interspike interval. There was no significant difference in the firing frequency values recorded in the control and transgenic groups at any interval (t-test; P values ranged from 0.181 to 0.992).

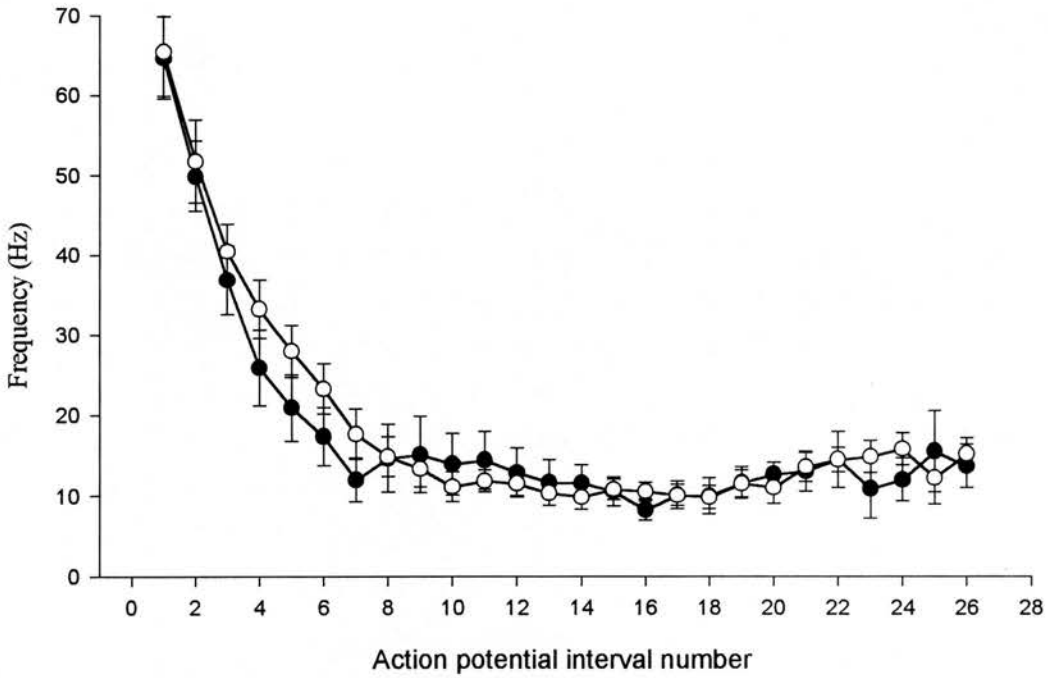

Figure 5.27 Action potential firing frequency adaptation

Trains of action potentials were generated using a 660pA current pulse. Both control (black) and transgenic (white) neurones showed rapid adaptation, reaching a steady state firing frequency by the 8th interspike interval. There was no significant difference in adaptation in control and transgenic groups (t-tests performed at each interval. P values ranged from 0.181 to 0.992).

5.9 Medium and slow afterhyperpolarization

Hippocampal pyramidal neurones show periods of membrane hyperpolarization following bursts of action potentials (APs). To investigate if these hyperpolarizations were altered in the transgenic rats, burst of 8, 12, 16 and 20 action potentials APs were evoked to generate medium and slow afterdepolarizations (mAHP and sAHP). The mAHP last for less than 1 second and its amplitude was taken as the maximal level of hyperpolarization following the burst. The sAHP lasts for upto 4 seconds. The peak amplitude of the sAHP was often obscured by the mAHP and so the level of hyperpolarization recorded 1 second following the end of the burst was taken as a representative value for the sAHP amplitude. Figure 5.28 shows examples of mAHPs and sAHPs generated in neurones from control and transgenic animals.

The mAHP amplitude varied greatly with control values ranging from 1.300 to 7.825mV following an 8 AP burst (x=4.082mV ± 0.282), 1.738 to 8.431mV following a 12 AP burst (x=5.173mV ± 0.336), 1.825 to 8.881mV following a 16 AP burst (x=5.297mV ± 0.349) and 1.806 to 9.050mV following a 20 AP burst (x=5.170mV ± 0.369) (figure 5.30B, C, D &E). Ranges in the transgenic group were 1.138 to 8.738mV following an 8 AP burst (x=3.830mV ± 0.228), 1.463 to 9.481mV following a 12 AP burst (x=4.557mV ± 0.249), 1.863 to 10.838mV following a 16 AP burst (x=4.794mV ± 0.319) and 1.931 to 11.450mV following a 20 AP burst (x=5.039mV ± 0.311). The change in mAHP amplitude with the number of APs in the conditioning burst is shown in figure 5.29A. The mAHP amplitude generated following a 12 AP burst was significantly greater than that generated following an 8 AP burst in both control and transgenic groups (t-test; control P=0.015, 8 AP burst n=36, 12 AP burst n=32. Transgenic P=0.034, 8 AP burst n=46, 12 AP burst n=44). The increase in the mAHP amplitude generated by 16 AP bursts and 20 AP bursts was not significantly greater than that generated by 12 AP bursts in either control or transgenic groups (t-test; control 12 & 16 AP bursts P=0.798, 12 & 20 AP bursts P=0.804, 16 AP bursts n=32, 20 APs n=25. Transgenic 12 & 16 AP bursts P=0.557, 12 & 20 AP bursts P=0.586, 16 AP bursts n=44, 20 AP bursts n=38). The difference in mAHP amplitude generated in control and transgenic groups was not significant (t-test; 8 AP burst P=0.485, 12 AP burst P=0.137, 16 AP burst P=0.295, 20 AP burst P=0.788).

The sAHP amplitude varied greatly with control values ranging from 0.600 to 7.363mV following an 8 AP burst (x=3.471mV ± 0.268), 0.931 to 7.575mV following a 12 AP burst (x=4.230mV ± 0.325), 1.306 to 7.856mV following a 16 AP burst (x=4.158mV ± 0.320) and 1.100 to 7.869mV following a 20 AP burst (x=4.214mV ± 0.375) (figure 5.31B, C, D &E). Ranges in the transgenic group were 0.894 to 8.350mV following an 8 AP burst (x=3.178mV ± 0.224), 0.969 to 8.456mV following a 12 AP burst (x=3.603mV ± 0.231), 1.219 to 9.738mV following a 16 AP burst (x=3.679mV ± 0.292) and 1.056 to 10.588mV following a 20 AP burst (x=3.829mV ± 0.290). The relationship between sAHP amplitude and the number of APs in the conditioning burst is shown in figure 5.30A. The increase in the sAHP amplitude generated by 12, 16 and 20 AP bursts was not significantly greater than that generated by 8 AP bursts in either control or transgenic groups (t-test; control comparing 8 & 12 AP bursts P=0.074, 8 & 16 AP bursts P=0.102, 8 & 20 AP bursts P=0.103. Transgenic comparing 8 & 12 AP bursts P=0.190, 8 & 16 AP bursts P=0.171, 8 & 20 AP bursts P=0.075). The difference in sAHP amplitude generated in control and transgenic groups was not significant (t-test; 8 AP bursts P=0.402, 12 AP bursts P=0.110, 16 AP bursts P=0.276, 20 AP bursts P=0.415).

Figures 5.32 and 5.33 show scatter plots of slow and medium AHP amplitudes respectively against resting membrane potential for control and transgenic groups. There was no significant correlation between the medium AHP amplitude and resting membrane potential (Pearson correlation: Control; mAHP8 P=0.056, mAHP12 P=0.082, mAHP16 P=0.098, mAHP20 P=0.140. Transgenic; mAHP8 P=0.213, mAHP12 P=0.319, mAHP16 P=0.196, mAHP20 P=0.150). There was no significant correlation between the slow AHP amplitude and resting membrane potential (Pearson correlation: Control; sAHP8 P=0.036, sAHP12 P=0.072, sAHP16 P=0.090, sAHP20 P=0.075. Transgenic sAHP8 P=0.700, sAHP12 P=0.804, sAHP16 P=0.489, sAHP20 P=0.458).

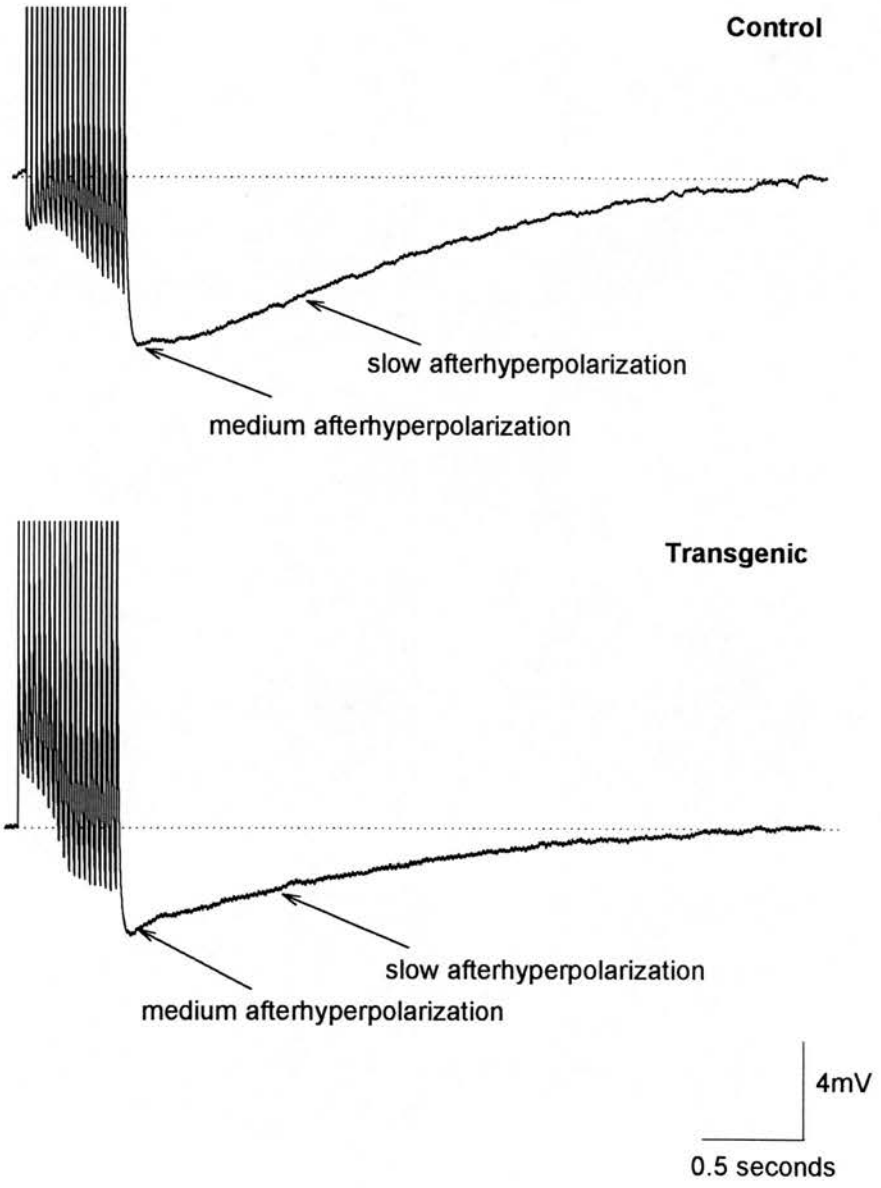

Figure 5.28 Medium and slow afterhyperpolarization
Medium and slow afterhyperpolarizing responses to a train of 20 action potentials are shown for control and transgenic groups.

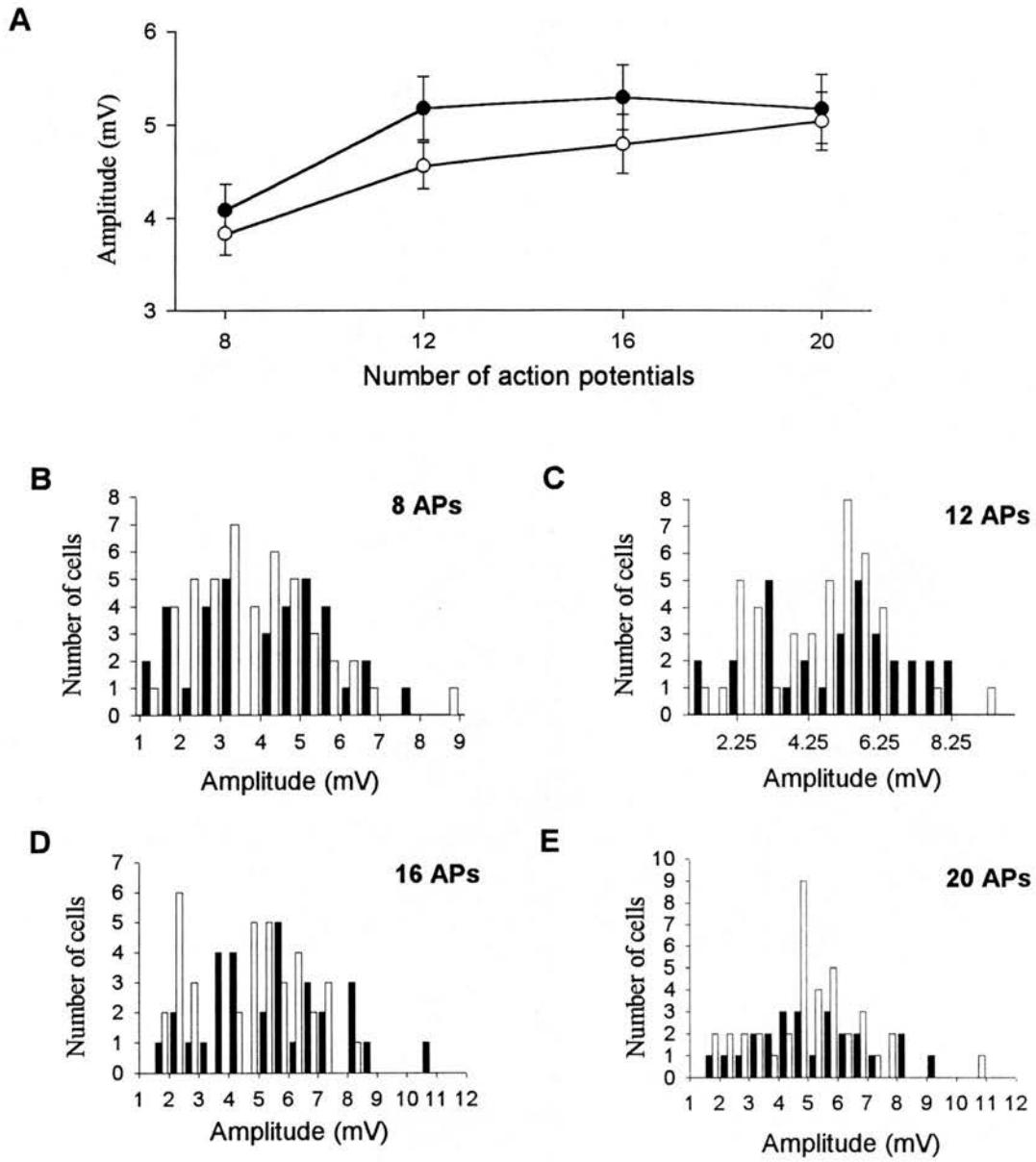

Figure 5.29 Medium AHP amplitude

(A) *The amplitude of the mAHP increased significantly when the number of action potentials (APs) in the conditioning train was increased from 8 to 12 (t-test; control P=0.015 8 APs n=36 12 APs n=32. Transgenic P=0.034, 8 APs n=46 12 APs n=44.) The difference in mAHP amplitude generated by 12 APs and 16 or 20 APs was not statistically significant (t-test; control 12 & 16 APs P=0.798, 12 & 20 APs P=0.804, 16 APs n=32, 20 APs n=25. Transgenic 12 & 16 APs P=0.557, 12 & 20 APs P=0.586, 16 APs n=44, 20 APs n=38). The difference in mAHP amplitude generated in control and transgenic groups was not significant (t-test; 8 APs P=0.485, 12 APs P=0.137, 16 APs P=0.295, 20 APs P=0.788). Frequency distributions are shown for mAHP amplitudes generated in control and transgenic groups in response to* ***(B)*** *8,* ***(C)*** *12,* ***(D)*** *16 &* ***(E)*** *20 APs. (mAHP amplitude values all grouped into 0.5mV bins).*

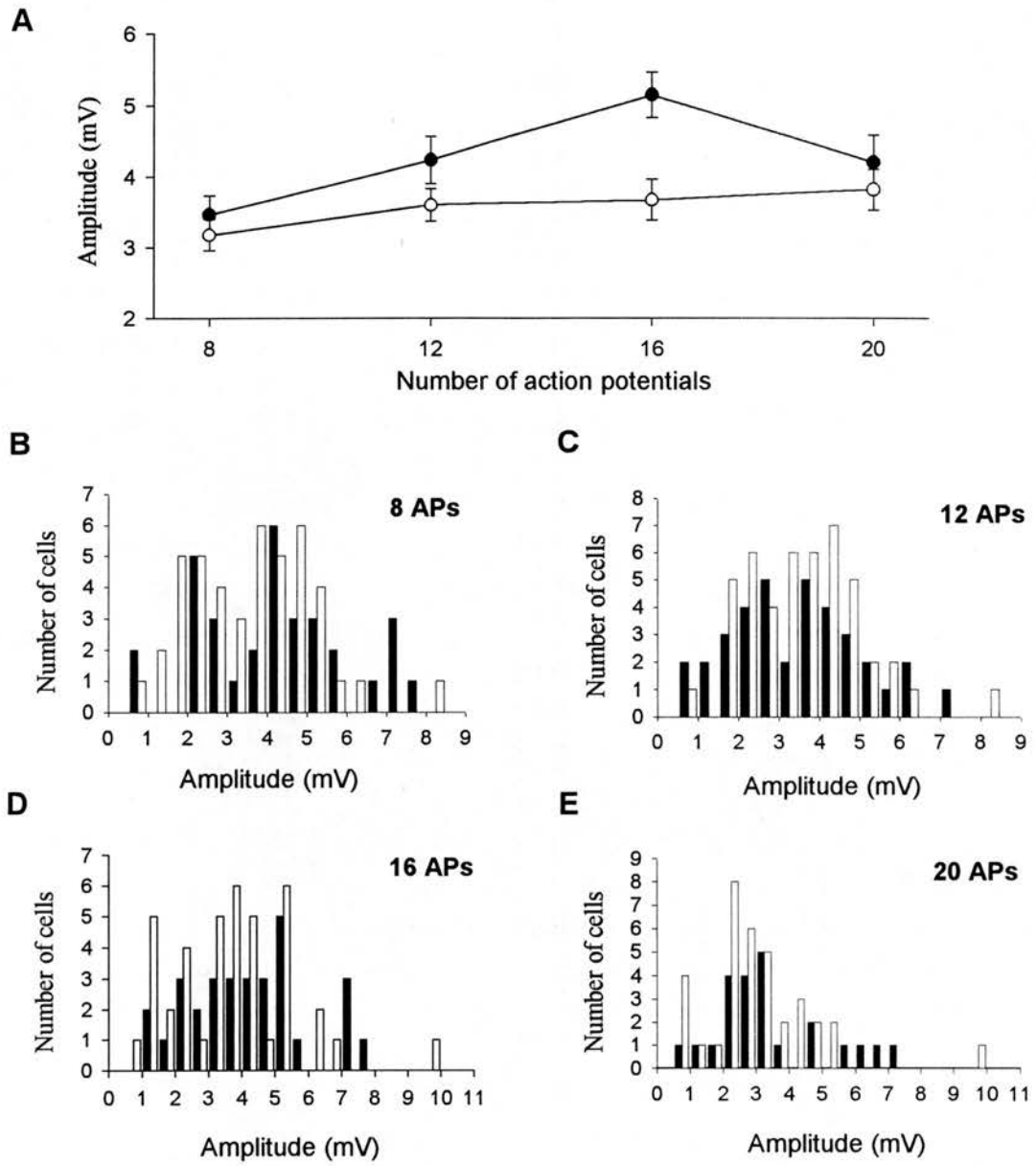

Figure 5.30 Slow afterhyperpolarization amplitude

(A) *The amplitude of the slow AHP increased when the number of conditioning action potentials (APs) was increased from 8, but this was not significant (t-test control comparing 8 & 12 APs P=0.074, 8 & 16 APs P=0.102, 8 & 20 APs P=0.103. Transgenic comparing 8 & 12 APs P=0.190, 8 & 16 APs P=0.171, 8 & 20 APs P=0.075.)*

The difference in sAHP generated in control and transgenic groups was not statistically significant (t-test; 8 APs P=0.402, 12 APs P=0.110, 16 APs P=0.276. Mann-Whitney rank sum test; 20 APs P=0.395). Frequency distributions are shown for the sAHP amplitudes generated in control and transgenic groups in response to ***(B)*** *8,* ***(C)*** *12,* ***(D)*** *16 and* ***(E)*** *20 APs.(Control 8 APs n=36, 12 AP2 n=30, 16 APs n=32, 20 APs n=25. Transgenic 8 APs n=46, 12 APs n=40, 16 APs n=44, 20 APs n=38).*

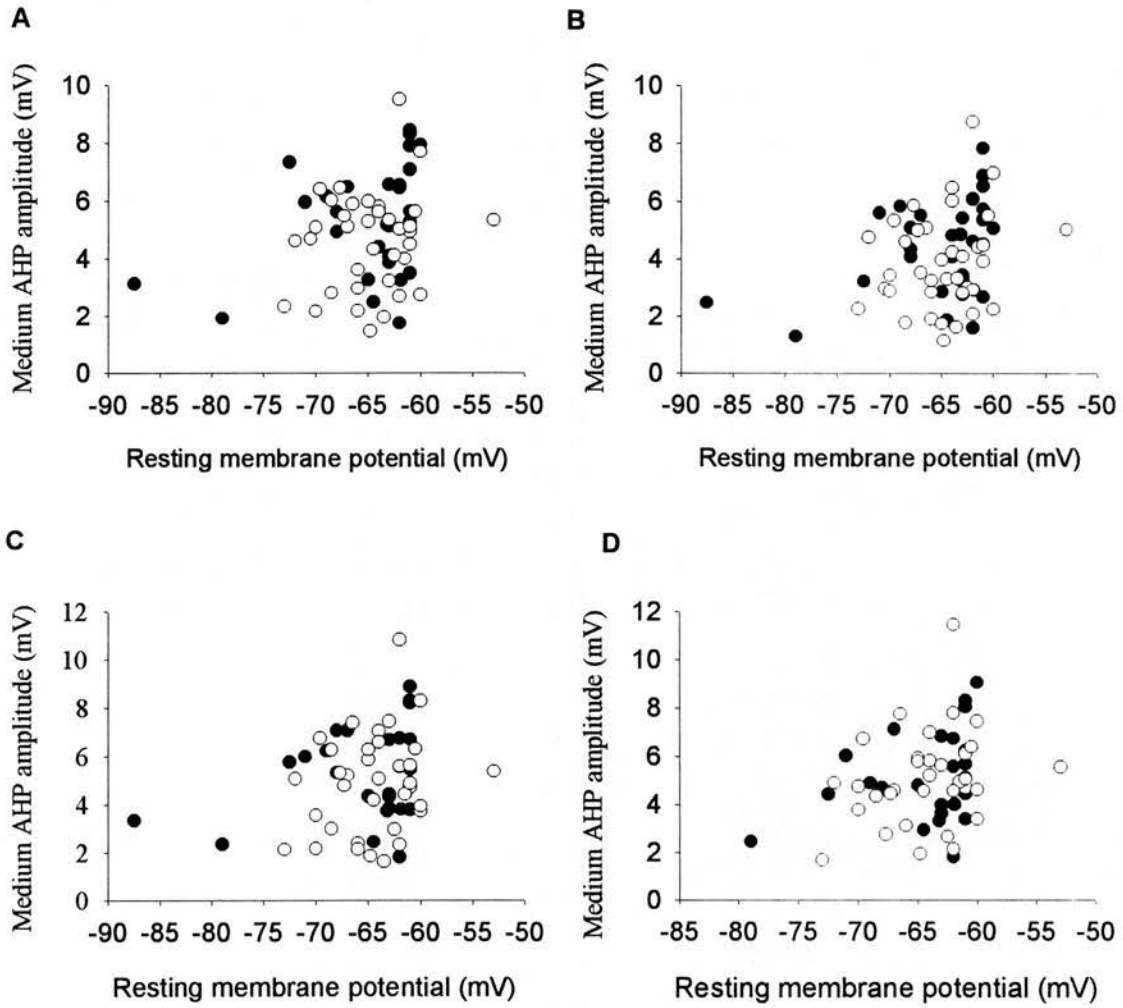

Figure 5.31 Medium AHP amplitude and resting membrane potential
Scatter plots show the relationship between the resting membrane potential and the medium AHP amplitude following a train of ***(A)*** *8,* ***(B)*** *12,* ***(C)*** *16 and* ***(D)*** *20 action potentials in control (black circles) and transgenic (open circles) groups.*
There was no significant correlation between the resting membrane potential and the medium AHP amplitude in control (mAHP8 P=0.056, mAHP12 P=0.082, mAHP16 P=0.098, mAHP20 P=0.140) or transgenic (mAHP8 P=0.213, mAHP12 P=0.319, mAHP16 P=0.196, mAHP20 P=0.150) groups (Pearson correlation).

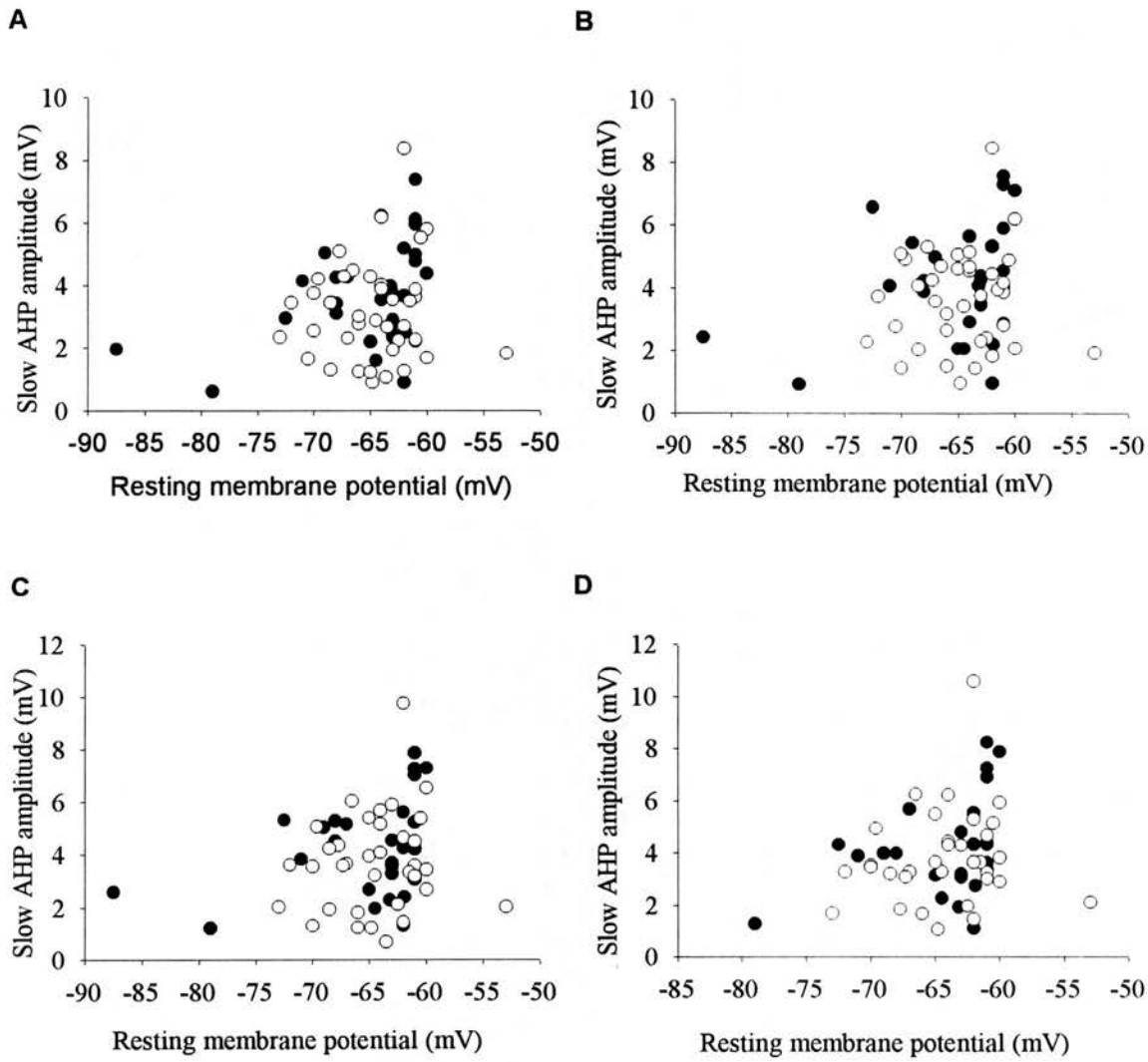

Figure 5.32 Slow AHP amplitude and resting membrane potential
Scatter plots show the relationship between the resting membrane potential and the slow AHP amplitude following a train of ***(A)*** *8,* ***(B)*** *12,* ***(C)*** *16 and* ***(D)*** *20 action potentials in control (black circles) and transgenic (open circles) groups.*
There was no significant correlation between the resting membrane potential and the slow AHP amplitude in control (sAHP8 P=0.036, sAHP12 P=0.072, sAHP16 P=0.090, sAHP20 P=0.075) or transgenic (sAHP8 P=0.700, sAHP12 P=0.804, sAHP16 P=0.489, sAHP20 P=0.458) groups (Pearson correlation).

Table 5.3 Properties of CA1 pyramidal neurones

	Control (Mean ± SEM)	Transgenic (Mean ± SEM)	P value †
Basic properties			
RMP (mV)	-66.49±1.23 (34)	-63.39±0.61 (48)	*P*=0.513 M-W
Rm (MΩ)	38.39±2.19 (33)	40.18±1.94 (50)	*P*=0.549
Time constant (ms)	30.62±2.41 (28)	27.81±1.79 (41)	*P*=0.343
Action potential properties			
Firing threshold (mV)			
Amplitude (mV)	72.867±0.686 (29)	71.703±0.772 (51)	*P*=0.465 M-W
Rise time (ms)	0.589±0.013 (29)	0.594±0.012 (51)	*P*=0.877 M-W
Decay time (ms)	1.078±0.023 (29)	1.068±0.024 (51)	*P*=0.778
Half width (ms)	0.851±0.010 (29)	0.869±0.011 (51)	*P*=0.264
ADP amplitude (mV)	4.507±0.838 (18)	4.058±0.612 (22)	*P*=0.661
fAHP amplitude (mV)	1.530±0.350 (21)	1.271±0.267 (34)	*P*=0.562 M-W
½ maximal EPSP properties			
Amplitude (mV)	5.704±0.512 (22)	5.995±0.369 (30)	*P*=0.638
Rise time (ms)	5.645±0.488 (22)	6.029±0.335 (30)	*P*=0.251 M-W
Decay time (ms)	19.659±4.901 (22)	30.697±4.502 (30)	*P*=0.060 M-W
Half width (ms)	10.718±1.964 (22)	14.847±1.497 (30)	*P*=0.016 M-W*
mAHP amplitude (mV)			
8 APs	4.082±0.282 (36)	3.830±0.228(46)	*P*=0.485
12 APs	5.173±0.336 (32)	4.557±0.249(44)	*P*=0.137
16 APs	5.297±0.349 (30)	4.794±0.319(40)	*P*=0.295
20 APs	5.170±0.369 (25)	5.039±0.311 (38)	*P*=0.788
sAHP amplitude (mV)			
8 APs	3.471±0.268 (36)	3.178±0.224 (46)	*P*=0.402
12 APs	4.230±0.325 (30)	3.603±0.231 (40)	*P*=0.110
16 APs	4.158±0.320 (32)	3.679±0.292 (44)	*P*=0.276
20 APs	4.214±0.375 (25)	3.829±0.290 (38)	*P*=0.415

RMP resting membrane potential. Rm membrane resistance. ADP after-depolarizing potential. f,m,s AHP slow, medium, fast hyperpolarizing potentials. APs action potentials.
†Statistics; t-test (unmarked) or Mann-Whitney rank sum test (M-W).
*$P<0.05$

Part III

Histology

Parasaggital section of rat brain including transverse sections of the hippocampus were fixed in paraformaldehyde and stained with haematoxylin and eosin or congo red. Human cortex from an Alzheimer's disease subject was stained alongside the rat sections as a positive control.

Both haematoxylin and eosin and congo red stains successfully demonstrated the presence of pathology in the human AD tissue. Figure 5.34 shows an amyloid plaque in human AD cortex stained with haematoxylin and eosin at x200 magnification. An amyloid plaque stained with congo red observed under x400 magnification is shown illuminated with normal light (figure 5.35A) and showing bifringence when viewed under polarized light (figure 5.35B). Congo red staining also showed accumulation of neurofibrillary tangles in pyramidal cell bodies at x400 magnification (figure 5.36).

Between 25 and 50 sections were examined from 3 control and 5 transgenic rats. No signs of amyloid plaque formation were observed in any of the sections whether stained using haematoxylin and eosin or congo red. Examination of congo red-stained sections under polarized light gave no evidence for the presence of amyloid plaques. Figure 5.37 shows part of the CA1 in a section from a transgenic rat at x100 magnification stained with haematoxylin and eosin demonstrating the complete lack of pathology. Similarly, examples of CA1 hippocampal sections from the same transgenic rat are shown stained with congo red at 100x magnification illuminated with normal (figure 5.38A) and polarized light (figure 5.38B).

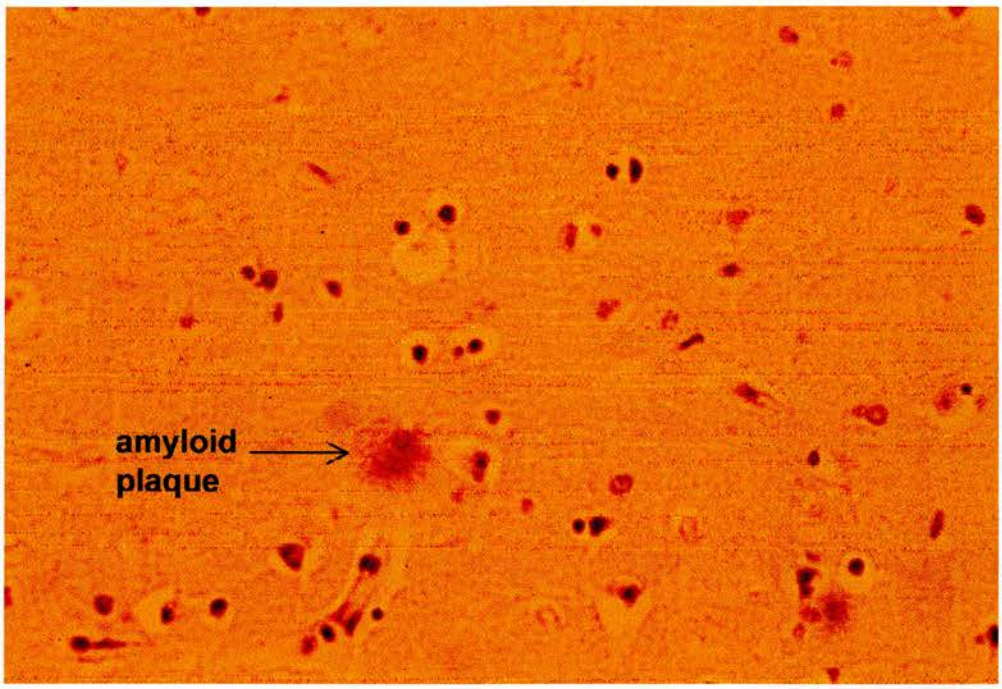

Figure 5.34 Human AD cortex sections showing amyloid plaques stained with H & E

An amyloid plaque in the human AD cortex stained with haematoxylin and eosin and observed

at x200 magnification.

A

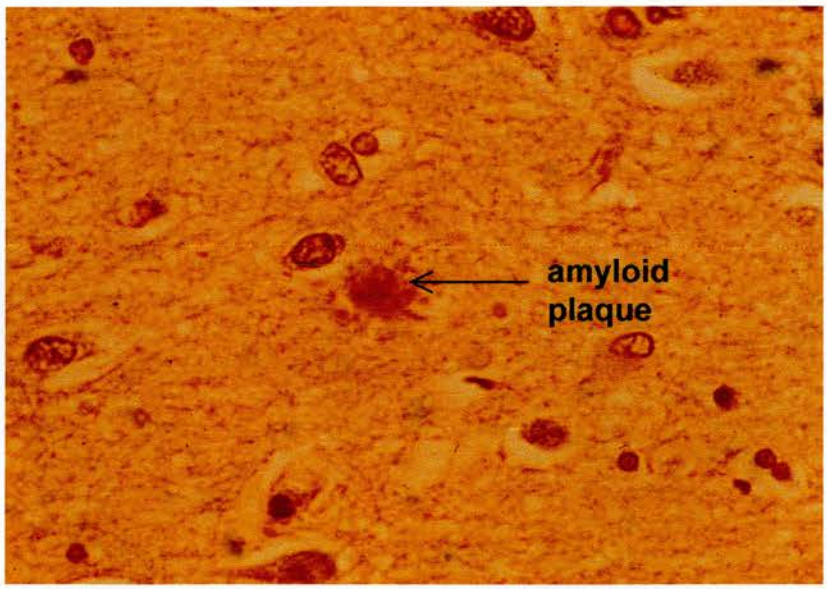

B

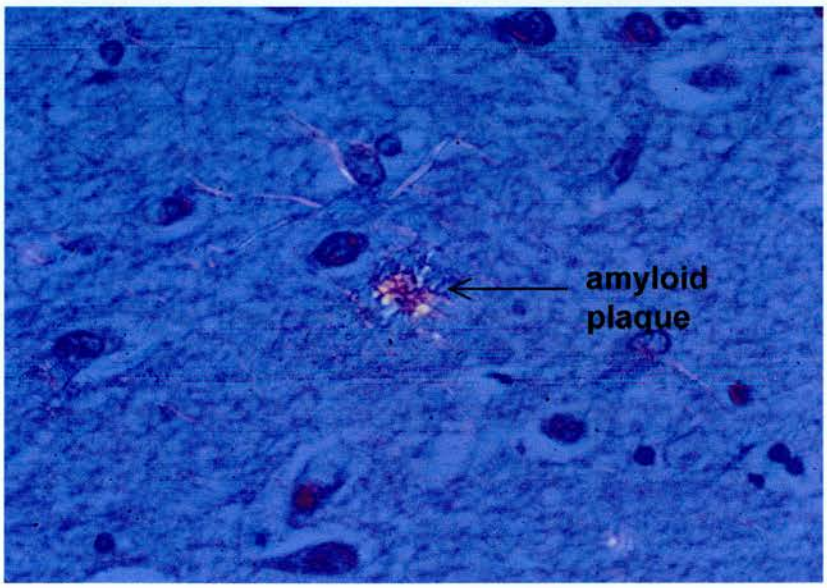

Figure 5.35 Human AD cortex sections showing amyloid plaques stained with congo red

Photographs of the same plaque revealed using congo red staining observed at x400 magnification under ***(A)*** *normal light and* ***(B)*** *polarized light.*

A

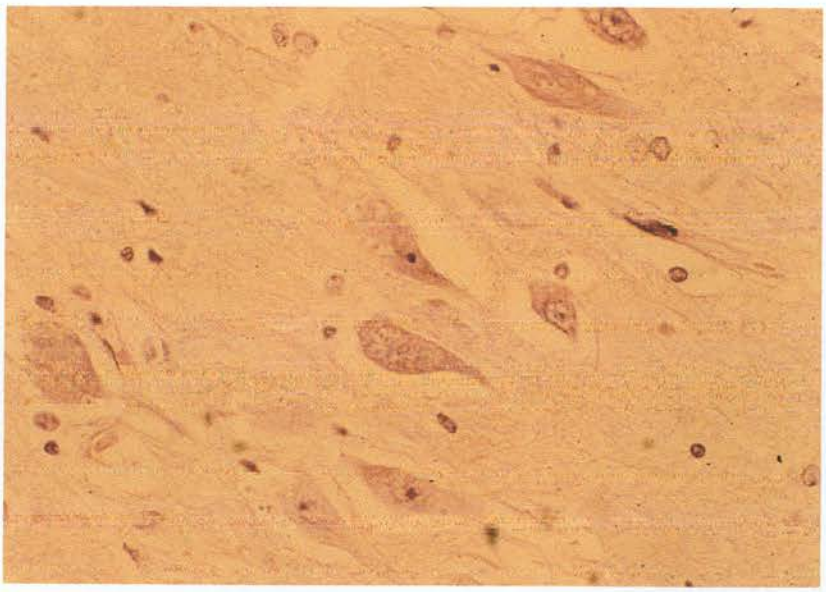

B

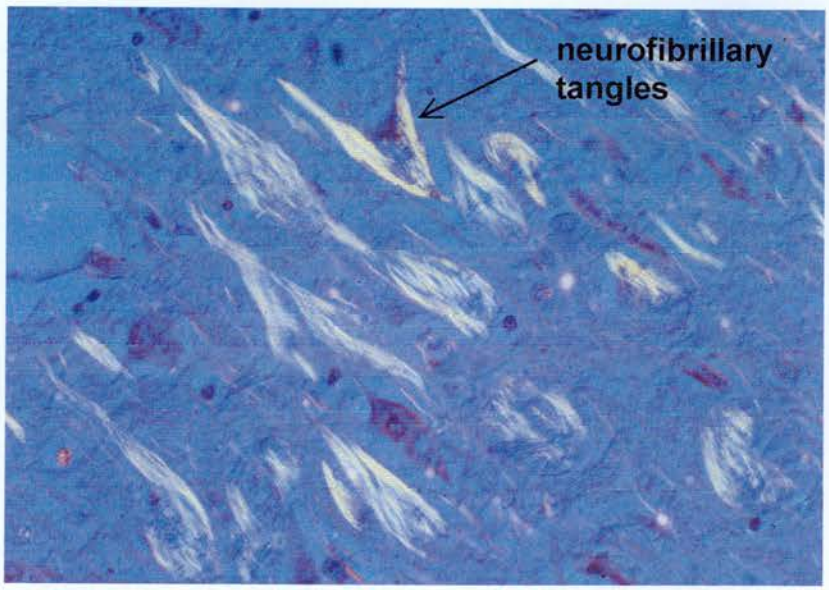

Figure 5.36 Human AD cortex sections showing neurofbrillary tangles

Photographs of neurofibrillary tangles revealed using congo red staining observed at x400 magnification under ***(A)*** *normal light and* ***(B)*** *polarized light. (Images show different sets of cells).*

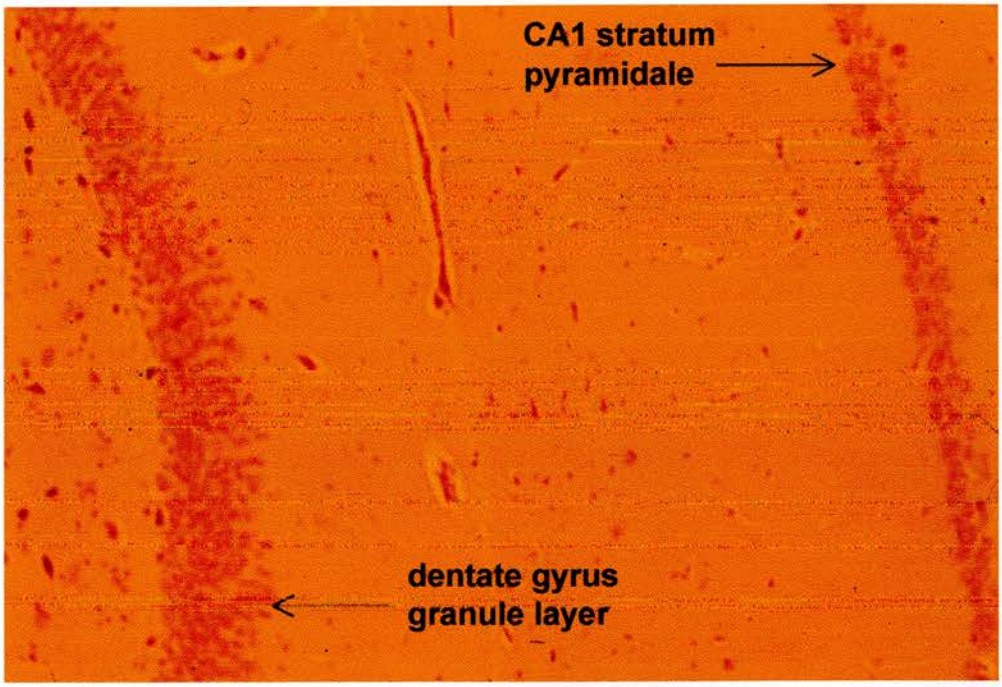

Figure 5.37 M146V rat hippocampus section stained with haematoxylin and eosin

Sections of rat hippocampus stained with haematoxyllin and eosin, observed at x100 magnification showed no evidence of amyloid plaques.

A

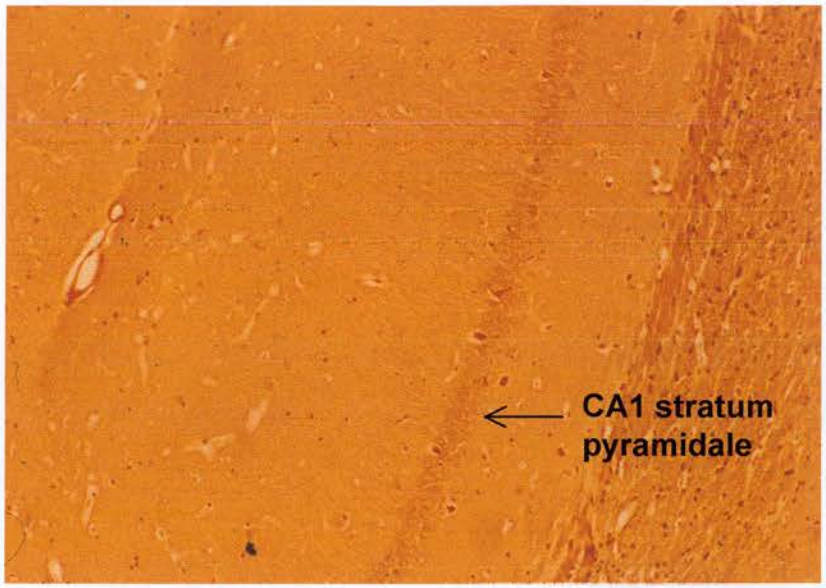

B

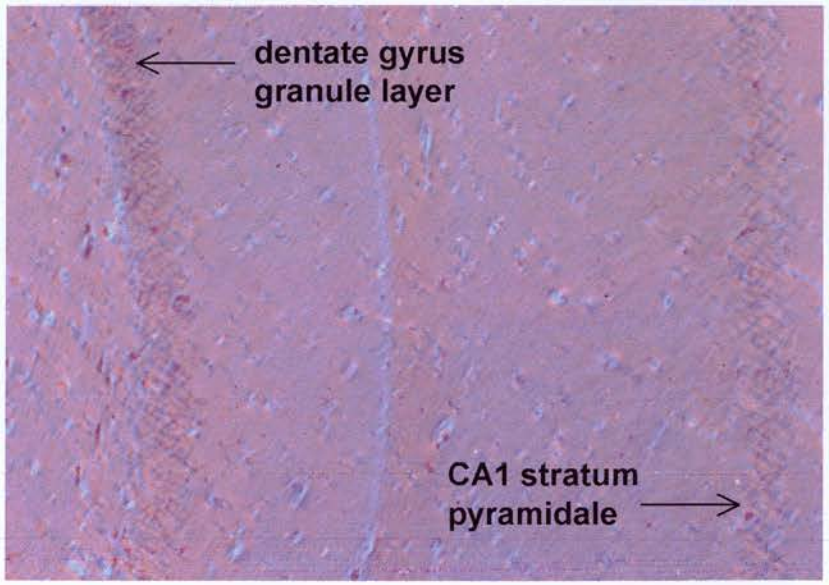

Figure 5.38 M146V rat hippocampus section stained with congo red

Sections of rat hippocampus stained with congo red, observed at x100 magnification showed no evidence of amyloid plaques under ***(A)*** *normal or* ***(B)*** *polarized light.*

Chapter 6

Discussion

Fischer rats were genetically engineered to express the human PS1 protein carrying the familial Alzheimer's disease-causing M146V mutation. Using electrophysiological and histological techniques, the suitability of these transgenic rats to be used as a model for Alzheimer's disease was assessed.

6.1 Summary of Results

The strength of LTP expression was increased in the $PS1_{M146V}$ rat in both an age-dependent and pathway-specific manner. The increase in LTP strength was only observed in the Schaffer collateral/CA1 pathway in aged animals. Paired pulse plasticity and post-tetanic potentiation were unchanged in this pathway. There was no change in perforant pathway/dentate gyrus synaptic plasticity, even in aged animals.

PPF in the CA1 was stronger in aged animals in both control and transgenic groups. This age-dependent change in PPF strength was not observed in the DG.

The amplitude and rising slope of field EPSPs recorded in the dentate gyrus were elevated in the transgenic rats.

Intracellular recordings revealed no differences in the basic membrane properties and non-synaptically driven activity in CA1 pyramidal neurones. However, synaptically evoked EPSPs did have an increased half width. Since there was no trend towards an increase in the EPSP rise time or amplitude, this was most likely attributable to the increased, (though not statistically significant) duration of the decay time.

No evidence of amyloid plaques was seen in the congo red or haemotoxylin and eosin stained sections of brain from the $PS1_{M146V}$ rat. Sections from the cortex of a human AD subject did show evidence of plaques and tangles when processed alongside the $PS1_{M146V}$ rat tissue. The absence of amyloid deposition was confirmed by immunohistological staining of slices from the same animals (Professor Ironside and co-workers, CJD Unit, Western General Hospital, Edinburgh).

6.2 Elevated LTP expression

Elevated LTP expression, as observed in the aged $PS1_{M146V}$ rat, has been reported in the CA1 of transgenic mouse models carrying PS1 mutations (Barrow et al 2000, Parent et al 1999, Zaman et al 2000). Animal models of AD using AβPP mutations have shown a decrease in LTP expression levels (Moechers et al 1999, Chapman et al 1999) although older mice have shown a reversal to elevated LTP expression (Larson et al 1999). Mutations to both proteins lead to altered AβPP processing, which has suggested that changes in the abundance of different AβPP cleavage products constitutes a common mechanism by which all known FAD-causing mutations act. However, whilst AβPP mutations such as the Swedish mutation (concentrated around the β-secretase cleavage site) promote β-secretase processing, leading to an upregulation of both $Aβ_{40}$ and $Aβ_{42}$, with a concomitant decrease in the neuroprotective sAβPPα, PS1 mutations, along with AβPP mutations concentrated around the γ-secretase cleavage site such as the London mutation) cause selective upregulation of $Aβ_{42}$ without generating a significant change in the level of other cleavage products (Dewachter et al 2000, Xia et al 1998). This is consistent with the observed (though not yet characterized) role of PS1 in γ-secretase activity and suggests that it is the ratio of $Aβ_{42}/Aβ_{40}$ rather than the absolute level of Aβ that is pathogenic in AD induced by PS1 mutations. Although the differences in LTP response to AβPP and PS1 mutations could be due to difference in the way they alter AβPP processing, it is also possible that PS1 mutations can disrupt normal neurophysiology by mechanisms unrelated to AβPP processing pathways to initiate AD progression.

PS1 levels are usually tightly regulated, and whilst AβPP can be overexpressed at high levels, significant upregulation of PS1 is difficult to achieve, suggesting that even small changes in PS1 levels can perturb normal cellular physiology. PS1 mutations A246E and M146L lead to an increase in levels of N- and C-terminal fragments, which seems to be due to increased stability of fragments from the mutated protein (Lee et al 1997). Therefore, FAD mutations in PS1 may allow subtle changes in PS1 activity by impairing clearance of excess protein, suggesting a possible pathogenic gain of function.

Lack of altered CA1 PPF recorded in brain slices showing enhanced LTP expression has been reported in other PS1 models (Parent et al 1999, Zaman et al 2000). The lack of altered PPF in the CA1 of the aged $PS1_{M146V}$ rat suggests that the enhanced LTP expression was not caused by changes in Ca^{2+} homeostasis in the CA3 pyramidal neurone axon terminals.

PTP was also not altered in the $PS1_{M146V}$ rat, suggesting that enhanced LTP expression was not caused by abnormal Ca^{2+} buffering by presynaptic mitochondria or by altered numbers of mitochondria.

Intracellularly recorded EPSP parametres have not been investigated in other PS1 models of AD. Both NMDA receptor and GABA receptor mediated currents contribute strongly to the late phase of the EPSP and so it is possible that the increased half width observed in the $PS1_{M146V}$ rat represents either enhanced NMDA activity or depressed GABAergic activity. The contribution of NMDA currents to the EPSP was measured in a PS1 ΔE9 transgenic mouse and was unchanged with respect to the control group (Zaman et al 2000), suggesting that PS1 mutations do not influence NMDA activity.

An increase in EPSP half width has been observed in the conditioned response during paired pulse facilitation and this has been attributed to inhibition of GABAergic interneurones by GABA released during the first pulse acting on presynaptic $GABA_B$ receptors (Nathan et al 1990). GABAergic activity also influences CA1 LTP induction; inhibiting $GABA_A$ transmission with picrotoxin enhances LTP expression (Wigstrom & Gustafsson 1985) and enhancing $GABA_A$ transmission with benzodiazepines decreased LTP expression (Del Cerro et al 1992).

The importance of GABAergic activity in modulating LTP is also indicated by a study of how choice of cutting solution during the preparation of hippocampal brain slices affects subsequent LTP generation. Cutting slices in a solution that replaced NaCl with sucrose helped to preserve neurones against anoxic damage during slicing. Slices cut in sucrose-substituted aCSF expressed weaker LTP and this was attributed to better preservation of GABAergic interneurones (Kuenzi et al 2000). Anoxia, which is unavoidable during preparation of brain slices, leads to neuronal depolarization and excitotoxicity, which has been attributed to influx of Cl^- and cations. This draws water into the cell, which causes swelling and cell lysis. The NaCl/sucrose substitution in the cutting solution preserves neuronal stability and allows more reliable preparation of healthy slices from adult tissue (Aghajanian

& Rasmusen 1989). Therefore, enhanced $GABA_B$ mediated suppression of GABAergic interneurones could potentiate facilitation of postsynaptic responses to HFS and so explain the increase in LTP expression in the $PS1_{M146V}$ rat. However, the time course of $GABA_B$-mediated autoinhibition is too slow to explain the increase in EPSP half width.

$GABA_A$ currents were also measured in the ΔE9 mouse and rather than being depressed, $GABA_A$ activity was actually increased (Zaman et al 1999). They observed that blocking $GABA_A$ with picrotoxin in slices from control animals enhanced CA1 LTP to levels comparable to the transgenic group. However, transgenic slices perfused with picrotoxin failed to show additional LTP expression, suggesting that the modulation of LTP by $GABA_A$ and by the PS1 mutation act independently on a common pathway.

The authors suggested that the link between the effects of the PS1 mutation and enhanced $GABA_A$ activity on LTP expression could be Ca^{2+} homeostasis. Enhanced Ca^{2+} responses to depolarization and Aβ have been recorded in PC12 cells transfected with $PS1_{L286V}$ (Guo et al 1996), cells from PS1 FAD transgenic animals (Guo et al 1998) and fibroblasts from affected human subjects (Etcheberrigaray et al 1998). This led to increased neuronal vulnerability to apoptosis (Guo et al 1998, Begley et al 1999). The adverse effects of PS1 mutations were alleviated using intracellular Ca^{2+} buffers and inhibitors of Ca^{2+}-induced Ca^{2+} release from intracellular stores (Begley et al 1999). Zamen et al suggested that the PS1 mutation causes enhanced release of Ca^{2+} from intracellular stores in response to Ca^{2+} influx through NMDA receptors and that the observed increase in $GABA_A$ currents was an (inadequate) compensatory reaction to the resulting increase in neuronal excitability (Zaman et al 2000). They also suggested that the PS1-induced increase in intracellular Ca^{2+} levels may promote Aβ production, as has been induced by promoting Ca^{2+} release from intracellular stores in cultured cells (Querfurth & Selkoe 1994).

Two recently published papers have addressed the question of how $PS1_{FAD}$ causes altered Ca^{2+} homeostasis (Leissring et al 2000, Yoo et al 2000). Both studied the effects of $PS1_{FAD}$ on the regulation of endoplasmic reticulum (ER) Ca^{2+} stores. Before the results of these papers are discussed, the proposed mechanisms of ER Ca^{2+} homeostasis will be outlined.

Receptor activity at the cell membrane can result in release of Ca^{2+} from the endoplasmic reticulum by two mechanisms. G-protein coupled receptors that activate PKC cause release of IP_3,

which activates Ca^{2+} channel linked receptors (IP_3R) in the ER membrane. A second Ca^{2+} channel linked receptor, ryanodine (RyR), is activated by Ca^{2+} and mediates Ca^{2+}-induced Ca^{2+} release. Stimulation of these receptors induces a biphasic pattern of Ca^{2+} activity; the initial peak caused by release from the ER is followed by a second peak, which is due to Ca^{2+} influx through store-activated calcium channels (SOCC) in the plasma membrane and serves to replenish ER Ca^{2+} levels. This second peak can be induced in the absence of receptor activation by artificially depleting ER Ca^{2+} stores with thapsigargin, indicating that this response is independent of second messenger cascades initiated by receptor activation and is induced solely by the drop in ER Ca^{2+} levels. This direct coupling between ER Ca^{2+} depletion and influx of extracellular Ca^{2+} is known as capacitative calcium entry (CCE) (Putney et al 1986). The precise mechanisms are still to be elucidated and the SOCC has not been isolated, (although the resulting current, I_{CRAC} has been characterized electrophysiologically), however, recent research has discounted many of the theories formerly proposed and has allowed a clearer understanding of the events involved.

Evidence supports the theory that coupling involves direct physical interaction between the ER and the plasma membrane (Ma et al 2000). The proteins involved in this interaction are SOCC in the plasma membrane and IP_3R in the ER membrane, although in its coupling role, IP_3R does not bind IP_3. IP_3R is believed to interact with and cause conformational change in the SOCC, which allows direct influx of extracellular Ca^{2+} into the ER. IP_3R is morphologically suited for this putative role since it has an intraluminal C-terminal domain, which could monitor ER Ca^{2+} levels, and a cytosolic N-terminal domain that is large enough to span the gap between the ER and the plasma membrane, and so could interact with SOCC.

Cells expressing FAD PS1 are associated with depressed CCE activity (Leissring et al 2000, Yoo et al 2000). Cells in which PS1 is absent or non-functional have increased CCE activity (Yoo et al 2000), which suggests that PS1 is a modulator of CCE and that the depression of CCE activity in cells carrying FAD PS1 reflects a gain of function. However, Leissring et al observed that the level of Ca^{2+} in the ER was strongly elevated in cells carrying $PS1_{M146V}$ and that treatment with thapsigargin to deplete ER Ca^{2+} stores elicited a normal CCE response, indicating that CCE mechanisms are not impaired (Leissring et al 2000). Therefore, the CCE underactivity associated with FAD PS1 is probably due to insufficient Ca^{2+} depletion during neuronal activity to create a drive for coupling

rather than dysfunction of the pairing mechanism. This suggests that the initial deleterious event caused by FAD PS1 is elevated ER Ca^{2+} concentration. Although the mechanisms causing this are yet to be determined it has been observed that RyR mRNA and protein levels are elevated in the brains of mice expressing $PS1_{M146V}$ or $PS1_{L286V}$. This is accompanied by an increased Ca^{2+} response to caffeine (which binds RyR), susceptibility to excitotoxicity and apoptosis (Chan et al 2000).

Yoo et al also observed that normal cells in which CCE was inhibited using SKF96365 showed increased Aβ production, and that this required the expression of functional PS1 (Yoo et al 2000). Therefore, the elevated $A\beta_{42}$ levels that are associated with cells carrying FAD PS1 are likely to be a response to CCE depression. This may even be a protective compensatory response. Animal models of FAD PS1, including the $PS1_{M146V}$ rat, all show enhanced LTP expression, which could potentially saturate synaptic capacity for plastic change. Intracerebroventricular injection of $A\beta_{42}$ into rat brain has been shown to promote CA1 LTD expression and can depotentiate LTP if applied within 10 minutes of an LTP-inducing tetanus (Kim et al 2001). Hippocampal slices perfused with $A\beta_{40}$, which is downregulated in FAD PS1, show elevated LTP expression (Wu et al 1995) whilst perfusion with the active $A\beta_{25\text{-}35}$ fragment depresses LTP (Freir et al 2001). Therefore, the increased ratio of $A\beta_{42}/A\beta_{40}$ in cells expressing FAD PS1 may reflect a bias towards the synaptic plasticity-suppressing longer isoform, intended to protect against saturation of synaptic plasticity and excitotoxicity.

The CCE studies used cultured fibroblasts and neurones from neonatal (Leissring et al 2000) or embryonic (Yoo et al 2000) mice carrying the M146V or M146L mutations, showing that Ca^{2+} homeostasis dysfunction is an early and probably an initiating event in FAD PS1 pathogenesis. This suggests that the development of AD symptoms and pathology in human cases is a result of years of physiological changes intended to compensate for the effects of, but failure to reverse, elevated Ca^{2+} levels. These compensatory mechanisms eventually generate deleterious side-effects possibly initiated by the accumulation of Aβ, as detailed in the introduction. Given the importance of Ca^{2+} in cellular physiology, the extent of the spectrum of systems, including inflammatory responses, mitochondria, tau function, AβPP processing, metal ion regulation and oxidant clearance, which present deficits in AD cases is certainly not surprising.

These observations support a possible role for enhanced Ca^{2+} activity in the generation of elevated LTP in the $PS1_{M146V}$ rat. The elevated Ca2+ response may also lead to the increase in EPSP

half width since GABA responses are suppressed by high Ca^{2+} levels, leading to decrease in the duration, but not amplitude of IPSCs (Koninck & Mody 1996).

6.3 Phenotypic change in LTP expression

CA1 LTP in slices from transgenic rats was not only enhanced but showed a consistent difference in the pattern of development. The usual response to high frequency tetanization is an initially powerful post-tetanic potentiation which declines exponentially into early LTP. The level of potentiation gradually falls for often over thirty minutes before a stable level of LTP expression is established. LTP in the CA1 of aged transgenic rats showed normal PTP but rather than showing a gradually declining early LTP phase, the postsynaptic response increased in strength briefly and slightly before reliably establishing a robust plateau of LTP expression within 15 minutes. This phenotypic change suggests that the observed increase in LTP involves an increased potency of early LTP expression mechanisms and is not merely caused by facilitation of induction by a lowered threshold for LTP or enhancement of the Ca^{2+} response increasing the probability that the threshold is reached, (although these may contribute, or even be necessary for the later effects).

The rapid stabilization of LTP expression level may be due to altered activity of NMDA and AMPA receptors following the tetanus. Blockade of NMDA receptors following tetanization leads to enhanced stability of the AMPA receptor response to test stimuli with a time course that is similar to that seen for the stabilization of LTP expression in the $PS1_{M146V}$ rat (Xiao et al 1996). This leads to the possibility that NMDAR activity in the $PS1_{M146V}$ rat following tetanus is unusually low and the changes in LTP expression pattern and strength are mediated by a lack of decay in AMPA receptor activity. This conflicts with the idea proposed in chapter 3 that enhanced NMDA receptor activity by PKC-dependent *src* tyrosine kinase phosphorylation of NR2B (Huang & Hsin 1999a) facilitates establishment of LTP. Instead, it suggests that such NMDA receptor-enhancing mechanisms may negatively regulate the expression level of LTP and their impairment would be a possible explanation for the observations in the $PS1_{M146V}$ rat. Zamen et al failed to show a change in the NMDA receptor contribution to the EPSP in the PS1ΔE9 mouse model during 4-pulse bursts at 100 Hertz (Zaman et al 2000). There are several possible explanations for this discrepancy. It is possible that altered NMDA

receptor activity would only be apparent following prolonged tetanic stimulation, such as the 100-pulse 100 Hertz stimulation used in the $PS1_{M146V}$ rat study. Also, the response to APV antagonism of NMDA receptor activity in the control group showed a large variance, suggesting a larger sample would be needed to reveal potential differences in NMDA activity in the $PS1_{\Delta E9}$ mouse. Alternatively, it is possible that the $PS1_{M146V}$ mutation has a different effect on neurophysiology. This is possible since the $PS1_{\Delta E9}$ mutation prevents PS1 cleavage and so the pathogenic species is full length PS1 rather than the persistent C- and N-terminal fragments generated by other PS1 mutations. However, if the lack of change in NMDA receptor activity is confirmed, then other mechanisms must be responsible for the observed phenotypic changes in LTP expression pattern. An extensive (though not exhaustive) search of the literature failed to find reports of manipulations that had generated elevated LTP in conjunction with phenotypic changes mimicking those observed in the $PS1_{M146V}$ rat and so current research fails to suggest alternative mechanisms.

6.4 Amyoid-beta production

Cells from subjects carrying PS1 mutations show upregulation of $A\beta_{42}$ production. The levels of $A\beta_{42}$ and $A\beta_{40}$ in the $PS1_{M146V}$ rat were not assayed due to the lack of a commercially available ELISA kit for rodent Aβ protein. However, mouse models of FAD PS1 mutations that have been tested all show an increase in the $A\beta_{42}$ levels in the absence of significant changes in the level of total Aβ (Duff et al 1996, Citron et al 1997). The increase in $A\beta_{42}$ expression in these mice was not determined by the level of mutated PS1 protein expression, which suggests that the low level of human PS1 protein detected in the $PS1_{M146V}$ rat does not preclude the possibility of significant $A\beta_{42}$ upregulation. Indeed, the ability of the $PS1_{M146V}$ rat to replicate the changes in synaptic plasticity observed in the mouse models suggests that upregulation of $A\beta_{42}$ will eventually be confirmed.

6.5 Enhanced LTP and memory

The hippocampus is important for spatial memory in rodents. Procedures that interfere with normal dorsal hippocampal function lead to impaired performance in behavioural tests such as the water maze and the T-maze (McDonald et al 1998, Hock et al 1998).

T-maze testing of spatial memory was attempted in the aged $PS1_{M146V}$ rat. However, both control and transgenic rats failed to perform sufficiently well during extensive pretraining (lasting over a week) to proceed with experiments. Both control and transgenic rats showed poor exploratory behaviour, which seemed to be due to nervousness in the new environment. They typically took a long time to begin exploring the maze and spent the majority of their time cowering. They showed head swaying behaviour, suggesting fear. They did eat the food reward, which was scattered throughout the maze, but only after a long delay (sometimes over an hour) even when the food was found quickly. The same food rewards were consumed readily when presented to the rats in their home cage. Better performance might have been achieved by pretraining the animals at an earlier age to familiarize them with the maze environment.

Enhance performance in spatial memory tasks has been observed in conjunction with elevated LTP expression (Madani et al 1999, Routtenberg et al 2000). However, current theory on synaptic plasticity and its possible role in memory formation, can also support the possibility of impaired memory formation in response to enhanced LTP expression. Memory encoding is thought to involve not only potentiation at strongly activated synapses but also depotentiation at weakly activated synapses, as a means of improving memory pattern resolution. Therefore, inappropriate overexpression of LTP (as generated by LTP expression in an unusually large number of the activated synapses) may impair pattern discrimination. It may also lead to saturation of synaptic capacity for plastic change, although saturation was not observed in the $PS1_{M146V}$ rat when just 2 episodes of tetanic stimulation were used.

Impaired memory in response to treatments that elevate LTP expression levels have been observed. Mice lacking the protein tyrosine phosphatase δ receptor show elevated LTP expression levels but have impaired memory when tested in the water maze, T-maze or radial arm maze (Uetani et al 2000). Transverse rat hippocampal slices perfused with $A\beta_{40}$ showed elevated LTP expression

(Wu et al 1995), but intracerebral injection of Aβ resulted in impaired performance of treated rats in the radial arm maze test (Yamaguchi & Kawashima 2001). Mutation of the postsynaptic density-95 protein enhanced long-term potentiation in mice but impaired learning in a water maze (Migaud et al 1998). Although selective inhibition of postsynaptic $GABA_B$ receptors using CGP 35348 facilitated LTP generated by HFS in a dose dependent manner, the change in performance of mice in a spatial delayed nonmatch-to-sample task following intraperitoneal injections of CGP 35348 did not follow the dose response relationship of altered LTP expression (Staubli et al 1999).

Therefore, it is possible that the increased LTP expression in the $PS1_{M146V}$ rat may not have correlated with improved memory and learning in behavioural tests, but may have been an inappropriate increase in synaptic strength that could actually disrupt memory formation. Behavioural tests have been performed on mice carrying FAD PS1 mutations and failed to show a difference in performance at 6 or 9 months old (Janus et al 2000b).

6.6 Ca^{2+} dependent events recorded intracellularly

The Ca^{2+} explanation of the elevated LTP response in the $PS1_{M146V}$ rat was not supported by the intracellular study. AHPs and action potential firing frequency adaptation are Ca^{2+} dependent events (mediated by Ca^{2+}-dependent K^+ currents) and these were unchanged in the $PS1_{M146V}$ rat. If Ca^{2+} responses were enhanced in these animals, the expected intracellular observations would be larger AHPs and more rapid action potential firing frequency adaptation.

A possible explanation is that cells with significantly higher Ca^{2+} responses were less viable due to excitotoxicity and did not tolerate impalement by sharp electrodes. However, these neurones would have been available to contribute to extracellular field recordings. An increase in the medium and slow AHP amplitudes have been reported in CA3 pyramidal neurones of two lines of mice carrying different PS1 mutations (Barrow et al 2000), although it should be noted that the sample sizes used were extremely low (control n=4 cells, $PS1_{M146L}$ n=3 and $PS1_{M146V}$ n=4 cells).

6.7 Enhanced PPF expression in the CA1 of aged rats

The observed increase in PPF expression in the CA1 of both control and transgenic groups is contrary to a previously published study that showed a decrease in PPF expression in 16 month old rats compared to 2 month old rats (Papatheodoropoulos & Kostopoulos 1998), however, they assessed PPF based on field EPSP area rather than slope.

At single synapses, stronger PPF is associated with a smaller conditioning response (Debanne et al 1996), however, the amplitude of field EPSPs was increased in the older rats. This suggests that the stronger PPF recorded in the old rats may be due to increased level of synaptic coupling that has been observed between both CA1 pyramidal neurones and dentate gyrus granule cells in the aged hippocampus (Barnes et al 1987).

6.8 Enhanced field EPSP amplitude and slope in the dentate gyrus

The amplitude and slope of field EPSPs recorded in the dentate gyrus were increased in aged transgenic rats. This is contrary to a previous report of decreased fEPSP slope recorded from aged rat dentate gyrus granule cells (Levkovitz & Segal 1998). However, this did not lead to a change in dentate gyrus LTP or PPD expression levels. Since recordings in the dentate gyrus were made in the presence of picrotoxin, it is unlikely that the age related changes were due to a decrease in intrinsic GABA release. Also, changes in GABA receptor activity would be unlikely to affect the rising slope of the field EPSP. This suggests that the increase in field EPSP slope and amplitude may be mediated by increased AMPA and/or NMDA receptor activity. Alternatively, there could be a change in the pattern of synaptic input onto granule cell dendrites resulting in greater uniformity in the parts of the dendritic tree that receive synaptic input, which could cause the increased fEPSP slope and amplitude by decreased variability in the time course of EPSP generation throughout the population of activated cells.

6.9 Absence of amyloid plaques

The lack of amyloid deposition in animal models of PS1 FAD has been previously reported (Chui et al 1999, Lamb et al 1999). Cerebral amyloid deposition is commonly observed in the brain from elderly human subjects but is not seen in aged rodent brain. Rodent Aβ differs from human Aβ in at least 2 residues (Podlisny et al 1991). Human Aβ seems to aggregate more readily than rodent Aβ; human Aβ is aggregated in the presence of CuII, especially in acidic conditions, whilst rat Aβ (and human Aβ in which histidine residues had been substituted to mimic the species differences in amino acid sequence) failed to aggregate under these conditions (Atwood et al 1998). Transgenic rats expressing FAD AβPP mutations do show amyloid deposition and this is likely to be due to the presence of human AβPP.

6.10 Choice of control group

The control animals used in this study do not express human PS1, therefore it is possible that the observed difference in the transgenic group are due to upregulation of PS1 and are independent of the mutation. PS1 upregulation is difficult to achieve since its expression level is tightly regulated. Therefore, even small changes in PS1 activity could be physiologically important and upregulated PS1 could be the reason for the differences in electrophysiology observed in the $PS1_{M146V}$ rat. Increased PS1 expression can saturate PS1 cleavage (Borchelt et al 1996) and so it is possible the changes observed here are induced by elevated full-length PS1, which is physiologically active (Levitan et al 1996).

This discrepancy could be controlled by using a control group that expresses wild-type human PS1, however the control and experimental lines would then need to be bred independently, which could introduce genetic drift and false positive results. Using non-transgenic controls allowed transgenic animals to be compared with their littermates and removed the risk of errors due to genetic drift. Mating of the control and transgenic rats gave litters that were about fifty per cent control and fifty per cent transgenic hemizygotes. The use of hemizygotes was appropriate since this is the genotype of human subjects.

However, enhanced LTP expression has been observed when animals expressing FAD PS1 are compared with controls that carry human wild-type PS1 suggesting that the increase in LTP is induced by the mutation (Duff et al 1996, Zaman et al 2000). Zaman et al used both non-transgenic and wild-type human PS1 transgenic control groups, and these showed no significant differences in their electrophysiology (Zaman et al 2000). A $PS1_{M146V}$ mouse model has provided a particularly rigorous model of AD since the human gene was inserted using knock-in techniques, which simultaneously ablates the endogenous mouse PS1 (Guo et al 1999a). This allowed the human protein to be expressed not only at the level normally exhibited by endogenous mouse PS1 but also preserved the site-specificity of expression. These observations support the PS1 mutation and not altered PS1 expression levels as the source of the changes observed in the $PS1_{M146V}$ rat.

Conclusion

The $PS1_{M146V}$ rat has successfully demonstrated some important features of AD. The increase in LTP expression indicates that the level of transgenic protein expression, although small, was sufficient to generate strongly significant physiological change. The literature suggests that this increase was due to altered Ca^{2+} homeostasis, which seems to be an early and possibly causative event in AD pathogenesis, at least in PS1 FAD cases. Although the levels of $A\beta_{42}$ were not investigated in these animals, other PS1 models of AD have shown a selective increase in $A\beta_{42}$. The $PS1_{M146V}$ rat has shown elevated LTP expression as seen in other PS1 models in which elevated $A\beta_{42}$ has been measured. It has been suggested that the increase in LTP expression is caused by elevated Ca^{2+} levels and elevated Ca^{2+} levels can lead to increased $A\beta_{42}$ production. The elevated expression of LTP in the $PS1_{M146V}$ rat therefore suggests that altered AβPP processing will also be demonstrated in this model. In addition, the change in LTP expression was both age-dependent and site-specific with a pattern that was consistent with human AD progression.

The observations made in the $PS1_{M146V}$ rat were consistent with those that have been reported for mice carrying $PS1_{FAD}$. However, the rats showed an additional stark qualitative difference in the pattern, as well as amplitude, of CA1 LTP expression in the aged animals. This may reflect specific abnormalities in the interaction of STP/LTP and further research will be needed to identify the mechanisms involved. Depression of NMDA receptor activity during early LTP expression can facilitate LTP strength, suggesting a possible focus for further investigation.

Although no evidence of plaques or tangles were observed, this is in line with other similar studies. Cross-breeding the $PS1_{M146V}$ rat with transgenic animals expressing $A\beta PP_{FAD}$, wildtype human AβPP or human tau protein may allow the species differences that have prevented these pathologies to develop to be overcome. Cross-breeding could also possibly reduce the incidence of tumour development in animals approaching 18 months and so allow older animals to be studied.

Appendix I

Criteria for Clinical Diagnosis of Alzheimer's Disease

I The criteria for the clinical diagnosis of PROBABLE Alzheimer's disease include:

dementia established by clinical examination and documented by the Mini-Mental Test, Blessed Dementia Scale, or some similar examination, and confirmed by neuropsychological test;

deficits in two or more areas of cognition;

progressive worsening of memory and other cognitive functions;

no disturbance of consciousness;

onset between ages 40 and 90, most often after age 65; and

absence of systemic disorders or other brain diseases that in and of themselves could account for the progressive deficits in memory and cognition.

II The diagnosis of PROBABLE Alzheimer's disease is supported by :

progressive deterioration of specific cognitive functions such as language (aphasia), motor skills (apraxia), and perception (agnosia);

impaired activities of daily living and altered patterns of behavior;

family history of similar disorders, particularly if confirmed neuropathologically; and

laboratory results of normal lumbar puncture as evaluated by standard techniques,

normal pattern of nonspecific changes in EEG, such as increased slow-wave activity, and

evidence of cerebral atrophy on CT with progression documented by serial observation.

III Other clinical features consistent with the diagnosis of PROBABLE Alzheimer's disease, after exclusion of causes of dementia other than Alzheimer's disease, include:

plateaus in the course of progression of the illness;

associated symptoms of depression, insomnia, incontinence, delusions, illusions, hallucinations,

catastrophic verbal, emotional, or physical outbursts, sexual disorders, and weight loss;

other neurologic abnormalities in some patients, especially with more advanced disease and including motor signs such as increased muscle tone, myoclonus, or gait disorder;

seizures in advanced disease; and

CT normal for age.

IV Features that make the diagnosis of PROBABLE Alzheimer's disease uncertain or unlikely include:

sudden, apoplectic onset;

focal neurologic findings such as hemiparesis, sensory loss, visual field deficits, and incoordination early in the course of the illness; and

seizures or gait disturbances at the onset or very early in the course of the illness.

V Clinical diagnosis of POSSIBLE Alzheimer's disease:

may be made on the basis of the dementia syndrome, in the absence of other neurologic, psychiatric, or systemic disorders sufficient to produce dementia, which is not considered to be *the* cause of the dementia; and

should be used in research studies when a single, gradually progressive severe cognitive deficit is identified in the absence of other identifiable cause.

VI Criteria for diagnosis of DEFINITE Alzheimer's disease are;

the clinical criteria for probable Alzheimer's disease; and

histopathologic evidence obtained from biopsy or autopsy.

VII Classification of Alzheimer's disease for research purposes should specify features that may differentiate subtypes of the disorder, such as:

familial occurrence;

onset before age of 65;

presence of trisomy-21; and

coexistence of other relevant conditions such as Parkinson's disease.

(Reproduced with permission; Lippincott, Williams & Wilkins, Philadelphia)

Appendix II

FAD-causing Pathogenic Mutations of the Amyloid-beta Precursor Protein

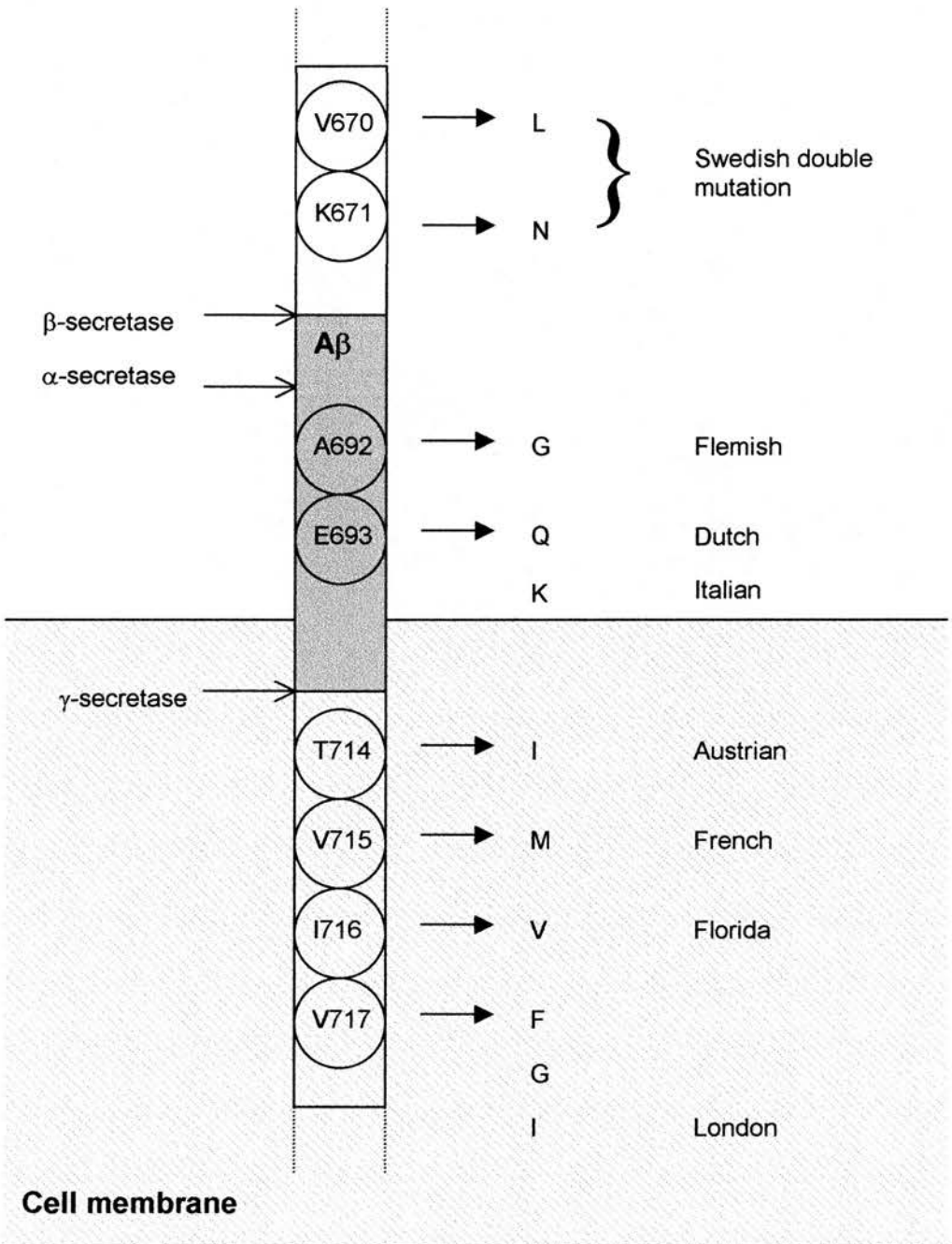

Appendix III

FAD-causing Pathogenic Mutations of the Presenilin 1 Protein

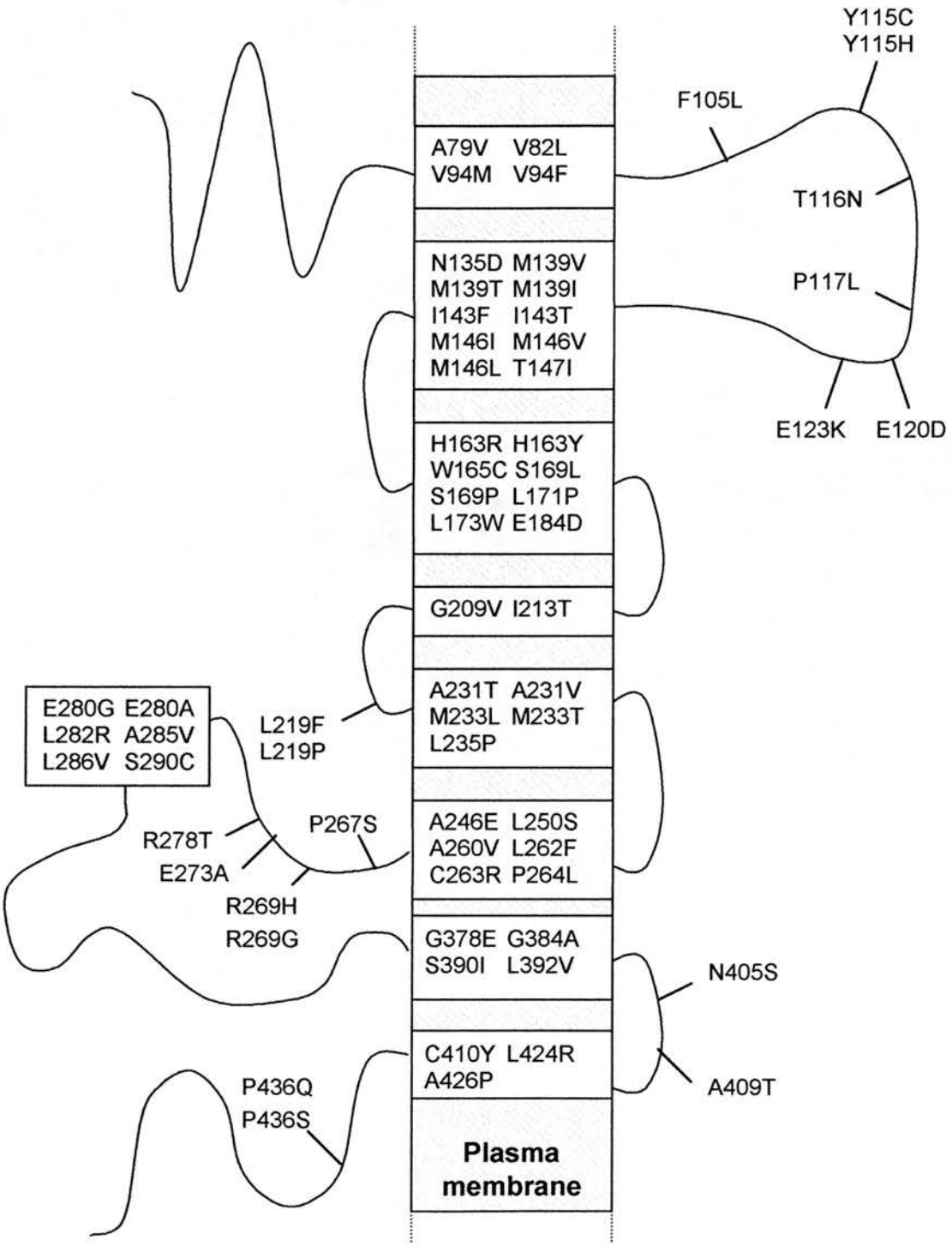

Appendix IV

FAD-causing Pathogenic Mutations of the Presenilin 2 Protein

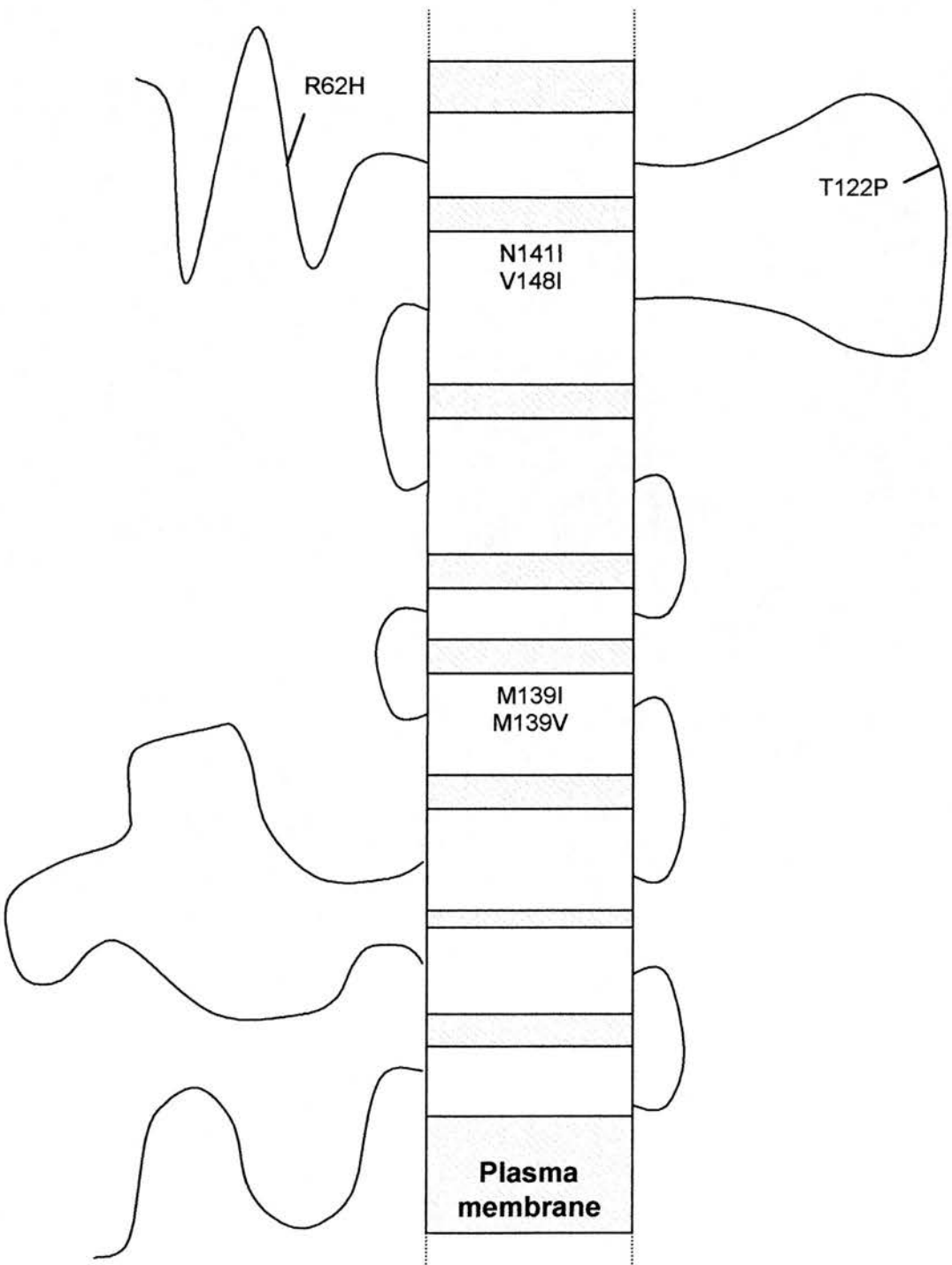

AGHAJANIAN G.K. & RASMUSSEN K. (1989) Intracellular studies in the facial nucleus illustrating a simple new method for obtaining viable motoneurones in adult rat brain slices. Synapse **3**, 331-338.

AKAMA K.T. & VAN ELDIC L.J. (2000) β-Amyloid stimulation of inducible nitric-oxide synthase in astrocytes is interleukin-1β- and tumour necrosis factor-α(TNF α)-dependent, and involves a TNFα receptor-associated factor- and NFκB-inducing kinase-dependent signalling mechanism. The Journal of Biological Chemistry **275**, 7918-7924.

AKSENOV M.Y., TUCKER H.M., NAIR P., AKSENOVA M.V., BUTTERFIELD D.A., ESTUS S. & MARKESBERY W.R. (1999) The expression of several mitochondrial and nuclear genes encoding the subunits of electron transport chain enzyme complexes, cytochrome c oxidase, and NADH dehydrogenase, in different brain regions in Alzheimer's disease. Neurochemical Research **24**, 767-774.

ALONSO A. DEL C., GRUNDKE-IQBAL I., BARRA H.S. & IQBAL K. (1997) Abnormal phosphorylation of tau and the mechanism of Alzheimer neurofibrillary degeneration: sequestration of microtubule-associated proteins 1 and 2 and the disassembly of microtubules by the abnormal tau. Proceedings of the National Academy of Sciences USA **94**, 298-303.

ALZHEIMER A. (1907) Über eine eigenartige Erkrankung der Hirnrinde. Allgemeine Zeitschrift fur Psychiatrie und Psychisch-gerichtliche Medizin **64**, 146-148. English translation posted at: www.alzforum.org/members/research/milestones/abstracts/alzheimer.html#english.

ANCOLIO K., MARAMBAUD P., DAUCH P. & CHECLER F. (1997) β-Secretase-derived product of β-amyloid precursor protein is decreased by presenilin 1 mutations linked to familial Alzheimer's disease. Journal of Neurochemistry **69**, 2494-2499.

ANDERSEN P., SUNDBERG S.H., SVEEN O. & WIGSTROM H. (1977) Specific long-lasting potentiation of synaptic transmission in hippocampal slices. Nature **266**, 736-737.

ANNAERT W. & DE STROOPER B. (1999) Presenilins: molecular switches between proteolysis and signal transduction. Trends in Neurosciences **22**, 439-443.

APPELT D.M. & BALIN B.J. (1997) The association of tissue transglutaminase with human recombinant tau results in the formation of insoluble filamentous structures. Brain Research **745**, 21-31.

ARENDT T., BRUCKNER M.K., GERTZ H.J. & MARCOVA L. (1998) Cortical distribution of neurofibrillary tangles in Alzheimer's disease matches the pattern of neurons that retain their capacity of plastic remodelling in the adult brain. Neuroscience **83**, 991-1002.

ARENDT T., SCHINDLER C., BRUCKNER M.K., ESCHRICH K., BIGL V., ZEDLICK D. & MARCOVA L. (1997) Plastic neuronal remodeling is impaired in patients with Alzheimer's disease carrying apolipoprotein epsilon 4 allele. Journal of Neuroscience. **17**, 516-29.

ARENDT T., HOLZER M., FRUTH R., BRUCKNER M.K. & GARTNER U. (1995) Paired helical filament-like phosphorylation of tau, deposition of β\A4-amyloid and memory impairment in rat induced by chronic inhibition of phosphatase 1 and 2A. Neuroscience **69**, 691-698.

ATWOOD C.S., SCARPA R.C., HUANG X., MOIR R.D., JONES W.D., FAIRLIE D.P., TANZI R.E. & BUSH A.I. (2000) Characterization of copper interactions with Alzheimer amyloid β peptides: identification of an attomolar-affinity copper binding site on amyloid β_{1-42}. Journal of Neurochemistry **75**, 1219-1233.

ATWOOD C.S., MOIR R.D., HUANG X., SCARPA R.C., MICHAEL N., BACARRA E., ROMANO D.M., HARTSHORN M.A., TANZI R.E. & BUSH A.I. (1998) Dramatic aggregation of Alzheimer Aβ by Cu(II) is induced by conditions representing physiological acidosis. The Journal of Biological Chemistry **273,** 12817-12826.

AXELMAN K., BASUN H., WINBLAD B. & LANNFELT L. (1994) A large Swedish family with Alzheimer's disease with a codon 670/671 amyloid precursor protein mutation: a clinical and genealogical investigation. Archives of Neurology **51**, 1193-1197.

BACHMAN D.L., WOLF P.A., LINN R., KNOEFEL J.E., COBB J., BELANGER A., D'AGOSTINO R.B. & WHITE L.R. (1992) Prevalence of dementia and probable senile dementia of the Alzheimer type in the Framingham study. Neurology **42**, 115-119.

BALL M.J. (1978) Topographic distribution of neurofibrillary tangles and granulovacuolar degeneration in hippocampal cortex of aging and demented patients. A quantitative study. Acta Neuropathologica **42**, 73-80.

BARGER S.W. & HARMON A.D. (1997) Microglial activation by Alzheimer amyloid precursor protein and modulation by apolipoprotein E. Nature **388,** 878-881.

BARGER S.W., FISCUS R.R., RUTH P., HOFMANN F. & MATTSON M.P. (1995) Role of cyclic GMP in the regulation of neuronal calcium and survival by secreted forms of β-amyloid precursor. Journal of Neurochemistry **64**, 2087-2096.

BARNES C.A., RAO G. & MCNAUGHTON B.L. (1987) Increased electrotonic coupling in aged rat hippocampus: A possible mechanism for cellular excitability changes. Journal of Comparative Neurology **259**, 549-558.

BARRIA A., MULLER D., DERKACH V., GRIFFITH L.C. & SODERLING T.R. (1997) Regulatory phosphorylation of AMPA-type glutamate receptors by CaMKII during long-term potentiation. Science **276**, 2042-2045.

BARROW P.A., EMPSON R.M., GLADWELL S.J., ANDERSON C.M., KILLICK R., YU X., JEFFERYS J.G.R. & DUFF K. (2000) Functional phenotype in transgenic mice expressing mutant human presenilin-1. Neurobiology of disease **7**, 119-126.

BAUER J., PLASCHKE K., MARTIN E., BARDENHEUER H.J. & HOYER S. (1997) Causes and consequences of neuronal energy deficit in sporadic Alzheimer's disease. Annals of the New York Academy of Science **826**, 379-381.

BEAR M.F. (1996) A synaptic basis for memory storage in the cerebral cortex. Proceeding of the National Academy of Sciences USA **93**, 13453-13459.

BEGLEY J.G., DUAN W., CHAN S., DUFF K. & MATTSON M.P. (1999) Altered calcium homeostasis and mitochondrial dysfunction in cortical synaptic compartments of presenilin-1 mutant mice. Journal of Neurochemistry **72**, 1030-1039.

BENEVENISTE H., EINSTEIN G., KIM K.R., HULETTE C. & JOHNSON G.A. (1999) Detection of neuritic plaques in Alzheimer's disease by magnetic resonance microscopy. Proceeding of the National Academy of Sciences USA **96**, 14079-14084.

BENZING W.C. & MUFSON E.J. (1995) Apolipoprotein E immunoreactivity within neurofibrillary tangles: relationship to Tau and PHF in Alzheimer's disease. Experimental Neurology. **132**, 162-71.

BENZING W.C., WUJEK J.R., WARD E.K., SHAFFER D., ASHE K.H., YOUNKIN S.G. & BRUNDEN K.R. (1999) Evidence for glial-mediated inflammation in aged APP(SW) transgenic mice. Neurobiology of Aging **20**, 581-589.

BIERER L.M., HOF P.R., PUROHIT D.P., CARLIN L., SCHMEIDLER J., DAVIS K.L. & PERL D.P. (1995) Neocortical neurofibrillary tangles correlate with dementia severity in Alzheimer's disease. Archives of Neurology **52**, 81-88.

BIRD T.D., LEVY-LAHAD E., POORKAJ P., SHARMA V., NEMENS E., LAHAD A., LAMPE T.H. & SCHELLENBERG G.D. (1996) Wide range in age of onset for chromosome 1-related familial Alzheimer's disease. Annals of Neurology **40**, 932-936.

BLASKO I., MARX F., STEINER E., HARTMANN T. & GRUBECK-LOEBENSTEIN B. (1999) TNFα plus IFNγ induce the production of Alzheimer β-amyloid peptides and decrease the secretion of APPs. FASEB J **13**, 63-68.

BLISS T.V.P., DOUGLAS R.M., ERRINGTON M.L. & LYNCH M.A. (1986) Correlation between long-term potentiation and release of endogenous amino acids from dentate gyrus of anaesthetized rats. Journal of Physiology **377**, 391-408.

BLISS T.V. & LOMO T. (1973) Long-lasting potentiation of synaptic transmission in the dentate area of the anaesthetized rabbit following stimulation of the perforant path. Journal of Physiology **232**. 331-356.

BOGDANOVIC N., DAVIDSSON P., VOLKMANN I., WINBLAD B. & BLENNOW K. (2000) Growth-associated protein GAP-43 in the frontal cortex and in the hippocampus in Alzheimer's disease: an immunohistochemical and quantitative study. Journal of Neural Transmission **107**, 463-478.

BOLSHAKOV V.Y., CARBONI L., COBB M.H., SIEGELBAUM S.A. & BELARDETTI F. (2000) Dual MAP kinase pathways mediate opposing forms of long-term plasticity at CA3-CA1 synapses. Nature Neuroscience **3**, 1107-1112.

BONFOCO E., KRAINC D., ANKARCRONA M., NICOTERA P. & LIPTON S.A. (1995) Apoptosis and necrosis: two distinct events induced, respectively, by mild and intense insults with N-methyl-D-aspartate or nitric oxide/superoxide in cortical cell cultures. Proceedings of the National Academy of Sciences of the United States of America **92**, 7162-7166.

BORCHELT D.R., RATOVITSKY T., VAN LARE J., LEE M.K., GONZALES V., JENKINS N.A., COPELAND N.G., PRICE D.L. & SISODIA S.S. (1997) Accelerated amyloid deposition in the brains of transgenic mice coexpressing mutant presenilin 1 and amyloid precursor proteins. Neuron **19**, 939-945.

BORCHELT D.R., THINAKARAN G., ECKMAN C.B., LEE M.K., DAVENPORT F., RATOVITSKY T., PRADA C.-M., KIM G., SEEKINS S., YAGER D., SLUNT H.H., WANG R., SEEGER M., LEVEY A.I., GANDY S.E., COPELAND N.G., JENKINS N.A., PRICE D.L., YOUNKIN S.G. & SISODIA S.S. (1996) Familial Alzheimer's disease-linked presenilin 1 variants elevate Aβ1-42/1-40 ratio *in vitro* and *in vivo*. Neuron **17**, 1005-1013.

BORNEMANN K.D., WIEDERHOLD K.-H., PAULI C., ERMINI F., STALDER M., SCHNELL L., SOMMER B., JUCKER M. & STAUFENBIEL M. (2001) Aβ-induced inflammatory processes in microglia cells of APP23 transgenic mice. American Journal of Pathology **158**, 63-73.

BORTOLOTTO Z.A. & COLLINGRIDGE G.L. (2000) A role for protein kinase C in a form of metaplasticity that regulates the induction of long-term potentiation at CA1 synapses of the adult rat hippocampus. European Journal of Neuroscience **12**, 4055-4062.

BOWER J.M. & HABERLY L.B. (1986) Facilitating and nonfacilitating synapses on pyramidal cells: a correlation between physiology and morphology. Proceedings of the National Academy of Sciences USA **83**, 1115-1119.

BOYLES JK. PITAS RE. WILSON E. MAHLEY RW. TAYLOR JM. (1985) Apolipoprotein E associated with astrocytic glia of the central nervous system and with nonmyelinating glia of the peripheral nervous system. Journal of Clinical Investigation **76**, 1501-13.

BRAAK H. & BRAAK E. (1991) Neuropathological stageing of Alzheimer-related changes. Acta Neuropathologica **82**, 239-259.

BRADLEY A., EVANS M., KAUFMAN M.H. & ROBERTSON E. (1984) Formation of germ-line chimaeras from embryo-derived teratocarcinoma cell lines. Nature **309**, 255-256.

BRADT B.M., KOLB W.P. & COOPER N.R. (1998) Complement-dependent proinflammatory properties of the Alzheimer's disease β-peptide. Journal of Experimental Medicine **188**, 431-438.

BRETELER M.M.B., VAN DUIJN C.M., CHANDRA V., FRATIGLIONI L., GRAVES A.B., HEYMAN A., JORM A.F., KOKMEN K., KONDO K., MORTIMER J.A., ROCCA W.A., SHALAT S.L., SOININEN H. & HOFMAN A. (1991) Medical history and the risk of Alzheimer's disease: a collaborative re-analysis of case-control studies. International Journal of Epidemiology **20**, S36-S42.

BRINSTER R.L., ALLEN J.M., BEHRINGER R.R., GELINAS R.E. & PALMITER R.D. (1988) Introns increase transcriptional efficiency in transgenic mice. Proceedings of the National Academy of Sciences USA **85**, 836-840.

BRINSTER R.L. (1974) The effects of cells transferred into the mouse blastocyst on subsequent development. The Journal of Experimental Medicine **140**, 1049-1056.

BROCHER S., ARTOLA A. & SINGER S. (1992) Intracellular injection of Ca^{2+} chelators blocks induction of long-term depression in rat visual cortex. Proceedings of the National Academy of Sciences USA **89**, 123-127.

BROUTMAN G. & BAUDRY M. (2001) Involvement of the secretory pathway for AMPA receptors in NMDA-induced potentiation in hippocampus. Journal of Neuroscience **21**, 27-34.

BUDD S.L. & NICHOLLS D.G. (1996) A reevaluation of the role of mitochondria in neuronal Ca2+ homeostasis. Journal of Neurochemistry **66**, 403-11.

BUEE L., DING W., ANDERSON J.P., NARINDRASORASAK S., KISILEVSKY R., BOYLE N.J., ROBAKIS N.K., DELACOURTE A., GREENBERG B. & FILLIT H.M. (1993) Binding of vascular heparan sulfate proteoglycan to Alzheimer's amyloid precursor protein is mediated in part by the N-terminal region of A4 peptide. Brain Research **627**, 199-204.

BUNDGAARD M.J., REGEUR L., GUNDERSEN H.J. & PAKKENBERG B. (2001) Size of neocortical neurons in control subjects and in Alzheimer's disease. Journal of Anatomy **198**, 481-9.

BURDETTE L.J. & GILBERT M.E. (1995) Stimulus parameters affecting paired-pulse depression of dentate granule cell field potentials. I. Stimulus Intensity. Brain Research **680**, 53-62.

BURSZTAJN S., DESOUZA R., MCPHIE D.L., BARMAN S.A., SHIOI J., ROBAKIS N.K. & NEVE R.L. (1998) Overexpression in neurons of human presenilin-1 or a presenilin-1 familial Alzheimer disease mutant does not enhance apoptosis. Journal of Neuroscience **18**, 9790-9799.

BUSCIGLIO J., LORENZO A., YEH J. & YANKNER B.A. (1995) β-Amyloid fibrils induce tau phosphorylation and loss of microtubule binding. Neuron **14**, 879-888.

BUXBAUM J.D., CHOI E.-K., LUO Y., LILLIEHOOK C., CROWLEY A.C., MERRIAM D.E. & WASCO W. (1998) Calsenilin: a calcium-binding protein that interacts with the presenilins and regulates the levels of a presenilin fragment. Nature Medicine **4**, 1177-1181.

CAI H., WANG Y., MCCARTHY D., WEN H., BORCHELT D.R., PRICE D.L. & WONG P.C. (2001) BACE 1 is the major β-secretase for generation of Aβ peptides by neurons. Nature Neuroscience **4**, 233-234.

CAI X.-D., GOLDE T.E. & YOUNKIN S.G. (1993) Release of excess amyloid β protein from a mutant amyloid β protein precursor. Science **259**, 514-516.

CALHOUN M.E., WIEDERHOLD K.-H., ABRAMOWSKI D., PHINNEY A.L., PROBST A., STURCHLER-PIERRAT C., STAUFENBIEL M., SOMMER B. & JUCKER M. (1998) Neuron loss in APP transgenic mice. Nature **395**, 755-756.

CALLAHAN L.M., CHOW N., CHEETHAM J.E., COX C. & COLEMAN P.D. (1998) Analysis of message expression in single neurons of Alzheimer's disease brain. Neurobiology of Aging **19**, S99-S105.

CAMPION D., DUMANCHIN C., HANNEQUIN D., DUBOIS B., BELLIARD S., PUEL M., THOMAS-ANTERION C., MICHON A., MARTIN C., CHARBONNIER F., RAUX G., CAMUZAT A., PENET C., MESNAGE V., MARTINEZ M., CLERGET-DARPOUX F., BRICE A. & FREBOURG T. (1999) Early-onset autosomal dominant Alzheimer disease: prevalence, genetic heterogeneity, and mutation spectrum. American Journal of Human Genetics **65**, 664-70.

CASTELLANI R.J., SMITH M.A., NUNOMURA A., HARRIS P.L.R. & PERRY G. (1999) Is increased redox-active iron in Alzheimer disease a failure of the copper-binding protein ceruloplasmin. Free Radical Biology & Medicine **26**, 1508-1512.

CHAN S.L., MAYNE M., HOLDEN C.P., GEIGER J.D. & MATTSON M.P (2000) Presenilin-1 mutations increase levels of ryanodine receptors and calcium release in PC12 cells and cortical neurones. Journal of Biological Chemistry **275**, 18195-18200.

CHAPMAN P.F., WHITE G.L., JONES M.W., COOPER-BLACKETER D., MARSHALL V.J. IRIZARRY M., YOUNKIN L., GOOD M.A., BLISS T.V.P., HYMAN B.T., YOUNKIN S.G. & HSIAO K.K. (1999) Impaired synaptic plasticity and learning in aged amyloid precursor protein transgenic mice. Nature Neuroscience **2**, 271-276.

CHAUHAN V.P.S., RAY I., CHAUHAN A., WEGIEL J. & WISNIEWSKI H.M. (1997) Metal cations defibrillize the amyloid β-protein fibrils. Neurochemical Research **22**, 805-809.

CHAUHAN A., CHAUHAN V.P.S., BROCKERHOFF H. & WISNIEWSKI H.M. (1991) Action of amyloid β-protein on protein kinase C activity. Life Sciences **49**, 1555-1562.

CHEN G., CHEN K., KNOX J., INGLIS J., BERNARD A., MARTIN S.J., JUSTICE A., MCCONLOGUE L., GAMES D., FREEDMAN S.B. & MORRIS R.G.M. (2000) A learning deficit related to age and β-amyloid plaques in a mouse model of Alzheimer's disease. Nature **408**, 975-979.

CHEN S.-Y., WRIGHT J.W. & BARNES C.D. (1996) The neurochemical and behavioral effects of β-amyloid peptide (25-35). Brain Research **720**, 54-60.

CHRISTIE B.R. & ABRAHAM W.C. (1994) Differential regulation of paired-pulse plasticity following LTP in the dentate gyrus. Neuroreport **5**, 385-388.

CHUI D.-H., TANAHASHI H., OZAWA K., SACHITA I., CHECLER F., UEDA O., SUZUKI H., ARAKI W., INOUE H., SHIROTANI K., TAKAHASHI K., GALLYAS F. & TABIRA T. (1999) Transgenic mice with Alzheimer presenilin 1 mutations show accelerated neuordegeneration without amyloid plaque formation. Nature Medicine **5**, 560-564.

CITRON M., WESTAWAY D., XIA W., CARLSON G., DIEHL T., LEVELSQUE G., JOHNSON-WOOD K., LEE M., SEUBERT P., DAVIS A., KHOLODENKO K., MOTTER R., SHERRINGTON R., PERRY B., YAO H., STROME T., LIEBERBURG I., ROMMENS J., KIM S., SCHENK D.,

FRASER P., ST GEORGE-HYSLOP P & SELKOE D. (1997) Mutant presenilins of Alzheimer's disease increase production of 42-residue amyloid β-protein in both transfected cells and transgenic mice. Nature Medicine **3**, 67-72.

CITRON M., DIEHL T.S., GORDON G., BIERE A.L., SEUBERT P. & D.J. SELKOE (1996) Evidence that the 42- and 40-amino acid forms of amyloid protein are generated from the β-amyloid precursor protein by different protease. Proceedings of the National Academy of Sciences USA **93**. 13170-13175.

CITRON M., OLTERSDORF T., HAASS C., MCCONLOGUE L., HUNG A.Y., SEUBERT P.. VIGO-PELFREY C., LIEBERBURG I. & SELKOE D.J. (1992) Mutation in the β-amyloid precursor protein in familial Alzheimer's disease increases β-protein production. Nature **360**, 672-674.

CLARKE R., SMITH A.D., JOBST K.A., REFSUM H., SUTTON L. & UELAND P.M. (1998) Folate, vitamin B12, and serum total homocysteine levels in confirmed Alzheimer disease. Archives of Neurology **55**, 1449-1455.

CLARK R.F., HUTTON M., FULDNER R.A., FROELICH S., KARRAN E., TALBOT C., CROOK R., LENDON C., PRIHAR G., HE C., KORENBLAT K., MARTINEZ A., WRAGG M., BUSFIELD F., BEHRENS M.I., MYERS A., NORTON J., MORRIS J., MEHTA N., PEARSON C., LINCON S.. BAKER M., DUFF K., ZEHR C., PEREZ-TUR J., HOULDEN H., RUIZ A., OSSA J., LOPERA F.. ARCOS M., MADRIGAL L., COLLINGE J., HUMPHRESY C., ASHWORTH A., SARNER S.. GOX N., HARVEY R., KENNEDY A., ROQUES P., CLINE R.T., PHILIPS C.A., VENTER J.C.. FORSELL L., AXELMAN K., LILIUS L., JOHNSTON J., COWBURN R., VIITANEN M.. WINBLAD B., KOSIK K., HALTIA M., POYHONEN M., DICKSON D., MANN D., NEARY D.. SNOWDEN J., LANTOS P., LANNFELT L., ROSSOR M., ROBERTS G.W., ADAMS M.D.. HARDY J. & GOATE A. (1995) The structure of the presenilin 1 (S182) gene and identification of six novel mutations in early onset AD families. Nature Genetics **11**, 219-222.

CLEMENTI E., RACCHETTI G., MELINO G. & MELDOLESI J. (1996) Cytosolic Ca2+ buffering. a cell property that in some neurons markedly decreases during aging, has a protective effect against NMDA/nitric oxide-induced excitotoxicity. Life Sciences **59**, 389-97.

COLLINGRIDGE G.L., KEHL S.J. & MCLENNAN H. (1983) Excitatory amino acids in synaptic transmission in the Schaffer collateral-commissural pathway of the rat hippocampus. Journal of Physiology **334**, 33-46.

COLLINS J.S., PERRY R.T., WATSON B., HARRELL L.E., ACTON R.T., BLACKER D., ALBERT M.S., TANZI R.E., BASSETT S.S., MCINNIS M.G., CAMPBELL R.D. & GO R.C.P. (2000) Association of a haplotype for tumour necrosis factor in siblings with late-onset Alzheimer disease: The NIMH Alzheimer disease genetics initiative. American Journal of Medical Genetics **96**. 823-830.

COOGAN A.N., O'LEARY D.M. & O'CONNER J.J. (1999) P42/44 MAP kinase inhibitor PD98059 attenuates multiple forms of synaptic plasticity in rat dentate gyrus *in vitro*. Journal of Neurophysiology **81**, 103-110.

CORMIER R.J. & KELLY P.T. (1996) Glutamate-induced long-term potentiation enhances spontaneous EPSC amplitude but not frequency. Journal of Neurophysiology **75**, 1909-1918.

CORNETT C.R., MARKESBERY W.R. & EHMANN W.D. (1998) Imbalances of trace elements related to oxidative damage in Alzheimer's disease brain. Neurotoxicology **19**, 339-346.

CORRAL-DEBRINSKI M., HORTON T., LOTT M.T., SHOFFNER J.M., MCKEE A.C., BEAL M.F., GRAHAM B.H. & WALLACE D.C. (1994) Marked changes in mitochondrial DNA deletion levels in Alzheimer brains. Genomics **23**, 471-476.

COUSSENS C.M. & TEYLER T.J. (1996) Protein kinase and phosphatase activity regulate the form of synaptic plasticity expressed. Synapse **24**, 97-103.

CREAGER R., DUNWIDDIE T. & LYNCH G. (1980) Paired-pulse and frequency facilitation in the CA1 region of the *in vitro* rat hippocampus. Journal of Physiology **299**, 409-424.

CRUTS M., VAN DUIJN C.M., BACKHOVENS H., VAN DEN BROECK M., WEHNERT A., SERNEELS S., SHERRINGTON R., HUTTON M., HARDY J., ST GEORGE-HYSLOP P.H., HOFMAN A. & VAN BROECKHOVEN C. (1998) Estimation of the genetic contribution of presenilin-1 and -2 mutations in a population-based study of presenile Alzheimer disease. Human Molecular Genetics **7**, 43-51.

CUMMINGS J.A., MULKEY R.M., NICOLL R.A. & MALENKA R.C. (1996) Ca^{2+} signaling requirements for long-term depression in the hippocampus. Neuron **16**, 825-833.

CZECH C., LESORT M., TREMP G., TERRO F., BLANCHARD V., SCHOMBERT B., CARPENTIER N., DREISLER S., BONICI B., TAKASHIMA A., MOUSSAOUI S., HUGON J. & PRADIER L. (1998) Characterization of human presenilin 1 transgenic rats: increased sensitivity to apoptosis in primary neuronal cultures. Neuroscience **87**, 325-336.

DAVIES C.H., STARKEY S.J., POZZA M.F. & COLLINGRIDGE G.L. (1991) $GABA_B$ autoreceptors regulate the induction of LTP. Nature **349**, 609-611.

DAVIES C.H., DAVIES S.N. & COLLINGRIDGE G.L. (1990) Paired-pulse depression of monosynaptic GABA-mediated inhibitory postsynaptic responses in rat hippocampus. Journal of Physiology **424**, 513-531.

DAVIS J.A., NARUSE S., CHEN H., ECKMAN C., YOUNKIN S., PRICE D.L., BORCHELT D.R., SISODIA S.S. & WONG P.C. (1998) An Alzheimer's disease-linked PS1 variant rescues the developmental abnormalities of PS1-deficient embryos. Neuron **20**, 603-609.

DE GREY A.D. (1997) A proposed refinement of the mitochondrial free radical theory of aging. Bioessays **19**, 161-6.

DE LA MONTE S.M., NG S.-C. & HSU D.W. (1995) Aberrant GAP-43 gene expression in Alzheimer's disease. American Journal of Pathology **147**, 934-946.

DE RONCHI D., FRATIGLIONI L., RUCCI P., PATERNICO A., GRAZIANI S. & DALMONTE E. (1998) The effect of education on dementia occurrence in an Italian population with middle to high socioeconomic status. Neurology **50**, 1231-1238.

DE STROOPER B., SAFTIG P. CRAESSAERTS K., VANDERSTICHELE H., GUHDE G., ANNAERT W., VON FIGURA K. & VAN LEUVEN F. (1998) Deficiency of presenlin-1 inhibits the normal cleavage of amyloid precursor protein. Nature **391**, 387-339.

DEBANNE D., GAHWILER B. & THOMPSON S.M. (1999) Heterogeneity of synaptic plasticity at unitary CA3-CA1 and CA3-CA3 connections in rat hippocampal slice cultures. Journal of Neuroscience **19**, 10664-10671.

DEBANNE D., GUERINEAU N.C., GAHWILER B.H. & THOMPSON S.M. (1996) Paired-pulse facilitation and depression at unitary synapses in rat hippocampus: quantal fluctuation affects subsequent release. Journal of Physiology **491**, 163-176.

DEIBEL M.A., EHMANN W.D. & MARKESBERY W.R. (1996) Copper, iron, and zinc imbalances in severely degenerated brain regions in Alzheimer's disease: Possible relation to oxidative stress. Journal of the Neurological Sciences **143**, 137-142.

DEL CERRO S., JUNG M. & LYNCH G. (1992) Benzodiazepines block long-term potentiation in slices of hippocampus and piriform cortex. Neuroscience **49**, 1-6.

DENG G., PIKE C.J. & COTMAN C.W. (1996) Alzheimer-associated presenilin-2 confers increased sensitivity to apoptosis in PC12 cells. FEBS Letters **397**, 50-54.

DEWACHTER I., VAN DORPE J., SMEIJERS L., GILIS M., KUIPERI C., LAENEN I.. CALUWAERTS N., MOECHARS D., CHECLER F., VANDERSTICHELE H. & VAN LEUVEN F. (2000) Aging increased amyloid peptide and caused amyloid plaques in brain of old APP/V717I transgenic mice by a different mechanism than mutant presenilin 1. Journal of Neuroscience **20**, 6452-6458.

DEWEY M.E., DAVIDSON I.A. & COPELAND J.R.M. (1988) Risk factors for dementia: evidence from the Liverpool study of continuing health in the community. International Journal of Geriatric Psychiatry **3**, 245-249.

DICKSON D.W., LIU W.K., KRESS Y., KU J., DEJESUS O. & YEN S.H. (1993) Phosphorylated tau immunoreactivity of granulovacuolar bodies (GVB) of Alzheimer's disease: localization of two amino terminal tau epitopes in GVB. Acta Neuropathologica **85**, 463-70.

DOBRUNZ L.E. & STEVENS C.F. (1997) Heterogeneity of release probability, facilitation, and depletion at central synapses. Neuron **18**, 995–1008.

DODART J.-C., MATHIS C,. BALES K.R., PAUL S.M. & UNGERER A. (1999) Early regional cerebral glucose hypometabloism in transgenic mice overexpressing the V717F β-amyloid precursor protein. Neuroscience Letters **277**, 49-52.

DOLPHIN A.C., ERRINGTON M.L. & BLISS T.V.P. (1982) Long-term potentiation of the perforant path *in vivo* is associated with increased glutamate release. Nature **297**, 496-498.

DU Y., BALES K.R., DODEL R.C., LIU X., GLINN M.A., HORN J.W., LITTLE S.P. & PAUL S.M. (1998) α2-Macroglobulin attenuates β-amyloid peptide 1-40 fibril formation and associated neuortoxicity of cultured fetal rat cortical neurones. Journal of Neurochemistry **70**, 1182-1188.

DUBINSKY J.M. & LEVI Y. (1998) Calcium-induced activation of the mitochondrial permeability transition in hippocampal neurons. Journal of Neuroscience Research **53**, 728-41.

DUDEK S.M. & BEAR M.F. (1992) Homosynaptic long-term depression in area CA1 of hippocampus and effects of N-methyl-D-aspartate receptor blockade. Proceedings of the National Academy of Sciences USA **89**, 4363-4367.

DUFF K., ECKMAN C., ZEHR C., YU X., PRADA C.-M., PEREZ-TUR J., HUTTON M., BUEE L., HARIGAYA Y., YAGER D., MORGAN D., GORDON M.N., HOLCOMB L., REFOLO L., ZENK B., HARDY J. & YOUNKIN S. (1996) Increased amyloid-$\beta_{42(43)}$ in brains of mice expressing mutant presenilin 1. Nature **383**, 710-713.

DUTAR P., POTIER B. & LAMOUR Y. (1994) Short-term effects of β-amyloid protein on CA1 hippocampal neurons in young and aged rats: a study of calcium-dependent events. Neurodegeneration **3**, 119-128.

EDDLESTON M. & MUCKE L. (1993) Molecular profile of reactive astrocytes - implications for their role in neurologic disease. Neuroscience **54**, 15-36.

EL KHOURY J., HICKMAN S.E., THOMAS C.A., LOIKE J.D. & SILVERSTEIN S.C. (1998) Microglia, scavenger receptors, and pathogenesis of Alzheimer's disease. Neurobiology of Aging **19**. S81-84.

EL KHOURY J., HICKMAN S.E., THOMAS C.A., CAO L., SILVERSTEIN S.C. & LOIKE J.D. (1996) Scavenger receptor-mediated adhesion of microglia to β-amyloid fibrils. Nature **382**, 716-719.

EMPTAGE N., BLISS T.V.P. & FINE A. (1999) Single synaptic events evoke NMDA receptor-mediated release of calcium from internal stores in hippocampal dendritic spines. Neuron **22**, 115-124.

ENGERT F. & BONHOEFFER T. (1999) Dendritic spine changes associated with hippocampal long-term synaptic plasticity. Nature **399**, 66-70.

ENGERT F. & BONHOEFFER T. (1997) Synapse specificity of long-term potentiation breaks down at short distances. Nature **388**, 279-284.

ENGIDAWORK E., GULESSERIAN T., SEIDL R., CAIRNS N. & LUBEC G. (2001) Expression of apoptosis related proteins in brains of patients with Alzheimer's disease. Neuroscience Letters **303**. 79-82.

ERRINGTON M.L., LYNCH M.A. & BLISS T.V.P. (1987) Long-term potentiations in the dentate gyrus induction and increased glutamate release are blocked by D(-)aminophosphonovalerate. Neuroscience **20**, 279-284.

ERSHLER W.B. (1993) Interleukin-6: a cytokine for gerontologists. Journal of the American Geriatrics Society **41**, 176-181.

ETCHEBERRIGARAY R., HIRASHIMA N., NEE L., PRINCE J., GOVONI S., RACCHI M., TANZI R.E. & ALKON D.L. (1998) Calcium responses in fibroblasts from asymptomatic members of Alzheimer's disease families. Neurobiology of Disease **5**, 37-45.

EVANS D.A., FUNKENSTEIN H.H., ALBERT M.S., SCHERR P.A., COOK N.R., CHOWN M.J., HEBERT L.E., HENNEKENS C.H. & TAYLOR J.O. (1989) Prevalence of Alzheimer's disease in a community population of older persons. Higher than previously reported. Journal of the American Medical Association **262**, 2551-2556.

EVANS K.C., BERGER E.P., CHO C., WEISGRABER K.H. & LANSBURY P.T. (1995) Apolipoprotein E is a kinetic but not a thermodynamic inhibitor of amyloid formation: implications for the pathogenesis and treatment of Alzheimer disease. Proceeding of the National Academy of Sciences USA **92**, 763-767.

EVANS M.J. & KAUFMAN M.H. (1981) Establishment in culture of pluripotential cells from mouse embryos. Nature **292**, 154-156.

FABRIZI C., BUSINARO R., LAURO G.M., STARACE G. & FUMAGALLI L. (1999) Activated α2macroglobulin increases β-amyloid (25-35)-induced toxicity in LAN5 human heuroblastoma cells. Experimental Neurology **155,** 252-259.

FISCHER M., KAECH S., WAGNER U., BRINKHAUS H. & MATUS A. (2000) Glutamate receptors regulate actin-based plasticity in dendritic spines. Nature Neuroscience **3**, 887-894.

FLAHERTY D., LU Q., SORIA J. & WOOD J.G. (1999) Regulation of tau phosphorylation in microtubule fractions by apolipoprotein E. Journal of Neuroscience Research **56**, 271-274.

FRATIGLIONI L., VIITANEN M., VON STRAUSS E., TONTODONATI V., HERLITZ A. & WINBLAD B. (1997) Very old women at highest risk of dementia and Alzheimer's disease: incidence data from the Kungsholmen Project, Stockholm. Neurology **48**, 132-138.

FRAUTSHY S.A., BAIRD A. & COLE G.M. (1991) Effects of injected Alzheimer β-amyloid cores in rat brain. Proceedings of the National Academy of Sciences USA **88**, 8362-8366.

FRIER D.B., HOLSCHER C. & HERRON C.E. (2001) Blockade of long-term potentiation by β-amyloid peptides in the CA1 region of the rat hippocampus *in vivo*. Journal of Neurophysiology **85**. 708-713.

FUKUNAGA K., STOPPINI L., MIYAMOTO E. & MULLER D. (1993) Long-term potentiation is associated with an increased activity of Ca^{2+}/calmodulin-dependent protein kinase II. Journal of Biological Chemistry **268**, 7863-7867.

FURUKAWA K. & MATTSON M.P. (1998) Secreted amyloid precursor protein α selectively suppresses N-methyl-D-aspartate currents in hippocampal neurons: Involvement of cyclic GMP. Neuroscience **83**, 429-438.

FURUKAWA K., BARGER S.W., BLALOCK E.M. & MATTSON M.P. (1996) Activation of K^+ channels and suppression of neuronal activity by secreted β-amyloid-precursor protein. Nature **379**, 74-78.

FYKSE E.M., LI C. & SUDHOF T.C. (1995) Phosphorylation of rabphilin-3A by Ca^{2+}/calmodulin- and cAMP-dependent protein kinases *in vitro*. Journal of Neuroscience **15**, 2385-2395.

GALASKO D., HANSEN L.A., KATZMAN R., WIEDERHOLT W., MASLIAH E., TERRY R., HILL L.R., LESSIN P. & THAL L.J. (1994) Clinical-neuropathological correlation in Alzheimer's disease and related dementias. Archives of Neurology **51**, 888-895.

GAMES D., ADAMS D., ALESSANDRINI R., BARBOUR R., BERTHELETTE P., BLACKWELL C., CARR T., CLEMENS J., DONALDSON T., GILLESPIE F., GUIDO T., HAGOPIAN S., JOHNSON-WOOD K., KHAN K., LEE M., LEIBOWITZ P., LIEBERBURG I., LITTLE S., MASLIAH E., MCCONLOGUE L., MONTOYA-ZAVALA M., MUCKE L., PAGANINI L., PENNIMAN E., POWER M., SCHENK D., SEUBERT P., SNYDER B., SORIANO F., TAN H., VITALE J., WADSWORTH S., WOLOZIN B. & ZHAO J. (1995) Alzheimer-type neuropathology in transgenic mice overexpressing V717F β-amyloid precursor protein. Nature **373**, 523-527.

GARDNER R.L. (1968) Mouse chimaeras obtained by the injection of cells into the blastocyst. Nature **220**, 596-597.

GEULA C., MESULAM M.M., SAROFF D.M. & WU C.-K. (1998a) Relationship between plaques. tangles, and loss of cortical cholinergic fibres in Alzheimer disease. Journal of Neuropathology and Experimental Neurology **57**, 63-75.

GEULA C., WU C.-K., SAROFF D., LORENZO A., YUAN M. & YANKNER B.A. (1998b) Aging renders the brain vulnerable to Aβ-protein neurotoxicity. Nature Medicine **4**, 827-831.

GIBSON G.E., SHEU K.-F.R. & BLASS J.P. (1998) Abnormalities of mitochondrial enzymes in Alzheimer disease. Journal of Neural Transmission **105**, 855-870.

GOATE A., CHARTIER-HARLIN M.-C., MULLAN M., BROWN J., CRAWFORD F., FIDANI L.. GIUFFRA L., HAYNES A., IRVING N., JAMES L., MANT R., NEWTON P., ROOKE K.. ROQUES P., TALBOT C., PERICAK-VANCE M., ROSES A., WILLIAMSON R., ROSSER M.. OWEN M. & HARDY J. (1991) Segregation of a missense mutation in the amyloid precursor protein gene with familial Alzheimer's disease. Nature **349**, 704-706.

GOLDGABER D., LERMAN M.I., MCBRIDE W., SAFFIOTTI U. & GAJDUSEK D.C. (1987) Characterization and chromosomal localization of a cDNA encoding brain amyloid of Alzheimer's disease. Science **235**, 877-880.

GOLDE T.E., ESTUS S., YOUNKIN L.H., SELKOE D.J. & YOUNKIN S.G. (1992) Processing of the amyloid protein precursor to potentially amyloidogenic derivatives. Science **255**, 728-30.

GOMEZ-ISLA T., HOLLISTER R., WEST H., MUI S., GROWDON J.H., PETERSEN R.C., PARISI J.E. & HYMAN B.T. (1997) Neuronal loss correlates with but exceeds neurofibrillary tangles in Alzheimer's disease. Annals of Neurology **41**, 17-24.

GOMPERTS S.N., RAO A., CRAIG A.M., MALENKA R.C. & NICOLL R.A. (1998) Postsynaptically silent synapses in single neuron cultures. Neuron **21**, 1443-1451.

GONZALEZ C., MARTIN T., CACHO J., BRENAS M.T., ARROYO T., GARCIA-BERROCAL B., NAVAJO J.A. & GONZALEZ-BUITRAGO J.M. (1999) Serum zinc, copper, insulin and lipids in Alzheimer's disease ε4 apolipoprotein E allele carriers. European Journal of Clinical Investigation **29**, 637-642.

GOOD T.A., SMITH D.O. & MURPHY R.M. (1996) β-Amyloid peptide blocks the fast-inactivating K^+ current in rat hippocampal neurons. Biophysical Journal **70,** 296-304.

GORDON J.W., SCANGOS G.A., PLOTKIN D.J., BARBOSA J.A. & RUDDLE F.H. (1980) Genetic transfomation of mouse embryos by microinjection of purified DNA. Proceedings of the National Academy of Sciences USA **77**, 7380-7384.

GRAVES A.B., VAN DUIJN C.M., CHANDRA V., FRATIGLIONI L., HEYMAN A., JORM A.F., KOKMEN E., KONDO K., MORTIMER J.A., ROCCA W.A., SHALAT S.L., SOININEN H. & HOFMAN A. (1991) Alcohol and tobacco consumption as risk factors for Alzheimer's disease: A collaborative re-analysis of case-control studies. International Journal of Epidemiology **20**, S48-S57.

GRAY C.W. & PATEL A.J. (1993) Regulation of β-amyloid precursor protein isoform mRNAs by transforming growth factor-β1 and interleukin-1β in astrocytes. Molecular Brain Research **19**, 251-256.

GROVER L.M. & TEYLER T.J. (1990) Differential effects of NMDA receptor antagonist APV on tetanic stimulation induced and calcium induced potentiation. Neuroscience Letters **113**, 309-314.

GROVER L.M. & YAN C. (1999) Evidence for involvement of group II/III metabotropic glutamate receptors in NMDA receptor-independent long-term potentiation in area CA1 of rat hippocampus. Journal of Neurophysiology **82**, 2956-2969.

GUILLOZET A.L., SMILEY J.F., MASH D.C. & MESULAM M.-M. (1997) Butyrylcholinesterase in the life cycle of amyloid plaques. Annals of Neurology **42**, 909-918.

GUO Q., FU W., SOPHER B.L., MILLER M.W., WARE C.B., MARTIN G.M. & MATTSON M.P. (1999a) Increased vulnerability of hippocampal neurons to excitotoxic necrosis in presenilin-1 mutant knock-in mice. Nature Medicine **5**, 101-107.

GUO Q., FU W., HOLTSBERG F.W., STEINER S.M. & MATTSON M.P. (1999b) Superoxide mediates the cell-death-enhancing action of presenilin-1mutations. Journal of Neuroscience Research **56**, 457-470.

GUO Q., CHRISTAKOS S., ROBINSON N. & MATTSON M.P. (1998) Calbindin D28k blocks the proapoptotic actions of mutant presenilin 1: reduced oxidative stress and preserved mitochondrial function. Proceeding of the National Academy of Sciences USA **95**, 3227-3232.

GUO Q., SOPHER B.L., FURUKAWA K., PHAM D.G., ROBINSON N., MARTIN G.M. & MATTSON M.P. (1997) Alzheimer's presenilin mutation sensitizes neural cells to apoptosis induced by trophic factor withdrawal and amyloid β-peptide: Involvement of calcium and oxyradicals. Journal of Neuroscience **17**, 4212-4222.

GUO Q., FURUKAWA K., SOPHER B.L., PHAM D.G., XIE J., ROBINSON N., MARTIN G.M. & MATTSON MP. (1996) Alzheimer's PS-1 mutation perturbs calcium homeostasis and sensitizes PC12 cells to death induced by amyloid β-peptide. Neuroreport **8**, 379-383.

HAASS C., HUNG A.Y., SCHLOSSMACHER M.G., TEPLOW D.B. & SELKOE D.J. (1993a) beta-Amyloid peptide and a 3-kDa fragment are derived by distinct cellular mechanisms. Journal of Biological Chemistry. **268,** 3021-4.

HAASS C., HUNG A.Y., SCHLOSSMACHER M.G., OLTERSDORF T., TEPLOW D.B. & SELKOE D.J. (1993b) Normal cellular processing of the beta-amyloid precursor protein results in the secretion of the amyloid beta peptide and related molecules. Annals of the New York Academy of Sciences **695**, 109-16

HALEY J.E., WILCOX G.L. & CHAPMAN P.F. (1992) The role of nitric oxide in hippocampal long-term potentiation. Neuron **8**, 211-216.

HALTIA M., VIITANEN M., SULKAVA R., ALA-HURULA V., POYHONEN M., GOLDFARB L., BROWN P., LEVY E., HOULDEN H., CROOK R., GOATE A., CLARK R., KORENBLAT K., PANDIR S., KELLER H.D., LILIUS L., LIU L., AXELMAN K., FORSELL L., WINBLAD B., LANNFELT L. & HARDY J. (1994) Chromosome 14-encoded Alzheimer's disease: Genetic and clinicopathological description. Annals of Neurology **36**, 362-367.

HARDY J. (1994) Alzheimer's disease: Clinical molecular genetics. Clinics in Geriatric Medicine **10**. 239-247.

HARTLEY D.M., WALSH D.M., YE C.P., DIEHL T., VASQUEZ S., VASSILEV P.M., TEPLOW B. & SELKOE D.J. (1999) Protofibrillar intermediates of amyloid β-protein induce acute electrophysiological changes and progressive neurotoxicity in cortical neurons. Journal of Neuroscience **19**, 8876-8884.

HAUSS-WEGRZYNIAK B., DOBRZANSKI P., STOEHR J.D. & WENK G.L. (1998) Chronic neuroinflammation in rats reproduces components of the neurobiology of Alzheimer's disease. Brain Research **780**, 294-303.

HEBB D.O. (1949) In *The Organisation of Behavior: A Neuropsychological Theory.* New York: John Wiley, 335.

HEESE K., HOCK C. & OTTEN U. (1988) Inflammatory signals induce neurotrophin expression in human microglial cells. Journal of Neurochemistry **70**, 699-707.

HENDERSON V.W. (1997) The epidemiology of estrogen replacement therapy and Alzheimer's disease. Neurology **48**, S27-35.

HENDRIE H.C., OSUNTOKUN B.O., HALL K.S., OGUNNIYI A.O., HUI S.L., UNVERZAGT F.W., GUREJE O., RODENBERG C.A., BAIYEWU O., MUSICK B.S., ADEYINKA A., FARLOW M.R., OLUWOLE S.O., CLASS C.A., KOMOLAFE O., BRASHEAR A. & BURDINE V. (1995) Prevalence of Alzheimer's disease and dementia in two communities: Nigerian Africans and African Americans. American Journal of Psychiatry **152**, 1485-1492.

HESSLER N.A., SHIRKE A.M. & MALINOW R. (1993) The probability of transmitter release at a mammalian central synapse. Nature **366**, 569-572.

HEYMAN A., WILKINSON W.E., STAFFORD J.A., HELMS M.J., SIGMON A.H. & WEINBERG T. (1984) Alzheimer's disease: a study of epidemiological aspects. Annals of Neurology **15**, 335-341.

HEYSER C.J., MASLIAH E., SAMIMI A., CAMPBELL I.L. & GOLD L.H. (1997) Progressive decline in avoidance learning paralleled by inflammatory neurodegeneration in transgenic mice expressing interleukin 6 in the brain. Proceedings of the National Academy of Sciences USA **94**. 1500-1505.

HOCK B.J. & BUNSEY M.D. (1998) Differential effects of dorsal and ventral hippocampal lesions. Journal of Neuroscience **18**, 7027-7032.

HOLCOMB L., GORDON M.N., MCGOWAN E., YU X., BENKOVIC S., JANTZEN P., WRIGHT K., SAAD I., MUELLER R., MORGAN D., SANDERS S., ZEHR C., O'CAMPO K., HARDY J., PRADA C.-M., ECKMAN C., YOUNKIN S., HSIAO K. & DUFF K. (1998) Accelerated Alzheimer-type phenotype in transgenic mice carrying both mutant amyloid precursor protein and presenilin 1 transgenes. Nature Medicine **4**, 97-100.

HSIA A.Y., MASLIAH E., MCCONLOGUE L., YU G.-Q., TATSUNO G., HU K., KHOLODENKO D., MALENKA R.C., NICOLL R.A. & MUCKE L. (1999) Plaque-independent disruption of neural circuits in Alzheimer's disease mouse models. Proceedings of the National Academy of Sciences USA **96**, 3228-2322.

HSIAO K., CHAPMAN P., NILSEN S., ECKMAN C., HARIGAYA Y., YOUNKIN S., YANG F. & COLE G. (1996) Correlative memory deficits, Aβ elevation, and amyloid plaques in transgenic mice. Science **274**, 99-102.

HU J., AKAMA K.T., KRAFFT G.A., CHROMY B.A. & VAN ELDIK L.J. (1998a) Amyloid-β peptide activates cultured astrocytes: morophological alterations, cytokine induction and nitric oxide release. Brain Research **785**, 195-206.

HU J., LADU M.J. & VAN ELDIK L.J. (1998b) Apolipoprotein E attenuates β-amyloid-induced astrocyte activation. Journal of Neurochemistry **71**, 1626-1634.

HUANG Y.-Q., LU W.-Y., ALI D.W., PELKEY K.A., PITCHER G.M., LU Y.M., AOTO H., RODER J.C., SASAKI T., SALTER M.W. & MACDONALD J.F. (2001) CAKβ/Pyk2 kinase is a signaling link for induction of long-term potentiation in CA1 hippocampus. Neuron **29**, 485-496.

HUANG X., CUAJUNGCO M.P., ATWOOD C.S., MOIR R.D., TANZI R.E. & BUSH A.I. (2000) Alzheimer's disease, β-amyloid protein and zinc. Journal of Nutrition **130**, 1488S-1492S.

HUANG C.-C. & HSIN K.-S. (1999a) Protein tyrosine kinase is required for the induction of long-term potentiation in the rat hippocampus.Journal of Physiology **520**, 783-796.

HUANG X., ATWOOD C.S., HARTSHORN M.A., MULTHAUP G., GOLDSTEIN L.E., SCARPA R.C., CUAJUNGCO M.P., GRAY D.N., LIM J., MOIR R.D., TANZI R.E. & BUSH A.I. (1999b) The Aβ peptide of Alzheimer's disease directly produces hydrogen peroxide through metal ion reduction. Biochemistry **38**, 7609-7616.

HUANG X., CUAJUNGCO M.P., ATWOOD C.S., HARTSHORN M.A., TYNDALL J.D.A., HANSON G.R., STOKES K.C., LEOPOLD M., MULTHAUP G., GOLDSTEIN L.E., SCARPA R.C., SAUNDERS A.J., LIM J., MOIR R.D., GLABE C., BOWDEN E.F., MASTERS C.L., FAIRLIE D.P., TANZI R.E. & BUSH A.I. (1999c) Cu(II) potentiation of Alzheimer Aβ neurotoxicity: Correlation with cell-free hydrogen peroxide production and metal reduction. Journal of Biological Chemistry **274**, 37111-37116.

HUANG X., CUAJUNGCO M.P., ATWOOD C.S., HARTSHORN M.A., TYNDALL J.D.A., HANSON G.R., STOKES K.C., KALTSCHIMIDT C., KALTSCHMIDT B., NEUMANN H., WEKERLE H. & BAEUERLE P.A. (1994) Constitutive NF-κB activity in neurones. Molecular Cell Biology **14**, 3981-3992.

HUBER G., BAILLY Y., MARTIN J.R., MARIANI J. & BRUGG B. (1997) Synaptic β-amyloid precursor proteins increase with learning capacity in rats. Neuroscience **80**, 313-320.

HUBER L.A., XU Q.B., JURGENS G., BOCK G., BUHLER E., GEY K.F., SCHONITZER D., TRAILL K.N. & WICK G. (1991) Correlation of lymphocyte lipid composition membrane microviscosity and mitogen response in the aged. European Journal of Immunology **21**, 2761-5.

IMAHORI K., HOSHI M., ISHIGURO K., SATO K., TAKAHASHI M., SHIURBA R., YAMAGUCHI H., TAKASHIMA A. & UCHIDA T. (1998) Possible role of tau protein kinases in pathogenesis of Alzheimer's disease. Neurobiology of Aging 19, S93-S98.

INGELSON M., VANMECHELEN E. & LANNFELT L. (1996) Microtubule-associated protein tau in human fibroblasts with Swedish Alzheimer mutation. Neuroscience Letters **220**, 9-12.

IWATSUBO T. (1998) $A\beta_{42}$, presenilins and Alzheimer's disease. Neurobiology of Aging **19**, S11-S13.

IWATSUBO T., MANN D.M.A., ODAKA A., SUZUKI N. & IHARA Y. (1995) Amyloid β protein (Aβ) deposition: $A\beta_{42(43)}$ precedes $A\beta_{40}$ in Down's syndrome. Annals of Neurology **37**, 294-299.

JACK C.R., PETERSEN R.C., XU Y.C., O'BRIEN P.C., SMITH G.E., IVNIK R.J., BOEVE B.F., WARING S.C., TANGALOS E.G. & KOKMEN E. (1999) Prediction of AD with MRI-based hippocampal volume in mild cognitive impairment. Neurology **52**, 1397-1403.

JAHROMI B.S., ZHANG L., CARLEN P.L. & PENNEFATHER P. (1999) Differential time-course of slow afterhyperpolarizations and assiciated Ca^{2+} transients in rat CA1 pyramidal neurons: further dissociation by Ca^{2+} buffer. Neuroscience **88**, 719-726.

JALONEN T.O., CHARNIGA C.J. & WIELT D.B. (1997) β-amyloid peptide-induced morphological changes coincide with increased K^+ and Cl^- channel activity in rat cortical astrocytes. Brain Research **746**, 85-97.

JANICKI S. & MONTEIRO M.J. (1997) Increased apoptosis arising from increased expression of the Alzheimer's disease-associated presenilin-2 mutation (N141I). The Journal of Cell Biology **139**, 485-495.

JANUS C., PEARSON J., MCLAURIN J., MATHEWS P.M., JIANG Y., SCHMIDT S.D., CHISHTI M.A., HORNE P., HESLIN D., FRENCH J., MOUNT H.T.J., NIXON R.A., MERCKEN M., BERGERON C., FRASER P.E., ST GEORGE-HYSLOP P. & WESTWAY D. (2000a) Aβ peptide immunization reduces behavioural impairment and plaques in a mouse model of Alzheimer's disease. Nature **408**, 979-982.

JANUS C., D'AMELIO S., AMITAY O., CHISHTI M.A., STROME R., FRASER P., CARLSON G.A., RODER J.C., ST GEORGE-HYSLOP P. & WESTAWAY D. (2000b) Spatial learning in transgenic mice expressing human presenilin 1 (PS1) transgenes. Neurobiology of Aging **21**, 541-549.

JARRETT J.T., BERGER E.P. & LANSBURY P.T. (1993) The C-terminus of the Aβ protein is critical in amyloidogenisis. Annals of the New York Academy of Science **695**, 144-148.

JENSEN M., SCHRODER J., BLOMBERG M., ENGVALL B., PANTEL J., IDA N., BASUN H., WAHLUND L.-O., WERLE E., JAUSS M., BEYREUTHER K., LANNFELT L. & HARTMENN T. (1999) Cerebrospinal fluid $A\beta_{42}$ is increased early in sporidic Alzheimer's disease and declines with disease progression. Annals of Neurology **45**, 504-511.

JERVIS G.A. & THIELLS N.Y. (1948) Early senile dementia in mongoloid idiocy. American Journal of Psychiatry **105**, 102-106.

JIA Z., AGOPYAN N., MIU P., XIONG Z., HENDERSON J., GERLAI R., TAVERNA F.A., VELUMIAN A., MACDONALD J., CARLEN P., ABRAMOW-NEWERLY W. & RODER J. (1996) Enhanced LTP in mice deficient in the AMPA receptor GluR2. Neuron **17**, 945-956.

JOHNSON-WOOD K., LEE M., MOTTER R., HU K., GORDON G., BARBOUR R., KHAN K., GORDON M., TAN H., GAMES D., LIEBERBURG I., SCHENK D., SEUBERT P. & MCCONLOGUE L. (1997) Amyloid precursor protein processing and $A\beta_{42}$ deposition in a transgenic mouse model of Alzheimer disease. Proceedings of the National Academy of Sciences USA **94**, 1550-1555.

JORM A.F., VAN DUIJN C.M., CHANDRA V., FRATIGLIONI L., GRAVES A.B., HEYMAN A., KOKMEN E., KONDO K., MORTIMER J.A., ROCCA W.A., SHALAT S.L., SOININEN H. & HOFMAN A. (1991) Psychiatric history and related exposures as risk factors for Alzheimer's disease: a collaborative re-analysis of case-control studies. International Journal of Epidemiology **20**, S43-S47.

KALARIA R.N., COHEN D.L., GREENBERG B.D., SAVAGE M.J., BOGDANOVIC N.E., WINBLAD B., LANNFELT L. & ADAM A. (1996) Abundance of the longer $A\beta_{42}$ in neocortical and cerebrovascular amyloid β deposits in Swedish familial Alzheimer's disease and Down's syndrome. Neuroreport **7**, 1377-1381.

KALTSCHMIDT C., KALTSCHMIDT B., NEUMANN H., WEKERLE H. & BAEUERLE P.A. (1994) Constitutive NF-κB activity in neurons. Molecular & Cellular Biology **14**, 3981-3992.

KAMETANI F., TANAKA K., TOKUDA T. & ALLSOP D. (1995) The immunoreactive profile at the N-terminal region of $A\beta_{1\text{-}39/40}$ but not $A\beta_{1\text{-}42}$ changes with transition from monomer/dimer to further peptide aggregates. Brain Research **703**, 237-241.

KANAI M., SHIZUKA M., URAKAMI K., MATSUBARA E., HARIGAYA Y., OKAMOTO K. & SHOJI M. (1999) Apolipoprotein E4 accelerates dementia and increases cerebrospinal fluid tau levels in Alzheimer's disease. Neuroscience Letters **267**, 65-68.

KANAI M., MATSUBARA E., ISOE K., URAKAMI K., NAKASHIMA K., ARAI H., SASAKI H., ABE K., IWATSUBO T., KOSAKA T., WATANABE M., TOMIDOKORO Y., SHIZUKA M., MIZUSHIMA K., NAKAMURA T., IGETA Y., IKEDA Y., AMARI M., KAWARABAYASHI T., ISHIGURO K., HARIGAYA Y., WAKABAYASHI K., OKAMOTO K., HIRAI S. & SHOJI M. (1998) Longitudinal study of cerebrospinal fluid levels of tau, $A\beta_{1-40}$, and $A\beta_{1-42(43)}$ in Alzheimer's disease: A study in Japan. Annals of Neurology **44**, 17-26.

KANG J., LEMAIRE H.G., UNTERBECK A., SALBAUM J.M., MASTERS C.L., GRZESCHIK K.H., MULTHAUP G., BEYREUTHER K. & MULLER-HILL B. (1987) The precursor of Alzheimer's disease amyloid A4 protein resembles a cell-surface receptor. Nature **325**, 733-6.

KANTEREWICZ B.I., URBAN N.N., MCMAHON D.B.T., NORMAN E.D., GIFFEN L.J., FAVATA M.F., SCHERLE P.A., TRZASKOS J.M., BARRIONUEVO G. & KLANN E. (2000) The extracellular signal-regulated kinase cascade is required for NMDA receptor-independent LTP in area CA1 but not area A3 of the hippocampus. Journal of Neuroscience **20**, 3057-3066.

KAPUR A., YECKEL M.F., GRAY R. & JOHNSTON D. (1998) L-type calcium channels are required for one form of hippocampal mossy fiber LTP. Journal of Neurophysiology **79**, 2181-2190.

KATZ B. & MILEDI R. (1968) The role of calcium in neuromuscular facilitation. Journal of Physiology **195**, 481-492.

KAWARABAYASHI T., YOUNKIN L.H., SAIDO T., SHOJI M., HSIAO ASHE K. & YOUNKIN S.G. (2001) Age-dependent changes in brain, CSF, and plasma amyloid β protein in the Tg2576 transgenic mouse model of Alzheimer's disease. Journal of Neuroscience **21**, 372-381.

KAWAS C. (1998) Erratum: A prospective study of estrogen replacement therapy and the risk of developing Alzheimer's disease: The Baltimore longitudinal study of aging. Neurology **51**, 654.

KIM J.-H., ANWYL R., SUH Y.-H., DJAMGOZ M.B.A. & ROWAN M.J. (2001) Use-dependent effects of amyloidogenic fragments of β-amyloid precursor protein on synaptic plasticity in rat hippocampus *in vivo*. Journal of Neuroscience **21**, 1327-1333.

KING D.L., ARENDASH G.W., CRAWFORD F., STERK T., MENENDEZ J. & MULLAN M.J. (1999) Progressive and gender-dependent cognitive impairment in the APP_{SW} transgenic mouse model for Alzheimer's disease. Behavioural Brain Research **103**, 145-162.

KLESCHEVNIKOV A.M., SOKOLOV M.V., KUHNT U., DAWE G.S., STEPHENSON J.D. & VORONIN L.L. (1997) Changes in paired-pulse facilitation correlate with induction of long-term potentiation in area CA1 of rat hippocampal slices. Neuroscience **76**, 829-843.

KO G.Y. & KELLY P.T. (1999a) Nitric oxide acts as a postsynaptic signaling molecule in calcium/calmodulin-induced syanptic potentiation in hippocampal CA1 pyramidal neurons. Journal of Neuroscience **19**, 6784-6794.

KO L.-W., KO E.C., NACHARAJU P., LIU W.-K., CHANG E., KENESSEY A. & YEN S.-H.C. (1999b) An immunochemical study on tau glycation in paired helical filaments. Brain Research **830**. 301-313.

KOH J.-Y., YANG L.L. & COTMAN C.W. (1990) β-Amyloid protein increases the vulnerability of cultured cortical neurons to excitotoxic damage. Brain Research **533**, 315-320.

KOVACS D.M., MANCINI R., HENDERSON J., NA S.J., SCHMIDT S.D., KIM T.-W. & TANZI R.E. (1999) Staurosporine-induced activation of caspase-3 is potentiated by presenilin 1 familial Alzheimer's disease mutations in human neuroglioma cells. Journal of Neurochemistry **73**, 2278-2285.

KOVACS DM. FAUSETT HJ. PAGE KJ. KIM T-W. MOIR RD. MERRIAM DE. HOLLISTER RD. HALLMARK OG. MANCINI R. FELSENSTEIN KM. HYMAN BT. TANZI RE. WASCO W. (1996) Alzheimer-associated presenilins 1 and 2: Neuronal expression in brain and localization to intracellular membranes in mammalian cells. Nature Medicine **2**, 224-229.

KRUGERS H.J., MULDER M., KORF J., HAVEKES L., DE KLOET E.R. & JOELS M. (1997) Altered synaptic plasticity in hippocampal CA1 area of apolipoprotein E deficient mice. Neuroreport 8, 2505-10.

KRUMAN I., BRUCE-KELLER A.J., BREDESEN D., WAEG G. & MATTSON M.P. (1997) Evidence that 4-hydroxynonenal mediates oxidative stress-induced neuronal apoptosis. Journal of Neuroscience **17**, 5089-5100.

KUENZI F.M., FITZJOHN S.M., MORTON R.A., COLLINGRIDGE G.L. & SEABROOK G.R. (2000) Reduced long-term potentiation in hippocampal slices prepared using sucrose-based artificial cerebrospinal fluid. Journal of Neuroscience Methods **100**, 117-122.

KUHNT U. & VORONIN L.L. (1994) Interaction between paired-pulse facilitation and long-term potentiation in area CA1 of the guinea-pig hippocampal slices: application of quantal analysis. Neuroscience **62**, 391-397.

KUIPER M.A., MULDER C., VAN KAMP G.J., SCHELTENS P. & WOLTERS E.C. (1994) Cerebrospinal fluid ferritin levels of patients with Parkinson's disease, Alzheimer's disease, and multiple system atrophy. Journal of Neural Transmission - Parkinsons Disease & Dementia Section **7**. 109-114.

KULLMANN D.M. & NICOLL R.A. (1992) Long-term potentiation is associated with increases in quantal content and quantal amplitude. Nature **357**, 240-244.

KUMAR-SINGH S., DEWACHTER I., MOECHARS D., LUBKE U., DE JONGHE C., CEUTERICH C., CHECLER F., NAIDU A., CORDELL B., CRAS P., VAN BROECKHOVEN C. & VAN LEUVEN F. (2000) Behavioral disturbances without amyloid deposits in mice overexpressing human amyloid precursor protein with Flemish (A692G) or Dutch (E693Q) mutation. Neurobiology of Disease **7**, 9-22.

LAGANIERE S. & YU B.P. (1993) Modulation of membrane phospholipid fatty acid composition by age and food restriction. Gerontology **39**, 7-18.

LAMB B.T., BARDEL K.A., KULNANE L.S., ANDERSON J.J., HOLTZ G., WAGNER S.L., SISODIA S.S. & HOEGER E.J. (1999) Amyloid production and deposition in mutant amyloid precursor protein and presenilin-1 yeast artificial chromosome transgenic mice. Nature Neuroscience **2**, 695-697.

LAMB B.T., SISODIA S.S., LAWLER A.M., SLUNT H.H., KITT C.A., KEARNS W.G., PEASON P.L., PRICE D.L. & GEARHART J.D. (1993) Introduction and expression of the 400 kilobase precursor amyloid protein gene in transgenic mice. Nature Genetics **5**, 22-30.

LAMBERT M.P., BARLOW A.K., CHROMY B.A., EDWARDS C., FREED R., LIOSATOS M., MORGAN T.E., ROZOVSKY I., TROMMER B., VIOLA K.L., WALS P., ZHANG C., FINCH C.E., KRAFFT G.A. & KLEIN W.L. (1998) Diffusible, nonfibrillar ligands derived from $A\beta_{1-42}$ are potent central nervous system neurotoxins. Proceedings of the National Academy of Sciences USA **95**, 6448-6453.

LANNFELT L., APPEGREN H., AXELMAN K., LILIUS L., HANSSON G., SCHENK D., HARDY J. & WINBLAD B. (1994) Amyloid precursor protein mutation causes Alzheimer's disease in a Swedish family. Neuroscience Letters **168**, 254-256.

LARKMAN A., HANNAY T., STRATFORD K. & JACK J. (1992) Presynaptic release probability influences the locus of long-term potentiation. Nature **360**, 70-73.

LARSON J., LYNCH G., GAMES D. & SEUBERT P. (1999) Alterations in synaptic transmission and long-term potentiation in hippocampal slices from young and aged PDAPP mice. Brain Research **840**, 23-35.

LAUNER L.J., ANDERSEN K., DEWEY M.E., LETENNEUR L., OTT A., AMADUCCI L.A.. BRAYNE C., COPELAND J.R.M., DARTIGUES J.-F., KRAGH-SORENSEN P., LOBO A.. MARTINEZ-LAGE J.M., STIJNEN T., HOLMAN A., GREEN A., LOLK A., NIELSEN H.. COMMENGES D., VAN HARSKAMP B.F., HOFMAN A.. DE- LA-CAMARA C., DIA J.L.. MARCOS G., SAZ P., VENTURA T., MCCRACKEN C.F.M., WILSON K.C.M., DAY N.E.. DEVAKUMAR M., ESIRI M.M., EVANS J.G., FAIRBAIRN A.F., HUPPERT F.A., INCE P.G.. JOHNSON A.L., KAY D.W.K., LOWE J., MCKEITH I.G., NICKSON J., PAYKEL E.S., ROSSI M.. WALKER N., XUEREB J., AURIACOMBE S., BALDERESCHI M., CLAYTON D. (1999) Rates and risk factors for dementia and Alzheimer's disease: Results from EURODEM pooled analyses. Neurology **52**, 78-84.

LAURI SE., KAUKINEN S., KINNUNEN T., YLINEN A., IMAI S., KAILA K., TAIRA T. & RAUVALA H. (1999) Regulatory role and molecular interactions of a cell-surface heparan sulfate proteoglycan (N-syndecan) in hippocampal long-term potentiation. Journal of Neuroscience **19**, 1226-1235.

LEE M.K., BORCHELT D.R., KIM G., THINAKARAN G., SLUNT H.H., RATOVITSKI T.. MARTIN L.J., KITTUR A., GANDY S., LEVEY A.L., JENKINS N., COPELAND N., PRICE D.L. & SISODIA S.S. (1997) Hyperaccumulation of FAD-linked presenilin 1 variants *in vivo*. Nature Medicine **3**, 756-760.

LEIBSON C.L., ROCCA W.A., HANSON V.A., CHA R., KOKMEN E., O'BRIEN P.C. & PALUMBO P.J. (1997) The risk of dementia among persons with diabetes mellitus: a population-based cohort study. Annals of the New York Academy of Science **826**, 422-427.

LEISSRING M.A., AKBARI Y., FANGER C.M., CAHALAN M.D., MATTSON M.P. & LAFERLA F.M. (2000) Capacitative calcium entry deficits and elevated luminal calcium content in mutant presenilin-1 knockin mice. Journal of Cell Biology **149**, 793-797.

LEONARD A.S., LIM I.A., HEMSWORTH D.E., HORNE M.C. & HELL J.W. (1999) Calcium/calmodulin-dependent protein kinase II is associated with the N-methyl-D-aspartate receptor. Proceedings of the National Academy of Sciences USA **96**, 3236-3244.

LEOPOLD M., MULTHAUP G., GOLDSTEIN L.E., SCARPA R.C., SAUNDERS A.J., LIM J., MOIR R.D., GLABE C., BOWDEN E.F., MASTERS C.L., FAIRLIE D.P., TANZI R.E. & Bush A.L. (1999) Cu(II) potentiation of Alzheimer Aβ neurotoxicity. Correlation with cell-free hydrogen peroxide production and metal reduction. Journal of Biological Chemistry **274**, 37111-37116.

LEVEUGLE B., DING W., DURKIN J.T., MISTRETTA S., EISLE J., MATIC M., SIMAN R., GREENBERG B.D. & FILLIT H.M. (1997) Heparin promotes β-secretase cleavage of the Alzheimer's amyloid precursor protein. Neurochemistry International **30**, 543-548.

LEVITAN D., DOYLE T.G., BROUSSEAU D., LEE M.K. THINAKARAN G., SLUNT H.H., SISODIA S.S. & GREENWALD I. (1996) Assessment of normal and mutant human presenilin function in *Caenorhabditis elegans*. Proceedings of the National Academy of Sciences USA **93**. 14940-14944.

LEVKOVITZ Y. & SEGAL M. (1998) Age-dependent local modulation of hippocampal-evoked responses to perforant path stimulation. Neurobiology of Aging. **19**, 317-324.

Levy W.B. & Steward O. (1979) Synapses as associative memory elements in the hippocampal formation. Brain Research. **175**, 233-45.

LI Y.-M., XU M., LAI M.-T., HUANG Q., CASTRO J. L., DIMUZIO-MOWER J., HARRISON T.. LELLIS C., NADIN A., NEDUVELIL J.G., REGISTER R.B., SARDANA M.K., SHEARMAN M.S.. SMITH A.L., SHI X.-P., YIN K.-C., SHAFER J.A. & GARDELL S.J. (2000a) Photoactivated γ-secretase inhibitors directed to the active site covalently label presenilin 1. Nature **405**, 689-694.

LI Y., BARGER S.W., LIU L., MRAK R.E. & GRIFFIN W.S.T. (2000b) S100β induction of the proinflammatory cytokine interleukin-6 in neurons. Journal of Neurochemistry **74**, 143-150.

LI Y.-P., BUSHNELL A.F., LEE C.-M., PERLMUTTER L.S. & WONG S.K.-F. (1996) β-Amyloid induces apoptosis in human-derived neurotypic SH-SY5Y cells. Brain Research **738**, 196-204.

LIBERINI P., MEMO M. & SPANO P. (1995) Lewy body pathology and heterogeneity of Alzheimer's disease. Journal of the American Medical Association **274**, 1199.

LICASTRO F., PEDRINI S., CAPUTO L., ANNONI G., DAVIS L.J., FERRI C., CASADEI V. & GRIMALDI L.M.E. (2000) Increased plasma levels of interleukin-1, interleukin-6 and α1-antichymotrypsin in patients with Alzheimer's disease: Peripheral inflammation or signals from the brain? Journal of Neuroimmunology **103**, 97-102.

LIU J., FUKUNAGA K., YAMAMOTO H., NISHI K. & MIYAMOTO E. (1999) Differential roles of Ca^{2+}/calmodulin-dependent protein kinase II and mitogen-activated protein kinase activation in hippocampal long-term potentiation. Journal of Neuroscience **19**, 8292-8299.

LLANSOLA M., SÁEZ R. & FELIPO V. (2001) NMDA-induced phosphorylation of the microtubule-associated protein MAP-2 is mediated by activation of nitric oxide synthase and MAP kinase. European Journal of Neuroscience **13**, 1283-1291.

LODISH H. (2000) *Molecular Cell Biology* (4th ed). New York: W.H. Freeman.

LOEFFLER D.A., LEWITT P.A., JUNEAU P.L., SIMA A.A.F., NGUYEN H.-U., DEMAGGIO A.J., BRICKMAN C.M., BREWER G.J., DICK R.D., TROYER M.D. & KANALEY L. (1996) Increased regional brain concentrations of ceruloplasmin in neurodegenerative disorders. Brain Research **738**, 265-274.

LOMBARDI V.R.M., GARCIA M. & CACABELOS R. (1998) Microglial activation induced by factor(s) contained in sera from Alzheimer-related ApoE genotypes. Journal of Neuroscience Research **54**, 539-553.

LOO D.T., COPANI A., PIKE C.J., WHITTEMORE E.R., WALENCEWICZ A.J. & COTMAN C.W. (1993) Apoptosis is induced by β-amyloid in cultured central nervous system neurons. Proceedings of the National Academy of Sciences USA **90**, 7951-7955.

LOVELL M.A., ROBERTSON J.D., TEESDALE W.J., CAMPBELL J.L. & MARKESBERY W.R. (1998) Copper, iron and zinc in Alzheimer's disease senile plaques. Journal of the Neurological Sciences **158**, 47-52.

LU W.-Y., MAN H.-Y., JU W., TRIMBLE W.S., MACDONALD J.F. & WANG Y.T. (2001) Activation of synaptic NMDA receptors induces membrane insertion of new AMPA receptors and LTP in cultured hippocampal neurons. Neuron **29**, 243-254.

LU P.-J., WULF G., ZHOU X.Z., DAVIES P. & LU K.P. (1999a) The prolyl isomerase Pin1 restores the function of Alzheimer-associated phosphorylated tau protein. Nature **399**, 784-788.

LU Y.-F., KOJIMA N., TOMIZAWA K., MORIWAKI A., MATSUSHITA M., OBATA K. & MATSUI H. (1999b) Enhanced synaptic transmission and reduced threshold for LTP induction in *fyn*-transgenic mice. European Journal of Neuroscience **11**, 75-82.

LUC G., BARD J.-M., ARVEILER D., EVANS A., CAMBOU J.-P., BINGHAM A., AMOUYEL P., SCHAFFER P., RUIDAVETS J.-B., CAMBIEN F., FRUCHART J.-C. & DUCIMETIERE P. (1994) Impact of apolipoprotein E polymorphism on lipoproteins and risk of myocardial infarction: The ECTIM study. Arteriosclerosis & Thrombosis **14**, 1412-1419.

LUE L.F., KUO Y.-M., ROHER A.E., BRACHOVA L., SHEN Y., SUE L., BEACH T., KURTH J.H., RYDEL R.E. & ROGERS J. (1999) Soluble amyloid β peptide concentration as a predictor of synaptic change in Alzheimer's disease. American Journal of Pathology **155**, 853-862.

LUND-KATZ S., WEISGRABER K.H., MAHLEY R.W. & PHILLIPS M.C. (1993) Conformation of apolipoprotein E in lipoproteins. Journal of Biological Chemistry **268**, 23008-23015.

LUTERMAN J.D., HAROUTUNIAN V., YEMUL S., HO L., PUROHIT D., AISEN P.S., MOHS R. & PASINETTI G.M. (2000) Cytokine gene expression as a function of the clinical progression of Alzheimer disease dementia. Archives of Neurology **57**, 1153-1160.

LUTHI A., CHITTAJALLU R., DUPRAT F., PALMRE M.J., BANKS T.A., KIDD F.L., HENLEY .M., ISASC J.T.R. & COLLINGRIDGE G.L. (1999) Hippocampal LTP expression involves a pool of AMPARs regulated by the NSF-GluR2 interaction. Neuron **24**, 389-399.

LYNCH G.S., DUNWIDDIE T. & GRIBKOFF V. (1977) Heterosynaptic depression: a postsynaptic correlate of long-term potentiation. Nature **266**, 737-9.

MA H.-T., PATTERSON R.L., VAN ROSSUM D.B., BIRNBAUMER L., MIKOSHIBA K. & GILL D.L. (2000) Requirement of the inositol trisphosphate receptor for activation of store-operated Ca2+ channels. Science **287**, 1647-1651.

MA L., ZABLOW L., KANDEL E.R. & SIEGELBAUM S.A. (1999) Cyclic AMP induces functional presynaptic boutons in hippocampal CA3-CA1 neuronal cultures. Nature Neuroscience **2**, 24-30.

MADANI R., HULO S., TONI N., MADANI H., STEIMER T., MULLER D. & VASSALLI J.-D. (1999) Enhanced hippocampal long-term potentiation and learning by increased neuronal expression of tissue-type plasminogen activator in transgneic mice. EMBO Journal **18**, 3007-3012.

MAKHINSON M., CHOTINER J.K., WATSON J.B. & O'DELL T.J. (1999) Adenylyl cyclase activation modulates activity-dependent changes in synaptic strength and Ca^{2+}/calmodulin-dependent kinase II autophosphorylation. Journal of Neuroscience **19**, 2500-2510.

MALCHIODI-ALBEDI F., PETRUCCI T.C., PICCONI B., IOSI F. & FALCHI M. (1997) Protein phosphatase inhibitors induce modification of synapse structure and tau hyperphosphorylation in cultured rat hippocampal neurons. Journal of Neuroscience Research **48**, 425-438.

MALEN P.L. & CHAPMAN P.F. (1997) Nitric oxide facilitates long-term potentiation, but not long-term depression. Journal of Neuroscience **17**, 2645-2651.

MALINOW R. (1991) Transmission between pairs of hippocampal slice neurones: quantal levels. oscillations and LTP. Science **252**, 722-724.

MANABE T. & NICOLL R.A. (1994) Long-term potentiation: Evidence against an increase in transmitter release probablility in the CA1 region of the hippocampus. Science **265**, 1888-1892.

MANABE T., WYLLIE D.J.A., PERKEL D.J. & NICOLL R.A. (1993) Modulation of synaptic transmission and long-term potentiation: effects on paired pulse facilitation and EPSC variance in the CA1 region of the hippocampus. Journal of Neurophysiology **70**, 1451-1459.

MARAMBAUD P., ANCOLIO K., ALVES DA COSTA C. & CHECLER F. (1999) Effect of protein kinase A inhibitors on the production of $A\beta_{40}$ and $A\beta_{42}$ by human cells expressing normal and Alzheimer's disease-linked mutated AβPP and presenilin 1. British Journal of Pharmacology **126**. 1186-1190.

MARRION N.V. & TAVALIN S.J. (1998) Selective activation of Ca^{2+}-activated K^+ channels by co-localized Ca^{2+} channels in hippocampal neurons. Nature **395**, 900-905.

MARTY S., DUSART I. & PESCHANSKI M. (1991) Glial changes following an exitotoxic lesion in the CNS - I Microglia/Macrophages. Neuroscience **45**, 529-539.

MARUYAMA K., KAMETANI F., USAMI M., YAMAO-HARIGAYA W. & TANAKA K. (1991) "Secretase," Alzheimer amyloid protein precursor secreting enzyme is not sequence-specific. Biochemical & Biophysical Research Communications **179**, 1670-6.

MATTSON M.P., ZHU H., YU J. & KINDY M.S. (2000) Presenilin-1 mutation increases neuronal vulnerability to focal ischemia *in vivo* and to hypoxia and glucose deprivation in cell culture: Involvement of perturbed calcium homeostasis. Journal of Neuroscience **20**, 1358-1364.

MAYEUX R., TANG M.-X., JACOBS D.M., MANLY J., BELL K., MERCHANT C., SMALL S.A., STERN Y., WISNIEWSKI H.M.& MEHTA P.D. (1999) Plasma amyloid β-peptide 1-42 and incipient Alzheimer's disease. Annals of Neurology **46**, 412-416.

MCCLEAN C.A., CHERNY R.A., FRASER F.W., FULLER S.J., SMITH M.J., BEYREUTHER K., BUSH A.I. & MASTERS C.L. (1999) Soluble pool of Aβ amyloid as a determinant of severity of neurodegeneration in Alzheimer's disease. Annals of Neurology **46**, 860-866.

MCDONALD M.P. GLEASON T.C., ROBINSON J.K. & CRAWLEY J.N. (1998) Galanin inhibits performance on rodent memory tasks. Annals of the New York Academy of Science **863**, 305-322.

MCGOWAN E., SANDERS S., IWATSUBO T., TAKEUCHI A., SAIDO T., ZEHR C., YU X., ULJON S., WANG R., MANN D., DICKSON D. & DUFF K. (1999) Amyloid phenotype characterization of transgenic mice overexpressing both mutant amyloid precursor protein and mutant presenilin 1 transgenes. Neurobiology of Disease **6**, 231-244.

MCKHANN G., DRACHMAN D., FOLSTEIN M., KATZMAN R., PRICE D. & STADLAN E.M. (1984) Clinical diagnosis of Alzheimer's disease: report of the NINCDS-ADRDA work group under the auspices of department of health and human services task force on Alzheimer's disease. Neurology **34**, 939-944.

MCLAURIN J., FRANKLIN T., KUHNS W.J. & FRASER P.E. (1999) A sulfated proteoglycan aggregation factor mediates amyloid-β peptide fibril formation and neurotoxicity. Amyloid **6**, 233-243.

MCLEAN C.A., CHERNY R.A., FRASER F.W., FULLER S.J., SMITH M.J., BEYREUTHER K., BUSH A.I. & MASTERS C.L. (1999) Soluble pool of Aβ amyloid as a determinant of severity of neurodegeneration in Alzheimer's disease. Annals of Neurology **46**, 860-866.

MCNAUGHTON B.L., DOUGLAS R.M. & GODDARD G.V. (1978) Synaptic enhancement in fascia dentata: cooperativity among coactive afferents. Brain Research **157,** 277-293.

MCNAUGHTON B.L. (1982) Long-term synaptic enhancement and short-term potentiation in rat fascia dentata act through different mechanisms. Journal of Physiology **324**, 239-262.

MCSHANE R., GEDLING K., READING M., MCDONALD B., ESIRI M.M. & HOPE T. (1995) Prospective study of relations between cortical Lewy bodies, poor eyesight, and hallucinations in Alzhemier's disease. Journal of Neurology, Neurosurgery & Psychiatry **59**, 185-188.

MEDA L., CASSATELLA M.A., SZENDREI G.I., OTVOS J.R.L., BARON P., VILLALBA M., FERRARI D. & ROSSI F. (1995) Activation of microglial cells by β-amyloid protein and interferon-gamma. Nature **374**, 647-650.

MEHLHORN G., HOLLBORN M. & SCHLIEBS R. (2000) Induction of cytokines in glial cells surrounding cortical β-amyloid plaques in transgenic Tg2576 mice with Alzheimer pathology. International Journal of Developmental Neuroscience **18**, 423-431.

MEHTA P.D., PIRTTILA T., MEHTA S.P., SERSEN E.A., AISEN P.S. & WISNIEWSKI H.M. (2000) Plasma and cerebrospinal fluid levels of amyloid β proteins 1-40 and 1-42 in Alzheimer disease. Archives of Neurology **57**, 100-105.

MELLOR J. & NICOLL R.A. (2001) Hippocampal mossy fibre LTP is independent of postsynaptic calcium. Nature Neuroscience **4**, 125-126.

MERCHANT C. (1999) The influence of smoking on the risk of Alzheimer's disease. Neurology **52**. 1408-1412.

MIGAUD M., CHARLESWORTH P., DEMPSTER M., WEBSTER L.C., WATABE A.M., MAKHINSON M., HE Y., RAMSAY M.F., MORRIS R.G., MORRISON J.H., O'DELL T.J. & GRANT S.G. (1998) Enhanced long-term potentiation and impaired learning in mice with mutant postsynaptic density-95 protein. Nature **396**, 433-439.

MILLS J., CHAREST D.L., LAM F., BEYREUTHER K., IDA N., PELECH S.L., & REINER P.B. (1997) Regulation of amyloid precursor protein catabolism involves the mitogen-activated protein kinase signal transduction pathway. Journal of Neuroscience **17**, 9415-9422.

MOECHARS D., DEWACHTER I., LORENT K., REVERSE D., BAEKELANDT V., NAIDU A., TESSEUR I., SPITTAELS K., VAN DEN HAUTE C., CHECLER F., GODAUX E., CORDELL B. & VAN LEUVEN F. (1999) Early phenotypic changes in mice that overexpress different mutants of amyloid precursor protein in brain. Journal of Biological Chemistry **274**, 6483-6492.

MOLINA, J.A., JIMENEZ-JIMENEZ F.J., AGUILAR M.V., MESEGUER I., MATEOS-VEGA C.J., GONZALEZ-MUNOZ M.J., DE BUSTOS F., PORTA J., ORTI-PAREJA M., ZURDO M., BARRIOS E. & MARTINEZ-PARA M.C. (1998) Cerebrospinal fluid levels of transition metals in patients with Alzheimer's disease. Journal of Neural Transmission **105**, 479-488.

MORGAN D., DIAMOND D.M., GOTTSCHALL P.E., UGEN K.E., DICKEY C., HARDY J., DUFF K., JANTZEN P., DICARLO G., WILCOCK D., CONNER K., HATCHER J., HOPE C., GORDON M. & ARANDASH G.W. (2000) Aβ peptide vaccination prevents memory loss in an animal model of Alzheimer's disease. Nature **408**, 982-985.

MORGAN S.L. & TEYLER T.J. (1999) VDCCs and NMDARs underly two forms of LTP in CA1 hippocampus *in vivo*. Journal of Neurophysiology **82**, 736-740.

MORRIS M.C., BECKETT L.A., SCHERR P.A., HEBERT L.E., BENNETT D.A., FIELD T.S. & EVANS D.A. (1998) Vitamin E and vitamin C supplement use and risk of incident Alzheimer disease. Alzheimer Disease & Associated Disorders **12**, 121-126.

MORTIMER J.A., VAN DUIJN C.M., CHANDRA V., FRATIGLIONI L., GRAVES A.B., HEYMAN A., JORM A.F., KOKMEN E., KONDO K., ROCCA W.A., SHALAT S.L., SOININEN & H. HOFMAN A. (1991) Head trauma as a risk factor for Alzheimer's disease: a collaborative re-analysis of case-control studies. International Journal of Epidemiology **20**, S28-S35.

MOSER E.I., KROBERT K.A., MOSER M.-B. & MORRIS R.G.M. (1998) Impaired spatial learning after saturation of long-term potentiation. Science **281**, 2038-2042.

MUCKE L., MASLIAH E., YU G.-Q., MALLORY M., ROCKENSTEIN E.M., TATSUNO G., HU K., KHOLODENKO D., JOHNSON-WOOD K. & MCCONLOGUE L. (2000) High-level neuronal expression of $A\beta_{1-42}$ in wild-type human amyloid protein precursor transgenic mice: synaptotoxicity without plaque formation. Journal of Neuroscience **20**, 4050-4058.

MUCKE L., MASLIAH E., JOHNSON W.B., RUPPE M.D., ALFORD M., ROCKENSTEIN E.M., FORSS-PETTER S., PIETROPAOLO M., MALLORY M. & ABRAHAM C.R. (1994) Synaptotrophic effects of human amyloid β protein precursors in the cortex of transgenic mice. Brain Research **666**, 151-167.

MULKEY R.M., ENDO S., SHENOLIKAR S. & MALENKA R.C. (1994) Involvement of a calineurin/inhibitor-1 phophatase cascade in hippocampal long-term depression. Nature **369**, 486-487.

MULKEY R.M., HERRON C.E. & MALENKA R.C. (1993) An essential role for protein phosphatases in hippocampal long-term depression. Science **261**, 1051-1055.

MULKEY R.M. & MALENKA R.C. (1992) Mechanisms underlying induction of homosynaptic long-term depression in area CA1 of the hippocampus. Neuron **9**, 967–975.

MULTHAUP G., RUPPERT T., SCHILICKSUPP A., HESSE L., BILL E., PIPKORN R., MASTERS C. & BEYREUTHER K. (1998) Copper-binding amyloid precursor protein undergoes a site-specific fragmentation in the reduction of hydrogen peroxide. Biochemistry **37**, 7224-7230.

MULTHAUP G., SCHLICKSUPP A., HESSE L., BEHER D., RUPPERT T., MASTERS C.L. & BEYREUTHER K. (1996) The amyloid precursor protein of Alzheimer's disease in the reduction of copper(II) to copper(I). Science **271**, 1406-1409.

MUNOZ D.G. (1998) Is exposure to aluminum a risk factor for the development of Alzheimer disease? - No. Archives of Neurology **55**, 737-739.

MURAYAMA M., TANAKA S., PALACINO J., MURAYAMA O., HONDA T., SUN X., YASUTAKE K., NIHONMATSU N., WOLOZIN B. & TAKASHIMA A. (1998) Direct association of presenilin-1 with β-catenin. FEBS Letters **433**, 73-77.

MURPHY G.M., ZHAO F., YANG L & CORDELL B. (2000) Expression of macrophage colony-stimulating factor receptor is increased in the $A\beta PP_{V717F}$ transgenic mouse model of Alzheimer's disease. American Journal of Pathology **157**, 895-904.

MURPHEY M.P., ULJON S.N., FRASER P.E., FAUQ A., LOOKINGBILL H.A., FINDLAY K.A., SMITH T.E., LEWIS P.A., MCLENDON D.C., WANG R. & GOLDE T.E. (2000) Presenilin 1 regulates pharmacologically distinct g-secretase activities. Journal of Biological Chemistry **275**, 26277-26284.

MURRELL J.R., HAKE A.M., QUAID K.A., FARLOW M.R. & GHETTI B. (2000) Early-onset Alzheimer disease caused by a new mutation (V717L) in the amyloid precursor protein gene. Archives of Neurology **57**, 885-887.

NAKAZAWA T., KOMAI S., TEZUKA T.O., HISATSUNI C., UMEMORI H., SEMBA K., MISHINA M., MANABE T. & YAMOMOTO T. (2001) Characterization of *fyn*-mediated tyrosine phosphorylation sites on GluRε2 (NR2B) subunit of the N-methyl-D-aspartate receptor. Journal of Biological Chemistry **276**, 693-699.

NAMBA Y., TOMONAGA M., KAWASAKI H., OTOMO E. & IKEDA K. (1991) Apolipoprotein E immunoreactivity in cerebral amyloid deposits and neurofibrillary tangles in Alzheimer's disease and kuru plaque amyloid in Creutzfeldt-Jakob disease. Brain Research **541**, 163-166.

NATHAN B.P., BELLOSTA S., SANAN D.A., WEISGRABER K.H., MAHLEY R.W. & PITAS R.E. (1994) Differential effects of apolipoproteins E3 and E4 on neuronal growth in vitro. Science. **264,** 850-2.

NATHAN T., JENSEN M.S. & LAMBERT J.D.C. (1990) $GABA_B$ receptors play a major role in paired-pulse facilitation in area CA1 of the rat hippocampus. Brain Research **531**, 55-65.

NELSON P.T., STEFANSSON K., GULCHER J. & SAPER C.B. (1996) Molecular evolution of tau protein: implications for Alzheimer's disease. Journal of Neurochemistry **67**, 1622-1632.

NGEZAHAYO A., SCHACHNER M. & ARTOLA A. (2000) Synaptic activity modulates the induction of bidirectional synaptic changes in adult mouse hippocampus. Journal of Neuroscience **20**. 2451-2458.

NIMPF J. & SCHNEIDER W.J. (2000) From cholesterol transport to signal transduction: low density lipoprotein receptor, very low density lipoprotein receptor, and apolipoprotein E receptor-2. Biochimica et Biophysica Acta **1529**, 287-98.

NOEL J., COLLINGRIDGE G.L. & HENLEY J.M. (1999) Surface expression of AMPA receptros in hippocampal neurones is regulated by an NSF-dependent mechanism. Neuron **23**, 365-376.

NOGUCHI S., MURAKAMI K., YAMADA N., PAYAMI H., KAYE J., HESTON L.L., BIRD T.D. & SCHELLENBERG G.D. (1993) Apolipoprotein E genotype and Alzheimer's disease. Lancet **342**. 737-738.

O'BARR S. & COOPER N.R. (2000) The C5a complement activation peptide increases IL-1β and IL-6 release from amyloid-β primed human monocytes: implications for Alzheimer's disease. Journal of Neuroimmunology **109,** 87-94.

OHYAGI Y., YAMADA T., NISHIOKA K., CLARKE N.J., TOMLINSON A.J., NAYLOR S., NAKABEPPU Y., KIRA J.-I. & YOUNKIN S.G. (2000) Selective increase in cellular $A\beta_{42}$ is related to apoptosis but not necrosis. Neuroreport **11**, 167-171.

OKA M., KATAYAMA S., WATANABE C., NODA K., MAO J.J. & NAKAMURA S. (1998) Argyrophilic stimulate glial reactions in neurofibrillary tangles and senile plaques. Neurological Research **20**, 121-126.

OLSON M.I. & SHAW C.-M. (1969) Presenile dementia and Alzheimer's disease in mongolism. Brain **92**, 147-156.

OTMAKHOVA N.A., OTMAKHOV N., MORTENSON L.H. & LISMAN J.E. (2000) Inhibition of the cAMP pathway decreases early long-term potentiation at CA1 hippocampal synapses. Journal of Neuroscience **20**, 4446-4451.

OTT A., STOLK R.P., HOFMAN A., VAN HARSKAMP F., GROBBEE D.E. & BRETELER M.M.B. (1996) Association of diabetes mellitus and dementia: the Rotterdam Study. Diabetologia **39**. 1392-1397.

OUYANG Y., ROSENSTEIN A., KREIMAN G., SCHUMAN E.M. & KENNEDY M.B. (1999) Tetanic stimulation leads to increased accumulation of Ca^{2+}/calmodulin-dependent protein kinase II via dendritic protein synthesis in hippocampal neurones. Journal of Neuroscience **19**, 7823-7833.

OVERMYER M., KRASZPULSKI M., HELISALMI S., SOININEN H. & ALAFUZOFF I. (2000) DNA fragmentation, gliosis and histological hallmards of Alzheimer's disease. Acta Neuropathologica **100**, 681-687.

OYAMA F., SAWAMURA N., KOBAYASHI K., MORISHIMA-KAWASHIMA M., KURAMOCHI T., ITO M., TOMITA T., MARUYAMA K., SAIDO T.C., IWATSUBO T., CAPELL A., WALTER J., GRUNBERG J., UEYAMA Y., HAASS C. & IHARA Y. (1998) Mutant presenilin 2 transgenic mouse: effect on an age-dependent increase of amyloid β-protein 42 in the brain. Journal of Neurobiology **71**, 313-322.

PANEGYRES P.K. (1997) The amyloid precursor protein gene: a neuropeptide gene with diverse functions in the central nervous system. Neuropeptides **31**, 523-535.

PAOLA D., DOMENICOTTI C., NITTI M., VITALI A., BORGHI R., COTTALASSO D., ZACCHEO D., ODETTI P., STROCCHI P., MARINARI U.M., TABATON M. & PRONZATO M.A. (2000) Oxidative stress induces increase in intracellular amyloid β-protein production and selective activation of βI and βII PKCs in NT2 cells. Biochemical & Biophysical Research Communications **268**, 642-646.

PAPAIOANNOU V.E., MCBURNEY M.W. & GARDNER R.L. (1975) Fate of teratocarcinoma cells injected into early mouse embryos. Nature **258**, 70-73.

PAPASSOTIROPOULOS A., BAGLI M., JESSEN F., BAYER T.A., MAIER W., RAO M.L. & HEUN R. (1999) A genetic variation of the inflammatory cytokine interleukin-6 delays the initial onset and reduces the risk for sporadic Alzheimer's disease. Annals of Neurology **45**, 666-668.

PAPATHEODOROPOULOS C. & KOSTOPOULOS G. (1998) Development of a transient increase in recurrent inhibition and paired-pulse facilitation in hippocampal CA1 region. Developmental Brain Research **108**, 273-285.

PARENT A., LINDEN D.J., SISODIA S.S. & BORCHELT D.R. (1999) Synaptic transmission and hippocampal long-term potentiation in transgenic mice expressing FAD-linked presenilin 1. Neurobiology of Disease **6**, 56-62.

PARPURA-GILL A., BEITZ D. & UEMURA E. (1997) The inhibitory effects of β-amyloid on glutamate and glucose uptakes by cultured astrocytes. Brain Research **754**, 65-71.

PEDERSEN W.A., CLUMSEE C., ZIEGLER C., HERMAN J.P. & MATTSON M.P. (1999) Aberrant stress response associated with severe hypoglycemia in a transgenic mouse model of Alzheimer's disease. Journal of Molecular Neuroscience **13**, 159-165.

PETERSEN C.C.H., MALENKA R.C., NICOLL R.A. & HOPFIELD J.J. (1998) All-or-none potentiation at CA3-CA1 synapses. Proceedings of the National Academy of Sciences USA **95**, 4732-4737.

PHINNEY A.L., DELLER T., STALDER M., CALHOUN M.E., FROTCHER M., SOMMER B., STAUFENBIEL M. & JUCKER M. (1999) Cerebral amyloid induces aberrant axonal sprouting and ectopic terminal formation in amyloid precursor protein transgenic mice. Journal of Neuroscience **19**. 8552-8559.

PIKE C.J., BURDICK D., WALENCEWICZ A.J., GLABE C.G., & COTMAN C.W. (1993) Neurodegeneration induced by β-amyloid peptides *in vitro*: the role of peptide assembly state. Journal of Neuroscience **13**, 1676-1687.

PODLISNY M.B., TOLAN D.R. & SELKOE D.J. (1991) Homology of the amyloid beta protein precursor in monkey and human supports a primate model for beta amyloidosis in Alzheimer's disease. American Journal of Pathology **138**, 1423-1435.

PRICE D.L., ALTSCHULER R.J., STRUBLE R.G., CASANOVA M.F., CORK L.C. & MURPHY D.B. (1986) Sequestration of tubulin in neurons in Alzheimer's disease. Brain Research **385**, 305-10.

PRO J.D., SMITH C.H. & SUMI S.M. (1980) Presenile Alzheimer disease: amyloid plaques in the cerebellum. Neurology **30**, 820-825.

PUKA-SUNDVALL M., GAJKOWSKA B., CHOLEWINSKI M., BLOMGREN K., LAZAREWICZ J.W. & HAGBERG H. (2000) Subcellular distribution of calcium and ultrastructural changes after cerebral hypoxia-ischemia in immature rats. Brain Research. Developmental Brain Research **125**, 31-41.

PUTNEY J.W. (1986) A model for receptor-regulated calcium entry. Cell Calcium 7, 1-12.

QIAN S., JIANG P., GUAN X.-M., SINGH G., TRUMBAUER M.E., YU H., CHEN H.Y., VAN DER PLOEG L.H.T. & ZHENG H. (1998) Mutant human presenilin 1 protects presenilin 1 null mouse against embryonic lethality and elevates $A\beta_{1-42/43}$ expression. Neuron **20**, 611-617.

QIU W.Q., BORTH W., YE Z., HAASS C., TEPLOW D.B. & SELKOE D.J. (1996) Degradation of amyloid β-protein by a serine protease-α-macroglobulin complex. Journal of Biological Chemistry **271**, 8443-8451.

QUERFURTH H.W. & SELKOE D.J. (1994) Calcium ionophore increases amyloid β peptide production by cultured cells. Biochemistry **33**, 4550-4561.

RABY C.A., MORGANTI-KOSSMANN M.C., KOSSMANN T., STAHEL P.F., WATSON M.D., EVANS L.M., MEHTA P.D., SPIEGEL K., KUO Y.-M., ROHER A.E. & EMMERLING M.R. (1998) Traumatic brain injury increases β-amyloid peptide 1-42 in cerebrospinal fluid. Journal of Neurochemistry **71**, 2505 - 2509.

RALL W (1969) Time constants and electrotonic length of membrane cylinders and neurones. Biophysical Journal **9**, 1483-1508.

RAUSCHE G., SARVEY J.M. & HEINEMANN U. (1989) Slow synaptic inhibition in relation to frequency habituation in dentate granule cells of rat hippocampal slices. Experimental Brain Research **78**, 233-242.

RAYMOND C.R., THOMPSON V.L., TATE W.P. & ABRAHAM W.C. (2000) Metabotropic glutamate receptors trigger homosynaptic protein synthesis to prolong long-term potentiation. Journal of Neuroscience **20**, 969-976.

REGEHR W.G., DELANEY K.R. & TANK D.W. (1994) The role of presynaptic calcium in short-term enhancement at the hippocampal mossy fibre synapse. Journal of Neuroscience **14**, 523-537.

RICHARDSON J.S., ZHOU Y. & KUMAR U. (1996) Free radicals in the neurotoxic action of β-amyloid. Annals of the New York Academy of Science **777**, 362-367.

RICHTER C., PARK J.W. & AMES B.N. (1988) Normal oxidative damage to mitochondrial and nuclear DNA is extensive. Proceedings of the National Academy of Sciences of the United States of America **85**, 6465-7.

RIGGS K.M., SPIRO III A., TUCKER K. & RUSH D. (1996) Relations of vitamin B-12, vitamin B-6, folate, and homocysteine to cognitive performance in the Normative Aging Study. American Journal of Clinical Nutrition **63**, 306-314.

ROCCA W.A., VAN DUIJN C.M., CLAYTON D., CHANDRA V., FRATIGLIONI L., GRAVES A.B., HEYMAN A., JORM A.F., KOKMEN E., KONDO K., MORTIMER J.A., SHALAT S.L.. SOININEN H. & HOFMAN A. (1991) Maternal age and Alzheimer's disease: A collaborative re-analysis of case-control studies. International Journal of Epidemiology **20**, S21-S27.

ROPERCH J.-P., ALVARO V., PRIEUR S., TUYNDER M., NEMANI M., LETHROSNE F.. PIOUFFRE L., GENDRON M.-C., ISRAELI D., DAUSSET J., OREN M., AMSON R. & TELERMAN A. (1998) Inhibition of presenilin I expression is promoted by p53 and p21(WAF-1) and results in apoptosis and tumor suppression. Nature Medicine **4**, 835-838.

ROSENBERG R.N. (1997) Molecular neurogenetics: The genome is settling the issue. Journal of the American Medical Association **278**, 1282-1283.

ROSSNER S., UEBERHAM U., SCHLIEBS R., PEREZ-POLO J.R. & BIGL V. (1998) The regulation of amyloid precursor protein metabolism by cholinergic mechanisms and neurotrophin receptor signaling. Progress in Neurobiology **56**, 541-569.

ROUTTENBERG A., CANTALLOPS I., ZAFFUTO S., SERRANO P. & NAMGUNG U. (2000) Enhanced learning after genetic overexpression of a brain growth protein. Proceedings of the National Academy of Sciences USA **97**, 7657-7662.

ROZEMULLER A.J., EIKELENBOOM P., THEEUWES J.W., JANSEN STEUR E.N. & DE VOS R.A. (2000) Activated microglial cells and complement factors are unrelated to cortical Lewy bodies. Acta Neuropathologica **100**, 701-708.

RÜLICKE T. & HÜBSCHER U. (2000) Germ line transformation of mammals by pronuclear microinjection. Experimental Physiology **85**, 589-601.

RULON L.L., ROBERTSON J.D., LOVELL M.A., DEIBEL M.A., EHMANN W.D. & MARKESBERY W.R. (2000) Serum zinc levels and Alzheimer's disease. Biological Trace Element Research **75**, 79-85.

SASTRY B.R. & BHAGAVATULA L.S. (1996) Quantal release of transmitter at a central synapse. Neuroscience **75**, 987-992.

SAURWEIN-TEISSL M. (2000) Inflammatory cytokines are believed to exhaserbated pathology and time course of age-related disorders (eg. AD). Cytokine **12**, 1160-1161.

SAYRE L.M., PERRY G., HARRIS P.L.R., LIU Y., SCHUBERT K.A. & SMITH M.A. (2000) In situ oxidative catalysis by neurofibrillary tangles and senile plaques in Alzheimer's disease: A central role for bound transition metals. Journal of Neurochemistry **74**, 270-279.

SCHELLENBERG G.D., BIRD T.D., WIJSMAN E.M., ORR H.T., ANDERSON L., NEMENS E., WHITE J.A., BONNYCASTLE L., WEBER J.L., ALONSO M.E., POTTER H., HESTON L.L. & MARTIN G.M. (1992) Genetic linkage evidence for a familial Alzheimer's disease locus on chromosome 14. Science **258**, 668-671.

SCHENK D., BARBOUR R., DUNN W., GORDON G., GRAJEDA H., GUIDO T., HU K., HUANG J., JOHNSON-WOOD K., KHAN K., KHOLODENKO K., LEE M., LIAO Z., LIEBERBURG I., MOTTER R., MUTTER L., SORIANO F., SHOPP G., VASQUEZ N., VANDEVERT C., WALKER S., WOGULIS M., YEDNOCK T., GAMES D. & SEUBERT P. (1999) Immunization with amyloid-β attenuates Alzheimer-disease-like pathology in the PDAPP mouse. Nature **400**, 173-177.

SCHEUNER D., ECKMAN C., JENSEN M., SONG X., CITRON M., SUZUKI N., BIRD T.D., HARDY J., HUTTON M., KUKULI W., LARSON E., LEVY-LAHAD E., VIITEN M., PESKIND E., POORKAJ P., SCHILLENBERG G., TANZI R., WASCO W. & YOUNKIN S. (1996) Secreted amyloid β-protein similar to that in the senile plaques of Alzheimer's disease is increased *in vivo* by the presenilin 1 and 2 and APP mutations linked to familial Alzheimer's disease. Nature Medicine **2**. 864-870.

SCHULZ P.E. (1997a) Long-term potentiation involves increases in the probablility of neurotransmitter release. Proceedings of the National Academy of Sciences USA **94**, 5888-5893.

SCHULZ P.E. & FITZGIBBONS J.C. (1997b) Differing mechanisms of expression for short- and long-term potentiation. Journal of Neurophysiology **78**, 321-334.

SCOTT B.L., WELCH K., DESERRANO V., MOSS N.C., ROSES A.D. & STRITTMATTER W.J. (1998) Human apolipoprotein E accelerates microtubule polymerization in vitro. Neuroscience Letters **245**, 105-8.

SELKOE D.J., PODLISNY M.B., JOACHIM C.L., VICKERS E.A., LEE G., FRITZ L.C. & OLTERSDORF T. (1988) Beta-amyloid precursor protein of Alzheimer disease occurs as 110- to 135-kilodalton membrane-associated proteins in neural and nonneural tissues. Proceedings of the National Academy of Sciences of the United States of America **85**, 7341-5.

SENNVIK K., BENEDIKZ E., FASTBOM J., SUNDSTROM E., WINBLAD B. & ANKARCRONA M. (2001) Calcium ionophore A23187 specifically decreases the secretion of β-secretase cleaved amyloid precursor protein during apoptosis in primary rat cortical cultures. Journal of Neuroscience Research **63**, 429-437.

SENNVIK K., FASTBOM J., BLOMBERG M., WAHLUND L.O., WINBLAD B. & BENEDIKZ E. (2000) Levels of α- and β-secretase cleaved amyloid precursor protein in the cerebrospinal fluid of Alzheimer's disease patients. Neuroscience Letters **278**, 169-172.

SHENG J.G., MRAK R.E., BALES K.R., CORDELL B., PAUL S.M., JONES R.A., WOODWARD S., ZHOU X.Q., MCGINNESS J.M. & GRIFFIN W.S.T. (2000) Overexpression of the neuritotrophic cytokine S100β precedes the appearance of neuritic β-amyloid plaques in APP_{V717F} mice. Journal of Neurochemistry **74**, 295-301.

SHEPHERD C.E., THIEL E., MCCANN H., HARDING A.J., & HALLIDAY G.M. (2000) Cortical inflammation in Alzheimer disease but not dementia with Lewy bodies. Archives of Neurology **57**. 817-822.

SHERRATT H.S. (1991) Mitochondria: structure and function. Revue Neurologique. **147**, 417-30.

SHERRINGTON R., FROELICH S., SORBI S., CAMPION D., CHI H., ROGAEVA E.A., LEVESQUE G., ROGAEV E.I., LIN C., LIANG Y., IKEDA M., MAR L., BRICE A., AGID Y., PERCY M.E., CLERGET-DARPOUX F., PIACENTINI S., MARCON G. & ST GEORGE-HYSLOP P.H. (1996) Alzheimer's disease associated with mutations in presenilin 2 is rare and variably penetrant. Human Molecular Genetics **5**, 985-988.

SHERRINGTON R., ROGAEV E.I., LIANG Y., ROGAEVA E.A., LEVESQUE G., IKEDA M., CHI H., LIN C., HOLMAN K., TSUDA T., MAR L., FONCIN J.-F., BRUNI A.C., MONTESI M.P., SORBI S., RAINERO I., PINESSI L., NEE L., CHUMAKOV I. & ST GEORGE-HYSLOP P.H. (1995) Cloning of a gene bearing missense mutations in early-onset familial Alzheimer's disease. Nature **375**, 754-760.

SHI S.-H., HAYASHI Y., PETRALIA R.S., ZAMAN S.H., WENTHOLD R.J., SVOBODA K. & MALINOW R. (1999) Rapid spine delivery and redistribution of AMPA receptors after synaptic NMDA receptor activation. Science **284**, 1811-1816.

SHIMOKAWA M., YANAGISAWA K., NISHIYE H. & MIYATAKE T. (1993) Identification of amyloid precursor protein in synaptic plasma membrane. Biochemical & Biophysical Research Communications. **196**, 240-4.

SHIN R.-W., BRAMBLETT G.T., LEE V.M. & TROJANOWSKI J.Q. (1993) Alzheimer disease A68 proteins injected into rat brain induce codeposit of β-amyloid, ubiquitin, and α1-antichymotrypsin. Proceedings of the National Academy of Sciences USA **90**, 6825-6828.

SHOFFNER J.M. & WALLACE D.C. (1994) Oxidative phosphorylation disease and mitochondrial DNA mutations: diagnosis and treatment. Annual Review of Nutrition **14**, 535-568.

SHOJI M., GOLDE T.E., GHISO J., CHEUNG T.T., ESTUS S., SHAFFER L.M., CAI X.D., MCKAY D.M., TINTNER R. & FRANGIONE B. (1992) Production of the Alzheimer amyloid beta protein by normal proteolytic processing. Science **258**, 126-9.

SILVA A.J., STEVENS C.F., TONEGAWA S. & WANG Y. (1992) Deficient hippocampal long-term potentiation in α-calcium-calmodulin kinase II mutant mice. Science **257**, 201-206.

SIMONS M., KELLER P., DE STROOPER B., BEYREUTHER K., DOTTI, C.G. & SIMONS K. (1998) Cholesterol depletion inhibits the generation of β-amyloid in hippocampal neurons Proceedings of the National Academy of Sciences USA **95**, 6460-6464.

SINGHRAO S.K., NEAL J.W., RUSHMERE N.K., MORGAN B.P. & GASQUE P. (1999) Differential expression of individual complement regulators in the brain and choroid plexus Laboratory Investigation **79**, 1247-1259.

SINHA S. & LIEBERBURG I. (1999) Cellular mechanisms of β-amyloid production and secretion Proceedings of the National Academy of Sciences USA **96**, 11049-11053.

SKOOG I., NILSSON L., PALMERTZ B., ANDREASSON L.-A. & SVANBORG A. (1993) A population-based study of dementia in 85-year-olds. New England Journal of Medicine **328**, 153-158.

SKOVRONSKY D.M., ZHANG B., KUNG M.-P., KUNG H.F., TROJANOWSKI J.Q. & LEE V.M.-Y. (2000a) *In vivo* detection of amyloid plaques in a mouse model of Alzheimer's disease Proceedings of the National Academy of Sciences USA **97**, 7609-7614.

SKOVRONSKY D.M., PIJAK D.S., DOMS R.W. & LEE V.M.-Y. (2000b) A distinct ER/IC γ-secretase competes with the proteosome for cleavage of APP. Biochemistry **39**, 810-817.

SMART T.G. (1992) A novel modulatory binding site for zinc on the $GABA_A$ receptor complex in cultured rat neurons. Journal of Physiology **447**, 587-625.

SNAEDAL J., KRISTINSSON J., GUNNARSDOTTIR S., OLAFSDOTTIR A., BALDVINSSON M. & JOHANNESSON T. (1998) Copper, ceruloplasmin and superoxide dismutase in patients with Alzheimer's disease. A case-control study. Dementia & Geriatric Cognitive Disorders **9**, 239-242.

SNIPES G.J., MCGUIRE C.B., NORDEN J.J. & FREEMAN J.A. (1986) Nerve injury stimulates the secretion of apolipoprotein E by nonneuronal cells. Proceedings of the National Academy of Sciences of the United States of America **83**, 1130-4.

SNYDER S.W., LADROR U.S., WADE W.S., WANG G.T., BARRETT L.W., MATAYOSHI E.D., HUFFAKER H.J., KRAFFT G.A., & HOLZMAN T.F. (1994) Amyloid-β aggregation: selective inhibition of aggregation in mixtures of amyloid with different chain lengths. Biophysical Journal **67**, 1216-1228.

SON H. & CARPENTER D.O. (1996) Interactions among paired-pulse facilitation and post-tetanic and long-term potentiation in the mossy fibre-CA3 pathway in rat hippocampus. Synapse **23**, 302-331.

SORRA K.E. & HARRIS K.M. (1998) Stability in synapse number and size at 2hrs after long-term potentiation in hippocampal area CA1. Journal of Neuroscience **18**, 658-671.

SORRA K.E. & HARRIS K.M. (1993) Occurrence and three-dimensional structure of multiple synapses between individual radiatum axons and their target pyramidal cells in hippocampal area CA1. Journal of Neuroscience **13**, 3736–3748.

ST GEORGE-HYSLOP P.H., TANZI R.E., POLINSKY R.J., HAINES J.L., NEE L., WATKINS P.C., MYERS R.H., FELDMAN R.G., POLLEN D., DRACHMAN D., GROWDON J., BRUNI A., FONCIN J.-F., SALMON D., FROMMELT P., AMADUCCI L., SORBI S., PIACENTINI S., STEWART G.D., HOBBS W.J., CONNEALLY P.M. & GUSELLA J.F. (1987) The genetic defect causing familial Alzheimer's disease maps on chromosome 21. Science **235**, 885-890.

STADELMANN C., DECKWERTH T.L., SRINIVASAN A., BANCHER C., BRUCK W., JELLINGER K. & LASSMANN H. (1999) Activation of caspase-3 in single neurons and autophagic granules of granulovacuolar degeneration in Alzheimer's disease. Evidence for apoptotic cell death. American Journal of Pathology **155**, 1459-1466.

STALDER M., PHINNEY A., PROBST A., SOMMER B., STAUFENBIEL M. & JUCKER M. (1999) Association of microglia with amyloid plaques in brains of APP23 transgenic mice. American Journal of Pathology **154**, 1673-1684.

STAUBLI U., SCAFIDI J. & CHUN D. (1999) $GABA_B$ receptor antagonism: facilitatory effects on memory parallel those on LTP induced by TBS but not HFS. Journal of Neuroscience **19**, 4609-4615.

STEEL P.M. & MAUK M.D. (1999) Inhibitory control of LTP and LTD: stability of synapse strength. Journal of Neurophysiology **81**, 1559-1566.

STEFFENSEN S.C. & HENRIKSEN S.J. (1991) Effects of baclofen and bicuculline on inhibition in the fascia dentata and hippocampus regio superior. Brain Research **538**, 46-53.

STEPHENSON D.T. & CLEMENS J.A. (1998) Metabotropic glutamate receptor activation *in vivo* induces intraneuronal amyloid immunoreactivity in guinea pig hippocampus. Neurochemistry International **33**, 83-93.

STIEF A., WINTER D.M., STRATLING W.H. & SIPPEL A.E. (1989) A nuclear DNA attachment element mediates elevated and position-independent gene activity. Nature **341**, 343-345.

STOLTZNER S.E., GRENFELL T.J., MORI C., WISNIEWSKI K.E., WISNIEWSKI T.M., SELKOE D.J. & LEMERE C.A. (2000) Temporal Accrual of Complement Proteins in Amyloid Plaques in Down's Syndrome with Alzheimer's Disease. American Journal of Pathology **156**, 489-499.

STRACK S. & COLBRAN R.J. (1998) Autophosphorylation-dependent targeting of calcium-calmodulin-dependent protein kinase II by the NR2B subunit of the N-methyl-D-aspartate receptor. Journal of Biological Chemistry **273**, 20689-20692.

STRICKER C., COWAN A.I., FIELD A.C. & REDMAN S.J. (1999) Analysis of NMDA-independent long-term potentiation induced at CA3-CA1 synapses in rat hippocampus. Journal of Physiology **520**, 513-525.

STRICKER C., FIELD A.C. & REDMAN S.J. (1996) Changes in quantal parameters of EPSCs in rat CA1 neurones *in vitro* after the induction of long-term potentiation. Journal of Physiology **490**, 443-454.

STRITTMATTER W.J., SAUNDERS A.M., SCHMECHEL D., PERICAK-VANCE M., ENGHILD J., SALVESEN G.S., & ROSES A.D. (1993) Apolipoprotein E: high-avidity binding to β-amyloid and increased frequency of type 4 allele in late-onset familial Alzheimer disease. Proceedings of the National Academy of Sciences **90**, 1977-1981.

STURCHLER-PIERRAT C. & STAUFENBIEL M. (2000) Pathogenic mechanisms of Alzheimer's disease analyzed in the APP23 transgenic mouse model. Annals of the New York Academy of Science **290**, 134-139.

STURCHLER-PIERRAT C., ABRAMOWSKI D., DUKE M., WIEDERHOLD K.-H., MISTL C., ROTHACHER S., LEDERMANN B., BURKI K., GREY P., PAGANETTI P.A., WARIDEL C., CALHOUN M.E., JUCKER M., PROBST A., STAUFENBIEL M. & SOMMER B. (1997) Two amyloid precursor protein transgenic mouse models with Alzheimer disease-like pathology. Proceedings of the National Academy of Sciences USA **94**, 13287-13292.

SUH S.W., JENSEN K.B., JENSEN M.S., SILVA D.S., KESSLAK P.J., DANSCHER G. & FREDERICKSON C.J. (2000) Histochemically-reactive zinc in amyloid plaques, angiopathy, and degenerating neurons of Alzheimer's diseased brains. Brain Research **852**, 274-278.

SUTTON E.T., HELLERMANN G.R. & THOMAS T. (1997) β-Amyloid-induced endothelial necrosis and inhibition of nitric oxide production. Experimental Cell Research **230**, 368-376.

SUZUKI A. (1997) Amyloid β-protein induces necrotic cell death mediated by ICE cascade in PC12 cells. Experimental Cell Research **234**, 507-511.

SWEARER J.M., O'DONNELL B.F., INGRAM S.M. & DRACHMAN DA. (1996) Rate of progression in familial Alzheimer's disease. Journal of Geriatric Psychiatry & Neurology **9**, 22-25.

SWEATT J.D. (2001) The neuronal MAP kinase cascade: a biochemical signal integration system subserving synaptic plasticity and memory. Journal of Neurochemistry **76**, 1-10.

SWEENEY W.A., LUEDTKE J., MCDONALD M.P. & OVERMIER J.B. (1997) Intrahippocampal injections of exogenous β-amyloid induce postdelay errors in an eight-arm radial maze. Neurobiology of Learning and Memory **68**, 97-101.

SZCZEPANIK A.M., FUNES S., PETKO W. & RINGHEIM G.E. (2001) IL-4, IL-10 and IL-13 modulate $A\beta_{1-42}$-induced cytokine and chemokine production in primary murine microglia and a human monocyte cell line. Journal of Neuroimmunology **113**, 49-62.

TAKASHIMA A., NOGUCHI K., SATO K., HOSHINO T. & IMAHORI K. (1993) Tau protein kinase 1 is essential for amyloid β-protein induced neurotoxicity. Proceedings of the National Academy of Sciences USA **90**, 7789-7793.

TAKEUCHI A., IRIZARRY M.C., DUFF K., SAIDO T.C., HSIAO ASHE K., HASEGAWA M., MANN D.M.A., HYMAN B.T. & IWATSUBO T. (2000) Age-related amyloid β deposition in transgenic mice overexpressing both Alzheimer mutant presenilin 1 and amyloid β precursor protein Swedish mutant is not associated with global neuronal loss. American Journal of Pathology **157**, 331-339.

TANAKA S., NAKAMURA S., UEDA K., KAMEYAMA M., SHIOJIRI S., TAKAHASHI Y., KITAGUCHI N. & ITO H. (1988) Three types of amyloid protein precursor mRNA in human brain: their differential expression in Alzheimer's disease. Biochemical & Biophysical Research Communications. **157**, 472-9.

TANG Y.-G. & ZUCKER R.S. (1997) Mitochondrial involvement in post-tetanic potentiation of synaptic transmission. Neuron **18**, 483-491.

TANII H., ANKARCRONA M., FLOOD F., NILSBERTH C., MEHTA N.D., PEREZ-TUR J., WINBLAD B., BENEDIKZ E. & COWBURN R.F (1999) Alzheimer's disease presenilin-1 exon 9 deletion and L250S mutations sensitize SH-SY5Y neuroblastoma cells to hyperosmotic stress-induced apoptosis. Neuroscience **95**, 593-601.

TANZI R.E., KOVACS D.M., KIM T.W., MOIR R.D., GUENETTE S.Y. & WASCO W. (1996) The gene defects responsible for familial Alzheimer's disease. Neurobiology of Disease **3**, 159-168.

TANZI R.E., GUSELLA J.F., WATKINS P.C., BRUNS G.A., ST GEORGE-HYSLOP P., VAN KEUREN M.L., PATTERSON D., PAGAN S., KURNIT D.M. & NEVE R.L. (1987) Amyloid β protein gene: cDNA, mRNA distribution and genetic linkage near the Alzheimer locus. Science **235**. 880-884.

TARKOWSKI E., RINGQVIST A., BLENNOW K., WALLIN A. & WENNMALM A. (2000) Intrathecal release of nitric oxide in Alzheimer's disease and vascular dementia. Dementia & Geriatric Cognitive Disorders **11**, 322-326.

TARKOWSKI A.K. (1961) Mouse chimaeras developed from fused eggs. Nature **190**, 857-860.

THINAKARAN G., HARRIS C.L., RATOVITSKI T., DAVENPORT F., SLUNT H.H., PRICE D.L., BORCHELT D.R. & SISODIA S. S. (1997) Evidence that levels of presenilins (PS1 and PS2) are coordinately regulated by competition for limiting cellular factors. Journal of Biological Chemistry **272**, 28415-28422.

THINAKARAN G., BORCHELT D.R., LEE M.K., SLUNT H.H., SPITZER L., KIM G., RATOVITSKY T., DAVENPORT F., NORDSTEDT C., SEEGER M., HARDY J., LEVEY A.I., GANDY S.E., JENKINS N.A., COPELAND N.G., PRICE D.L., & SISODIA S.S. (1996) Endoproteolysis of presenilin 1 and accumulation of processed derivatives *in vivo*. Neuron **17**, 181–190.

TIRET L., DE KNIJFF P., MENZEL H.-J., EHNHOLM C., NICAUD V. & HAVEKES L.M. (1994) ApoE polymorphism and predisposition to coronary heart disease in youths of different European population: the EARS study. Arteriosclerosis & Thrombosis **14**, 1617-1624.

TOKUHIRO S., TOMITA T., IWATA H., KOSAKA T., SAIDO T.C., MARUYAMA K. & IWATSUBO T. (1998) The presenilin 1 mutation (M146V) linked to familial Alzheimer's disease attenuates the neuronal differentiation of NTera 2 cells. Biochemical & Biophysical Research Communications **244**, 751-755.

TONI N., BUCKS P.-A., NIKONENKO I., BRON C.R. & MULLER D. (1999) LTP promotes formation of multiple spine synapses between a single axon terminal and a dendrite. Nature **402**, 421-425.

TSENG B.P., ESLER W.P., CLISH C.B., STIMSON E.R., GHILARDI J.R., VINTERS H.V., MANTYH P.W., LEE J.P. & MAGGIO J.E. (1999) Deposition of monomeric, not oligomeric, Aβ mediates growth of Alzheimer's disease amyloid plaques in human brain preparations. Biochemistry **38**, 10424-10431.

UEDA K., SHINOHARA S., YAGAMI Y., ASAKURA K. & KAWASAKI K. (1997) Amyloid β protein potentiates Ca^{2+} influx through L-type voltage-sensitive Ca^{2+} channels: a possible involvement of free radicals. Journal of Neurochemistry **68**, 265-271.

UEDA K., FUKUI Y. & KAGEYAMA H. (1994) Compromise of mitochondrial function induced by amyloid beta protein in PC12 cells and protection by cyclic AMP-dependent protein kinase inhibitors. Neuroscience Research Communications **15**, 195-200.

UETANI N., KATO K., OGURA H., MIZUNO K., KAWANO K., MIKOSHIBA K., YAKURA H., ASANO M. & IWAKURA Y. (2000) Impaired learning with enhanced hippocampal long-term potentiation in PTPδ-deficient mice. EMBO Journal **19**, 2775-2785.

VAN DORPE J., SMEIJERS L., DEWACHTER L., NUYENS D., SPITTAELS K., VAN DEN HAUTE C., MERCHEN M., MOECHARS D., LAENEN I., KUIPERI C., BRUYNSEELS K., TESSEUR I., LOOS R., VANDERSTICHELE H., CHECLER F., SCIOT R. & VAN LEUVEN F. (2000) Prominent cerebral amyloid angiopathy in transgenic mice overexpression the London mutant of human APP in neurons. American Journal of Pathology **157**, 1283-1298.

VAN DUIJN C.M., CLAYTON D., CHANDRA V., FRATIGLIONI L., GRAVES A.B., HEYMAN A., JORM A.F., KOKMEN E., KONDO K., MORTIMER J.A., ROCCA W.A., SHALAT S.L., SOININEN H. & HOFMAN A. (1991) Familial aggregation of Alzheimer's disease and related disorders: A collaborative re-analysis of case-control studies. International Journal of Epidemiology **20**, S13-S20.

VASSAR R., BENNETT B.D., BABU-KHAN S., KAHN S., MENDIAZ E.A., DENIS P., TEPLOW D.B., ROSS S., AMARANTE P., LOELOFF R., LUO Y., FISHER S., FULLER J., EDENSON S., LILE J., JAROSINSKI M.A., BIERE A.L., CURRAN E., BURGESS T., LOUIS J.-C., COLLINS F., TREANOR J., ROGERS G. & CITRON M. (1999) β-secretase cleavage of Alzheimer's amyloid precursor protein by the transmembrane aspartic protease BACE. Science **286**, 735-741.

VELAZQUEZ P., CRIBBS D.H., POULOS T.L. & TENNER A.J. (1997) Aspartate residue 7 in amyloid β-protein is critical for classical complement pathway activation:implications for Alzheimer's disease pathogenesis. Nature Medicine **3**, 77-79.

VERBEEK M.M., OTTE-HOLLER I., VAN DEN BORN J., VAN DEN HEUVEL L.P.W.J., DAVID G., WESSELING P. & DE WAAL R.M.W. (1999) Agrin is a major heparan sulfate proteoglycan accumulating in Alzheimer's disease brain. American Journal of Pathology **155**, 2115-2125.

VINCENT B. & SMITH JD. (2001) Astrocytes down-regulate neuronal beta-amyloid precursor protein expression and modify its processing in an apolipoprotein E isoform-specific manner. European Journal of Neuroscience **14**, 256-66.

VORONIN L.L., KUHNT U. & GUSEV A.G. (1992) Analysis of fluctuations of 'minimal' excitatory postsynaptic potentials during long-term potentiation in guinea pig hippocampal slices. Experimental Brain Research **89**, 288-299.

WAKABAYASHI K., HANSEN L.A. & MASLIAH E. (1995) Cortical Lewy body-containing neurons are pyramidal cells: laser confocal imaging of double-immunolabeled sections with anti-ubiquitin and SMI32. Acta Neuropathologica **89**, 404-408.

WANG J.C., KWON J.M., SHAH P., MORRIS J.C. & GOATE A. (2000) Effect of APOE genotype and promoter polymorphism on risk of Alzheimer's disease. Neurology **55**, 1644-1649.

WANG H. & WAGNER J.J. (1999) Priming-induced shift in synaptic plasticity in the rat hippocampus. Journal of Neurophysiology **82**, 2024-2028.

WANG J.-Z., GRUNDKE-IQBAL I. & IQBAL K. (1996a) Glycosylation of microtubule-associated protein tau: An abnormal posttranslational modification in Alzheimer's disease. Nature Medicine **2**. 871-875.

WANG S., WOJTOWICZ J.M. & ATWOOD H.L. (1996b) Synaptic recruitment during long-term potentiation at synapses of the medial perforant pathway in the dentate gyrus of the rat brain. Synapse **22**, 78-86.

WANG X., LUEBBE P., GRUENSTEIN E. & ZEMLAN F. (1998) Apolipoprotein E (ApoE) peptide regulates tau phosphorylation via two different signaling pathways. Journal of Neuroscience Research **51**, 658-65.

WEBSTER S.D., TENNER A.J., POULOS T.L. & CRIBBS D.H. (1999) The mouse C1q A-chain sequence alters β-amyloid-induced complement activation. Neurobiology of Aging **20**, 297-304.

WEIDERMANN A., PALIGA K., DÜRRWANG U., REINHARD F.B.M., SCHUCKERT O., EVIN G. & MASTERS C.L. (1999) Proteolytic Processing of the Alzheimer's Disease Amyloid Precursor Protein within Its Cytoplasmic Domain by Caspase-like Proteases. Journal of Biological Chemistry **274**, 5823-5829.

WENGENACK T.M., WHELAN S., CURRAN G.L., DUFF K.E. & PODUSLO J.F. (2000) Quantitative histological analysis of amyloid deposition in Alzheimer's double transgenic mouse brain. Neuroscience **101**, 939-944.

WICKNER S., MAURIZI M.R. & GOTTESMAN S. (1999) Posttranslational quality control: Folding, refolding, and degrading proteins. Science **286**, 1888-1893.

WIGSTROM H. & GUSTAFSSON B. (1985) Facilitation of hippocampal long-lasting potentiation by GABA antagonists. Acta Physiologica Scandinavica **125**, 159-172.

WILSON C.A., DOMS R.W. & LEE V.M.-Y. (1999) Intracellular APP processing and Aβ production in Alzheimer disease. Journal of Neuropathology and Experimental Neurology **58**, 787-794.

WISNIEWSKI T., CASTANO E.M., GOLABEK A., VOGEL T. & FRANGIONE B. (1994) Acceleration of Alzheimer's fibril formation by apolipoprotein E *in vitro*. American Journal of Pathology **145**, 1030-1035.

WISNIEWSKI K.E., DALTON A.J., MCLACHLAN C., WEN G.Y. & WISNIEWSKI H.M. (1985) Alzheimer's disease in Down's syndrome: clinicopathologic studies. Neurology **35**, 957-961.

WOLFE M.S., XIA W., OSTASZEWSKI B.L., DIEHL T.S., KIMBERLEY W.T. & SELKOE D.J. (1999) Two transmembrane aspartates in presenilin-1 required for presenilin endoproteolysis and β-secretase activity. Nature **398**, 513-517.

WONG T.P., DEBEIR T., DUFF K. & CUELLO C. (1999) Reorganization of cholinergic terminals in the cerebral cortex and hippocampus in transgenic mice carrying mutated presenilin-1 and amyloid precursor protein transgenes. Journal of Neuroscience **19**, 2706-2716.

WU J., ANWYL R. & ROWAN M.J. (1995) β-amyloid 1-40 increases long-term potentiation in rat hippocampus. European Journal of Pharmacology **284**, R1-R3.

WYSS-CORAY T., LIN C., YAN F., YU G.-Q., ROHDE M., MCCONLOGUE L., MASLIAH E. & MUCKE L. (2001) TGF-β promotes microglial amyloid-β clearance and reduces plaque burden in transgenic mice. Nature Medicine **7**, 612-618.

XIA W., ZHANG J., OSTASZEWSKI B.L., KIMBERLY W.T., SEUBERT P., KOO E.H., SHEN J. & SELKOE D.J. (1998) Presenilin 1 regulates the processing of β-amyloid precursor protein C-terminal fragments and the generation of amyloid β-protein in endoplasmic reticulum and golgi. Biochemistry **37**, 16465-16471.

XIA W., ZHANG J., KHOLODENKO D., CITRON M., PODLISNY M.B., TEPLOW D.B., HAASS C., SEUBERT P., KOO E.H. & SELKOE D.J. (1997) Enhanced production and oligomerization of the 42-residue amyloid β-protein by chinese hamster ovary cells stably expressing mutant presenilins. Journal of Biological Chemistry **272**, 7977-7982.

XIAO M.-Y., NIU Y.-P. & WIGSTROM H. (1996) Activity-dependent decay of early LTP revealed by dual EPSP recording in hippocampal slices from young rats. European Journal of Neuroscience **8**. 1916-1923.

XIE X., LIAW J.-S., BAUDRY M. & BERGER T.W. (1997) Novel expression mechanism for synaptic potentiation: Alignment of presynaptic release site and postsynaptic receptor. Proceedings of the National Academy of Sciences USA **92**, 6983-6988.

XIE X. & SMART T.G. (1994) Modulation of long-term potentiation in rat hippocampal pyramidal neurones by zinc. Pflugers Archives; European Journal of Physiology **427**, 481-486.

XIE X., GERBER U., GAHWILER B.H. & SMART T.G. (1993) Interaction of zinc with ionotropic and metabotropic glutamate receptors in rat hippocampal slices. Neuroscience Letters **159**, 46-50.

XIE X., BERGER T.W. & BARRIONUEVO G. (1992) Isolated NMDA receptor-mediated synaptic responses express both LTP and LTD. Journal of Neurophysiology **67**, 1009-1013.

XU P.-T., GILBERT J.R., QIU H.-L., ERVIN J., ROTHROCK-CHRISTIAN T.R., HULETTE C., AND SCHMECHEL D.E. (1999) Specific regional transcription of apolipoprotein E in human brain neurons. American Journal of Pathology **154**, 601-611.

YAMAGUCHI Y. & KAWASHIMA S. (2001) Effects of amyloid-β_{25-35} on passive avoidance, radial-arm maze learning and choline acetyltransferase activity in the rat. European Journal of Pharmacology **412**, 265-272.

YAN S.D., CHEN X., FU J., CHEN M., ZHU H., ROHER A., SLATTERY T., ZHAO L., NAGASHIMA M., MORSER J., MIGHELI A., NAWROTH P., STERN D. & SCHMIDT A.M. (1996) RAGE and amyloid-β peptide neurotoxicity in Alzheimer's disease. Nature **382**, 685-691.

YAN S.D., YAN S.F., CHEN X., FU J., CHEN M., KUPPUSAMY P., SMITH M.A., PERRY G., GODMAN G.C., NAWROTH P., ZWEIER J.L. & STERN D. (1995) Non-enzymatically glycated tau in Alzheimer's disease induces neuronal oxidant stress resulting in cytokine gene expression and release of amyloid β-peptide. Nature Medicine **1**, 693-699.

YANG D.-S., MCLAURIN J., QIN K., WESTAWAY D. & FRASER P.E. (2000a) Examining the zinc binding site of the amyloid-β peptide. European Journal of Biochemistry **267**, 6692-6698.

YANG F., UEDA K., CHEN P.-P., HSIAO ASHE K. & COLE G.M. (2000b) Plaque-associated α-synuclein in (NACP) pathology in aged transgenic mice expressing amyloid precursor protein. Brain Research **853**, 381-383.

YANG L.-S. & KSIEZAK-REDING H. (1999a) Ca^{2+} and Mg^{2+} selectively induce aggregates of PHF-Tau but not normal human Tau. Journal of Neuroscience Research **55**, 36-43.

YANG S.-N., TANG Y.-G. & ZUCKER R.S. (1999b) Selective induction of LTP and LTD by postsynaptic $[Ca^{2+}]_i$ elevation. Journal of Neurophysiology **81**, 781-787.

YANKNER B.A., DAWES L.R., FISHER S., VILLA-KOMAROFF L., OSTER-GRANITE M.L. & NEVE R.L. (1989) Neurotixicity of a fragment of the amyloid precursor associated with Alzheimer's disease. Science **245**, 417-420.

YASOJIMA K., SCHWAB C., MCGEER E.G. & MCGEER P.L. (1999) Up-regulated production and activation of the complement system in Alzheimer's disease brain. American Journal of Pathology **154**, 927-936.

YATES S.L., BURGESS L.H., KOCSIS-ANGLE J., ANTAL J.M., DORITY M.D., EMBURY P.B., PIOTRKOWSKI A.M. & BRUNDEN K.R. (2000) Amyloid β and amylin fibrils induce increases in proinflammatroy cytokine and chemokine production by THP-1 cells and murine microglia. Journal of Neurochemistry **74**, 1017-1025.

YATES C.M., BUTTERWORTH J., TENNANT M.C. & GORDON A. (1990) Enzyme activities in relation to pH and lactate in postmortem brain in Alzheimer-type and other dementias. Journal of Neurochemistry **55**, 1624-1630.

YE C., HO-PAO C.L., KANAZIRSKA M., QUINN S., ROGERS K., SEIDMAN C.E., SEIDMAN J.G., BROWN E.M. & VASSILEV P.M. (1997) Amyloid-β proteins activate Ca^{2+}-permeable channels through calcium-sensing receptors. Journal of Neuroscience Research **47**, 547-554.

YECKEL M.F., KAPUR A. & JOHNSON D. (1999) Multiple forms of LTP in hippocampal CA1 neurones use a common postsynaptic mechanism. Nature Neuroscience **2**, 625-633.

YOO A.S., CHENG I., CHUNG S., GRENFELL T.Z., LEE H., PACK-CHUNG E., HANDLER M., SHEN J., WIA W., TESCO G., SAUNDERS A.J., DING K., FROSCH M.P., TANZI R.E. & KIM T.-W. (2000) Presenilin-mediated modulation of capacitative calcium entry. Neuron **27**, 561-572.

YU S.P., FARHANGRAZI Z.S., YING H.S., YEH C.-H. & CHOI D.W. (1998) Enhancement of outward potassium current may participate in β-amyloid peptide-induced cortical neuronal death. Neurobiology of Disease **5**, 81-88.

ZAMAN S.H., PARENT A., LASKEY A., LEE M.K., BORCHELT D.R., SISODIA S.S. & MALINOW R. (2000) Enhanced synaptic potentiation in transgenic mice expressing presenilin 1 familial Alzheimer's disease mutation is normalized with a benzodiazepine. Neurobiology of Disease **7**, 54-63.

ZAMANILLO D., SPRENGEL R., HVALBY O., JENSEN V., BURNASHEV N., ROZOV A., KAISER K.M.M., KOSTER H.J., BORCHARDT T., WORLEY P., LUBKE J., FROTSCHER M., KELLY P.H., SOMMER B., ANDERSEN P., SEEBURG P.H. & SAKMANN B. (1999) Importance of AMPA receptors for hippocampal synaptic plasticity but not for spatial learning. Science **284**. 1805-1181.

ZHANG Z., HARTMANN H., DO V.M., ABRAMOWSKI D., STURCHLER-PIERRAT C., STAUFENBIEL M., SOMMER B., VAN DE WETERING M., CLEVERS H., SAFTIG P., DE STROOPER B., HE X. & YANKNER B. (1998) Destabilization of β-catenin by mutations in presenilin-1 potentiates neuronal apoptosis. Nature **395**, 698-702.

ZHANG F., ECKMAN C., YOUNKIN S,. HSIAO K.K. & IADECOLA C. (1997) Increased susceptibility to ischemic brain damage in transgenic mice overexpressing the amyloid precursor protein. Journal of Neuroscience **17**, 7655-7661.

ZHANG E.Y., DETURE M.A., BUBB M.R., CAVISTON T.L., ERDOS G.W., WHITTAKER S.D. & PURICH D.L. (1996) Self-assembly of the brain MAP-2 microtubule binding region into polymeric structures resembling Alzheimer filaments. Biochemical and Biophysical Research Communications **229**, 176-181.

ZIELASEK J. HARTUNG HP. (1996) Molecular mechanisms of microglial activation. Advances in Neuroimmunology **6**, 191-22.